ABSTRACT

Title of Dissertation: EXPLORING THE FUNCTION AND REGULATION OF ARABIDOPSIS EIN2 IN ETHYLENE SIGNALING

Jennifer Marie Shemansky, Doctor of Philosophy, 2016

Dissertation directed by: Dr. Caren Chang, Department of Cell Biology and Molecular Genetics

Ethylene is an essential plant hormone involved in nearly all stages of plant growth and development. EIN2 (ETHYLENE INSENSITIVE2) is a master positive regulator in the ethylene signaling pathway, consisting of an N-terminal domain and a C-terminal domain. The EIN2 N-terminal domain localizes to the endoplasmic reticulum (ER) membrane and shows sequence similarity to Nramp metal ion transporters. The cytosolic C-terminal domain is unique to plants and signals downstream. There have been several major gaps in our knowledge of EIN2 function. It was unknown how the ethylene signal gets relayed from the known upstream component CTR1 (CONSTITUTIVE RESPONSE1) a Ser/Thr kinase at the ER, to EIN2. How the ethylene signal was transduced from EIN2 to the next downstream component transcription factor EIN3 (ETHYLENE INSENSITIVE3) in the nucleus was also unknown. The N-terminal domain of EIN2 shows homology to Nramp

metal ion transporters and whether EIN2 can also function as a metal transporter has been a question plaguing the ethylene field for almost two decades. Here, EIN2 was found to interact with the CTR1 protein kinase, leading to the discovery that CTR1 phosphorylates the C-terminal domain of EIN2 in *Arabidopsis thaliana*. Using tags at the termini of EIN2, it was deduced that in the presence of ethylene, the EIN2 C-terminal domain is cleaved and translocates into the nucleus, where it could somehow activate downstream ethylene responses. The EIN2 C-terminal domain interacts with nuclear proteins, RTE3 and EER5, which are components of the TREX-2 mRNA export complex, although the role of these interactions remains unclear.

The EIN2 N-terminal domain was found to be capable of divalent metal transport when expressed in *E. coli* and *S. cerevisiae* leading to the hypothesis that metal transport plays a role in ethylene signaling. This hypothesis was tested using a novel missense allele, *ein2 G36E*, substituting a highly conserved residue that is required for metal transport in Nramp proteins. This G36E substitution did not disrupt metal ion transport of EIN2, but the ethylene insensitive phenotype of this mutant indicates that the EIN2 N-terminal domain is important for positively regulating the C-terminal domain. The defect of the *ein2* G36E mutant does not prevent proper expression or subcellular localization, but might affect protein modifications. The *ein2 G36E* allele is partially dominant, mostly likely displaying haploinsufficiency. Overexpression of the EIN2 N-terminal domain in the *ein2 G36E* mutant did not rescue ethylene insensitivity, suggesting the N-terminal domain functions *in cis* to regulate the C-terminal domain. These findings advance our knowledge of EIN2, which is critical to understanding ethylene signaling

EXPLORING THE FUNCTION AND REGULATION OF ARABIDOPSIS EIN2 IN ETHYLENE SIGNALING

by

Jennifer Marie Shemansky

Dissertation submitted to the Faculty of the Graduate School of the
University of Maryland, College Park, in partial fulfillment
of the requirements for the degree of
Doctorate of Philosophy
2016

Advisory Committee:
Dr. Caren Chang, Chair
Dr. Zhongchi Liu
Dr. Stephen Mount
Dr. Daniel Nelson
Dr. Gary Coleman, Dean's Representative

Dedication

"Our greatest weakness lies in giving up. The most certain way to succeed is to try one more time" Thomas Edison

Acknowledgements

As I reflect on my graduate career, there have been many people who have helped me along the way. Most importantly, Dr. Caren Chang who has been a wonderful mentor and friend. She has been there for me, providing advice, encouragement and a shoulder to cry on. I am a better scientist and person because of her and although there are a ton of words in this thesis, there are really no words to describe how wonderful a person Caren is and what a pleasure is has been to work with her for all these years. From the bottom of my heart, thank you for everything you have done for me, Caren.

Additionally, much thanks to John Clay, Roxane Bouten, David Lin and all the other members of the Chang Lab over the years. I honestly do not know how I would have made it all the way to the end without their help and encouragement. Much thanks to my thesis committee, who have given me valuable comments and suggestions over the years as well as their comments on this beast of a thesis. Dr. Sébastien Thomine and Pierre Longerstay for the yeast strains, advice with the transport assays, and atomic absorption results. Lastly, I would like to thank the NIH MOCB Training Grant Fellowship as well as the Ann G. Wylie Dissertation Fellowship, which combined funded me for 2.5 years of my graduate career and allowed me to focus solely on my research.

Lastly, thanks Mom ☺

Table of Contents

List of Tables

List of Figures

List of Abbreviations

3-AT – 3-Amino-1,2,4-triazole
ABA – Abscisic acid
ABRC - Arabidopsis Biological Resource Center
ACC - 1-Aminocyclopropane-1-carboxylic acid
Ade - adenine
Ala - alanine
AtNRAMP4 – Arabidopsis NATRUAL RESISTANCE-ASSOCIATED MACROPHAGE PROTEIN4
AVG – Aminoethoxyvinylglycine
BiFC – Bimolecular Fluorescence Complementation
BPDS - Bathophenanthrolinedisulfonic acid
BSD2 – BYPASS SOD1p DEFECTS 2
CCC1 – Cross-Complements Ca^{2+} phenotype of *csg1*
CDC31 – CELL DIVISION CYCLE 31
Col-0 – *Arabidopsis thaliana* Columbia ecotype
COT1 - CObalt Toxicity 1
CNB1 - CalciNeurin subunit B 1
CSN – COP9 signalosome
CSNAP – COP9 SIGNALOSOME ASSOCIATED PROTEIN
CSN3 - COP9 signalosome subunit 3
CSN8 - COP9 signalosome, subunit 8
CTR1 - CONSTITUTIVE RESPONSE 1
CTR1 (yeast) - Copper TRansport 1
CTR1-1 – containing the D694E mutation
CTR2 (yeast) - Copper TRansport 2
DAPI - 4',6-diamidino-2-phenylindole
DCT1 – DIVALENT CATION TRANSPORTER 1
DMT1 – DIVALENT METAL TRANSPORTER 1
EBF1 - EIN3 BINDING F-BOX PROTEIN 2
EBF2 – EIN3 BINDING F-BOX PROTEIN 2
EER5 – ENHANCED ETHYLENE RESPONSE 5
EGTA - ethylene glycol-bis(β-aminoethyl ether)-N,N,N',N'-tetraacetic acid
eiF3 – eukaryotic initiation factor 3
EIL1 – EIN3-LIKE 1
EIN2 - ETHYLENE INSENSITIVE 2
EIN2 C-terminal domain – Residues 516-1294
EIN2 hybrid – *E. coli* codon optimized EIN2 N-terminal domain (residues 1-524), with residues 1-15 replaced with MntH protein sequence
EIN2/MntH chimera – *E. coli* codon optimized EIN2 N-terminal domain (residues 1-481), with residues 1-15 replaced with MntH protein sequence
EIN2 N-terminal domain – Residues 1-524
EIN2-9 – containing the H1143P mutation
EIN3 - ETHYLENE INSENSITIVE 3

EIN4 - ETHYLENE INSENSITIVE 4
EIN5 - ETHYLENE INSENSITIVE 5
EMS - Ethyl methanesulfonate
EPR - Electron Paramagnetic Resonance
EREBP – ETHYLENE-RESPONSIVE-ELEMENT-BINDING PROTEINS
ERF1 – ETHYLENE RESPONSIVE FACTOR 1
ETP1 - EIN2 TARGETING PROTEIN 1
ETP2 – EIN2 TARGETING PROTEIN 2
ETRI – ETHYLENE RESPONSE 1
ETR2 – ETHYLENE RESPONSE 2
ERS1 – ETHYLENE RESPONSE SENSOR 1
ERS2 - ETHYLENE RESPONSE SENSOR 2
FET3 - FErrous Transport 3
FET4 - FErrous Transport 4
FOA - 5-Fluoroorotic acid
FRET – Fluorescence Resonance Energy Transfer assay
G418 - Geneticin
GANP - GERMINAL CENTER ASSOCIATED NUCLEAR PROTEIN
GFP – GREEN FLUORESCENT PROTEIN
Glu – glutamic acid
Gly - glycine
GUS - β-GLUCURONIDASE
His - histidine
L*er* – *Arabidopsis thaliana* Landsberg erecta ecotype
ICP-MS – Inductively Coupled Plasma-Mass Spectrometry
Leu - leucine
IRT1 - IRON REGULATED TRANSPORTER 1
JAZ1 - JASOMANTE-ZIM-domain protein 1
M^{2+} - Generic metal with a 2+ charge (divalent cation)
M^{3+} - Generic metal with a 3+ charge (trivalent cation)
Map80 - 80 kDa MCM3 ASSOCIATED PROTEIN
MCM3 - MINI CHROMOSOMAL MAINTAINENCE 3
MCM3AP - MINI CHROMOSOMAL MAINTAINENCE 3 ASSOCIATED PROTEIN
MES - 2-(*N*-morpholino) ethanesulfonic acid
Met - methionine
MICKEY - Metal Ion Compensation of Killing Efficiency and Yield assay
MIF1 – MITOCHONDRIAL ASSEMBLY 1
MntH – Manganese transport system of *E. coli*, H+ dependent
MPN domain - Mpr1-Pad1-N-terminal
MS – Murashige and Skoog medium
MUSCLE – Multiple Sequence Comparison by Log-Expectation
NanoSIMS - high-resolution Secondary Ion Mass Spectrometry
NLS – Nuclear localization sequence
NMR - Nuclear Magnetic Resonance
NPC – Nuclear Pore Complexes

NRAMP – Natural Resistance-Associated Macrophage Protein
NRAMP4 – NATRUAL RESISTANCE-ASSOCIATED MACROPHAGE PROTEIN4
NRAT1 - NRAMP ALUMINUM TRANSPORTER1
NUP1 – NUCLEOPORE COMPLEX PROTEIN
PAM domain – PCI/PINT associated module
PCI domain – Proteasome, COP9 signalosome, initiation factor 3
PDF1.2 – PLANT DEFENSIN 1.2
PINT domain- Proteasome subunits, Int-6, Nip-1, and TRIP-15
PMC1 – PLASMA MEMBRANE CALCIUM 1
PMR1 – PLASMA MEMBRANE ATP-ASE RELATED 1
RAN1 – RESONSE-TO-ANTAGONIST 1
RFP – RED FLUORESCENT PROTEIN
ROS – Reactive oxygen species
RTE1 – REVERSION-TO-ETHYLENE-SENSITIVITY 1
RTE3 – REVERSION-TO-ETHYLENE-SENSITIVITY 3
RTE3-1 – containing the W1143* substitution
SAC3 – SUPPRESSOR OF ACTIN 3
SEC62 – SECrectory, subunit of the Sec63 complex
SED5 – SUPPRESSOR OR ERD2 DELETION
Ser - serine
SMF1 – SUPRESSOR OF MITOCHONDRIA IMPORT FUNCTION 1
SMF2 – SUPRESSOR OF MITOCHONDRIA IMPORT FUNCTION 2
SNC1 – SUPPRESSOR OF THE NULL ALLELE OF CAP
SOD – SUPEROXIDE DISMUTASE
SOD2 – SUPEROXIDE DISMUTASE 2
SPF1 – SENSITIVITY TO PICHIA FARINOSA KILLER TOXIN 1
Split-Ub - Split-Ubiquitin assay
SSO1 – SUPPRESSOR OF SEC ONE
SUS1 – SUCROSE SYNTHASE 1
S-XRF - Synchrotron-X-ray Fluorescence
TAIR - The *Arabidopsis* Information Resource
TAP – Tandem Affinity Purification
TBP2 - TATA-BOX BINDING PROTEIN 2
THP1 - Tho2/Hpr1 Phenotype 1
Thr - threonine
TREX-2 – TRANSCRIPTION EXPORT 2 complex
Trp – tryptophan
Ura - uracil
UTR – untranslated region
VCX1 - VaCuolar H^+/Ca^{2+} eXchanger 1
X-gal - 5-bromo-4-chloro-3-indolyl-β-D-galactopyranoside
XRN4 – EXORIBONUCLEASE 4
YCF1 – YEAST CADMIUM FACTOR 1
YFP – YELLOW FLUORESCENT PROTEIN
ZRC1 - ZINC RESISTANCE CONFERRIN

Chapter 1: Introduction

The Ethylene Signaling Pathway

Ethylene, although a very simple gaseous molecule, plays a vital role as a plant hormone. It affects all stages of plant growth and development, from seed germination and seedling growth and development to fruit development and senescence (Abeles et al., 1992). For example, ethylene is most known for its role in promoting fruit development and senescence. As a result, ethylene and ethylene related studies are commercially useful, as a means to selectively promote or inhibit ripening of fruit.

Many of the core signaling pathway components have been elucidated utilizing the signature triple response phenotype (Knight and Crocker, 1913; Bleecker et al., 1988; Guzmán and Ecker, 1990; Kieber, et al., 1993; Roman et al., 1995), first described by Dimitry Neljubow (1901) as an ethylene response in etiolated pea seedlings. In Arabidopsis, ethylene causes shortening and thickening of the hypocotyl, shortening and thickening of the root, and production of an apical hook, termed the triple response phenotype (Figure 1.1). This phenotype is specific to etiolated seedlings in the presence of ethylene, and therefore has been a vital tool in elucidating the ethylene pathway (through the screening of mutants), as well as a useful readout for an ethylene response.

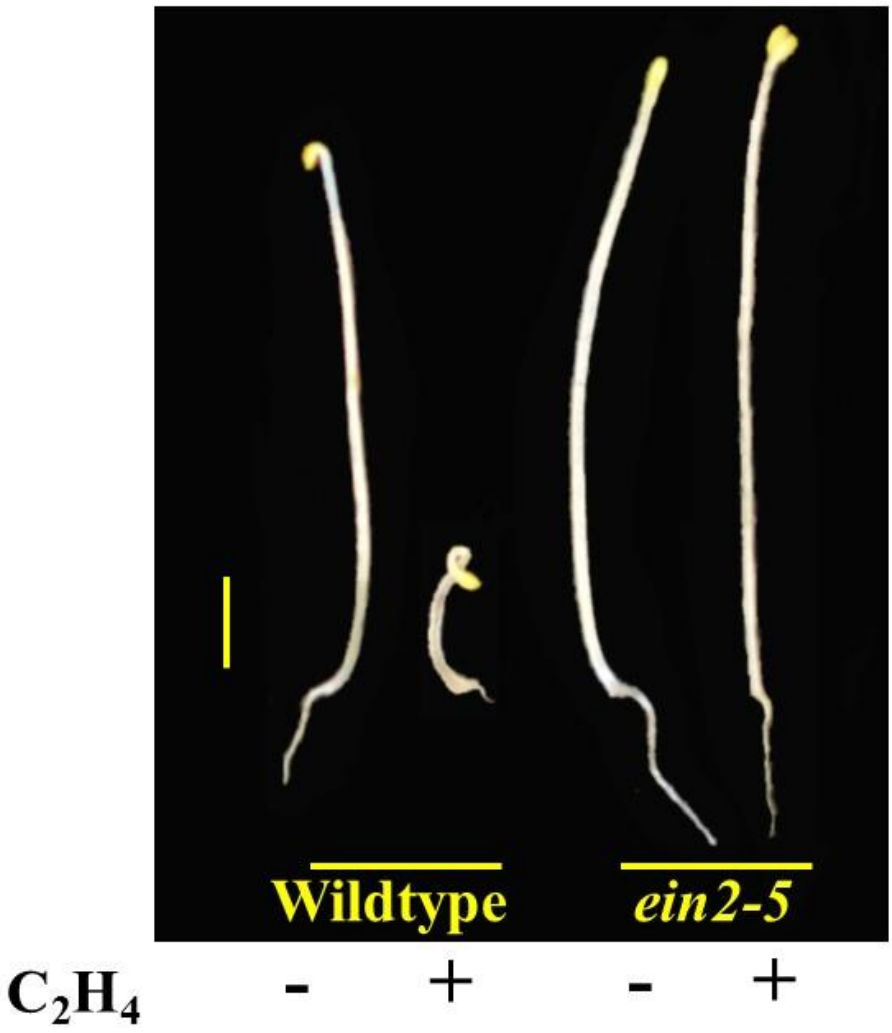

Figure 1.1 Triple response phenotype in four day-old etiolated Arabidopsis seedlings. When ethylene biosynthesis is blocked via AVG (10 μM Aminoethoxyvinylglycine) wildtype (Col-0) seedlings have long hypocotyls and roots. However, in the presence of ethylene, via the precursor ACC (20 μM 1-Aminocyclopropane-1-carboxylic acid) seedlings display the signature triple response phenotype, in contrast to the *ein2-5* null allele, which confers ethylene insensitivity. Scale bar represents 2 mm.

In Arabidopsis, ethylene is perceived by a family of five ethylene receptors (ETR1, ERS1, ETR2, ERS2, EIN4; ETHYLENE RECEPTOR 1, ETHYLENE RESPONSE SENSOR 1, ETHYLENE RECEPTOR 2, ETHYLENE RESPONSE SENSOR 2, ETHYLENE INSENSITIVE 4) localized to both the Golgi and the endoplasmic reticulum (ER) membranes (Dong et al., 2008; Chen et al., 2010). These receptors were found to negatively regulate the signaling pathway (Hua and Meyerowitz, 1998; Hall et al., 1999; Qu et al., 2007). In other words, when ethylene is bound, the receptors are considered to be inactive in terms of their signaling.

All five receptors are comprised of a hydrophobic N-terminal domain, where the ethylene molecule binds (Schaller and Bleecker, 1995; Hall et al., 1999; Rodriguez et al., 1999; O'Malley et al., 2005), followed by a cytosolic GAF domain, which plays a role in protein-protein interactions between receptors (Xie et al., 2006; Grefen et al., 2008; Gao et al., 2008). Following the GAF domain, is a histidine kinase domain, and some receptors contain an additional receiver domain. The receptors named ERS (ETHYLENE RESPONSE SENSOR) lack a receiver domain.

The receptors are subdivided into two subfamilies. Subfamily I is composed of ETR1 and ERS1. They contain three transmembrane domains and have histidine autokinase activity (ERS1 also shows serine/threonine kinase activity) (Gamble et al., 1998; Moussatche and Klee, 2004; Chen et al., 2009). ETR2, ERS2, and EIN4 are grouped into subfamily II, which contain four N-terminal trans-membrane domains and have serine/threonine kinase activity (Gamble et al., 1998; Moussatche and Klee, 2004; Chen et al., 2009). However, there is debate concerning the extent to which the

kinase domain plays a role in ethylene signaling (Gamble et al., 2002; Wang et al., 2003; Hall and Bleecker, 2003; Qu and Schaller, 2004; Hall et al., 2012).

Interacting with the receptors, is the next downstream component, CTR1 (CONSTITUTIVE TRIPLE RESPONSE 1), a serine/threonine protein kinase, also a negative regulator of ethylene signaling. CTR1 is inactive when ethylene is bound by the ethylene receptors (Kieber et al., 1993; REF). The physical association of CTR1 and the receptors is required for the CTR1 kinase activity (Clark et al., 1998; Cancel and Larsen, 2002; Gao et al., 2003; Huang et al., 2003). The receptors were also found to interact with the EIN2 C-terminal domain (ETHYLENE INSENSITIVE 2), the next downstream component from CTR1 and a positive regulator of ethylene signaling (Bisson et al., 2009; Bisson and Groth, 2010; Alonso et al., 1999). This could suggest that there is a large ethylene signaling complex at the ER, however, the components may not all interact with each other at the same time (Chapter 2 describes this in more detail). When no ethylene is present, the receptors and CTR1 are active.

A long term question has been to identify the phosphorylated substrate of CTR1. Since CTR1 was thought to be a Raf-like kinase (a MAPKKK), for many years a MAPK cascade was proposed to be part of the ethylene signaling pathway (Novikova et al., 2000; Quaked et al., 2003; Yoo et al., 2008). However, to my knowledge, there have not been any CTR1-containing MAPK pathways identified. Perhaps CTR1 has a different substrate?

Ethylene binding to the receptors requires a Cu^{+} cofactor, delivered by the Golgi localized RAN1 (RESPONSE-TO-ANTAGONIST1), a copper transporting P-type ATPase homologous to the human Menkes/Wilson proteins (Hirayama et al.,

1999). Once ethylene is bound, the receptors and CTR1 are signaling inactive. This somehow leads to the activation of EIN2, which somehow signals to the downstream component, transcription factors EIN3 (ETHYLENE INSENSITIVE 3) and EIL1 (EIN3-LIKE 1) (Chao et al., 1997).

EIN2 – the Central Regulator of the Ethylene Signaling Pathway

EIN2 is one of the key components of this signaling pathway. In 2012, more than a decade after it was initially cloned (Alonso et al., 1999), three independent labs simultaneously helped uncover the mechanism of how EIN2 can bridge the gap in the ethylene signal from the ER membrane to the nucleus (Ju et al., 2012; Qiao et al., 2012; Wen et al., 2012) and between CTR1 and EIN2 (Ju et al., 2012). My role in these discoveries will be described in Chapter 2. However, the biochemical function of EIN2 still remains elusive.

EIN2 consists of two different domains; an N-terminal domain and a C-terminal domain. The N-terminal domain consists of twelve predicted transmembrane domains (ARAMEMNON; Alonso et al., 1999), localizes to the ER membrane (Bisson et al., 2009), and shows homology to Nramp metal ion transporters. Alonso et al. (1999) proposed that the N-terminal domain might control the C-terminal domain and have involvement in seedling skotomorphogenesis, but they were not able show any metal transport ability. Beyond that, not much is known regarding the N-terminal domain or its role in ethylene signaling. The EIN2 C-terminal domain, on the other hand, is a novel hydrophilic domain and is considered the ethylene signaling portion of the protein.

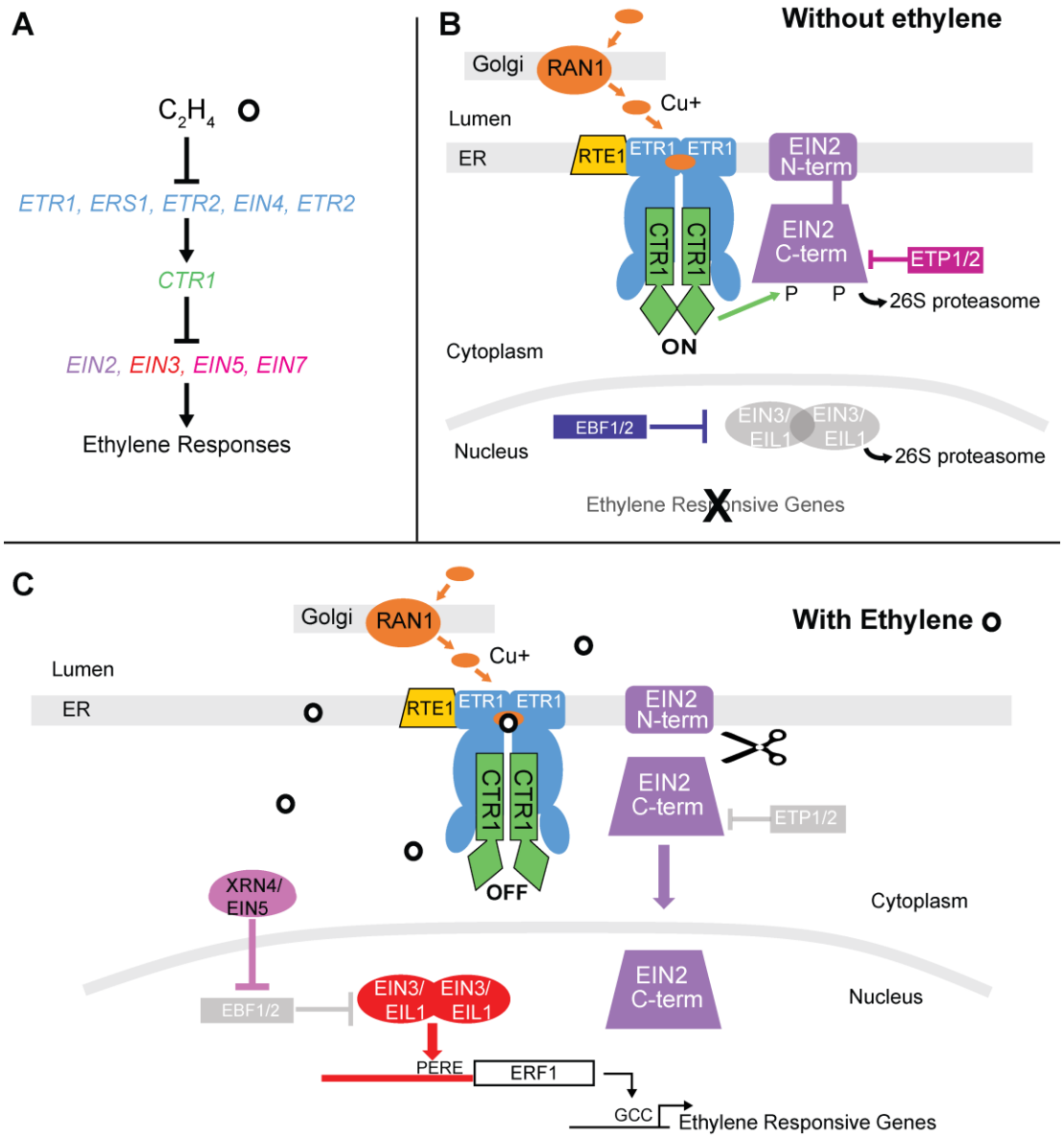

Figure 1.2. Models of the ethylene signaling pathway. (A) Model based on epistastic relationships, circa 1998. Many of these components were identified in the Roman et al. (1995) study. (B and C) Current model of ethylene signaling pathway without (B) and with ethylene (C).Ethylene (white circle) is perceived by a family of five ethylene receptors (depicted is ETR1 dimer). The copper cofactor required for ethylene binding is delivered by the Golgi localized copper transporter protein RAN1. The RTE1 interaction is specific to ETR1 and is believed to help promote proper

confirmation of the ETR1 receptor. Without ethylene (B) ETR1 is in a signaling active state, leading to the activation of CTR1 protein kinase, which in turn phosphorylates specific residues on the C-terminal domain of EIN2. This phosphorylation on EIN2 potentially leads to degradation by the 26S proteasome via two F-box proteins (ETP1/2). Two F-box proteins also target the EIN3/EIL1 dimer for degradation by the 26S proteasome as well, inhibiting ethylene responses. In the presence of ethylene (C) both receptors and CTR1 are signaling inactive and therefore CTR1 is unable to phosphorylate the specific residues in EIN2 C-terminal domain. The unphosphorylated EIN2 C-terminal domain is cleaved (via an unknown protease, depicted as scissors) and translocated to the nucleus where it plays a role in activating downstream ethylene responses. The EIN3/EIL1 are stabilized by the downregulation of EBF1/2 via their 3'UTR interaction with EIN5 and EIN2 C-terminal domain in the P-bodies (not depicted above, Liu et al., 2015). Homodimers of transcription factors EIN3/EIL1 bind to PERE elements of target genes, such as ERF1, to activate their expression. These target genes, such as transcription factor ERF1, in turn bind to the GCC box in the promoter of secondary target genes, leading to an ethylene response. Figure taken from Bakshi et al., 2015.

EIN2 was originally isolated in a screen to identify ethylene response mutants that exhibit severe ethylene insensitivity (Roman et al., 1995, Appendix A). It took until 1999 to clone *EIN2* (Alonso et al., 1999) making it the last of the core signaling components to be identified. Epistasis analysis places it downstream of *CTR1* (Roman et al., 1995) and for years EIN2 was predicted to localize to the nuclear membrane, where it could signal to the next downstream component, transcription factor EIN3. In 2009, EIN2 was finally localized to the ER membrane (Bisson et al., 2009).

EIN2 has been termed the "central regulator of ethylene signaling" since *ein2* mutants are the most insensitive of all ethylene mutants (Alonso et al., 1999; Roman et al., 1995) and over-expression of the C-terminal domain leads to a constitutive ethylene response in adult plants (Alonso et al., 1999) suggesting that EIN2, or at least its C-terminal domain, plays an important role as a positive regulator in ethylene signaling.

However, the N-terminal domain comprises a large portion of EIN2 (residues 1-461 out of 1294) and there has really been no work to better understand the function of this elusive domain, or how it functions in relation to the C-terminal domain. One of the major reasons that it has been difficult to decipher the function of the N-terminal domain is the lack of available mutant alleles. To address the function of the N-terminal domain, it would be helpful to have missense mutations in the N-terminal domain. However, there is only one published missense mutation in EIN2, *ein2-9*, located in the C-terminal domain. There are no published missense mutations in the N-terminal domain. Chapter 3 utilizes a novel missense mutant/mutation, in a

conserved Nramp motif in the N-terminal domain, in order to address the function of the N-terminal domain.

EIN2 is Regulated by F-box Proteins, ETP1/2

One reason why information regarding the function of EIN2 has slowly trickled in over the years is that EIN2 is notoriously difficult to work with. It is a very short lived protein. Although stabilized by ethylene perception (presumably via the ethylene receptors) it has a half-life of around 30 minutes (Qiao et al., 2009). In this same study, Qiao et al. (2009) found that EIN2 turnover was mediated by the 26S proteasome via two F-box proteins, ETP1/2 (EIN2 TARGETING PROTEIN1/2). These proteins were found to interact with a very highly conserved region at the very end the EIN2 C-terminal domain (last 250 residues). Ethylene caused the accumulation of EIN2 by hindering the interaction between EIN2 C-terminal domain and the ETPs.

Knowledge Gaps in the Ethylene Signaling Pathway

However, prior to 2012, there were huge gaps in our knowledge of the ethylene signaling pathway. It was unknown how the ethylene signal was passed from CTR1 to EIN2, at the ER membrane. As mentioned above, there were many attempts to place a MAPK cascade between CTR1 and EIN2 (Novikova et al., 2000; Quaked et al., 2003; Yoo et al., 2008). In addition, it was unknown how the ethylene signal was transduced from EIN2 (at the ER membrane) to the next known downstream component EIN3 (in the nucleus).

EIN2 contains a NLS (nuclear localization sequence) near the C-terminus, residues 1261-1268 out of 1294 (Bisson and Groth, 2011). Therefore, it is possible

that a portion of the C-terminal domain of EIN2 has a separate localization from the ER localized N-terminal domain (Bisson et al., 2009). In fact, it is possible that EIN2 could rely on the NLS to relay the ethylene signal to the next downstream component, transcription factor EIN3, within the nucleus. Chapter 2 focuses on filling in these gaps in our knowledge in the ethylene signaling pathway.

The EIN3 and EIL1 Transcription Factors

Two redundant plant specific transcription factors *EIN3* and *EIL1* (Binder et al., 2007; An et al., 2010) are positive regulators of ethylene signaling and were first cloned in 1997 (Chao et al., 1997). However, the *ein3* mutant was first identified a few years prior, in the same screen that identified the *ein2* mutant, as well as placed *EIN3* epistatically downstream of *CTR1* (Roman et al., 1995). The fact that EIN3 is a transcription factor suggested that *EIN3* acts downstream of *EIN2* (Guo and Ecker, 2003).

EIN3 levels were found to be highly responsive to ethylene in that EIN3 protein levels start accumulating 15 min after ethylene treatment and turned over within 30 minutes of ethylene removal (Guo and Ecker, 2003). In fact, overexpression of EIN3 results in a constitutive highly exaggerated triple response phenotype (similar to the U-shape phenotype seen with overexpression of EIN2- Appendix A; An et al., 2010), suggesting that over-expression of EIN3 leads to over activation of the ethylene response pathway.

Similar to EIN2, EIN3 protein levels are also regulated by protein turnover, mediated by the 26S proteasome, via two F-box proteins, EBF1/2 (EIN3 BINDING F-BOX PROTEINS 1/2). This was simultaneously discovered by three independent

laboratories (Guo and Ecker, 2003; Potuschak et al., 2003; Gagne et al., 2004). Protein turnover at the level of both EIN2 and EIN3 can help explain why ethylene responses can be so rapid.

Interestingly, it was very recently discovered that the EIN2 C-terminal domain interacts with the 3'UTR of EBF1/2 and that this interaction is necessary for translational repression of EBF mRNAs (Li et al., 2015; Merchante et al., 2015). Li et al. (2015) also discovered that in the presence of ethylene, the EIN2 C-terminal domain localized to the P-bodies together with EBF1/2-3'UTRs, where it interacts with P-body factors such as EIN5 (ETHYLENE INSENSITIVE 5), a 5' to 3' exoribonuclease, also known as XRN4 (EXORIBONUCLEASE 4). However, it is not clear whether the EIN2 C-terminal domain is first translocated to the nucleus and then exported to the P-bodies, or whether a subset of the EIN2 C-terminal domain localizes to the P-bodies instead of translocating to the nucleus.

The *ein5* mutant was originally identified in the same screen identifying both the *ein2* and *ein3* mutants (Roman et al., 1995) and was found to indirectly regulate EBF1/2 expression, which in turn, affected EIN3 protein levels (Potuschak et al., 2006; Olmedo et al., 2006). It is possible that this indirect regulation of EBF1/2 is via the interaction between EIN5 and EIN2 C-terminal domain, within the P-bodies. This could suggest EIN2 is a master regulator of the ethylene signaling pathway.

Downstream Nuclear Components in Ethylene Signaling

Ethylene signaling leads to a transcriptional cascade (Chang et al., 2013). Starting off this transcriptional cascade are the transcription factors EIN3 and EIL1. EIN3 functions as a homodimer, binding that binds to a conserved promoter elements

(PERE element) in ethylene target genes (EREBPs, ETHYLENE-RESPONSIVE ELEMENT-BINDING PROTEINS) such as ERF1 (ETHYLENE RESPONSIVE FACTOR 1), which is another transcription factor (Solano et al., 1998). ERF1 and some of the other target genes then bind to GCC elements in the promoters of secondary responsive genes, such as chitinase and PDF1.2, resulting in an ethylene response cascade. (Figure 1.2)

Cross-talk Between Ethylene and Other Plant Hormone Signaling Pathways

Of course ethylene signaling does not function alone, but functions in conjunction with other plant hormone signaling pathways to regulate proper plant growth and development. As a transcription factor, EIN3 provides a major point of cross-talk between the ethylene signaling pathway and other plant hormone signaling pathways. For example, EIN3 is induced in the presence of auxin, in particular with root elongation and gravitropism (He et al., 2012). In gibberellic acid signaling, the DELLA proteins (negative regulators of gibberellic acid signaling) function to repress EIN3, which in turn allow for repression of ethylene signaling (An et al., 2012). In this study, An et al. (2012) discovered that both ethylene and the gibberellins play a role in the apical hook formation of the triple response phenotype.

Cross-talk between ethylene signaling and other plant hormone signaling pathways can occur upstream of EIN3 as well. Cytokinin-induced root growth was found to require both ETR1 and EIN2 (Kushwah et al., 2011). Similarly, EIN2 also plays an important role in ABA regulated germination and root elongation (Wang et al., 2011). *ein2* mutants have been isolated from genetic screens for ABA, auxin, and

cytokinin (Su and Howell, 1992; Fujita and Syono, 1996; Ghassemian et al., 2000) suggesting a role for EIN2 in these hormone signaling pathways.

Ethylene and jasmonic acid work together to regulate root growth, abscission, and the timing and onset of senescence (Kim et al., 2015). Jasmonic acid is believed to inhibit ethylene signaling using an EIN2-independent pathway, which is only discernable when jasmonic acid levels are low (Kim et al., 2013). Whereas downstream of EIN2, JAZ1 (JASOMANTE-ZIM-domain protein 1, a jasmonic acid mediated transcriptional repressor) was also found to interact with and repress the activity of EIN3 and EIL1, inhibiting ethylene signaling (Zhu et al., 2011).

Nuclear Pore Complexes

Nuclear pore complexes (NPC) are highly dynamic structures involved in import and export of macromolecules through the nuclear pore. Other complexes tether to the nuclear pores, via NPC, to facilitate rapid shuttling of macromolecules between the nucleus and the cytoplasm. As a result, nuclear pores are involved in many diverse processes, such as mRNA processing and export, protein import and export, gene expression, and cytoskeleton organization (Meier and Brkljacic, 2010). For many years, the complex dynamic structure and large size (40 to 60 MDa) has been a major limitation to studying the structure of these NPC and the complexes that associate with them. However, recent advances in technology and techniques have made more advances possible.

Nuclear pores are thought to be utilized as a level of control over cellular processes, by "gating" certain genes to the pore to facilitate rapid transcription and export of mRNAs (Blobel, 1985). This allows the cell a level of control over such

processes such as transcription and translation, by controlling which mRNAs are produced, modified, and exported rapidly, as well as cell cycle, by controlling the rate and concentration of the proteins imported. Since movement in and out of nuclear pores affects many diverse processes in the cell, the mutant phenotypes of these NPC and large complexes that associate with the nuclear pores are just as diverse (Meier and Brkljacic, 2010). These mutants demonstrate a wide array of morphological and developmental defects, as well as altered responses to hormones and external stresses (Merkle, 2011).

Most of what is currently known about NPC has been discovered using yeast and mammalian systems. Unfortunately, in plants even less is known about NPC and the complexes that associate with them. Some of the complexes that associate with NPC are highly conserved between yeast, plants, and mammalian cells, however some are not.

The Arabidopsis TREX-2 mRNA Export Complex

The TREX-2 (TRANSCRIPTION EXPORT 2) complex is evolutionarily conserved among eukaryotes and has been shown to play a role in many processes, including transcription and mRNA export (Gallardo et al., 2003), gene gating (Cabal et al., 2006), genome stability (González-Aguilera et al., 2008) and DNA replication (Bermejo et al., 2011).

The *Arabidopsis* TREX-2 mRNA export complex is a nuclear pore complex that is only partially conserved, since not all the homologous yeast interactions have been observed in *Arabidopsis* (Lu et al., 2010). For example, in yeast, the SAC3 (SUPRESSOR OF ACTIN) protein component of this complex binds two SUS1

(SUCROSE SYNTHASE 1) proteins but in Arabidopsis, RTE3 (REVERSION TO ETHYLENE SENSITIVITY 3, also called SAC3B) was not able to bind to the AtSUS1 protein (Jani et al., 2009; Liu et al., 2010). In addition, yeast SAC3 binds to NUP1 (NUCLEAR PORE COMPLEX PROTEIN) allowing the TREX-2 complex to dock directly at the nuclear pore (Jani et al, 2009). However, in the Arabidopsis TREX-2 complex, EER5 (ENHANCED ETHYLENE RESPONSE 5, also known as THP1) is the mediator protein and forms a bridge between RTE3 and AtNUP1 since a direct protein interaction between RTE3 and AtNUP1 was not detected (Liu et al., 2010). This could suggest that the *Arabidopsis* TREX-2 complex may be composed of slightly different proteins (or interaction combinations) and behaving differently than the yeast homolog. Chapter 5 discusses RTE3, a member of the Arabidopsis TREX-2 complex, and how an EIN2 C-terminal domain protein export defect might be causing the ethylene related phenotype of the *rte3-1* mutant. There are no homologs of EIN2 C-terminal domain in any other homologous TREX-2 complexes, and the C-terminal domain of EIN2 is only found in plants (Alonso et al., 1999)

The COP9 Signalosome

The COP9 signalosome (CSN) is a highly conserved protein complex, conserved in eukaryotes (Wei and Deng, 2008; Mundt et al., 1999). It is very large complex (450-550 kDa) composed of eight subunits (CSN1-8) that show homology to the 26S proteasome lid (Wei and Deng, 2003; Glickman et al., 1998). Recently, a ninth subunit was discovered, CSNAP, but is does not seem to be well conserved in plants (only in the C-terminal CSN integration domain). However it is completely

absent in yeast, and only found in lower eukaryotes and chordates (Rozen et al., 2015).

Just like the 26S proteasome lid, six of the COP9 subunits (CSN1-4, 7 and 8) contain a PCI/PINT (Proteasome, COP9 signalosome, initiation factor 3/Proteasome subunits, Int-6, Nip-1, and TRIP-15) domain and two subunits (CSN5 and 6) contain an MPN (Mpr1-Pad1-N-terminal) domains (Hoffmann and Bucher, 1998; Cope et al. 2002). In fact, they were found to be so similar that it was predicted that the CSN complex could act as an alternative lid for the 26S proteasome (Schwechheimer and Deng, 2001; Serino and Deng, 2003), which suggests a common evolutionary ancestry between the 26S proteasome lid and the CSN complex (Glickman et al., 1998). The eIF3 complex (eukaryotic Initiation Factor 3) also shows homology, but is more distantly related since it is composed of three PCI domains and two MPN domains (Kim et al., 2001).

This COP9 complex was originally identified in Arabidopsis due to the constitutive photomorphogenic response shown in loss-of-function mutants, which look like light-grown seedlings when grown in the dark (Wei and Deng, 1992). These mutants are notoriously difficult to work with due to their seedling lethal phenotype. In fact, protein-protein interactions between subunits, as well as loss of any one of the eight subunits results in the same seedling lethal phenotype, indicate that the CSN functions as an interconnected regulatory unit (Wei and Deng, 2003). The COP9 signalosome has been shown to play an important function in many cellular processes, a few examples are; cell cycle progression, nuclear export, and the DNA damage repair pathway (Tomoda et al., 2001; Doronkin et al., 2002; Doronkin

et al., 2003; Liu et al., 2013; Füzesi-Levi et al., 2014). So, it is not surprising that the mutants are lethal and have pleiotropic effects.

It is possible that there are additional undiscovered functions of the COP9 signalosome. A smaller subset of the CSN subunits was detected, containing CSN4-8 located in the cytoplasm (Tomoda et al., 2002), whereas normally the COP9 complex is nuclear localized (Wei and Deng, 1998; Mundt et al., 1999). However the function of this smaller subset complex (termed "Mini-CSN") is not fully understood, but it is believe to help the CSN complex adapt to the many cellular functions (Sharon et al., 2009).

CSN5 has also been detected in both the CSN complex, but also in monomeric form (Kwok et al., 1998). Interestingly, in the *csn5* mutants, CSN5 only accumulates in the monomeric form (Kwok et al., 1998; Wang et al., 2002) suggesting this subunit can function independently, but also that its role in the COP9 complex is required. Recently, CSN3 was also found to have independent functioning, beyond the COP9 signalosome, in auxin signaling (Huang et al., 2013). Perhaps future studies will uncover other independent functions these subunits as well as independent functions of the other subunits as well.

Transition Metal Transport

Transition metals (such as Cu, Fe, Mn, Zn), are essential elements needed for proper growth and development of all cells since they are essential cofactors for many cellular processes. They are also are important due to their redox activity. For example, Cu is an essential cofactor for cytochrome c oxidase (Tsukihara et al., 1995) and Mn is an essential cofactor for Mn-SOD (SUPEROXIDE DISMUSTASE),

helping plants adapt to conditions of high oxidative stress (Alscher et al., 2002). However, since these heavy metals readily give up an electron, creating reactive oxygen species (ROS), they are easily toxic (Zitka et al., 2013).

Iron, copper, and cobalt are the most reactive of the essential transition metals, manganese to a lesser extent, while zinc and calcium are considered non-redox reactive. These non-redox reactive metals are more suitable for use in transcription factors and other enzymes involved in DNA metabolism. For example, if a redox reactive metal were used instead of a non-redox reactive metal, the ROS generated could lead to nucleic acid damage (Stohs and Bagchi, 1995; Zitka et al., 2013).

One of the many effects of metal toxicity is disruption of the electron transfer chain, in turn disrupting the production of ATP in the cell. A toxic level of any one of these metals could also suppress plant growth via interference with transport and function of other essential metals and overall metal homeostasis. Therefore, these transition metal concentrations in the cell need to be highly regulated. The cell regulates these metals using a variety of metal ion transporters. One family of highly conserved metal transporters are the Nramp proteins. (Zitka et al., 2013)

Nramp Metal Ion Transporters

Nramp proteins (Natural resistance-associated macrophage protein) are a family of highly conserved divalent metal ion transporters, found in all species from bacteria to humans. Much of what is known regarding Nramp proteins and their function, has been discovered studying *E. coli* and *S. cerevisiae*. Work with other systems, such as mouse Nramp1 and 2 or human Nramp2 (also known as DMT1 - DIVALENT METAL TRANSPORTER 1 or DCT1 - DIVALENT CATION

TRANSPORTER 1), have helped to further support the functional yeast and bacterial studies as well as highlight differences between species and suggest additional roles for Nramp proteins. For example, DMT1 was shown to transport Cu^{+} in intestinal cells, whereas normally Nramp proteins are known to transport divalent metals (or Cu^{2+}) (Arredondo et al., 2003). Additionally, using other systems, polymorphisms in these Nramp genes were found to play a role in disease susceptibility, such as anemia, tuberculosis, Crohn's disease, and leprosy (Abel et al., 1998; Fleming et al., 1997; Hsu et al. 2006; Gazouli et al., 2008).

In general, these Nramp metal transporters are integral membrane proteins, which usually consist of a core of ten hydrophobic transmembrane domains, plus one or two additional hydrophobic less conserved domains. The first transmembrane domain is usually involved in metal ion binding and proton coupling, whereas the 4^{th} and 6^{th} transmembrane domains are usually involved in formation of the selective channel (Nevo and Nelson, 2006). However, they do localize to different cellular membranes. In general, Nramp proteins are broad range metal transporters, but their metal specificities differ slightly.

The *E. coli* Nramp Homolog, MntH

EIN2 shows homology to the *E.coli* Nramp homolog, MntH A (Manganese transport system of *E. coli*, H^{+} -dependent), a broad range divalent metal transporter with a preference for Mn^{2+} and Fe^{2+} (Makui et al., 2000). Studies suggest that MntH functions as a pH dependent protein symporter found at the cell inner membrane (Makui et al, 2000; Courville et al., 2004). There are other MntH homologs, but these other MntH proteins (B and C) but they are found are in other types of bacteria or

other organisms. For example, MntH B is present in anaerobic bacteria, whereas MntH C is found in unicellular eukaryotic organisms, such as amoebae, fungi, and algae (Richer et al., 2004).

Site-directed mutagenic studies have revealed the function of critical residues and highly conserved Nramp motifs within MntH. For example, using this technique, it was discovered that the DPGN motif (residues 34-37 of MntH), highly conserved among all Nramp proteins and found within the first transmembrane domain of MntH, is important for metal transport. Altering any of the residues within this DPGN motif hindered transport ability of MntH (Courville et al., 2004; Haemig and Brooker, 2004; Chaloupka et al., 2005). Other conserved residues in transmembrane domain three (Asp109 and Glu112) are believed to play a role in metal binding along with the DPGN motif (Haemig and Brooker, 2004).

There are also other highly conserved residues, which were found to be important for the metal transport ability of MntH and other Nramps, using this same technique. Critical residues in both transmembrane domains 4 and 6 (such as the MPH motif in transmembrane domain six) were also found to be important for metal uptake and transport (Haemig et al., 2010; Fleming et al., 1997). In mouse NRAMP2, the His 267 and His 272 residues (within transmembrane domain six) were found to have an important role in pH regulation (Lam-Yuk-Tseung et al., 2003).

Nramp Homologs in Yeast

Although *E. coli* studies have provided much information regarding Nramp function, studies using yeast had provided the initial hints at Nramp protein functions (Cellier and Gros, 2004). The yeast *Saccharomyces cerevisiae* contains three Nramp

homologs, SMF1, 2 and 3. SMF1 (SUPRESSOR OF MIF1) is mainly a Mn^{2+} and Fe^{2+} transporter. Under low Mn^{2+}conditions, expression of SMF1 is induced and SMF1 localizes to the plasma membrane, in order to facilitate Mn^{2+} uptake into the cell (Supek et al., 1996; Portnoy et al., 2000). However, when Mn^{2+} levels are high, SMF1 is translocated to internal membranes or the vacuole for degradation (Portnoy et al., 2000). Expression of SMF1 was also found to be downregulated under toxic Mn^{2+} conditions (Jensen et al., 2009) further supporting a role of SMF1 in manganese homeostasis.

In addition to Mn^{2+}, SMF1 has also been shown to transport Zn^{2+} and Cu^{2+}, Fe^{2+}, Cd^{2+}, Ni^{2+}, and Co^{2+} suggesting that SMF1 (like MntH) is a broad range divalent metal transporter (Sacher et al., 2001; Supek et al., 1996; Supek et al., 1997; Liu et al., 1997; Chen et al., 1999). Expression studies using *Xenopus* oocytes suggest that SMF1 is (like MntH) an H^{+}-dependent divalent metal ion transporter (Chen et al., 1999).

SMF2 was found to localize to intracellular vesicles and is believed to transport Mn^{2+} towards the cytoplasm (Luk and Culotta, 2001). Similar to other Nramp proteins, SMF2 is a broad range divalent metal ion transporter and has been shown to play a role in transport of Mn^{2+}, Fe^{2+}, Co^{2+}, Cu^{2+} (Portnoy et al., 2000; Liu et al, 1997; Cohen et al., 2000). However, unlike SMF1, it was shown to be required for Mn^{2+} homeostasis and although they both are Mn^{2+} transporters they do not have redundant functions (Luk and Culotta, 2001; Liu et al., 1997). SMF2 functions to provide Mn^{2+} to targets, such as SOD2 (SUPEROXIDE DISMUTASE 2) in the mitochondria (Luk and Culotta, 2001). Another potential target is PMR1 (PLASMA

MEMBRANE ATP-ASE RELATED 1), which provides the required Mn^{2+} and Ca^{2+} co-factors to sugar transferases in the Golgi (Rudolph et al., 1989; Luk and Culotta, 2001), whereas SMF1 functions to bring Mn^{2+} into the cell (Supek et al., 1996).

Both SMF1 and SMF2 proteins are regulated by an ER membrane protein BSD2 (BYPASS SOD1 DEFECTS 2). Under conditions of excess Mn^{2+}, BSD2 facilitates the translocation of SMF1 and SMF2 to the vacuole for degradation (Portnoy et al., 2000; Liu et al, 1997). SMF3, on the other hand, is the least similar of the three yeast Nramps. SMF3 localizes to the vacuolar membrane and is regulated by Fe^{2+}, not Mn^{2+}, nor is it regulated by BSD2 (Portnoy et al., 2000; 2002).

Nramp Proteins in Arabidopsis

Arabidopsis contains six Nramp proteins (AtNramp 1-6), plus EIN2. The N-terminal domain of EIN2 is homologous to Nramp metal ion transporters. The N-terminal domain of EIN2 shows less than 20% identity with other Nramps. Other Nramp proteins lack the long C-terminal domain that EIN2 contains. Yet, to my knowledge, no published studies have shown any transport ability for EIN2.

Functional redundancy has been suggested, since Arabidopsis contains six Nramp transporters, however they have different metal specificity and localize to different membranes. For example, AtNramp1 is a plasma membrane localized transporter of Fe^{2+}, Mn^{2+} and Cd^{2+}, whereas AtNramp2 may not play an important role in Fe^{2+} transport (Curie et al., 2000; Lanquar et al., 2000; Thomine et al., 2000; Cailliatte et al., 2010). However, the role of AtNramp1 in Fe^{2+} transport has been controversial (Curie et al., 2000, Thomine et al, 2000, Cailliatte et al, 2009). AtNramp3 and AtNramp4 localize to the vacuole and has been shown to play a role

in the transport of Fe^{2+}, Mn^{2+}, and Cd^{2+}, but only AtNramp4 plays a role in Zn^{2+} transport (Thomine et al., 2000; Lanquar et al., 2010; Lanquar et al.,2005; Lanquar et al., 2004). Only Nramp1, 3 and 4 have been definitively localized in planta.

Hints of Metal Transport by EIN2

Since the N-terminal domain of EIN2 shows homology to Nramp metal ion transporters, whether EIN2 is capable of metal transport has been a question plaguing the ethylene field for almost two decades. To my knowledge, no studies have been successful in demonstrating transport ability of EIN2 (Alonso et al., 1999; Thomine et al., 2000; Thomine and Schroeder, unpublished). However, there have been hints that EIN2 may function like an Nramp metal transporter. For example, the *ein2-1* mutant showed an enhance sensitivity to lead, suggesting a role for *EIN2* in lead resistance (Cao et al., 2009), however, transport of lead was not tested. This is similar to other Nramp mutants, such as *nramp1*, which is hypersensitive to Mn^{2+} deficiency (Cailliatte et al., 2010), or *nramp3 and nramp4*, again more sensitive to Mn^{2+} as well as Fe^{2+} deficiency (Lanquar et al., 2005; Lanquar et al., 2010).

Another example is with bacterial susceptibility. Mutants in Arabidopsis *nramp3*, and *nramp4* were shown to be more susceptible to *Erwinia chrysanthemi* infection (Segond et al., 2009). Similarly, *EIN2* was found to be involved in resistance to *Botrytis cinerea* (Thomma et al., 1999; Ferrari et al., 2003) and *Pythium irregular* (Adie et al., 2007) infections. Taken together these could suggest that *EIN2* could have some conserved Nramp functions. Chapter 4 provides data to suggest EIN2 may indeed function as a metal transporter, further supporting its functioning as an Nramp protein.

Materials and Methods

Triple Response Assay – Seeds for both *Arabidopsis thaliana* ecotype Columbia (Col-0, used as the wild-type) and the *ein2-5* mutant were plated onto Murashige and Skoog (MS) media (Caisson Labs) containing 0.8% agar. For ethylene response, 20 μM ACC (Sigma Aldrich) was added to the plates. Plates were cold stratified at 4 C, in the dark, for 4 days prior to the 20 C dark treatment for 4 days. Seedlings were photographed and hypocotyls were measured using the ImageJ software (https://imagej.nih.gov/ij/).

Chapter 2: EIN2 is in an ER Ethylene Signaling Complex and Bridges the Signaling Gap Between the ER and the Nucleus

Introduction

Gaps in the Ethylene Signaling Pathway

Although there is still much to be discovered regarding the ethylene signaling pathway, prior to 2012, there were two major gaps in our understanding of how the ethylene signal was relayed. Epistasis analysis placed CTR1 upstream of *EIN2* and *EIN3* (Roman et al., 1995) and further studies placed *EIN3* downstream of EIN2 (Guo and Ecker, 2003). However, it was unknown how the ethylene signal is biochemically relayed from CTR1 to EIN2 and then from EIN2 (at the ER membrane) to EIN3 (in the nucleus). In 2012, three independent laboratories helped fill in those gaps (Ju et al., 2012; Qiao et al., 2012; Wen et al., 2012). This chapter discusses my contributions to the Ju et al., (2012) study.

CTR1 – a Negative Regulator of the Ethylene Signaling Pathway

Directly interacting with the ethylene receptors (ETR1, ETR2, ERS1, ERS2, EIN4) is the next downstream component, CTR1 (CONSTITUTIVE TRIPLE RESPONSE 1) a serine/threonine protein kinase (Roman et al., 1995; Clark et al., 1998; Cancel and Larsen, 2003, Gao et al., 2003). CTR1 is a negative regulator of ethylene signaling and inactive when ethylene is bound by the receptors (Kieber et al., 1993). Although the CTR1 interaction with the ethylene receptors is required for CTR1 kinase activity (Clark et al., 1998; Cancel and Larsen, 2002; Gao et al., 2003; Huang et al., 2003) this activation does not seem to involve ETR1 histidine kinase activity (Gao et al., 2003).

Since CTR1 was thought to be a Raf-like kinase (a MAPKKK) there were many attempts to place a MAPK cascade in the ethylene signaling pathway. There were a few MAPK cascades proposed (Novikova et al., 2000; Quaked et al., 2003; Yoo et al., 2008) however, no CTR1-containing MAPK pathway has yet been identified. The substrate of the CTR1 kinase was not discovered until the Ju et al. (2012) study, EIN2.

EIN2 C-terminal Domain is Phosphorylated in the Absence of Ethylene

Previous genetic techniques were unsuccessful in identifying new components in the ethylene signaling pathway. This prompted the Chang lab and collaborators to use a different approach identifying phosphorylated proteins in ethylene signaling (Chen et al. 2011). They looked for differences in protein phosphorylation in the microsomal protein fraction, in response to ethylene treatment of 4-day old etiolated Arabidopsis seedlings using mass spectrometry. As a result, it was uncovered that EIN2 is phosphorylated in the absence of ethylene (Chen et al., 2011).

They were next curious as to what protein(s) could be phosphorylating EIN2 at these specific residues, Ser645 and Ser924, which were the most highly conserved among higher plants (Chen et al., 2011). Since CTR1, a kinase, was the next identified upstream component, they speculated that perhaps CTR1 could be phosphorylating the EIN2 C-terminal domain in the absence of ethylene. My contributions to the subsequent discoveries in the Ju et al. (2012) study are described in this chapter.

EIN2 C-terminal Domain Contains an NLS Sequence

EIN2 contains an NLS (nuclear localization sequence) close to the C-terminus, consisting of residues 1261-1268 of 1294 (Bisson and Groth, 2011), raising the question of where the EIN2 protein is localized, since the EIN2 N-terminal domain was localized to the ER membrane (Bisson et al., 2009). In fact, it is possible that EIN2 could relay the ethylene signal to the next downstream component, transcription factor EIN3, in the nucleus. Could EIN2 be the master regulator protein bridging the ethylene signaling gap between the ER membrane and the nucleus?

Results

EIN2 Interacts with ETR1, With and Without Ethylene

Previously, it was discovered that the C-terminal domain of EIN2 can interact with ETR1 (Figure 2.1a; Bisson et al., 2009), placing EIN2 at the ER and potentially in the same protein complex with CTR1, since it has been shown that the receptors can also interact with CTR1 (Clark et al., 1998, Gao et al., 2003). ETR1 and other ethylene receptors interact with the EIN2 C-terminal domain in the presence of ethylene (Bisson et al (2009; Bisson and Groth, 2010). However, this model is somewhat contradictory as to how EIN2 is believed to function since the receptors would be signaling inactive in the presence of ethylene. In the absence of ethylene, when they are active, they should be actively repressing EIN2 function.

However, when I repeated the protein interaction using both full-length EIN2 and ETR1, I found the ETR1-EIN2 interaction occurred in both the presence and absence of ethylene (Figure 2.1), when expressed in onion epidermal cells. This suggests the EIN2-receptor interaction (or at least with ETR1) may be necessary for

EIN2 function. This indicates that EIN2 is in an ethylene signaling protein complex, at the ER, with ETR1 and other receptors.

CTR1 Interacts with EIN2 C-terminal Domain

The Chen et al. (2011) study indicated that EIN2 is phosphorylated in the absence of ethylene. However, there was still a gap in the ethylene signaling pathway between CTR1 (a kinase) and EIN2, both localized at the ER membrane (CTR1 localization REF, Bisson et al., 2009). As a means to bridge that gap, I decided to test whether EIN2 and CTR1 could physically interact. Using the yeast 2-hybrid assay, I found that the kinase domain (C-terminus) of CTR1 can interact with the C-terminal domain of EIN2 (Figure 2.2), and further tested this interaction *in planta* using BiFC (Figure 2.3) suggesting that EIN2, ETR1 and CTR1 are in one large ethylene signaling protein complex at the ER membrane.

Next, I was curious as to whether the CTR1 kinase domain is necessary for EIN2 regulation. We know that CTR1 and EIN2 physically interact (Figures 2.2 and 2.3) and that EIN2 is phosphorylated in the absence of ethylene (Chen et al., 2011). Is CTR1 the kinase responsible for this phosphorylation? To test this, I attempted to disrupt the EIN2-CTR1 yeast-2 hybrid interaction by introducing a D694E substitution into the CTR1 kinase domain construct (termed CTR1-1) to mimic the *ctr1-1* mutant allele (Kieber et al., 1993). This mutation, which rendered CTR1 catalytically inactive (Huang et al., 2003) also disrupted the interaction with the EIN2 C-terminal domain (Figure 2.2). This suggests the kinase domain of CTR1 is important for the EIN2 C-terminal domain -CTR1 kinase domain interaction, or perhaps that the D694E substitution could be causing the kinase domain of CTR1 to

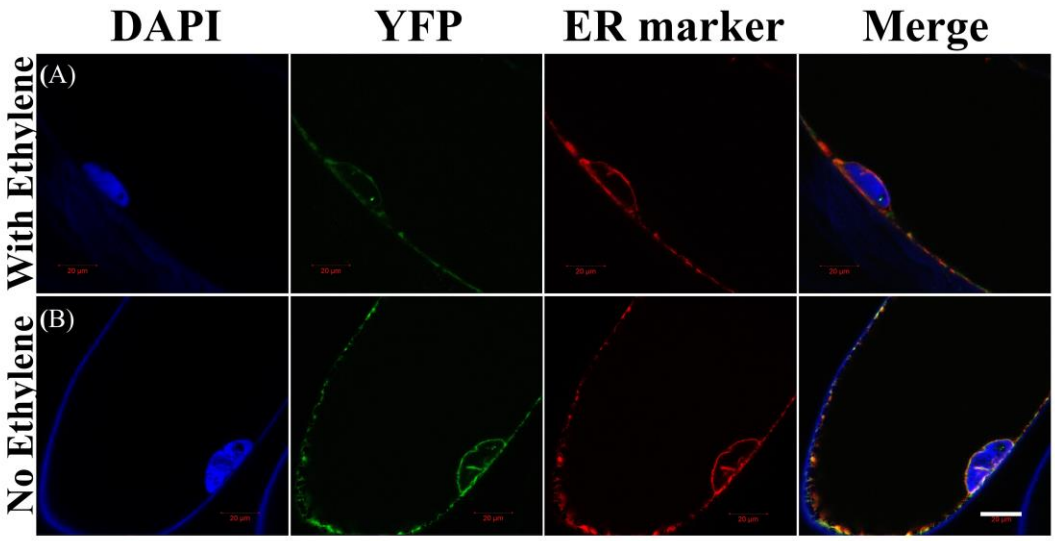

Figure 2.1. EIN2 interacts with ETR1 at the ER in onion epidermal cells. BiFC interaction of full length Arabidopsis EIN2 and full length Arabidopsis ETR1, transiently expressed using particle bombardment in onion epidermal cells either (A) treated with or (B) without 100 ppm ethylene for 3 hours before visualization with Zeiss LSM confocal microscope. Onions were transformed using particle bombardment. Merged image shows DAPI (20 µg/mL), ER marker (HDEL::mCherry), and YFP (BiFC signal). Scale bar represents 20 µm.

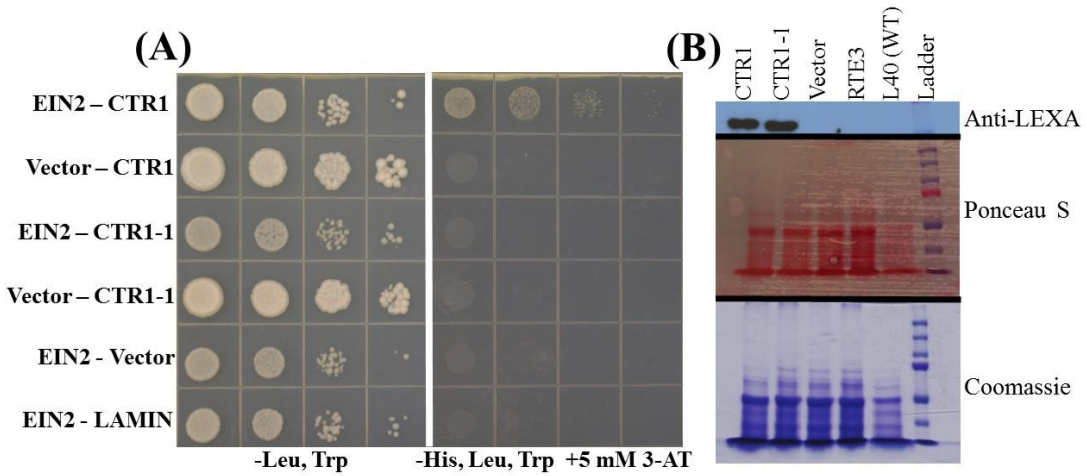

Figure 2.2. EIN2 C-terminal domain interacts with CTR1 kinase domain, in yeast. Using the yeast 2-hybrid assay (A) EIN2 C-terminal domain (residues 516-1294) was found to interact with the CTR1 kinase domain (residues 551-821). Whereas CTR1-1 (containing the D694E substitution) did not interact. Both pLEXA (bait plasmid) and pACTII (prey plasmid) were used as an empty vector negative controls, as was the human lamin protein (LAMIN). (B) Both CTRI and CTR1-1 were expressed to similar levels in yeast. Yeast cultures were grown containing both CTR1 and EIN2 and expression of CTR1 was visualized by Western Blot, using an anti-LEXA antibody (Abcam). Band is approximately 60 kDa. The empty vector and untransformed WT (L40) yeast were used as a negative controls. RTE3 was intended as a positive control, but did not work. Ponceau S staining of the blot and a Coomassie Stained Gel were used as a loading controls.

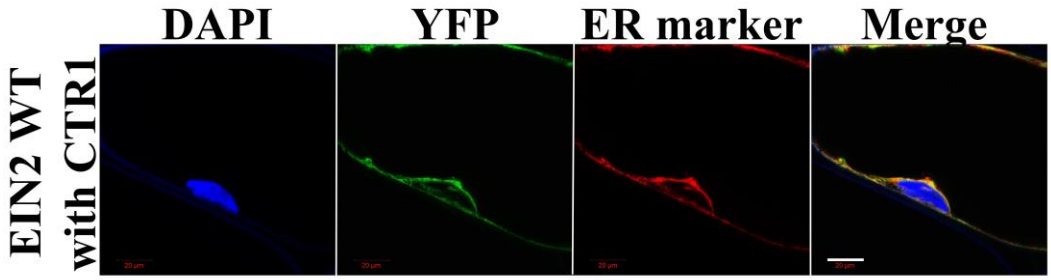

Figure 2.3. EIN2 interacts with CTR1 at the ER, *in planta*. BiFC interaction of full-length EIN2 and full-length CTR1, transiently expressed using particle bombardment in onion epidermal cells. Merged image shows DAPI (20 µg/mL), ER marker (HDEL::mCherry), and YFP (BiFC signal), visualized using confocal microscopy. Scale bar represents 20 µm.

misfold rendering it nonfunctional.

Since CTR1 and EIN2 C-terminal domain can physically interact (Figures 2.2 and 2.3) it is possible that the phosphorylation seen on specific residues of the EIN2 C-terminal domain in the Chen et al. (2011) is from the kinase CTR1. Dr. Gyeong Mee Yoon and Dr. Joseph Kieber tested whether CTR1 can directly phosphorylate those specific residues of EIN2 and found using an *in vitro* kinase assay that CTR1 was the kinase responsible for the phosphorylation of EIN2 at Ser645 and Ser924 in the absence of ethylene (Ju et al., 2012). This also indicates that a MAPK cascade is not required to relay the ethylene signal from CTR1 to EIN2.

To test the effect of phosphorylation on EIN2, Dr. Chuanli Ju created transgenic lines expressing EIN2 where alanine substitutions were introduced at two of the most highly phosphorylated residues *in vitro*, Ser645 and Ser924. These two residues are also highly conserved among land plant EIN2 homologs (Ju et al., 2012). When both of these sites, or just Ser924, were changed to an alanine, blocking phosphorylation at these sites, Ju et al. observed a constitutive ethylene response when using the native *EIN2* promoter. Ser645Ala conferred only a slight constitutive response. These results suggest that phosphorylation of EIN2 at Ser645 and Ser924 by CTR1 are involved in EIN2 repression of ethylene signaling and that Ser924 plays a more prominent role in this repression. (Ju et al., 2012).

Upon Ethylene Treatment, the EIN2 C-terminal Domain Translocates to the Nucleus

The next major gap in our understanding of ethylene signaling transduction was how is the ethylene signal relayed from EIN2 at the ER to EIN3 in the nucleus?

In addition, how does this lack of phosphorylation by CTR1 result in a constitutive ethylene response?

Interestingly, the EIN2 C-terminus contains a nuclear localization signal (residues 1261-1268; Bisson and Groth, 2011), which raised the possibility that EIN2 itself could bridge the signaling gap between the ER and the nucleus, if the soluble C-terminal domain was cleaved from the ER localized N-terminal domain. To test this possibility, I created two different constructs; the first of which would express an N-terminally tagged full length EIN2 protein and the second a C-terminally tagged full length EIN2 protein, when expressed in onion epidermal cells. This way, I would be able to observe what happens to both halves of the protein, both with and without ethylene treatment. In air, or without added ethylene, both the N-terminally tagged and C-terminally tagged EIN2 proteins localized to the ER (Figure 2.4a and 2.4c). However, with ethylene the N-terminus remained at the ER membrane (Figure 2.4b) while the C-terminus localized to the nucleus as well as the ER (Figure 2.4d). This suggests that in the presence of ethylene, a portion of the C-terminal domain of EIN2 is cleaved and translocates to the nucleus.

This is significant because bridges the ethylene signaling gap between the ER membrane and the nucleus. In addition, this discovery allowed us to better understand the defect with the alanine substitution mutants, since the constitutive response phenotypes observed were due to a constitutive nuclear localization of EIN2 C-terminal domain. Dr. Chuanli Ju saw a constitutive nuclear localization of C-terminally tagged EIN2 in the *ctr1-1* (kinase defective) mutant, further supporting phosphorylation by CTR1 is required for repression of ethylene signaling by EIN2.

(Ju et al., 2012). However, the fate of the EIN2 C-terminal domain inside the nucleus is still unknown

Discussion

Bridging the Gaps in the Ethylene Signaling Pathway

Many of the components in the ethylene signaling pathway had been discovered since the 1990s, and genetic epistasis as well as functional studies have allowed for construction of most of the signaling pathway (Bakshi et al., 2015). However, there were still gaps in our knowledge, such as how is the ethylene signal relayed from CTR1 to EIN2, both at the ER, and then transduced from EIN2 to the next known downstream component (EIN3) in the nucleus? Since CTR1 can phosphorylate EIN2 directly, this fills the gap between CTR1 and EIN2, suggesting that there does not need to be a MAPK cascade between CTR1 and EIN2. However this does not rule out the possibility of an EIN2 bypass involving a MAPK cascade.

Another large unknown gap in the signaling pathway was between the ER membrane and the nucleus, from EIN2 to the next downstream component, the transcription factor EIN3. Our data suggests that in the presence of ethylene, the C-terminal domain of EIN2 is cleaved and translocates into the nucleus, while the N-terminal domain remains at the ER (Figure 2.4). Simultaneously, two independent labs had similar stories regarding the nuclear localization of EIN2 in the presence of ethylene (Qiao et al., 2012; Wen et al., 2012). These findings are significant because this makes EIN2 the central regulatory protein in the ethylene signaling pathway, bridging the gap between the ER and the nucleus.

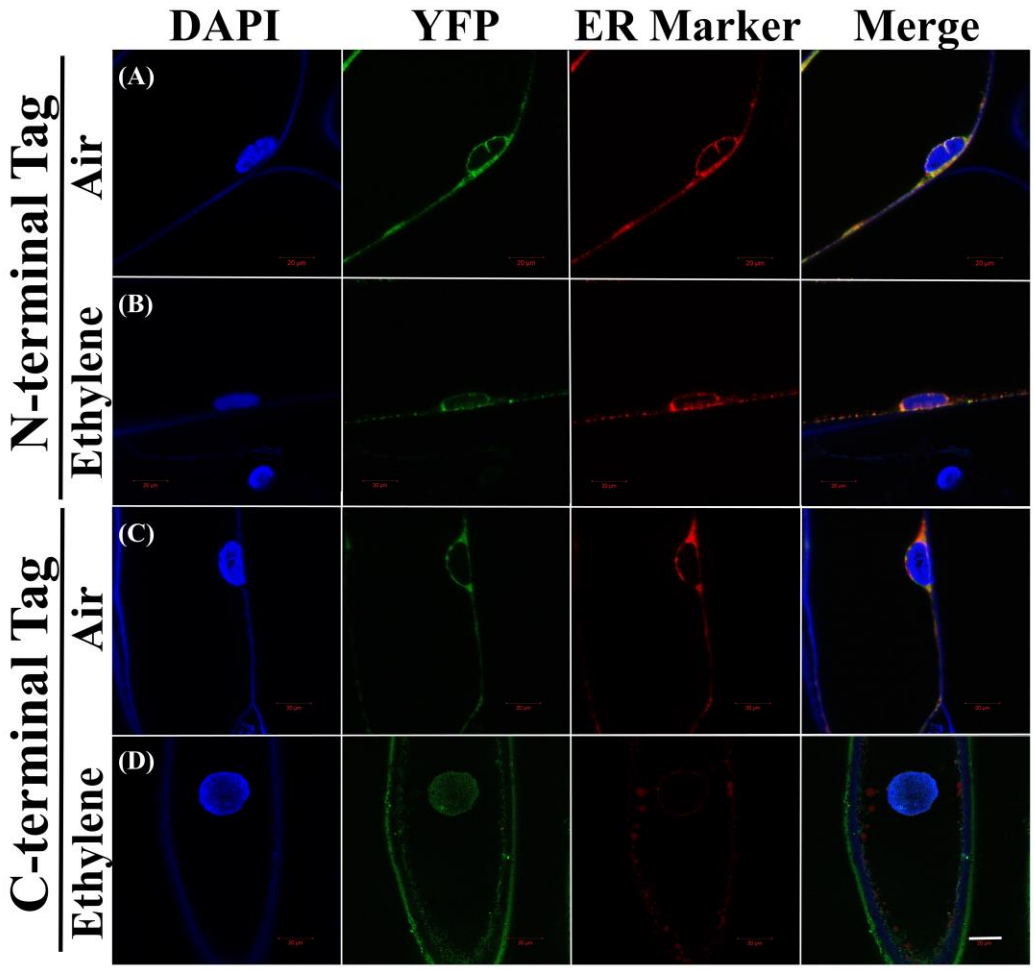

Figure 2.4. Ethylene causes nuclear localization of the EIN2 C-terminal domain. When tagged at the N-terminus, full length wild-type Arabidopsis EIN2 localized to the ER membrane in onion epidermal cells transiently expressed using particle bombardment. EIN2 was expressed either (A) without or (B) with 100 ppm ethylene treatment for 3 hours. When tagged at the C-terminus, the untreated (C) onion cells also demonstrated ER localization of EIN2. With ethylene treatment, C-terminally tagged full-length EIN2 localized to both ER membrane and the nucleus (D). Merged image shows DAPI (20 µg/mL), ER marker (HDEL::mCherry), and YFP (BiFC signal), visualized using confocal microscopy. Scale bar represents 20 µm.

The data in Ju et al. (2012) culminated in a model where, in the absence of ethylene, active CTR1 phosphorylates the C-terminal domain of EIN2 at specific residues. In the presence of ethylene, CTR1 is inactive, so therefore does not phosphorylate EIN2, and EIN2 is then cleaved and the C-terminal domain is translocated to the nucleus where it activates downstream responses (Figure 2.5). The constitutive responses seen in the EIN2 S924A single mutant and EIN2 S645A S924A double mutant can be explained by unphosphorylated EIN2 resulting in the accumulation of nuclear localized C-terminal EIN2. Another possibility is that the constitutive response phenotype seen was a result of a subset of EIN2 C-terminal domain being translocated to the P-bodies (Liu et al., 2015)

EIN2 Interacts with ETR1 in the Absence of Ethylene Too

Data suggests EIN2 interacts with ETR1 both in the absence and presence of ethylene (Figure 2.1). However, this is contradictory to the Bisson et al (2009) study, which stated that EIN2 C-terminal domain interacts with ETR1 and other receptors (Bisson and Groth, 2010) only in the presence of ethylene. I believe that both our results are valid. The Bisson et al., 2009 study definitely had a better technique to test the protein interactions, they used FRET whereas I used BiFC. One possibility for the discrepancy is the piece of the EIN2 fragment used. I used full-length EIN2 compared to just the C-terminal portion used in the Bisson et al. (2009) study. This could affect protein expression of that fragment and availability of the receptor binding site, if there is a confirmational change in the EIN2 protein. Perhaps the EIN2 C-terminal domain piece is folded in such a way that the receptor binding site is unavailable in the absence of ethylene, in the fragment that was used in the Bisson et

al. (2009; Bisson and Groth, 2010) studies. Another possibility is that ETR1 is interacting with the N-terminal domain of EIN2. Regardless, both studies place EIN2 at the ER with ETR1, and indirectly with CTR1, forming a large ethylene signaling complex at the ER. This work suggests all three proteins interact with each other (Figures 2.1-2.3).

EIN2 Functionally Requires Interaction With the CTR1 Kinase Domain

The CTR1 interaction with the EIN2 C-terminal domain allowed us to discover CTR1 can directly phosphorylate EIN2 at particular residues, and it is the lack of phosphorylation by CTR1 that causes the nuclear translocation of the EIN2 C-terminal domain (Ju et al., 2012). The importance of the functional role of the CTR1 kinase on the nuclear localization of EIN2 was confirmed by transforming full-length wild-type *EIN2* into the *ctr1-1* mutant, which showed constitutive nuclear localization of EIN2 (Ju et al., 2012). This suggests that CTR1 kinase represses nuclear localization of EIN2, thereby repressing downstream ethylene responses.

During this study, we discovered that too much overexpression of EIN2 driven by the strong CaMV 35S promoter could result in 4-day old etiolated seedlings showing an extreme triple response phenotype that we refer to as a U-shaped phenotype (See Appendix A). This U-shape is very similar to what is seen with overexpression of EIN3 (An et al., 2010) suggesting that the ethylene pathway is over activated. This could be a result of too much EIN2 and not enough CTR1 to regulate it properly, causing an excess of EIN2 C-terminal domain translocating to the nucleus activating downstream ethylene responses. The use of the 35S promoter with *EIN2* is

the topic of quite a bit of controversy, as is which residue of EIN2 is the most critical phosphorylation residue regulating cleavage (Cooper, 2013; Qiao et al., 2013).

Phosphorylation of EIN2 could also be a signal to target EIN2 for degradation since there is evidence that EIN2 is targeted for degradation by the 26S proteasome by two F-box proteins ETP1/2 (Qiao et al., 2009). Lack of phosphorylation inhibits degradation leading to cleavage and nuclear localization of the EIN2 C-terminal domain and activation of downstream responses (Figure 2.5).

However the EIN2-CTR1 interaction (Figure 2.2 and 2.3) as well as the EIN2-ethylene receptor interaction (Bisson and Groth, 2010) could also help to keep the components in proximity to each other and help to tether EIN2 at the ER. Perhaps EIN2 and ETR1 or EIN2 and CTR1 do not interact at the same time with each other, as Bisson et al. (2009) suggested. However, between the EIN2-CTR1 interaction and the EIN2-ethylene receptor interaction, at some time the EIN2 protein is in an ethylene regulatory complex, tethered to the ER. Upon ethylene treatment only the C-terminal domain is translocated to the nucleus. What happens to the remaining N-terminal domain of EIN2? How does this other half of the protein relate to ethylene signaling?

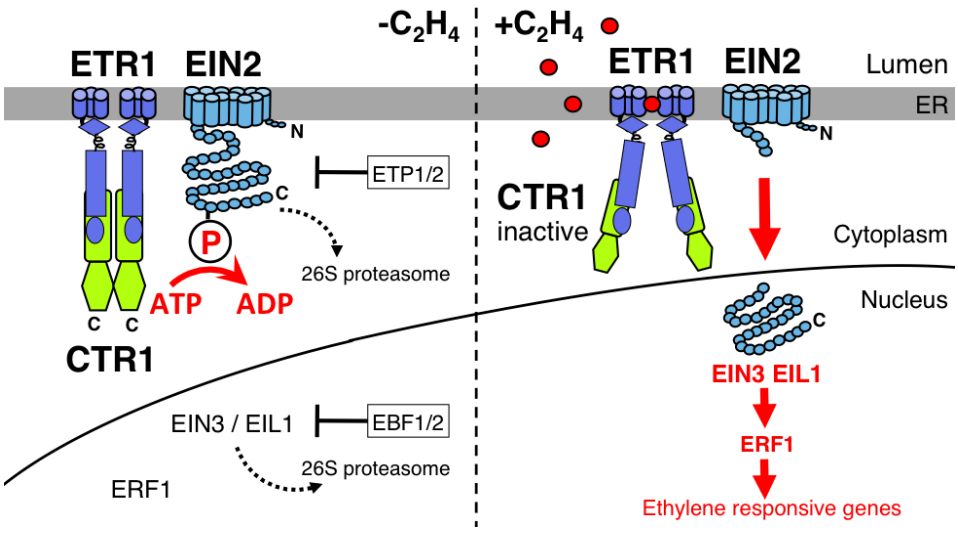

Figure 2.5. Model of the ethylene signaling pathway. In the absence of ethylene (left panel), both ETR1 and CTR1 (both active) interact with EIN2, resulting in phosphorylation of the EIN2 C-terminal domain (by CTR1). This phosphorylation acts as a signal to prevent nuclear localization of EIN2 C-terminal domain. In the presence of ethylene (right panel), EIN2 is no longer phosphorylated by CTR1 (inactive), somehow leading to nuclear translocation of EIN2 C-terminal domain and activation of downstream ethylene responses. Image taken from Ju et al., 2012.

Materials and Methods

Bimolecular Fluorescence Complementation (BiFC) in Onion Epidermal Cells – The full-length coding sequence for *EIN2* was transferred from pDONR221 into the pSPYCE-35S vector (Schütze et al., 2009). The EIN2 full-length (with no stop codon) construct was created by PCR-amplifying the *EIN2* coding sequence from pEIN2 (Arabidopsis Biological Resource Center, ABRC) using same primers listed in the table below (EIN2 pDONR221 no stop) and cloned into the pDONR221 vector. Dr. Mandy Bish created both of the *CTR1* pDONR221 and *ETR1* pDONR221 constructs. The full length ETR1 and CTR1 pSPYNE constructs were created by Dr. Chunhai Dong (with help from Andrew Scaggs) and David Lin, respectively. Both constructs were created by transferring the full-length coding sequence of ETR1 or CTR1 from pDONR221 to the pSPYNE 35S vector (Schütze et al., 2009). Onion epidermal cells were transformed via particle bombardment (BioRad Helios Gene Gun) using white onions purchased from the grocery store, as described in Hollender and Liu (2010). Bullets were prepared for the above construct together with an ER-marker (ER-rB, RFP-HDEL, Nelson et al., 2007) obtained from the ABRC. After room temperature incubation in the dark for 16 hrs, onion epidermal pieces were incubated in 20 μg/mL DAPI for 15 min before interactions were visualized using a LSM 710 confocal microscope. For ethylene treatment, onion pieces were placed in jars filled with 100 ppm ethylene gas for 3 hrs prior to DAPI treatment, and slides remained in ethylene during 15 min incubation with DAPI.

Subcellular Localization of EIN2 in Onion Epidermal Cells- The full-length *EIN2* coding sequence was PCR amplified from pEIN2 (ABRC), with and without the stop

codon, using the primers listed below and cloned into the pDONR221 vector. To create the 35S-*EIN2*-*GFP* construct, the full-length coding sequence (with no stop codon) was transferred from the pDONR221 vector to the pEarleyGate103 vector (Earley et al., 2006, obtained from ABRC). Full-length EIN2 coding sequence (with the stop codon) was transferred from the pDONR221 vector to the pEarleyGate104 vector (Earley et al., 2006, obtained from ABRC). Constructs were transformed into white onions, purchased from the grocery store, using particle bombardment with a Helios Gene Gun (Bio-Rad) as described in Hollender and Liu (2010). Bullets were prepared for the above constructs together with an ER-marker (ER-rB, RFP-HDEL, Nelson et al., 2007) obtained from the ABRC. After room temperature incubation in the dark for 16 hrs, onion epidermal pieces were incubated in 20 μg/mL DAPI for 15 min before interactions were visualized using a LSM 710 confocal microscope. For ethylene treatment, onion pieces were placed in jars filled with 100 ppm ethylene gas for 3 hrs prior to DAPI treatment, and slides remained in ethylene during 15 min incubation with DAPI.

Construct	Forward or Reverse	Primer Sequence (5'-3')
EIN2 pDONR221 no stop	F	GGGGACAAGTTTGTACAAAAAAGCAGGCTATATGGAAGCTGAAATTGTGAATGTG
	R	GGGGACCACTTTGTACAAGAAAGCTGGGTAACCCAATGATCCGTACGCAGTCACGTTTTTTC
EIN2 pDONR221 with stop	F	GGGGACAAGTTTGTACAAAAAAGCAGGCTATATGGAAGCTGAAATTGTGAATGTG
	R	GGGGACCACTTTGTACAAGAAAGCTGGGTCCTAACCCAATGATCCGTACGCAGT

Yeast 2-Hybrid Assay- The EIN2 pACTII construct was created by Dr. Christopher McClellan and contains the coding sequence encoding the EIN2 C-terminal domain (residues 516-1294). The CTR1 pLEXA-NLS construct was created by Dr. Jason Shockey and contains the coding sequence encoding the CTR1 kinase domain (residues 551-821). The *CTR1-1* (D694E) pLEXA-NLS construct was created by

using site directed mutagenesis (Agilent Technologies) to add in the substitution to the *CTR1* pLEXA-NLS construct, also done by Dr. Jason Shockey. Plasmids were transformed into the L40 yeast strain. Yeast 2-hybrid interactions were selected on plates lacking histidine with the addition of 5 mM 3-AT. Yeasts were spotted in serial dilutions (10-1 each) on both growth control (only lacking leucine and tryptophan) and selection plates, then grown at 30C for two to four days.

Western Blot-Yeast cultures were grown overnight and total protein was extracted using YPER buffer (Thermo Fisher Scientific). Protein samples were heated to 95 C for 10 min prior to separation by 10% SDS-PAGE, transferred to PVDF membrane (Bio-Rad) via semi-dry transfer. Membrane was stained with Ponceau S to verify transfer of proteins before immunoblotting with a 1:2000 dilution of an anti-LEXA antibody (Abcam), used to detect the expression of the CTR1 kinase domain protein fragment. An additional 10% gel was identically loaded and stained with Coomassie Blue.

Chapter 3: The N-terminal Domain of EIN2 is Involved in Regulation of the C-terminal Ethylene Signaling Domain

Introduction

EIN2 - the Central Regulator of Ethylene Signaling

EIN2 is one of the key components of the ethylene signaling pathway. However, the biochemical function of EIN2 still remains a mystery. *EIN2* was originally isolated in a genetic screen to identify ethylene insensitive mutants (Roman et al., 1995, Appendix A). In fact, *ein2* mutants are the most insensitive of all the ethylene insensitive mutants (Roman et al., 1995; Alonso et al., 1999). *EIN2* was placed downstream of *CTR1* based on genetic epistasis and was proposed to act upstream of *EIN3* (Roman et al., 1995; Guo and Ecker, 2003).

The EIN2 protein consists of two domains: an N-terminal domain and a C-terminal domain. As mentioned above, the hydrophilic C-terminal domain (approximately residue 516-1294) is found only in plant EIN2 homologs (Alonso et al., 1999). Over-expression of just the C-terminal domain (residues 516-1294) confers a constitutive ethylene response in adult plants (Alonso et al., 1999), suggesting EIN2, or at least the C-terminal domain, plays an important role in ethylene signaling. As a result, most studies have focused on the signaling portion of EIN2, the C-terminal domain.

The N-terminal Domain of EIN2 – the Mysterious Half of the Protein

As Chapter 2 describes, EIN2 C-terminal domain is responsible for bridging the gaps in the ethylene signaling pathway from CTR1 to EIN2 (via CTR1 directly

phosphorylating EIN2) and between EIN2 (at the ER membrane) and EIN3 (in the nucleus). The N-terminal domain, which comprises a large portion of EIN2 (residues 1-461 out of 1294), consists of twelve predicted transmembrane domains (ARAMEMNON; Alonso et al., 1999) that localize to the ER (Bisson et al., 2009) and shows homology to Nramp metal ion transporters. Since overexpression of full-length EIN2 did not show the same constitutive response as overexpression of the C-terminal domain alone, it was predicted that the N-terminal domain might be controlling the C-terminal domain. Alonso et al. (1999) did not see rescue of the *ein2-5* insensitive phenotype by overexpressing just the EIN2 C-terminal domain, seedlings remained insensitive but showed adult constitutive ethylene responses. However, since *EIN2* C-terminal domain was not sufficient to invoke the triple response phenotype (only full-length EIN2 could) it suggests the N-terminal domain plays a role in seedling skotomorphogenesis (Alonso et al., 1999). However, beyond that, the function of the N-terminal domain and its role in ethylene signaling remain elusive.

The *ein2 G36E* Mutant

One of the major reasons that it has been difficult to decipher the function of the N-terminal domain and how it functions in relation to the C-terminal domain is the lack of informative mutant alleles that affect the N-terminal domain. There are frameshifts and nonsense mutations in the portion of EIN2 that codes for the N-terminal domain. However, there are no known missense mutations that could help to address the function of this domain. One published missense mutation in *EIN2* exists, *ein2-9* (coding for an H1143P substitution), but this substitution is located in the C-

terminal domain. Although informative, this allele would not provide information regarding the N-terminal domain.

In 2012, we receive a gift from Dr. Zhizhong Gong (China Agricultural University) of an Arabidopsis *ein2* mutant isolated from an EMS mutagenized population (in the Landsberg *erecta* ecotype) in a screen for ABA insensitivity. This allele is a missense mutation encoding amino acid substitution (a G36E substitution) within a conserved motif (DPGK) in the N-terminal domain of EIN2 (Figure 3.1). In fact, it is within a motif (DPGN) that is highly conserved among Nramp proteins from a diversity of organisms (to be discussed in Chapter 4). We refer to this mutant as *ein2 G36E*. This chapter analyzes this novel mutant, *ein2 G36E* for insight into the function for the N-terminal domain.

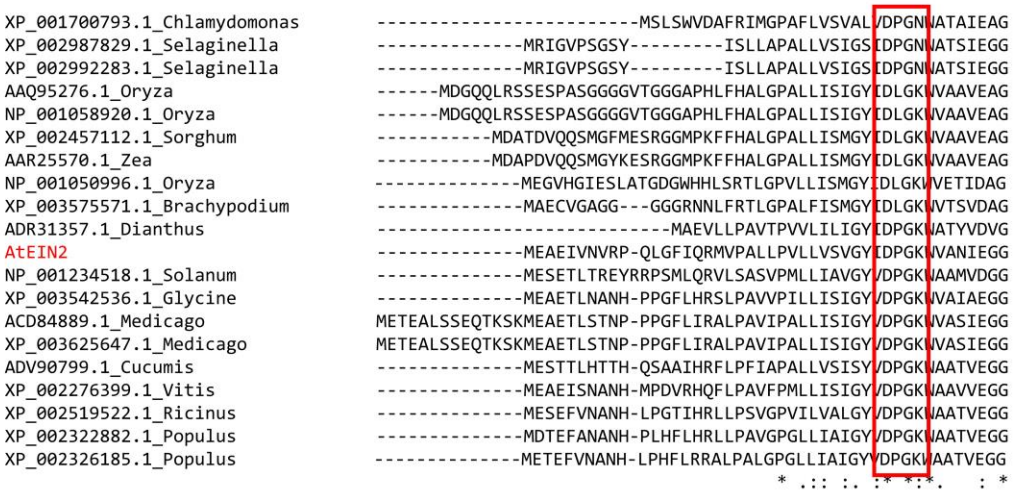

Figure 3.1. The DPGK motif is a highly conserved motif in EIN2 proteins in vascular plants. Protein sequence alignment of EIN2s from various vascular plants, in addition to the green algae *Chlamydomonas* and the vascular moss *Selaginella*, both of which contain a DPGN motif like other Nramp proteins. The Arabidopsis EIN2 (AtEIN2) protein sequence name is highlighted in red. The conserved DPGK motif is highlighted with a red box. Multiple Sequence Alignment done using MUSCLE (3.8) (Edgar, 2004) and accession numbers are listed.

Results

ein2 G36E Confers Ethylene Insensitivity and is a Partially Dominant Allele

A novel *ein2* allele with a point mutation in the N-terminal domain was a valuable discovery that was worth investigating. After backcrossing to clean-up the genetic background, I wanted to characterize the *ein2 G36E* mutant in terms of its ethylene response. As seen in Figure 3.2, *ein2 G36E* confers ethylene insensitivity in 4-day old dark grown seedlings. (The mutant was compared to wild-type Landsberg *erecta* (L*er*) ecotype, which is the genetic background of *ein2 G36E*.) The insensitivity of the *ein2 G36E* mutant was also observed in adult plants (Figure 3.3).

Given that the null *ein2-5* mutant is ethylene insensitive (Alonso et al., 1999) suggests the *ein2 G36E* mutant is also a loss-of function allele. This result indicates that the N-terminal domain is a positive regulator of ethylene signaling. This also suggests that perhaps the DPGK motif in EIN2 is important for ethylene signaling function since mutating an important residue in this highly conserved motif (Figure 3.1) resulted in ethylene insensitivity. In addition, this indicates that the EIN2 N-terminal domain negatively regulates the EIN2 C-terminal domain to control ethylene signaling, as hypothesized in the Alonso et al. (1999) study based on evidence of constitutive signaling activity of the C-terminal domain when the N-terminal domain was removed.

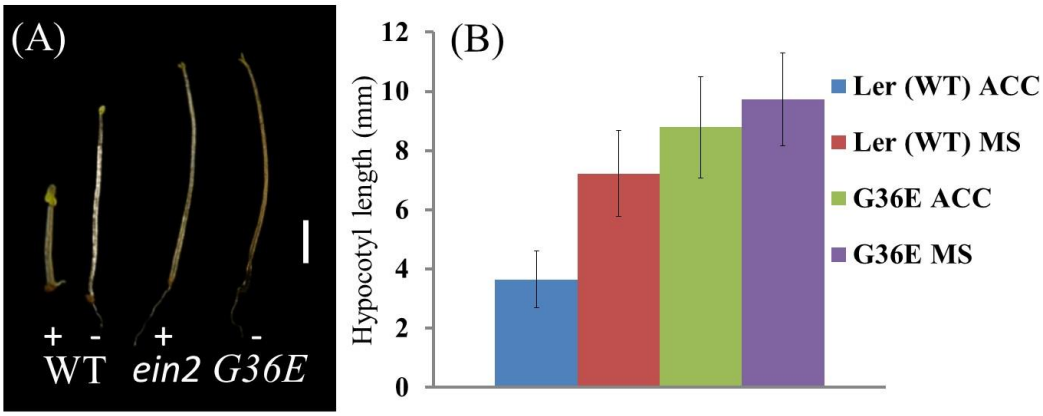

Figure 3.2. The *ein2 G36E* mutant confers ethylene insensitivity. Four day-old etiolated seedlings, wild-type (L*er*) and *ein2 G36E* were grown on MS plates with or without 20 µM ACC. (A) Representative sample. Scale bar represents 2 mm. (B) Hypocotyl measurements of seedlings where $50<n<66$ seedlings.

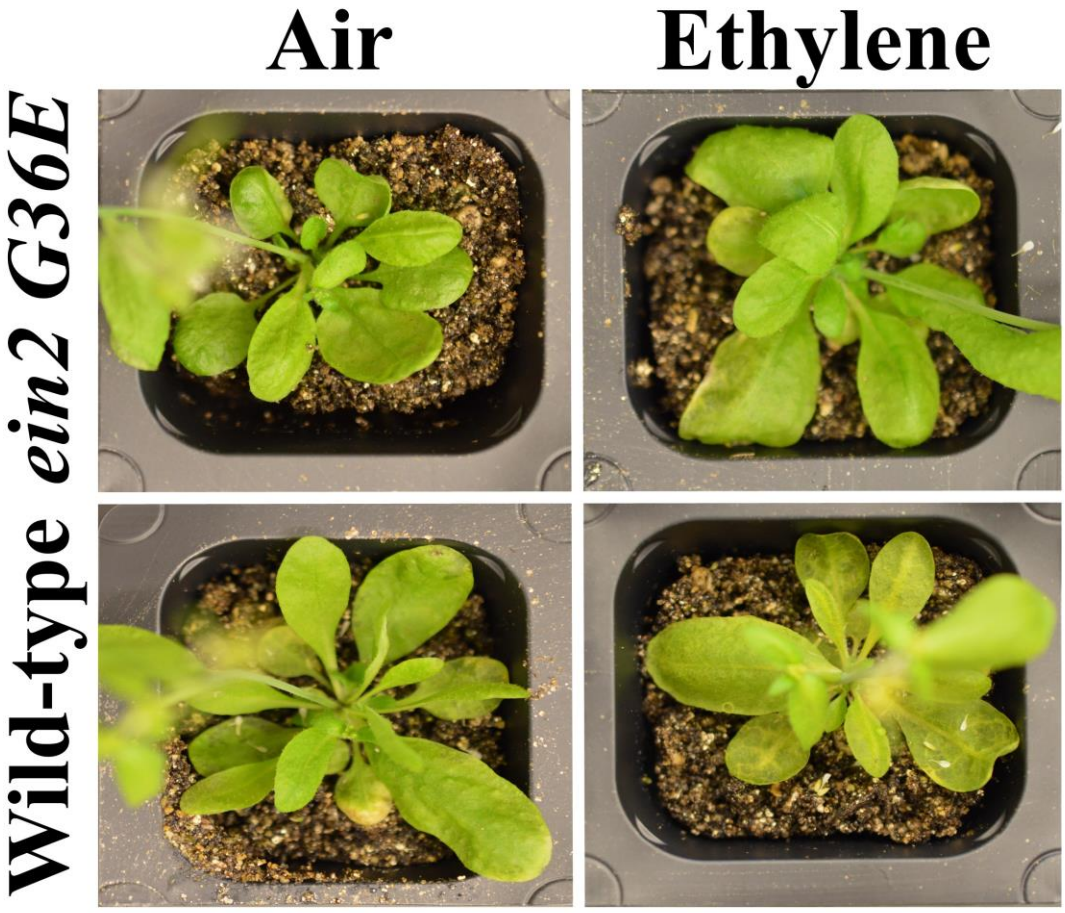

Figure 3.3. The ethylene insensitivity of the *ein2 G36E* mutant is also seen in adult plants. Three-week old wild-type (L*er*) and *ein2 G36E* mutant plants were treated with or without 100 ppm ethylene gas for 3 days. The *ein2 G36E* mutant did not seem to senesce as fast as wildtype as indicated by the browning of the leaves in the wildtype plant with ethylene treatment that is not as advanced in the *ein2 G36E* mutant.

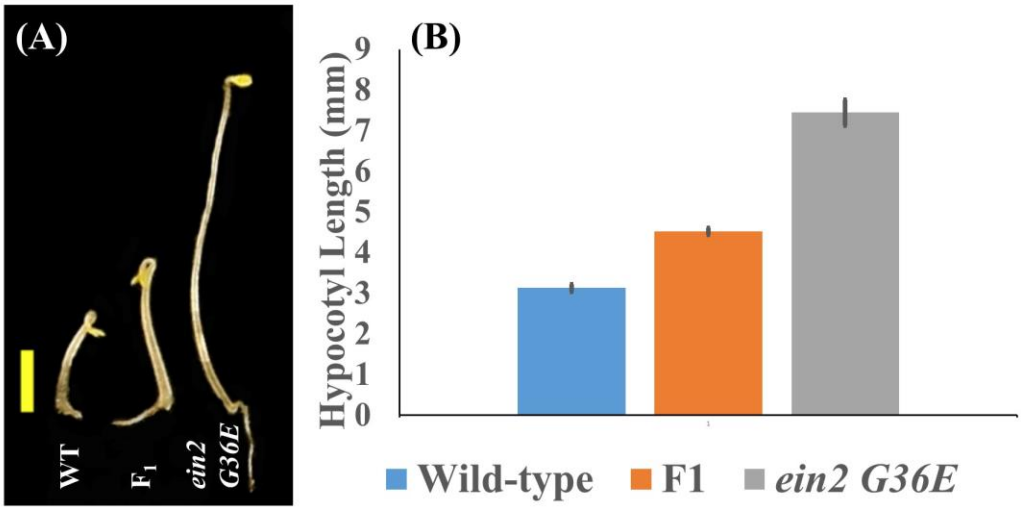

Figure 3.4. When back-crossed, the F_1 population of the *ein2 G36E* mutant shows partial insensitivity. The *ein2 G36E* mutant was back-crossed to *Ler* (wild-type) and etiolated seedlings were grown on MS plates with 20 μM ACC plates for 4 days. The F_1 population conferred partial insensitivity. (A) Representative sample of seedlings (B) Hypocotyl length measurements. The F_1 bar represents a pool of eight independent crosses. Error bars represent standard error. $35<n<100$ seedlings.

Next, I wanted to explore the basis as to how this single mutation in the N-terminus could result in the observed ethylene insensitive phenotype. Since the mutant allele was obtained from an EMS screen, it was possible that other mutations were present in the *EIN2* sequence. An undergraduate working with me, Jordon Limsky, PCR-amplified and sequenced the *EIN2* gene from the *ein2 G36E* mutant to verify that the *G36E* mutation was indeed the only mutation present in the *EIN2* gene. He also found a single sequence polymorphism present in the wild-type L*er EIN2* sequence relative to the Col-0 *EIN2* sequence (discussed in Chapter 4).

Interestingly, during the initial backcrossing, I discovered in the F_1 generation that the *ein2 G36E* mutant showed partial dominance (Figure 3.4). This could indicate that the *ein2 G36E* mutant protein interferes with the function of the wild-type EIN2 protein in a dominant negative fashion. Another possibility is that EIN2 functions in a dose-dependent fashion, and that the EIN2 G36E mutant version reveals EIN2 haploinsufficiency.

The *ein2 G36E* Mutant is Not a Null Allele

Since this G36E substitution falls in a highly conserved motif in EIN2 (Figure 3.1) it is possible that the G36E substitution could result in protein degradation of EIN2 causing the ethylene insensitive phenotype observed (Figure 3.2). To test this, I examined the EIN2 protein from the *ein2 G36E* mutant, using a Western Blot (Figure 3.5). Under conditions where ethylene biosynthesis is blocked (with AVG), the *ein2 G36E* mutant produced a full-length protein. However the EIN2 protein level in the *ein2 G36E* mutant was slightly reduced compared to wild-type EIN2 (L*er*) indicating a full-length EIN2 protein is present. Therefore the G36E substitution is not causing

degradation of EIN2, which could result in ethylene insensitivity. However, there is possibly a lower level of EIN2 protein in the *ein2 G36E* mutant for unknown reasons.

Additionally, in the presence of ethylene (with the ethylene precursor ACC) the *ein2 G36E* mutant produced a protein that is slightly smaller than the wild-type EIN2 protein (Figure 3.5). This suggests that there may be some sort of protein modification occurring in the *ein2 G36E* mutant or lack thereof causing a slight decrease in protein size. This slight shift in size could not be accounted for by cleavage of EIN2 because of the location of the antibody. The anti-EIN2 antibody used in this Western Blot (Figure 3.5) bound to the last 20 residues at the very C-terminus of EIN2. If cleavage occurred, the protein would not have been detected using this antibody.

When assayed for the triple response the *ein2 G36E* mutant did have a slight shortening of the hypocotyl in the presence of the ethylene precursor ACC and a slight increase in the hypocotyl length in presence of AVG (an ethylene biosynthesis inhibitor) (Figure 3.6). This suggests that ethylene signaling is still slightly activated in this *ein2 G36E* mutant, resulting in a residual ethylene response. This also indicates that the *ein2 G36E* mutant is not a null allele. Therefore, something else is causing the observed ethylene insensitivity.

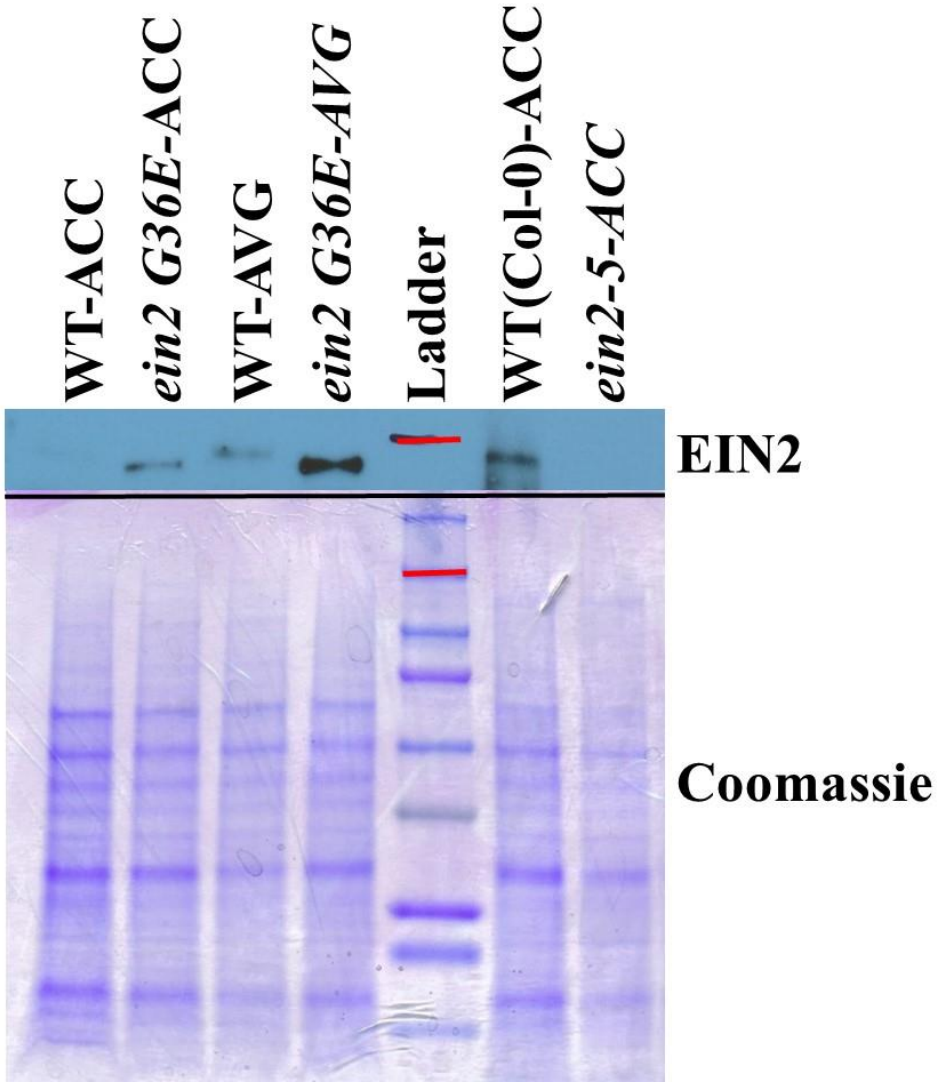

Figure 3.5. The *ein2 G36E* mutant expressed a full length EIN2 protein. Western Blot of EIN2 from microsomal fractions of 4 day-old etiolated seedlings grown on MS plates with either 20 µM ACC (an ethylene precursor) or 10 µM AVG (an ethylene biosynthesis inhibitor). Microsomal fractions were analyzed by Western Blot using an anti-EIN2 antibody (Agrisera), which detects a peptide within the last 20 residues of the C-terminus of EIN2. WT samples on left side were L*er* ecotype (lanes 1 and 3), control for *ein2 G36E* (lanes 2 and 4), and WT samples on right side were Col-0 ecotype (lane 6), the control for *ein2-5* (null allele and negative control,

lane 7). Red marker bar in the ladder (lane 5) represents 150 kDa, also labeled on the Coomassie gel. Coomassie gel used as loading control.

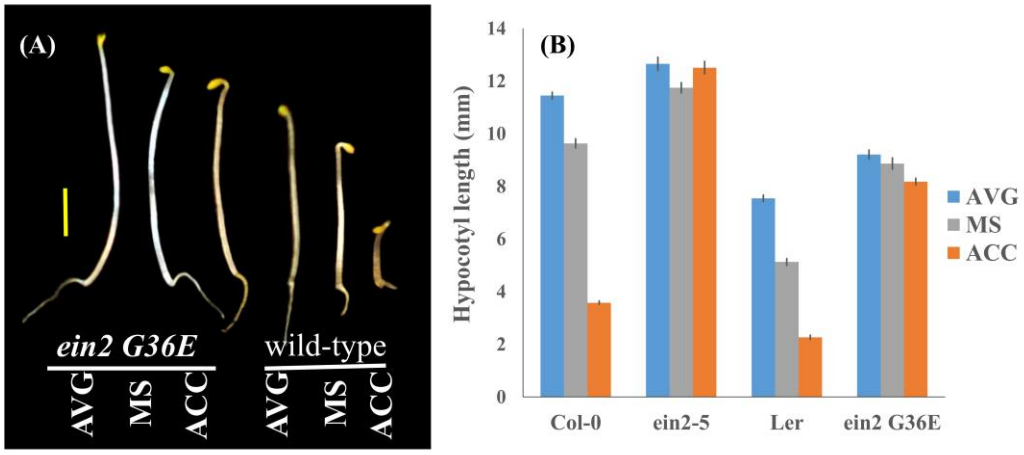

Figure 3.6. *The ein2 G36E* mutant has a residual ethylene response. Four day-old etiolated seedlings were grown on either MS, or with the addition of ACC (an ethylene precursor, 20 µM), or AVG (an ethylene biosynthesis inhibitor, 10 µM). When grown on ACC, the *ein2 G36E* mutant is insensitive to ethylene. However, with the addition of AVG, the hypocotyl length increases slightly, indicating there is some ethylene response in this mutant. Panel (A) is a representative sample of seedlings, that were photographed and measured using Image J (B). Scale bar represents 2 mm and error bars represent standard deviation.

The G36E substitution could cause EIN2 to misfold, resulting in the observed ethylene insensitivity conferred by the *ein2 G36E* mutant (Figure 3.2). To test this possibility, I tested the seedling triple response of the *ein2 G36E* mutant at various temperatures, both warmer and cooler than normal (Figure 3.7) to see if temperature could aid in correct folding of EIN2 G36E, rescuing the ethylene insensitive phenotype of the *ein2 G36E* mutant. However, temperature did not result in rescue of the ethylene insensitivity, so it remains inconclusive whether the ethylene insensitivity observed in the *ein2 G36E* mutant is due to a protein folding error.

The EIN2 (G36E) Protein Localizes to the Ethylene Receptor Complex at the ER in Onion Epidermal Cells

To better understand the function of EIN2 and why the G36E substitution confers ethylene insensitivity, I next wanted to ensure that the EIN2 protein properly localizes to the ER membrane verifying that the G36E substitution does not disrupt the proper subcellular localization of the EIN2. When tagged at the N-terminus with YFP, full length wild-type EIN2 localizes to the ER as expected (Figure 3.8a). I found the G36E substitution did not disrupt this ER localization (Figure 3.8b) despite the substitution being located near the first transmembrane domain. This indicates that the N-terminus of EIN2, both wild-type and EIN2 G36E, is located at the ER, that the G36E substitution does not disrupt the localization of the N-terminal domain, and that the N-terminus could be folded properly at the gross level. Interestingly, the strength of the YFP signal between wild-type and EIN2 G36E were similar suggesting that the G36E substitution does not affect the expression of the N-terminal domain.

It is possible that the EIN2 G36E substitution could alter the confirmation of EIN2 disrupting essential protein interactions, such as with CTR1 (Chapter 2- Figure 2.2, and 2.3; Ju et al. 2012). To explore this possibility, I tested whether EIN2 G36E was could interact with CTR1 using BiFC in onion epidermal cells. EIN2 G36E, like wild-type EIN2, still interacted with CTR1 (Figure 3.9) suggesting the C-terminal domain of EIN2 is most likely folded properly since the C-terminal domain of EIN2 interacts with CTR1. This also places both EIN2 and the mutant EIN2 G36E in an ethylene receptor protein complex at the ER membrane.

EIN2 Interacts With Itself *in planta* and When Expressed in Yeast

The partial dominant effect observed in the *ein2 G36E* heterozygotes (Figure 3.4) was intriguing and warranted further exploration. One possibility is the partial dominance is due to a dominant negative effect, which can be obtained via EIN2 self-interaction. Therefore, I decided to test whether or not EIN2 is able to self-interact. Full length EIN2 was able to self-interact using a yeast split Ubiquitin assay (Figure 3.10). This EIN2 self-interaction was also observed *in planta* using BiFC in onion epidermal cells (Figure 3.11) suggesting there is an oligomer of EIN2 proteins at the ER. This also suggests that the G36E substitution does not disrupt the EIN2 self-interaction at the ER (Figure 3.10c).

So, if full length EIN2 is capable of self-interaction, which portion of EIN2 is responsible for this self-interaction? To partially address this question, I dissected EIN2 into smaller fragments and tested these fragments for self-interaction in yeast. The EIN2 N-terminal domain (residues 1-524 and residues 1-481 Figure 3.12) self-interacted as well as the EIN2 C-terminal domain (residues 516- 1294; Figure 13).

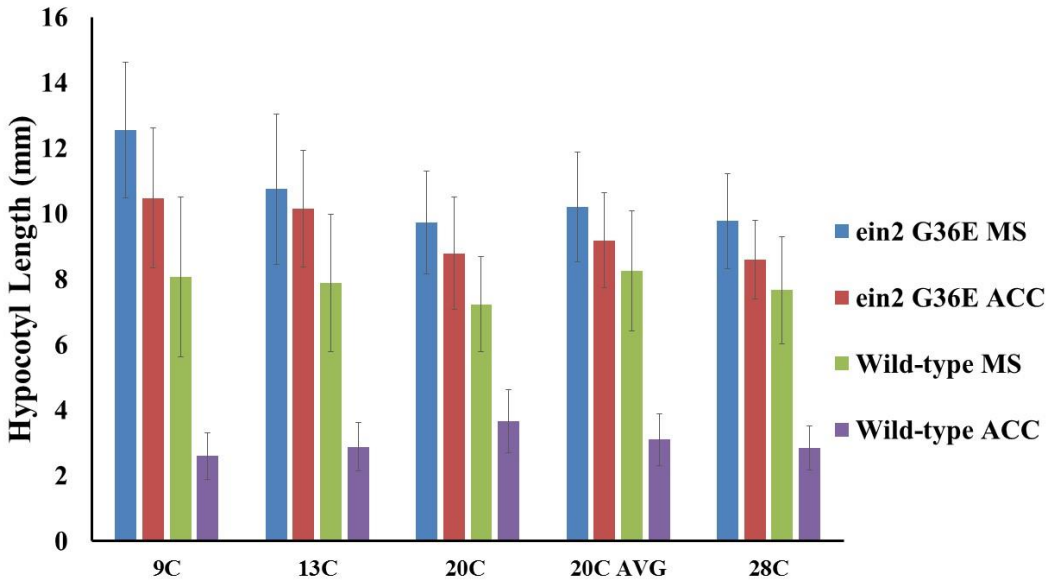

Figure 3.7. Temperature did not rescue the insensitivity of the *ein2 G36E* mutant. Etiolated seedlings, both wildtype (L*er*) and *ein2 G36E*, were grown on MS with and without the addition of ACC or AVG and grown at various temperatures; 9^{o}C for 19 days, 13^{o}C for 11 days, 20^{o}C for 4 days, and 28^{o}C for 2 days. Seedlings were photographed and hypocotyl lengths were measured using Image J. Error bars represent standard deviation.

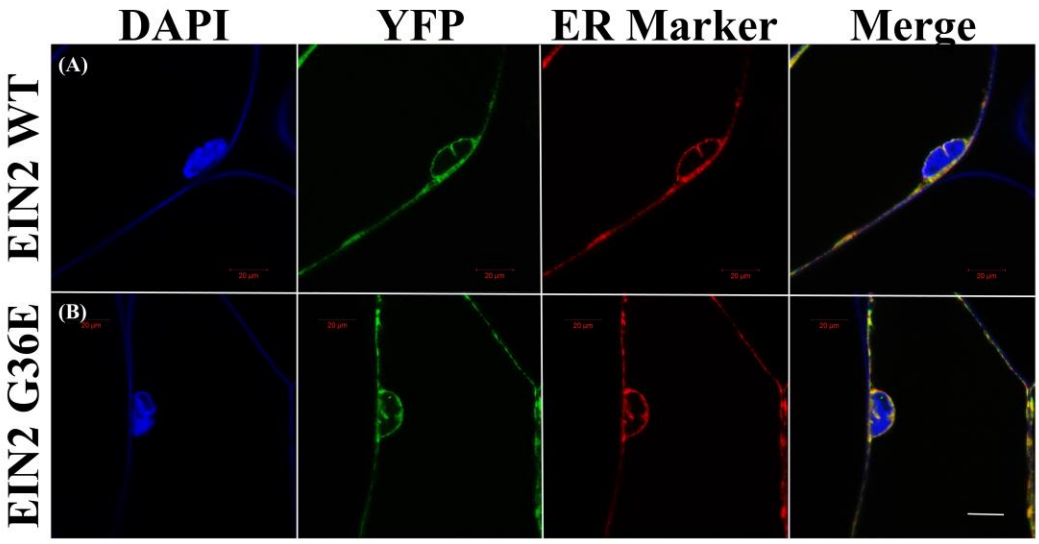

Figure 3.8. The EIN2 G36E substitution does not alter the ER localization of EIN2 N-terminal domain. Full-length wild-type EIN2 (A) with an N-terminal YFP tag was transiently expressed using particle bombardment in onion epidermal cells and found to localize to the ER (From Chapter 2, Figure 2.5A). Addition of the G36E substitution did not alter the localization pattern of EIN2 N-terminus (B). Merged image shows DAPI (20 µg/mL), ER marker (HDEL::mCherry), and YFP (EIN2 signal). Samples were visualized using confocal microscopy. Scale bar represents 20 µm.

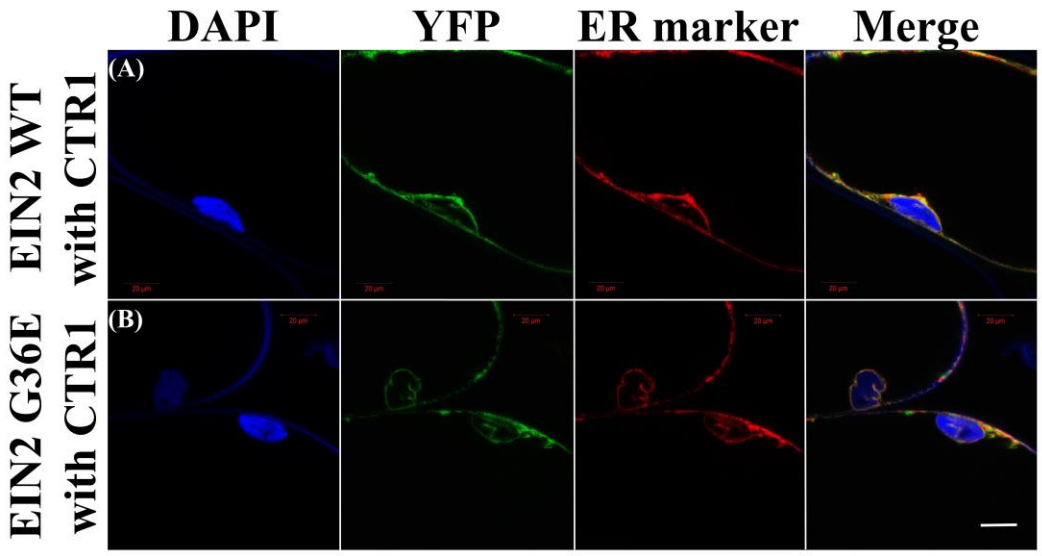

Figure 3.9. EIN2 G36E interacts with CTR1, *in planta*. BiFC interaction of full length EIN2, both wild-type (A) and EIN2 G36E (B) with full length CTR1 in onion epidermal cells. Addition of the G36E substitution did not disrupt the EIN2-CTR1 interaction or alter the ER localization of the interaction. Samples were visualized using confocal microscopy. Row A is also shown in Chapter 2 (Figure 2.4). Merged images show DAPI (20 µg/mL), ER marker (HDEL::mCherry), and BiFC (YFP signal). Scale bar represents 20 µm.

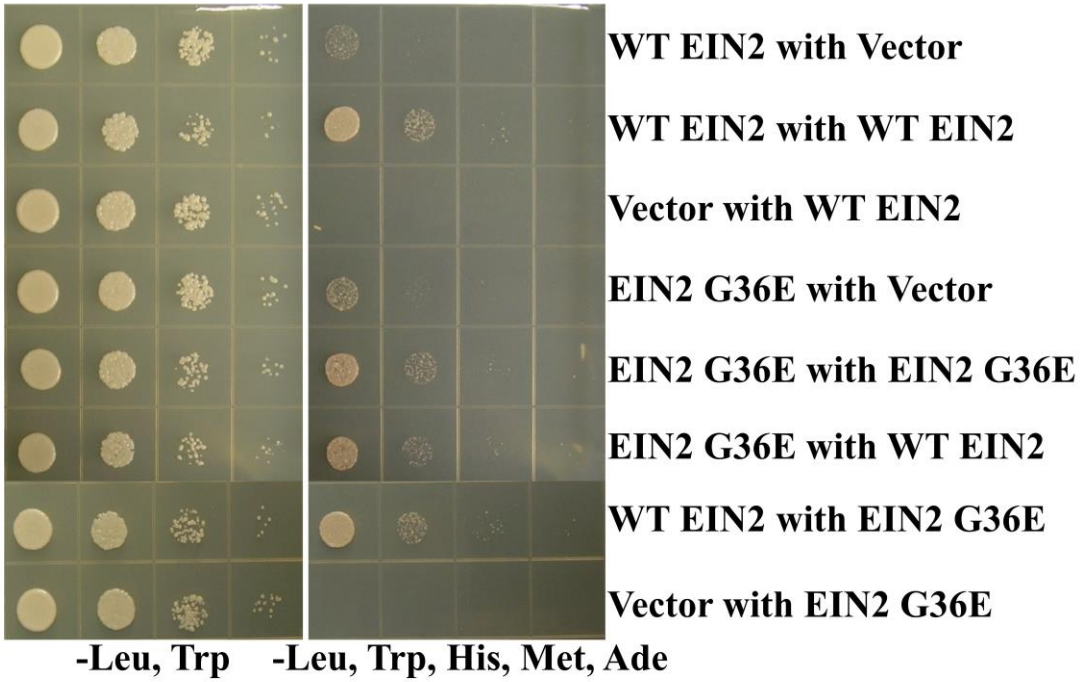

Figure 3.10. The EIN2 G36E substitution does not disrupt the EIN2 self-interaction, in yeast. Full length EIN2 was tested for self-interaction using a split-Ubiquitin assay, in yeast. Addition of the G36E substitution did not disrupt the self-interaction. Growth with empty vector (pNUB) and (pMET) were used as negative controls. Left panel was used as a growth control and right panel selected for interaction. Yeast were spotted on minimal media and grown for 2 days (growth control) or 4 days (selection plates) at 30C.

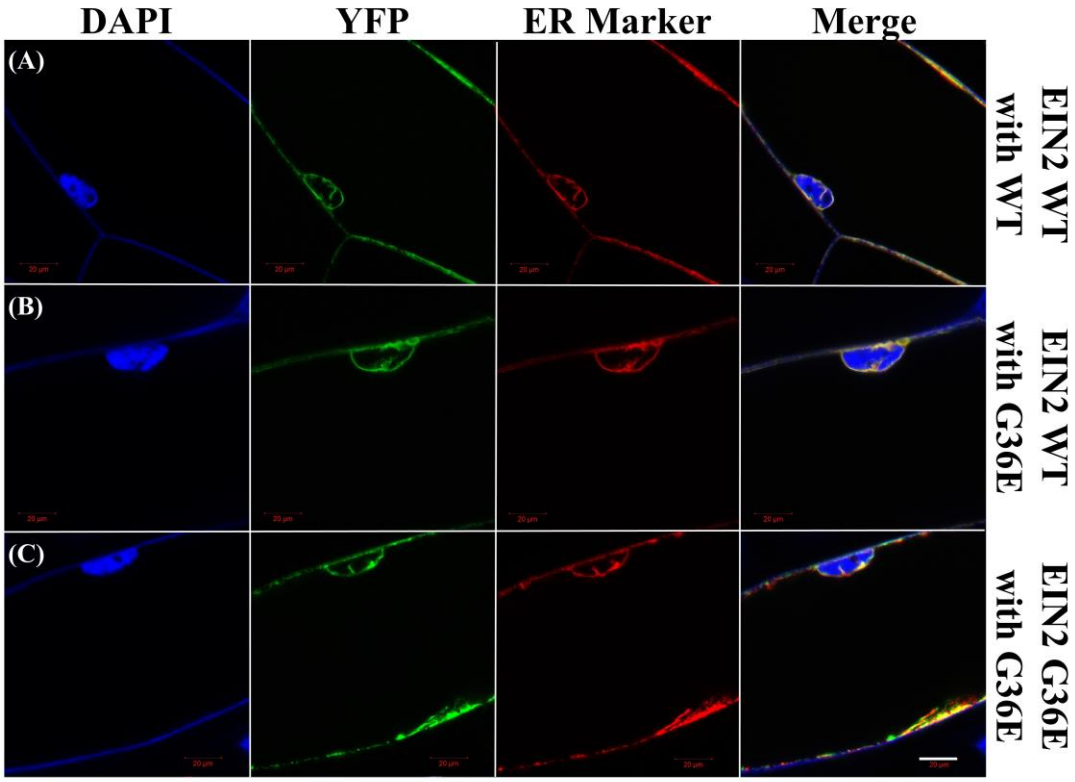

Figure 3.11. The EIN2 G36E substitution does not disrupt the EIN2 self-interaction, *in planta*. BiFC interactions, in onion epidermal cells, suggest that full-length wild-type EIN2 interacts with itself (A) at the ER membrane. Addition of one (B) or two copies (C) of the G36E substitution did not disrupt the EIN2 self-interaction. Merged images show DAPI (20 µg/mL), ER marker (HDEL::mCherry), and BiFC (YFP signal). Scale bar represents 20 µm.

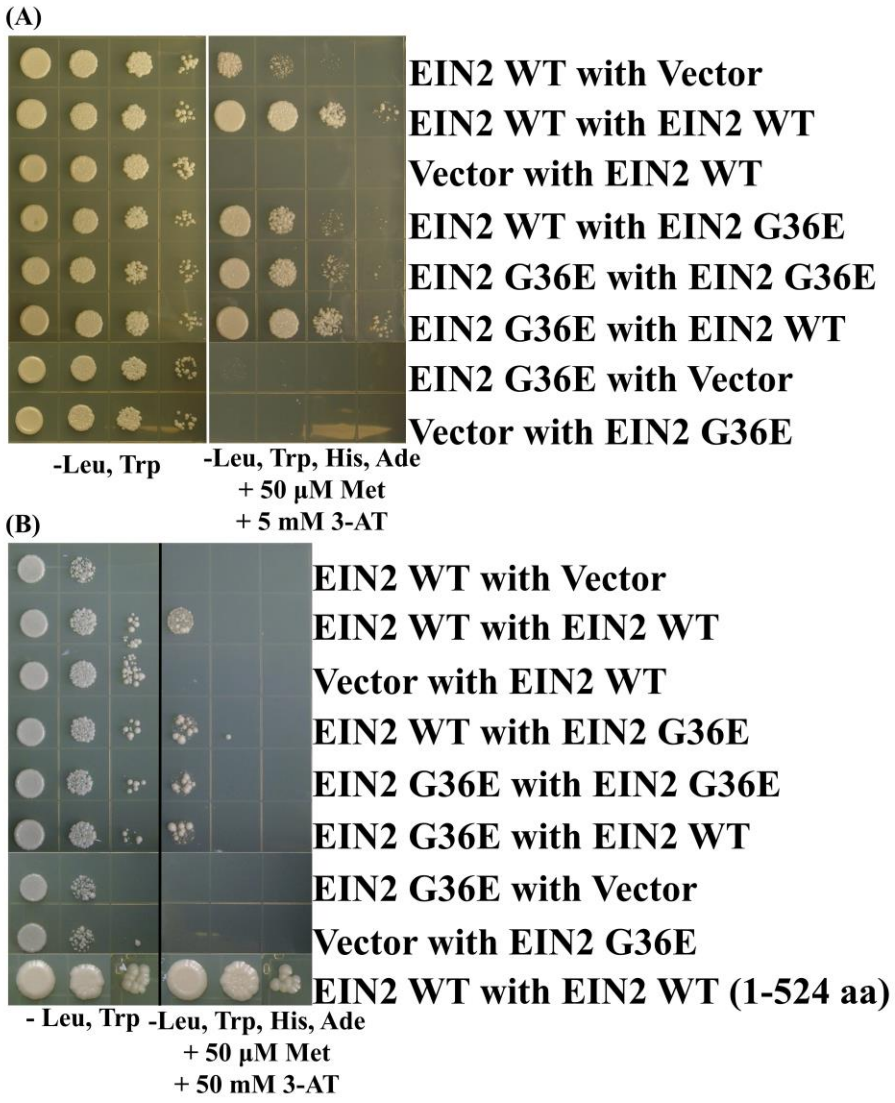

Figure 3.12. The EIN2 G36E substitution does not disrupt the self-interaction of EIN2 N-terminal domain, in yeast. Two different sized fragments of EIN2 N-terminal domain (A) residues 1-524 and (B) residues 1-481 were tested for self-interaction, using the split-ubiquitin assay. Addition of the G36E substitution did not disrupt the EIN2 self-interaction. However, expression of the smaller EIN2 fragment (residues 1-481) did seem to inhibit yeast growth compared to the larger (residues 1-524) N-terminal piece (B). Growth with empty vector (pNUB) and (pMET) were used as negative controls. Left panel was used as a growth control and right panel selected for interaction. Plates were spotted and grown at 30C for 2-12 days.

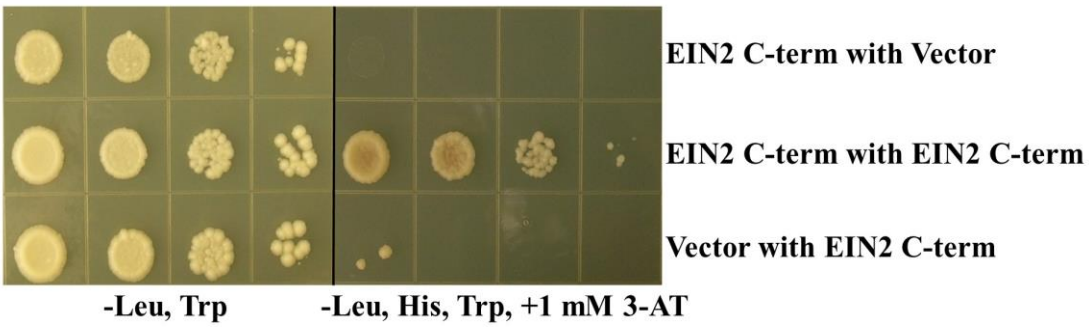

Figure 3.13. EIN2 C-terminal domain interacts with itself, in yeast. EIN2 C-terminal domain was found to self-interact using the yeast 2-hybrid assay. Empty vectors (pACTII and pLEXA) were used as negative controls for interaction (right panel). Left panel shows the growth control. Yeasts were grown at 30 C for 2 to 4 days.

The C-terminal domain of EIN2 was then further divided into smaller fragments selected to ensure highly conserved regions remained intact. An undergraduate working with me, Francine Ryan, help create the constructs and test these fragments using the yeast 2-hybrid assay, all of which were also found to self-interact (Figure 3.14). This suggests that EIN2 is a very "sticky" protein and appears that all fragments tested self-interact to some degree. It is also possible that EIN2 requires this self-interaction to function. Perhaps, the EIN2 self-interaction is important for EIN2 function at the ER in the absence of ethylene. Perhaps the EIN2 self-interaction plays a role in EIN2 protein confirmation or the protein interaction with CTR1, which is important for phosphorylation and regulation of EIN2.

Interestingly, with the addition of ethylene, the EIN2 full length self-interaction signal became stronger (Figure 3.15a and 3.15b) and remained at the ER. This is in contrast to how EIN2 is known to function, in that with the addition of ethylene, the C-terminal domain is supposed to move into the nucleus (Chapter 2 – Figure 2.4; Ju et al., 2012). This could suggest that the GFP tag at the C-terminus of EIN2 interfered with proper function of the C-terminal domain preventing nuclear localization. Although, compared to EIN2 G36E, the GFP signal was not as responsive to ethylene and ethylene treated sample had a similar GFP signal compared to the untreated sample (Figure 3.15c and 3.15d), similar to the wildtype untreated sample (Figure 3.15b). This is somewhat consistent with the *ein2 G36E* mutant, since the *ein2 G36E* mutant has a very subtle response to ethylene (Figure 3.6).

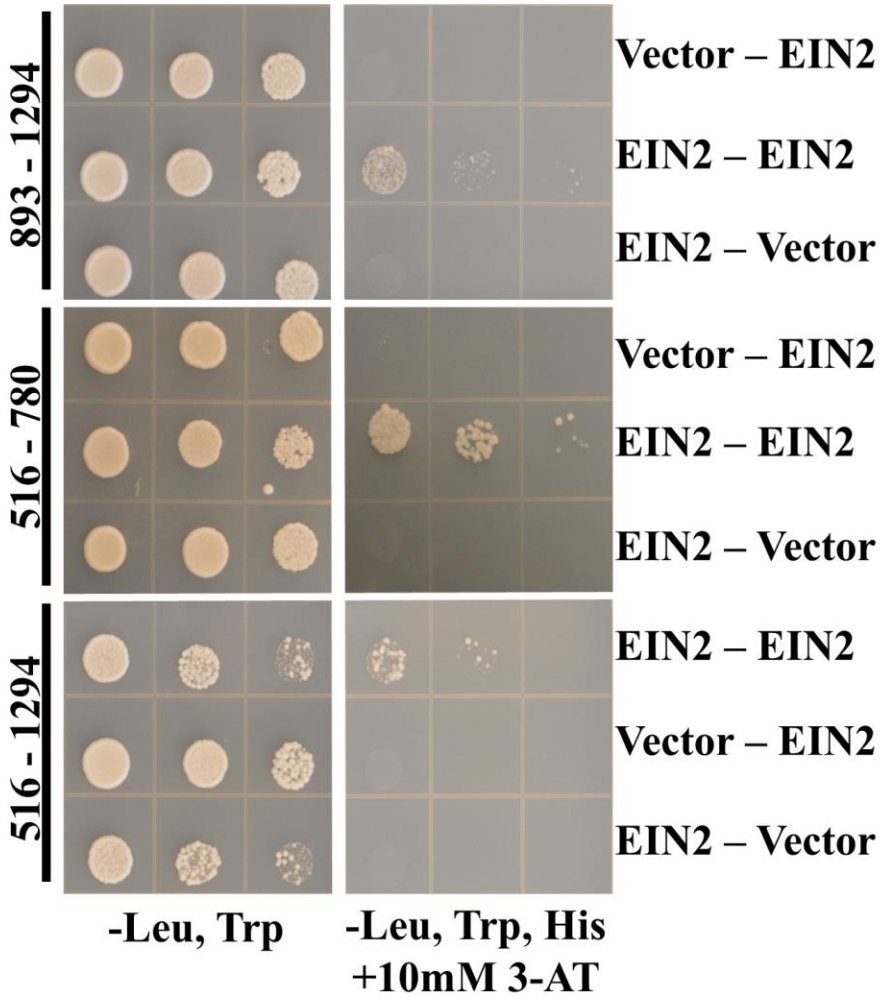

Figure 3.14. Smaller fragments of the EIN2 C-terminal domain also self –interact. Using a yeast 2-hybrid assay smaller fragments of the EIN2 C-terminal domain were tested for self-interaction. Like the full C-terminal domain (residues 516-1294) the smaller fragments were also found to self-interact. The EIN2 fragments were selected to ensure highly conserved regions of EIN2 remained intact as well as centered around important residues, such as the Ser924 and Ser645. Depicted are the fragments containing residues 893-1294 and 516-780 where growth on the self-

interaction plate (right panel) was similar to the full length C-terminal domain self-interaction (residues 516-1294). Additional fragments (containing residues 516-1040, 567-760, 767-1294, and 1041-1294, data not shown) showed similar growth as the full length C-terminal domain and fragments depicted above. Empty vectors (pACTII and pLEXA) were used as negative controls. Yeasts were plated on minimal media lacking Trp and Leu (growth control) and lacking Trp, Leu, and His with the addition of 10 mM 3-AT (selection plates) and grown at 30C for 2 to 4 days.

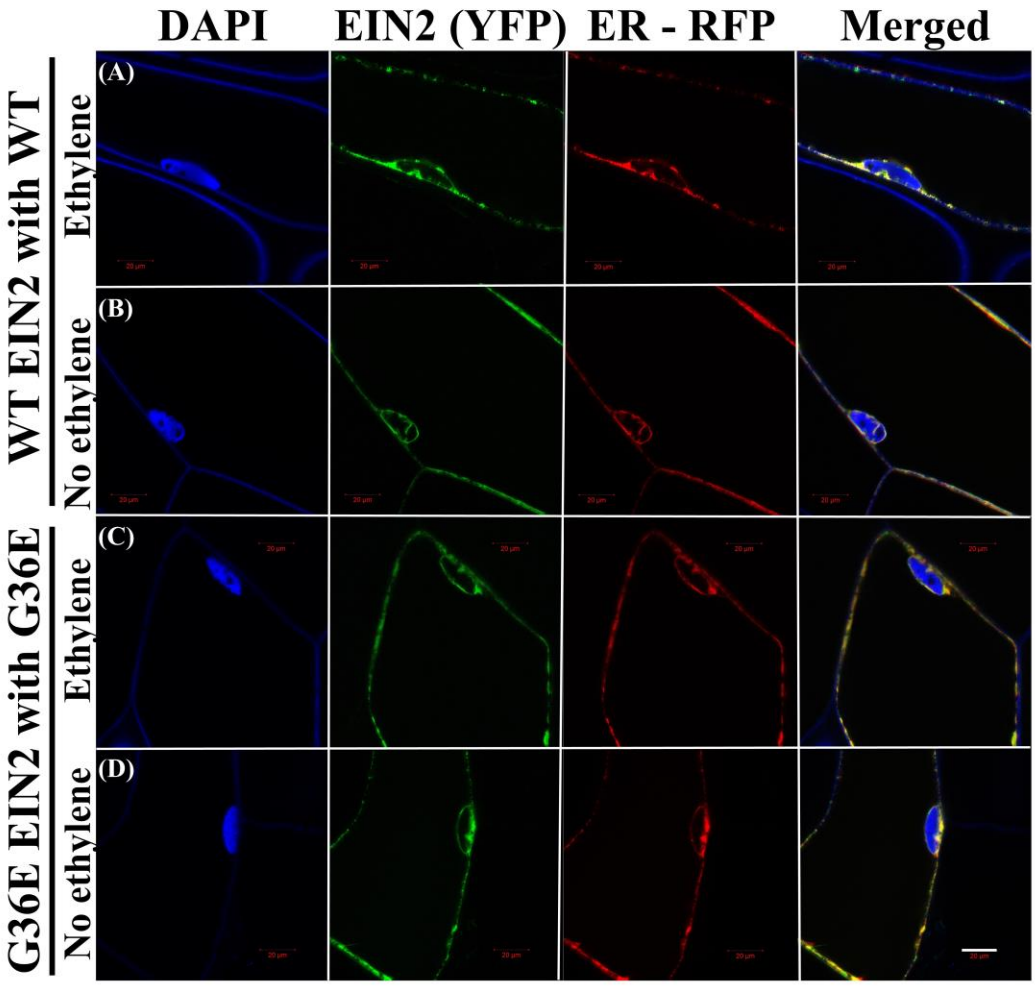

Figure 3.15. The EIN2 self-interaction remained at the ER and appeared stronger after ethylene treatment. BiFC interaction of full length EIN2 expressed in onion epidermal cells, wild-type EIN2 (A and B) and EIN2 G36E (C and D). Addition of ethylene (100 ppm for 3 hrs; A and C) did not alter ER localization of EIN2 (B and D) nor did the C-terminus translocate to the nucleus. The wild-type EIN2 interaction in the presence of ethylene (A) had a stronger BiFC signal compared to untreated samples (B). EIN2 G36E samples had a similar signal level between ethylene treated untreated samples (C and D). Merged images contain DAPI (20 µg/mL), ER marker (HDEL::mCherry), and BiFC (YFP). Scale bar represents 20 µm.

The H1143P Substitution Does Not Disrupt the EIN2 Self-Interaction

The *ein2-9* allele is another example of a missense allele of *EIN2*. However, this point mutation (H1143P) occurs in the C-terminal domain and confers weak ethylene insensitivity (Alonso et al., 1999). Since *ein2-9* currently the only published missense mutation in *EIN2*, I was curious as to whether the H1143P substitution would disrupt the EIN2-EIN2 self-interaction. Therefore, an undergraduate working with me, Lauren Nesi, introduced the *ein2-9* mutation into the EIN2 C-terminal domain fragment (residues 516-1294; termed EIN2-9) and tested EIN2-9 for self-interaction using the yeast two hybrid assay. Similar to G36E, the H1143P substitution did not disrupt the EIN2 self-interaction of the EIN2 C-terminal domain (Figure 3.16). This suggests that the His1143 residue is not an important site for the EIN2 self-interaction. Perhaps multiple sites would have to be mutated to disrupt this self-interaction. It is possible that this H1143P has other important roles in EIN2 function, perhaps in the P-body function of EIN2 C-terminal domain (Liu et al., 2015).

The *ein2 G36E* Mutant is Most Likely Not a Dominant Negative Allele

The EIN2 self-interaction supports the possibility that the G36E substitution could be interfering with wild-type EIN2 function in a dominant negative manner. To further explore this possibility, I created transgenic lines expressing just the N-terminal domain of EIN2 (both wild-type and with the G36E mutation; residues 1-524), in a wild-type (L*er*) background. If the overexpression of EIN2 G36E caused a dominant negative effect on wild-type EIN2 present in the background, it would suggest that this particular N-terminal point mutation affects the translocation of the

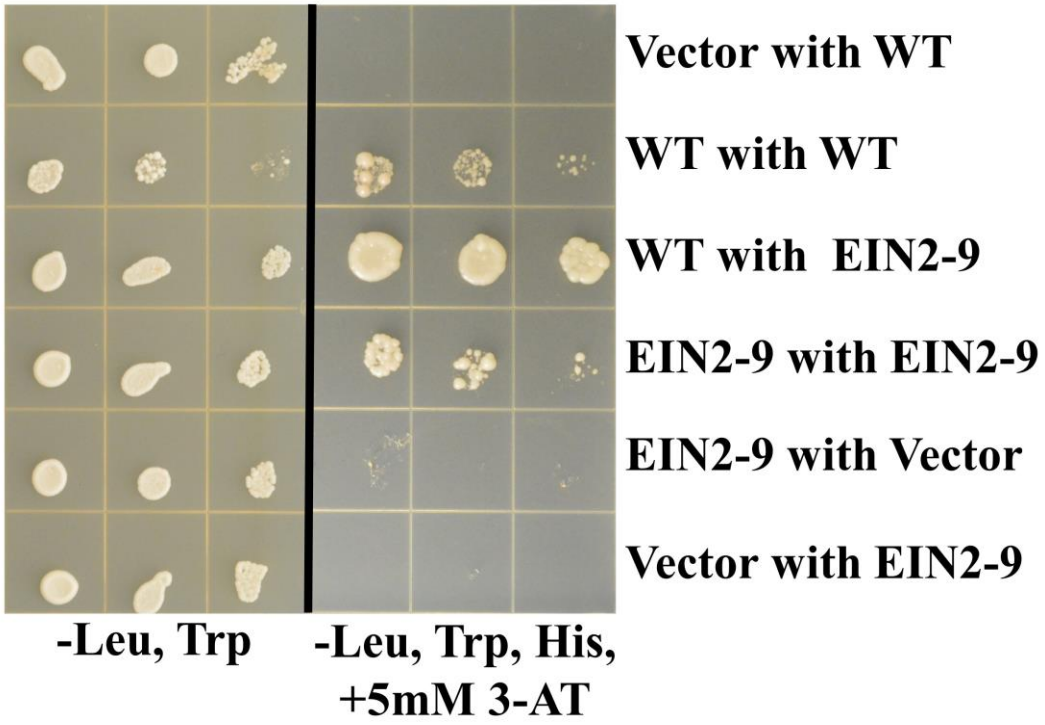

Figure 3.16. The H1143P substitution does not disrupt the EIN2 C-terminal domain self-interaction, in yeast. The nucleotide encoding the H1143P substitution was inserted into the EIN2 C-terminal domain mimicking the *ein2-9* mutant allele. This new construct (termed "EIN2-9") was used in the yeast 2-hybrid assay to test the EIN2 self-interaction. The EIN2-9 substitution did not disrupt the self-interaction of the EIN2 C-terminal domain. EIN2 self-interaction with wild-type EIN2 C-terminal domain (WT) was used as a positive control and the interaction with empty vector (pACTII or pLEXA) were used as negative controls. Yeasts were spotted on minimal media (-Leu, Trp; left panel) for a growth control and interactions were selected using minimal media lacking -Leu, Trp, His, with the addition of 5 mM 3-AT (right panel, selection plate). Plates were grown at 30C for 2-4 days.

C-terminal domain into the nucleus and therefore the signaling function of EIN2.

So, if EIN2 G36E functioned in a dominant negative manner, I would predict that overexpression of the N-terminal domain would inhibit the function of wild-type copies present in the L*er* background resulting in insensitivity or partial ethylene insensitivity, reminiscent of the F_1 heterozygote (Figure 3.4). However, overexpression of the EIN2 G36E N-terminal domain did not cause partial ethylene insensitivity (Figure 3.17) to the level seen in the F_1 heterozygote, nor alter the wild-type triple response phenotype at all, suggesting an absence of interference by the EIN2 G36E N-terminal domain on wild-type EIN2 function. Overexpression of wild-type EIN2 N-terminal domain similarly had no effect (Figure 3.17b). Therefore, the G36E substitution most likely does not function in a dominant negative manner to cause ethylene insensitivity. This finding also further suggests a requirement of both a functional C-terminal domain as well as an N-terminal domain to promote an ethylene response (Alonso et al., 1999).

Overexpression of full length *EIN2 G36E* in a wild-type background (Col-0), similar to full length wild-type *EIN2*, resulted in a full range of phenotypes from insensitive to rescue to U-shape (Appendix A, data not shown) and therefore were uninterpretable. This is similar to what was seen in the Alonso et al. (1999) study where overexpression of just the EIN2 C-terminal domain conferred a constitutive response. However, in that same study, they found that overexpression of full length EIN2 did not confer a constitutive response. This could suggest that perhaps there is some activation of downstream responses in the *ein2 G36E* mutant since some of the phenotypes were U-shaped and overexpression would just enhanced this response.

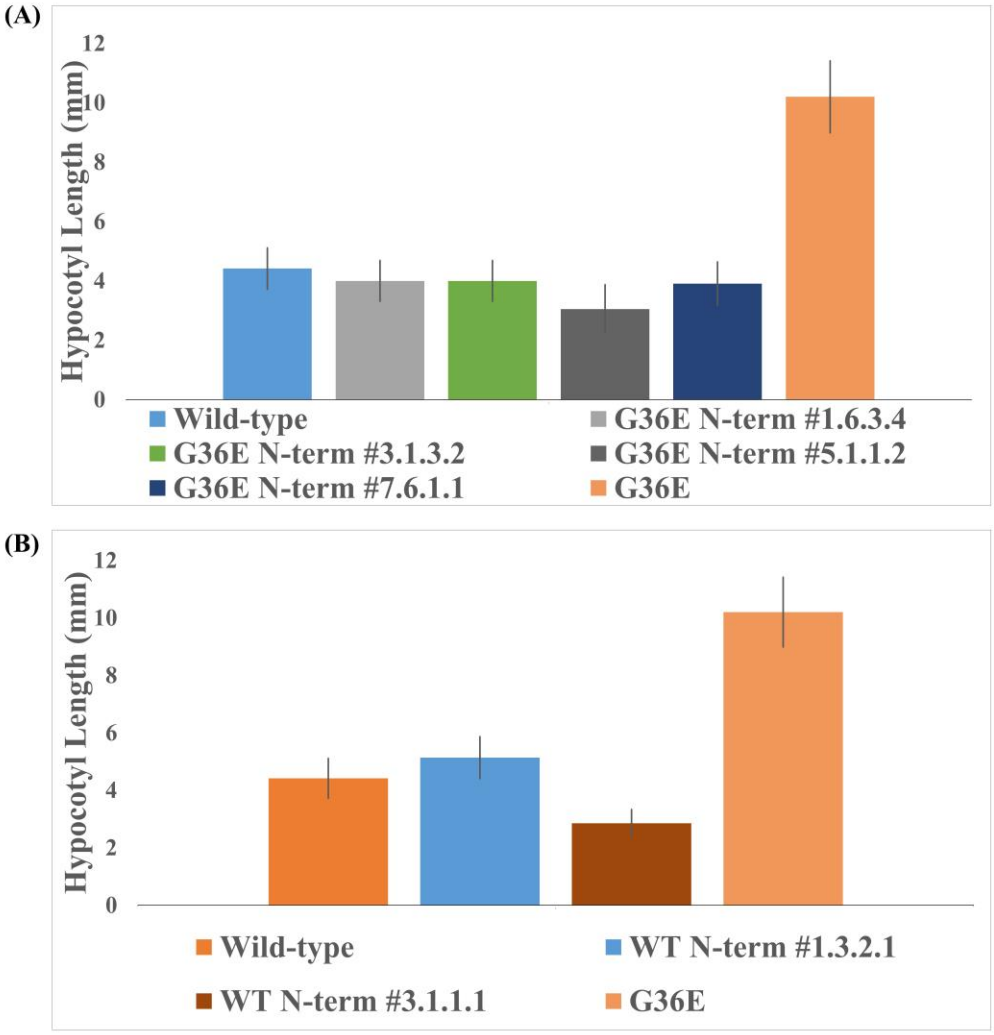

Figure 3.17. The EIN2 G36E substitution did not inhibit the function of EIN2 C-terminal domain. Transgenic lines were created, expressing just EIN2 N-terminal domain (residues 1-524), in a wild-type (L*er*) background. Addition of the G36E substitution (A) did not confer ethylene insensitivity when grown on 20 µM ACC and 4 day-old etiolated seedlings remained similar to wild-type. Four independent lines shown. Overexpression of wild-type EIN2 N-terminal domain (B) resulted in a similar phenotype. Two independent lines shown. Error bars represent standard deviation. Seedlings measured using Image J.

However, it also could be possible that there was just too much EIN2 and the EIN2 G36E was still processed and cleaved as wild-type. The background used in the Alonso et al. (1999) study was the *ein2-5* null mutant. This could suggest that the expression of EIN2 is sensitive to the genetic background. This could be an indicator of haploinsufficiency in the *EIN2* gene (Wilkie, 1994).

EIN2 Most Likely Functions in a Haploinsufficient Manner

When oligomerized, a dominant negative protein would show a stronger effect in an F_1 heterozygote (25% activity relative to wild-type) compared to a null allele (50% activity relative to wild-type) due to the mutant protein rendering the oligomer inactive (Veitia, 2007). If this is the case and EIN2 G36E protein has a dominant negative effect on wild-type EIN2 protein, the *ein2 G36E* mutant should have a stronger phenotype in the F_1 generation than the *ein2-5* null allele. To test this possibility, I compared the F_1's from the cross of *EIN2 G36E* x L*er* to *ein2-5* crossed with Col-0. Unfortunately, the two different *ein2* alleles are in two different ecotype backgrounds. There are no known null alleles of *EIN2* available in the L*er* ecotype.

When compared, the *ein2 G36E* x L*er* cross was not more severe than the F_1's produced from the null mutant (Figure 3.18) and therefore does not fit the simplest definition of a dominant negative mutation (Veitia, 2007). This is further evidence that EIN2 G36E substitution is not functioning in a dominant negative manner. However, this does not necessarily rule out the possibility that the G36E substitution is a less severe mutation, causing partial inhibition of wild-type EIN2, which also is in agreement with the slight response seen in the *ein2 G36E* mutant (Figure 3.6) when treated with AVG (an ethylene biosynthesis inhibitor) suggesting that the ethylene

signaling pathway is slightly activated in the *ein2 G36E* mutant. This could also suggest that the partial dominance of *ein2 G36E* (Figure 3.4 and 3.18) might result from EIN2 haploinsufficiency.

Overexpression of full length wild-type *EIN2*, in the *ein2-1* background, like in Col-0 background, gave a full range of phenotypes; from insensitive (a result of RNAi, data not shown) to rescue (similar to wild-type) to a U-shaped EIN2 overexpression phenotype (See Appendix A; An et al.; 2010) (data not shown). The addition of the G36E substitution was not able to rescue the insensitivity of the *ein2-1* mutation when C-terminally tagged, but it was able to rescue when N-terminally tagged (data not shown). This could also suggest that the dosage of EIN2 is important and that perhaps the GFP tag at the C-terminus is somehow interfering with the proper functioning of the C-terminal domain.

The EIN2 N-terminal Domain Functions *in cis* to Regulate the EIN2 C-terminal Domain

In further exploring the EIN2 self-interaction (Figure 3.11-3.17), I was curious as to whether the EIN2 N-terminal domain can function *in trans* to regulate the C-terminal domain. To test this hypothesis, I utilized the insensitivity of the *ein2 G36E* mutant and created transgenic lines where I overexpressed just the N-terminal domain (residues 1-524) of both wild type *EIN2* and *EIN2 G36E* in an *ein2 G36E* mutant background. The *ein2 G36E* mutant expresses a full length EIN2 protein (Figure 3.5), so if the EIN2 N-terminal domain is able to function *in trans*, then over-expressing just the wild-type EIN2 N-terminal domain would allow the C-terminal domain of *ein2 G36E* (from the background) to be cleaved and translocated to the

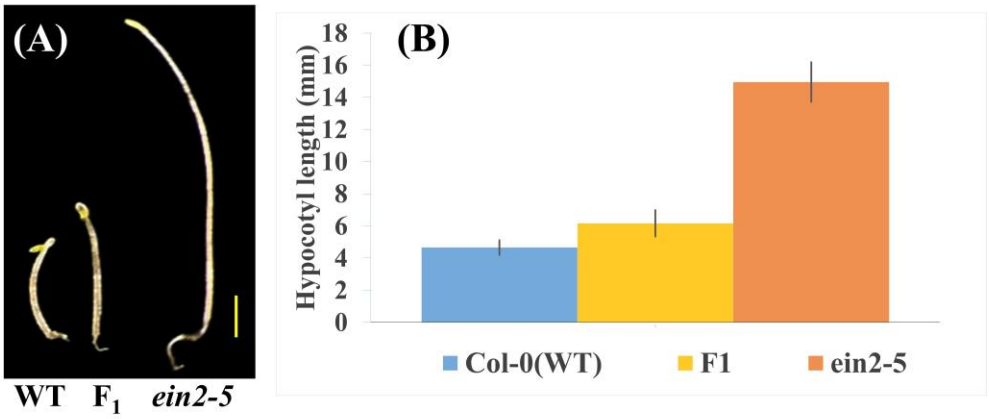

Figure 3.18. The F_1 progeny from the *ein2-5* backcross also showed partial dominance. The *ein2-5*, null allele, when backcrossed to Col-0 (wild-type) conferred partial insensitivity to ethylene, when grown on plates containing 20 µM ACC. A representative image of the seedlings are depicted in (A). F_1 bar and (B) is representative of hypocotyl measurements from two independent crosses, totaling 30 seedlings. Seedlings were grown in the dark for 4 days before photographed and measured using Image J. Scale bar is 2 mm. Error bars represent standard deviation.

nucleus causing full or partial rescue of the ethylene insensitivity.

However, overexpression of wild-type EIN2 N-terminal domain (Figure 3.19) did not cause partial rescue and the plants remained insensitive. Addition of the EIN2 G36E substitution did not have any effect either (Figure 3.19b). A similar result was observed from overexpression of the N-terminal domain of both wild-type and EIN2 G36E in an *ein2-5* null background (Figure 3.20). This suggests that the N-terminal domain of EIN2 does not function *in trans* to regulate the C-terminal domain in ethylene signaling, but instead functions *in cis*. Therefore, one N-terminal domain of EIN2 regulates one C-terminal domain, on the same molecule. However, questions still remain, such as; Why is the *ein2 G36E* mutant insensitive to ethylene? How does the N-terminal domain regulate the C-terminal domain? What else can this G36E substitution tell us about the function of EIN2?

Regulation of the EIN2 C-terminal Domain is Affected by the G36E Substitution

How is the EIN2 C-terminal domain affected by the G36E substitution? When N-terminally tagged with YFP, EIN2 G36E was properly localized to the ER membrane (Figure 3.8). However, we may only be seeing some of the picture, since we can only observe the N-terminus of EIN2 with this tag. Therefore, to observe what happens to the C-terminal domain as well, I created a C-terminally tagged EIN2 construct, both wild-type and *EIN2 G36E,* which then I localized using onion epidermal cells. Without ethylene, wild-type EIN2 localizes to the ER membrane (Figure 3.21a) and was translocated to the nucleus upon ethylene treatment (Figure 3.21b). However, when the G36E substitution was introduced, the overall YFP signal

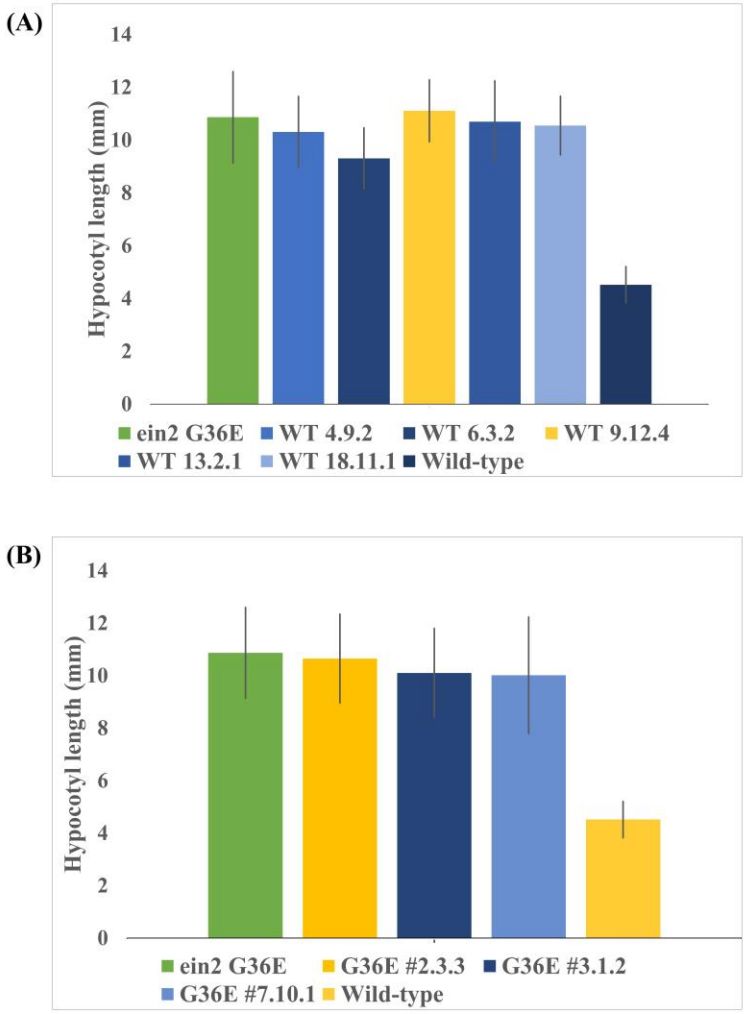

Figure 3.19. EIN2 N-terminal domain does not function *in trans* to regulate the C-terminal domain. Transgenic lines were created expressing just EIN2 N-terminal domain (residues 1-524) in an *ein2 G36E* mutant background. Wild-type EIN2 N-terminal domain was not able to rescue the 4 day-old etiolated ethylene insensitive phenotype of this mutant (A). Addition of the G36E substitution (B) similarly had no effect when grown on 20 µM ACC. For graph (A), five independent lines are shown, whereas three independent lines are shown for the graph in (B). Error bars represent standard deviation. Seedlings measured using Image J.

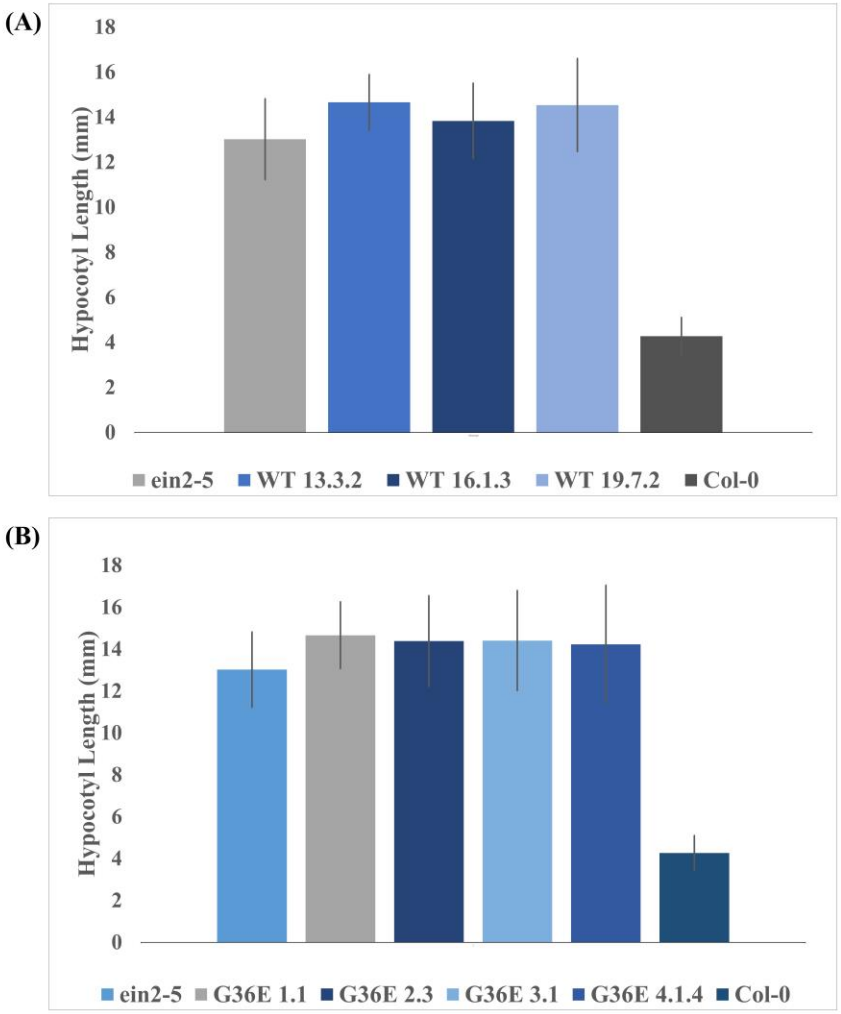

Figure 3.20. EIN2 N-terminal domain requires a C-terminal domain for the triple response phenotype. Transgenic lines were created, expressing just EIN2 N-terminal domain (residues 1-524), in an *ein2-5* null mutant background. Wild-type EIN2 N-terminal domain was not able to rescue the 4 day-old etiolated ethylene insensitive phenotype of this mutant (A). Addition of the G36E substitution (B) similarly had no effect when grown on 20 µM ACC. For graph (A), three independent lines are shown, whereas four independent lines are shown for the graph in (B). Error bars represent standard deviation. Seedlings measured using Image J.

was decreased compared to wild-type EIN2 (Figure 3.21), but there was no difference between the ethylene and untreated samples with the EIN2 G36E substitution (Figure 3.21c and d). This reduction in signal strength with EIN2 G36E compared to wildtype was much more severe than the reduction seen with the EIN2 protein level, in the *ein2 G36E* mutant compared to the EIN2 level in the wild-type (L*er*) plant (Figure 3.5). In fact, the signal was so low it was barely observable.

The EIN2 G36E signal was observed at the ER membrane, in the nucleus, and in the cytoplasm, regardless of ethylene treatment (Figure 3.21c and 3.21d). This suggests that the G36E substitution could be affecting the proper regulation of the EIN2 C-terminal domain, in that this substitution seems to be preventing proper nuclear localization, which would result in insensitivity. It is also possible that the G36E substitution is affecting the stability of EIN2, however, the Arabidopsis *ein2 G36E* mutant still expresses a full-length protein based on Western blotting (Figure 3.5) suggesting that altering stability cannot be the only result.

Since it looks as if the EIN2 G36E substitution is affecting the overall signal level of EIN2 C-terminal domain, at least in onion cells, I decided to test whether both the N and C- termini of EIN2 were affected at the same time in the same cell by simultaneously tagging both domains of EIN2. I created constructs expressing a fluorescent tag at each terminus of EIN2 (for both wild-type and EIN2 G36E) and transiently expressed them in onion epidermal cells. However, when observed under the microscope, the signal was extremely weak (for both EIN2 G36E and WT) and diffuse throughout the cell (data not shown). This suggests that the double-tagged

EIN2 might not localize properly. It could also suggest that the tags were causing EIN2 to be degraded, reducing the overall signal.

Discussion

ein2 G36E Confers Ethylene Insensitivity and is a Partially Dominant Allele

This *ein2 G36E* mutant has been useful in providing insight into the function of the N-terminal domain of EIN2. Currently, there are no published point mutations in the N-terminal domain. One possibility is that it plays a role in an undiscovered function of EIN2 and therefore has not been isolated from any genetic screens yet. However, the ethylene insensitivity of the *ein2 G36E* mutant indicates the N-terminal domain of EIN2 is a positive regulator of ethylene signaling and therefore is important in positively regulating the C-terminal, ethylene signaling domain.

Since the G36E substitution falls in a highly conserved motif in EIN2s (Figure 3.1) in the N-terminal Nramp-like domain, important for metal transport in Nramp proteins, and the *ein2 G36E* mutant is ethylene insensitive, it could suggest that metal transport may be involved in ethylene signaling. Chapter 4 provides data suggesting EIN2 can function as a metal transporter. However, it is also possible that although this substitution happens to fall in a highly conserved motif and confers a partial ethylene response (Figure 3.6) that metal transport may also be partially affected. Yet another possibility is that this particular substitution does not play a role in metal transport by EIN2.

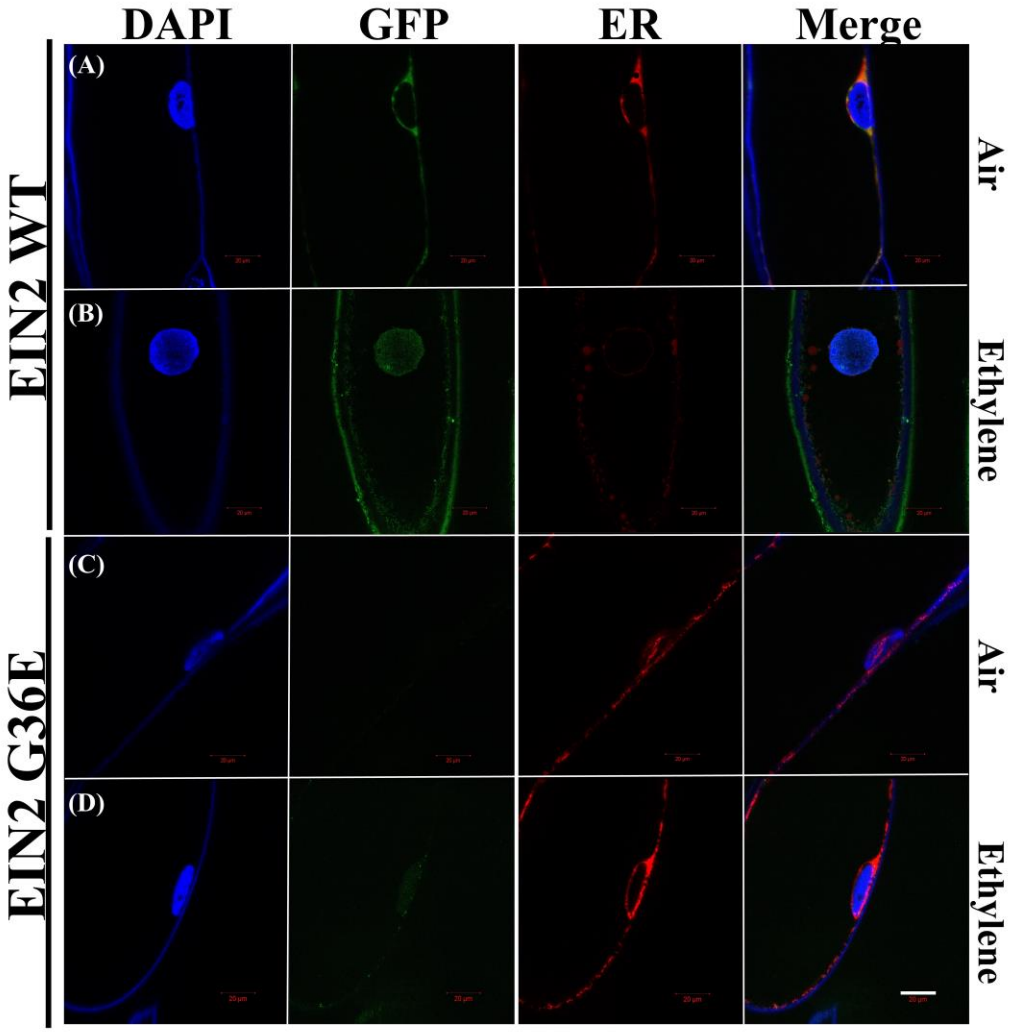

Figure 3.21. The EIN2 G36E substitution causes a misregulation of EIN2 C-terminal domain. When tagged at the C-terminus, full length wild-type EIN2 localized to the ER in the absence of ethylene (A) and a portion was translocated to the nucleus in the presence of 100 ppm ethylene for 3 hours (B), when visualized in onion epidermal cells. The addition of the EIN2 G36E substitution resulted in a reduction in overall signal level (C and D), and localization to the ER, nucleus, and cytoplasm, both without ethylene (C) and with ethylene treatment (D). Merged image shows DAPI (20 µg/mL), ER marker (HDEL::mCherry), and YFP (BiFC signal), visualized using

confocal microscopy. Scale bar = 20 μm. Panels A and B are also shown in Chapter 2, Figure 2.5.

The *ein2 G36E* Mutant is Not a Null Allele

Since the *ein2 G36E* mutant produces a full length EIN2 protein (Figure 3.5) and has some residual ethylene response (Figure 3.6) suggests the *ein2 G36E* mutant is not a null allele. Interestingly, there was a slight difference in protein size between *ein2 G36E* and L*er* (Figure 3.5). It was so subtle that this size difference was only observed on a gradient gel. Perhaps the size difference could be due to a lack of protein modifications, such as phosphorylation, glycosylation, or lipidation. However, since EIN2 is usually not phosphorylated in the presence of ethylene, it is possible that the EIN2 G36E substitution causes EIN2 to form a different confirmation than wild type, leading to slightly different protein modifications, leaving the correct sites unavailable for the necessary protein interactions or modifications.

Without ethylene, EIN2 is phosphorylated at specific sites by CTR1 (Ju et al., 2012). This does not rule out the possibility that there are other phosphorylation sites normally phosphorylated by other proteins that have not yet been identified, and as a result of the EIN2 G36E substitution, those sites are no longer available due to perhaps a different confirmation. Loss of phosphorylation like this could also result in a smaller sized EIN2 protein in the *ein2 G36E* mutant.

Another possibility is that the EIN2 G36E substitution is causing some proteolytic cleavage of EIN2, resulting in a smaller band in the presence of ethylene. I do not think this is the case, mainly due to the location of the antibody used in the Western Blot. The antibody (which I tested for Agrisera) recognizes a peptide very close to the C-terminus of EIN2, 20 residues away, and the *ein2 G36E* mutant showed

a full-length EIN2 protein band (Figure 3.5). If the protein was cleaved, it would most likely be cleaved at the very C-terminus, where the antibody binds. The difference in band size shift between the wild-type and ACC treated samples, detected by the antibody on a Western Blot (Figure 3.5), could not account for the amount cleaved off the C-terminus of EIN2 and still result in a protein that would be detected. Therefore the size difference could be due to some difference in protein modifications or how the protein is folded. This G36E substitution does not seem to disrupt the known protein interaction EIN2-CTR1 (Figure 3.9), but that does not rule out the possibility that other protein interactions are disrupted due to a change in confirmation.

However, the EIN2 G36E expression *in planta* was similar to wild-type (Figure 3.8) when tagged at the N-terminus, suggesting the EIN2 N-terminal domain is most likely folding properly, stable, and cleavage is not occurring from the N-terminal side. The EIN2 C-terminal domain is a bit more unstable, as seen from the difference in localization pattern when tagged at the C-terminus (Figure 3.21), suggesting the EIN2 G36E substitution is causing at least some degradation of EIN2 C-terminal domain. However, degradation could account for the slightly lower level of EIN2 present in the *ein2 G36E* mutant (Figure 3.5).

There was some nuclear EIN2 G36E protein observed, when tagged at the C-terminus (Figure 3.21c and 3.21d) but the overall GFP signal was seen at a very low level, present in both the ER and in the nucleus. One possibility is that the low level of EIN2 protein present in the nucleus with EIN2 G36E may be below the level to stimulate an ethylene response. I had to increase the laser power to 100% to be able to pull out a GFP signal above the background. This was not the case for the wild-

type EIN2. It is possible that in wild-type EIN2, there is also some EIN2 in the nucleus at 100% with no ethylene, but it is not enough to stimulate an ethylene response. It is only when ethylene is added that EIN2 is increased (as seen in Figure 3.15, when EIN2-EIN2 levels increase with ethylene) that the threshold is reached and an ethylene response is achieved. It is possible that the 35S promoter is functioning to amplify the partial response of the *ein2 G36E* mutant and the nuclear signal is that partial response being visualized (Figure 3.6; Figure 21c and 21d).

Another possibility is that the nuclear fragment in the *ein2 G36E* mutant may be the wrong size. It is possible that the EIN2 G36E substitution is causing EIN2 to be miscleaved, perhaps due to a different confirmation/modification, and therefore the ethylene signaling cascade is not further activated. Both of these possibilities could account for the ethylene insensitive of the *ein2 G36E* mutant.

EIN2 Interacts With Itself *in planta* and in Yeast

It is unclear as to why EIN2 self-interacts and how this self-interaction relates to ethylene signaling. However, many of the proteins in the ethylene pathway form dimers such as the ethylene receptors (Schaller et al., 1995; Gao et al., 2008), the CTR1 kinase domain (Mayerhofer et al., 2012) and EIN3 (Solano et al., 1998). Further exploration into this self-interaction could help us to gain better insight into how EIN2 functions and how it relates to how EIN2 functions in ethylene.

Since the EIN2-EIN2 self-interaction remained at the ER and became stronger with ethylene treatment (Figure 3.15) this could suggest that the C-terminal YFP tag is interfering with the proper function of EIN2. Perhaps EIN2 is not moving to the nucleus and/or not being cleaved like wild-type (Figure 3.21) due to some aspect of

the split YFP tag. However, Figure 3.21 also had a C-terminal tag, albeit a GFP tag. Perhaps this suggests that the EIN2 self-interaction is a mechanism to help EIN2 remain tethered to the ER membrane.

Another possibility is that when the EIN2 protein is induced, upon ethylene exposure, the EIN2 protein is first expressed as a full length protein at the ER membrane, which is what I am observing in Figure 3.15. This is consistent with what was observed in Qiao et al. (2009) where EIN2 levels were rapidly induced upon ethylene treatment. During ethylene treatment, the functional portion of EIN2 (C-terminal domain) is cleaved and moves into the nucleus, perhaps as a monomer, and therefore would not result in a BiFC signal.

Interestingly, the *ein2-9* substitution did seem to slightly enhance the EIN2-EIN2 self-interaction in yeast. The EIN2-9 self-interaction was slightly stronger than the wild-type EIN2 C-terminal domain self-interaction. Even more interesting was that the strongest interaction observed was with the wild-type EIN2 C-terminal domain and EIN2-9 (Figure 3.16) since this is not a natural situation. Perhaps this particular mutation enhances the EIN2 self-interaction, which could be necessary for EIN2 functioning, suggesting that the His1143 residue could be important or perhaps part of (or near) a critical motif involved in dissociation of EIN2 self-interaction. This could suggest that the *ein2-9* mutant and the H1143P substitution could be something for further exploration.

The N-terminal Domain of EIN2 Functions *in cis* to Regulate the C-terminal Domain

Since data suggests that the N-terminal domain is not functioning *in trans* to regulate the C-terminal domain, which indicates that it functions *in cis* (Figure 3.19). Ethylene is an essential plant hormone and required for many essential processes. It is feasible that a tightly stimulated response would be needed. If the N-terminal domain of EIN2 was functioning *in trans*, one EIN2 N-terminal domain could essentially activate many EIN2 C-termini, quickly overflowing the nucleus with an ethylene response. Since EIN2 functions seems to function in a haploinsufficient manner (Figure 3.18), that could quickly be disastrous for the cell.

But, if EIN2 functions *in cis* then there could be a slower and tighter control over the EIN2 response. EIN2 is induced by ethylene (Figure 3.15; Qiao et al., 2009), so one EIN2 N-terminal domain regulates the C-terminal domain of the same protein. Therefore it could potentially be easier to ensure the correct interactions, modifications, etc. occur to the C-terminal domain of EIN2 before it is translocated to the nucleus. This would ensure a more efficient yet tighter control over a central regulator protein, in an essential hormone signaling pathway.

The Stability of the EIN2 C-terminal Domain is Affected by the G36E Substitution

The localization of EIN2 G36E when tagged at the C-terminus (Figure 3.21) gave some clues into the defect in EIN2 caused by the EIN2 G36E substitution. Perhaps the C-terminal domain is cleaved and translocated into the nucleus less efficiently compared to wild-type. Another possibility is the G36E substitution could

be causing EIN2 to be miscleaved and therefore misregulated. Miscleavage is less likely since miscleavage could result in a smaller sized protein. However, as stated before, the *ein2 G36E* mutant showed a full length EIN2, or very close to full length EIN2, band on a Western Blot (Figure 3.5). Since the anti-EIN2 antibody detected a peptide very close to the C-terminal domain, this antibody would not detect any cleaved EIN2 fragments. Therefore, most likely the *ein2 G36E* mutation causes a misregulation of the C-terminal domain.

The misregulation of EIN2 C-terminal domain, caused by the G36E substitution, could account for the slight reduction in the signal in the *ein2 G36E* mutant (Figure 3.5) and the reduced signal in the C-terminally tagged construct (Figure 3.21 c and d). In this case, EIN2 G36E protein would be produced, just not sent to the nucleus and processed as it is supposed to be, resulting in the insensitive phenotype seen in the *ein2 G36E* mutant (Figure 3.2). When tagged at the C-terminus, the EIN2 G36E localized signal to the ER, the nucleus, and to the cytoplasm (Figure 3.21c and 3.21d). This disperse localization pattern and slight nuclear localization could account for the slight activation of the ethylene response in the *ein2 G36E* mutant, since the seedling became slightly longer with the addition of AVG and slightly shorter with ACC (Figure 3.6).

The signal level was also greatly reduced in the C-terminally tagged EIN2 G36E samples compared to wild-type (Figure 3.21). This is in contrast to N-terminally tagged EIN2, which showed similar EIN2 protein signal levels for both wild type and EIN2 G36E (Figure 3.8). This could suggest that adding a C-terminal tag interferes with the function of EIN2 C-terminal domain. However, wild-type

EIN2 was still able to translocate to the nucleus with the addition of ethylene (Figure 3.21b) suggesting a tag on the C-terminus, in this case, did not interfere with function. This suggests that the G36E substitution has an effect on how the C-terminal domain of EIN2 is regulated. Therefore, the G36E substitution tells us that the N-terminal domain of EIN2 is a necessary component of the ethylene signaling pathway, because it regulates the C-terminal domain, although cannot function alone.

Materials and Methods

Plant Growth and Conditions– *Arabidopsis thaliana* ecotype Landsberg (L*er*, used as the wild-type) because it is the background of the *ein2 G36E* mutant, unless otherwise stated. For the triple response assay, seeds were plated onto Murashige and Skoog (MS) media (Caisson Labs) containing 0.8% agar. For ethylene response, 20 μM ACC (Sigma Aldrich) was added to the plates. To block the ethylene response the ethylene inhibitor 10 μM AVG (Sigma) was added to the plates. Plates were cold stratified at 4 C, in the dark, for 4 days prior to the 20 C dark treatment for 4 days. Seedlings were photographed and hypocotyls were measured using the ImageJ software (https://imagej.nih.gov/ij/). For the triple response assay at different temperatures, the length of growth changed. So, after cold stratification, plates were grown in the dark for 19 days at 9C, 11 days at 13C or 2 days at 28C, before photographing. For the senescence assay, three-week old plants were placed in a dark gas chamber with 100 ppm ethylene for 3 days. Untreated plants were also place in a dark gas chamber with an equivalent injection of 100 ppm ambient air for 3 days.

Protein Sequence Alignment – Protein Sequences of monocot and dicot EIN2s were obtained from the NCBI database using the AtEIN2 protein sequence as a query. The

green algae *Chlamydomonas reinhardtii* and the vascular moss *Selaginella moellendorffii* were used as evolutionary outgroups. Sequences were aligned using MUSCLE (Edgar, 2004) (http://www.ebi.ac.uk/Tools/msa/muscle).

Western Blot - Microsomal fraction was extracted from 4-day old etiolated seedlings as done in the Ju et al. (2012) study. The L*er* (wild-type) served as the control for the *ein2 G36E* mutant and the Col-0 (wild-type) served as the control for the *ein2-5* null mutant. Protein samples were incubated for 1 hr at 37 C before separation by 4-20% gradient SDS-PAGE (Bio-Rad). An identical gel was loaded and used for Coomassie Blue stain. Proteins were transferred to a PVDF membrane via semi-dry transfer and immunoblotted with a 1:1000 dilution of an anti-EIN2 antibody (Agrisera).

Bimolecular Fluorescence Complementation (BiFC) in Onion Epidermal Cells – The full-length coding sequence for *EIN2* was transferred from pDONR221 into the pSPYCE-35S and pSPYNE-35S vectors (Schütze et al., 2009). The EIN2 full-length (with no stop codon) construct was created by PCR-amplifying the *EIN2* coding sequence from pEIN2 (Arabidopsis Biological Resource Center, ABRC) using same primers listed Chapter 2 (EIN2 pDONR221 no stop) and cloned into the pDONR221 vector. Dr. Mandy Bish created the *CTR1* pDONR221 and construct and it was transferred to the pSPYNE-35S vector by David Lin. The G36E substitution was added via site directed mutagenesis (Agilent Technologies, see EIN2 G36E mutagenesis primers), to the full-length *EIN2* pDONR221 construct and then *EIN2 G36E* was transferred from pDONR221 to the pSPYNE-35S and pSPYCE-35S vectors (Schütze et al., 2009). Onion epidermal cells were transformed via particle bombardment (BioRad Helios Gene Gun) using white onions purchased from the

grocery store, as described in Hollender and Liu (2010). Bullets were prepared for the above construct together with an ER-marker (ER-rB, RFP-HDEL, Nelson et al., 2007) obtained from the ABRC. After room temperature incubation in the dark for 16 hrs, onion epidermal pieces were incubated in 20 μg/mL DAPI for 15 min before interactions were visualized using a LSM 710 confocal microscope. For ethylene treatment, onion pieces were placed in jars filled with 100 ppm ethylene gas for 3 hrs prior to DAPI treatment and slides remained in ethylene during 15 min incubation with DAPI.

Split Ubiquitin EIN2 Self-Interaction in Yeast – The full-length *EIN2* pDONR221 constructs generated above (both wildtype and *EIN2 G36E*) were used to create the EIN2 yeast 2-hybrid expression constructs. Both full-length wildtype and EIN2 G36E were transferred from pDONR221 to pMETYCgate and pX-Nubgate vectors (Obrdlik et al., 2004). The full-length *EIN2* pDONR221 constructs were used as a template to PCR amplify smaller *EIN2* fragments. Other N-terminal fragments of *EIN2* were PCR amplified using primers listed below. The N-terminal fragment encoding residues 1-481 and the fragment encoding residues 1-524 were cloned into the pDONR221 vector (both wildtype *EIN2* and *EIN2 G36E*) and transferred to pMETYCgate and pX-Nubgate vectors (Obrdlik et al., 2004). Constructs were transformed into the THY.AP4 yeast strain. For full-length EIN2 self-interaction, split Ub interactions were selected on plates lacking histidine, methionine, and adenine. Both N-terminal fragments required the addition of 50 μM Met and either 50 mM or 5 mM 3-AT for the 1-481 fragment or the 1-524 fragment, respectively. Yeasts were spotted in serial dilutions (10-1 each) on both growth control (only lacking leucine and tryptophan)

and selection plates, then grown at 30C for two to four days. The selection plate for the EIN2 N-terminal fragment (1-481) was grown at 30 C for 12 days.

Primer name	Forward or Reverse	Primer Sequence (5'-3')
EIN2 1-481 pDONR221	F	GGGGACAAGTTTGTACAAAAAAGCAGGCTATATGGAAGCTGAAATTGTGAATGTG
	R	GGGGACCACTTTGTACAAGAAAGCTGGGTCTAAAGCATTTTGAGCATCCATG
EIN2 1-524 pDONR221	F	GGGGACAAGTTTGTACAAAAAAGCAGGCTATATGGAAGCTGAAATTGTGAATGTG
	R	GGGGACCACTTTGTACAAGAAAGCTGGGTCGACCGAGCTAGTAACAGACGTAG
EIN2 G36E mutagenesis	F	GTCGGATATATTGATCCCGAGAAATGGGTTGCAAATATC
	R	GATATTTGCAACCCATTTCTCGGGATCAATATATCCGAC

Subcellular Localization of EIN2 in Onion Epidermal Cells- To create the 35S-*EIN2-GFP* and the *35S-EIN2-GFP* constructs, the full-length coding sequence (with no stop codon) was transferred from the EIN2 no stop pDONR221 and the *EIN2 G36E* no stop pDONR221 constructs to the pEarleyGate103 vector (Earley et al., 2006, obtained from ABRC). In order to create the *35S-YFP-EIN2* and *35S-YFP-EIN2 G36E* constructs, the full length coding sequence (with a stop codon) was transferred from the corresponding pDONR221 vector to the pEarleyGate104 vector (Earley et al., 2006, obtained from ABRC). The pEarleyGate constructs were transformed into white onions, purchased from the grocery store, using particle bombardment with a Helios Gene Gun (Bio-Rad) as described in Hollender and Liu (2010). Bullets were prepared for the above constructs together with an ER-marker (ER-rB, RFP-HDEL, Nelson et al., 2007) obtained from the ABRC. After room temperature incubation in the dark for 16 hrs, onion epidermal pieces were incubated in 20 μg/mL DAPI for 15 min before interactions were visualized using a LSM 710 confocal microscope. For ethylene treatment, onion pieces were placed in jars filled

with 100 ppm ethylene gas for 3 hrs prior to DAPI treatment, and slides remained in ethylene during 15 min incubation with DAPI.

Yeast 2-Hybrid Assays With the EIN2 C-terminal Domain – The EIN2 self-interactions with the EIN2 C-terminal domain were tested using the full-length EIN2 pDONR221 (with no stop) construct as a template. Fragments destined for the pACTII vector were PCR amplified with the addition of *XmaI* and *EcoRI* restriction sites and with *Xmal* and *SalI* restriction sites for the pLEXA-NLS vector (Clark et al., 1998), using the primers below. All fragments were first cloned into the pGEMT vector (Promega) and then digested with either *XmaI* and *EcoRI* or *XmaI* and *SalI* and ligated into the corresponding pACTII or pLEXA-NLS (pBTM116) vector. The EIN2-9 substitution (encoding the H1143P residue substitution) was introduced via site directed mutagenesis (Agilent Technologies) into the 516-1294 pACTII and pLEXA-NLS constructs using primers listed below. All plasmids were transformed into the L40 yeast strain. Yeast 2-hybrid interactions were selected on plates lacking histidine and with varied amounts of 3-AT; selection plates for self-interaction with the 516-1294 fragment contained 1 mM 3-AT, both 516-780 and 893-1294 contained 10 mM 3-AT, and selection plates for the EIN2-9 substitution contained 5 mM 3-AT. Yeasts were spotted in serial dilutions (10-1 each) on both growth control (only lacking leucine and tryptophan) and selection plates, then grown at 30C for two to four days.

Primer name	Forward or Reverse	Primer Sequence (5'-3')
516-1294 pACTII	F	CCCGGGAGATACTACGTCTGTTAC
	R	GAATTCTCAACCCAATGATCCGTACG
516-1294 pLEXA	F	CCCGGGAATGGATACTACGTCTGTTACTAGC
	R	GTCGACTCAACCCAATGATCCGTACG
516-780 pACTII	F	CCCGGGAGATACTACGTCTGTTAC
	R	GAATTCTCACAACATCTGCATACGG
516-780 pLEXA	F	CCCGGGAATGGATACTACGTCTGTTACTAGC
	R	GTCGACTCACAACATCTGCATACGG
893-1294 pACTII	F	CCCGGGAATGTCGCGACAATCTGAAAG
	R	CTGCAGTCAACCCAATGATCCG
893-1294 pLEXA	F	CCCGGGAATGTCGCGACAATCTGAAAG
	R	GTCGACTCAACCCAATGATCCGTACG
EIN2-9 mutagenesis	F	CAAGTCAAGGACACGGGGAATGCACCAAACTCC
	R	GGAGTTTGGTGCATTCCCCGTGTCCTTGACTTG

Creation of Stably Transformed Arabidopsis Lines-All transgenic lines were transformed with either *35S-EIN2 (1-524)-GFP* or *35S-EIN2 G36E (1-524)-GFP*. The coding sequence of EIN2 N-terminal domain (encoding residues 1-524) both wildtype and containing the G36E substitution were transferred from the pDONR221 vector to the pEarleyGate103 vector (Earley et al., 2006). The pEarleyGate103 constructs were transformed into the *Agrobacterium tumefaciens* strain GV3101, and then Arabidopsis plants were transformed using the floral dip method (Clough and Bent, 1998) into L*er* wildtype, *ein2 G36E* and *ein2-5* mutant backgrounds. Transformants were selected using the herbicide Basta (Bayer Crop Science). Homozygous lines obtained in the T3 generation and phenotypes screened, using a triple response assay, in the T4 generation (for transformants with a L*er* or *ein2 G36E* background) or T3 generation (for transformants with an *ein2-5* background).

Chapter 4: Evidence for Divalent Metal Ion Transport by the EIN2 N-terminal Domain

Introduction

Since the N-terminal domain of EIN2 shows homology to Nramp metal ion transporters, the question remained as to whether EIN2 is capable of metal transport. However, to my knowledge, no transport activity has been shown (Alonso et al., 1999; Thomine et al., 2000; Thomine and Schroeder, unpublished).

Nramp Metal Ion Transporters in *E. coli* and *S. cerevisiae*

Nramps (Natural resistance-associated macrophage protein) are a family of highly conserved metal ion transporters, found in all species from bacteria to humans (Nevo and Nelson, 2006). In general, Nramp proteins are broad range divalent cation metal transporters, but their subcellular localizations and metal specificities differ.

EIN2 shows homology to the *E.coli* Nramp homolog, MntH A (Manganese transport system of *E. coli*, H^+ -dependent), a broad range divalent metal transporter with a preference for Mn^{2+} and Fe^{2+} (Makui et al., 2000). Studies suggest that MntH functions as a pH dependent protein symporter found at the cell inner membrane (Makui et al, 2000; Courville et al., 2004).

Site-directed mutagenesis studies have revealed the function of critical residues and highly conserved Nramp motifs within MntH. For example, using this technique, it was discovered that the DPGN motif, highly conserved among all Nramp proteins (found within the first transmembrane domain of MntH, Figure 4.1), was important for metal transport. Altering any of the residues within this DPGN

motif hindered transport ability of MntH (Couville et al., 2004; Haemig and Brooker, 2004; Chaloupka et al., 2005). This DPGN motif (residues 34-37 of MntH) is believed to play a role in metal binding along with other conserved residues in transmembrane domain 3 (Asp109 and Glu112) (Haemig and Brooker, 2004).

Saccharomyces cerevisiae Nramp Proteins

Yeast contains three Nramp homologs, SMF1-3. SMF1 (SUPRESSOR OF MIF1) is mainly a Mn^{2+} and Fe^{2+} transporter, which under low Mn^{2+}conditions expression of SMF1 is induced and localizes to the plasma membrane in order to facilitate Mn^{2+} uptake into the cell (Supek et al., 1996; Portnoy et al., 2000). However, when Mn^{2+} levels are high SMF1 is translocated to internal membranes or the vacuole for degradation (Portnoy et al., 2000). Expression of SMF1 was also found to be downregulated under toxic Mn^{2+} conditions (Jensen et al., 2009) further supporting a role of SMF1 in manganese homeostasis. SMF2 was found to localize to intracellular vesicles and is believed to transport Mn^{2+} towards the cytoplasm (Luk and Culotta, 2001). Similar to other Nramp proteins, SMF2 is a broad range divalent metal transporter and has been shown to play a role in transport of Mn^{2+}, Fe^{2+}, Co^{2+} and Cu^{2+} (Portnoy et al., 2000; Liu et al, 1997; Cohen et al., 2000). SMF1 and SMF2 do not have redundant functions (Luk and Culotta, 2001; Liu et al., 1997). SMF2 provides Mn^{2+} to target proteins, such as SOD2 (SUPEROXIDE DISMUTASE 2) in the mitochondria (Luk and Culotta, 2001). Another potential target of SMF2 is PMR1 (PLASMA MEMBRANE ATP-ASE RELATED 1), which provides the required Mn^{2+} and Ca^{2+} co-factors to sugar transferases in the Golgi (Rudolph et al., 1989; Luk

and Culotta, 2001), whereas SMF1 functions to bring Mn^{2+} into the cell (Supek et al., 1996).

Arabidopsis Nramp Proteins

Arabidopsis contains six Nramp proteins (AtNramp 1-6) plus EIN2, where the N-terminal domain of EIN2 shows less than 20% identity with the other Nramp proteins. No other Nramp protein contains a C-terminal domain like EIN2 does.

Since Arabidopsis contains six Nramp transporters, functional redundancy has been suggested, however they localize to different subcellular membranes and have different metal specificities. For example, AtNramp1 is a plasma membrane localized transporter of Fe^{2+}, Mn^{2+} and Cd^{2+}, whereas AtNramp2 may not play an important role in Fe^{2+} transport (Curie et al., 2000; Lanquar et al., 2000; Thomine et al., 2000; Cailliatte et al., 2010). The role of AtNramp1 in Fe^{2+} transport has been somewhat controversial (Curie et al., 2000, Thomine et al, 2000, Cailliatte et al, 2009). AtNramp3 and AtNramp4 localize to the vacuolar membrane and also have been shown to play a role in the transport of Fe^{2+}, Mn^{2+}, and Cd^{2+}, but only AtNramp4 plays a role in Zn^{2+} transport (Thomine et al., 2000; Lanquar et al., 2010; Lanquar et al.,2005; Lanquar et al., 2004). Only AtNramp1, AtNramp3 and AtNramp4 have been definitively localized subcellularly in Arabidopsis.

Hints of Metal Transport by EIN2

Since the N-terminal domain of EIN2 shows homology to Nramp metal ion transporters, whether EIN2 is capable of metal transport has been a question plaguing the ethylene field for almost two decades, ever since Arabidopsis EIN2 was identified in 1999. To my knowledge, no studies have been successful in demonstrating

transport ability of EIN2 (Alonso et al., 1999; Thomine et al., 2000; Thomine and Schroeder, unpublished). However, there have been hints that EIN2 may function like an Nramp metal transporter. For example, the *ein2-1* mutant showed enhanced sensitivity to lead, suggesting a role for *EIN2* in lead resistance (Cao et al., 2009) however, transport of lead was not tested. This is similar to other Nramp mutants, such as *nramp1,* which is hypersensitive to Mn^{2+} deficiency (Cailliatte et al., 2010), or *nramp3 and nramp4,* again more sensitive to Mn^{2+} as well as Fe^{2+} deficiency (Lanquar et al., 2005; Lanquar et al., 2010).

Bacterial susceptibility is another example of Nramp protein function. Mutants in Arabidopsis *nramp3,* and *nramp4* were shown to be more susceptible to *Erwinia chrysanthemi* infection (Segond et al., 2009). Similarly, *ein2* mutants showed increased susceptibility to *Botrytis cinerea* (Thomma et al., 1999; Ferrari et al., 2003) and *Pythium irregular* (Adie et al., 2007) infections. Taken together this could suggest *EIN2* may have some conserved Nramp functions.

The EIN2 G36E Substitution

The *ein2 G36E* mutant contains a missense substitution in a highly conserved motif in EIN2 proteins (discussed in Chapter 3). This glycine residue is also highly conserved among all Nramp proteins (Figure 4.1), and is part of a highly conserved motif (DPGN) that is believed to function as part of the metal binding site of the Nramp transporter (Haemig and Brooker, 2004). In fact, if this particular glycine (or any part of the DPGN motif) was changed (for example to a G36A or G36P), transport ability of MntH was greatly reduced (Haemig and Brooker, 2004). Similarly, in that same study, Haemig and Brooker (2004) found substitution of any

other residues within this DPGN motif disrupted transport. EIN2 consists of a DPGK motif (Chapter 3 – Figure 3.1) however, to my knowledge, this asparagine to lysine substitution has not been tested in *E. coli*.

Since the *ein2 G36E* mutant confers ethylene insensitive (Chapter 3-Figure 3.2) and this particular substitution falls in a highly conserved protein motif important for metal transport, it is possible that metal transport by EIN2 could suggest a role for metal transport, via EIN2, in ethylene signaling. This substitution could shed light on a new function of EIN2, possibly in terms of ethylene signaling.

However, the location of this DPGN motif seems to differ compared to MntH. In MntH, where many of the site-directed mutagenic studies were done and transport was found to be disrupted, using proteolytic cleavage assays as well as reporter fusion assays, the DPGN motif was found within the first transmembrane domain (Makui et al., 2000; Courville et al., 2004). However, in human DCT1, the DPGN motif was predicted to only be partially in the first transmembrane domain (Nevo, 2008). The DPGK motif in EIN2 is predicted (ARAMEMNON) to be outside the first transmembrane domain (in the first loop region, in the lumen). It is possible that this difference in membrane localization of this critical metal binding motif could suggest an evolutionary difference in their use of this motif for metal binding. It is also possible that predicted motif locations of DCT1 and EIN2 differ from each other as well as MntH due to a difference in modeling.

Results

Part 1 – EIN2 Expression and Possible Metal Transport in *E. coli*

Testing metal transport *in planta* could be rather difficult since besides EIN2, Arabidopsis contains six Nramp homologs (AtNramp1-6), in addition to numerous other metal transporters. Since EIN2 shows homology to the *E. coli* Nramp homolog MntH A (Figure 4.1), which localizes to the inner cell membrane (Makui et al., 2000), *E. coli* could be a useful expression system to test whether EIN2 is capable of metal transport. It is not complicated by internal membranes, such as eukaryotic systems, and only has one Nramp homolog, MntH A. Therefore, I decided to pursue expression of the EIN2 N-terminal, Nramp-like, domain in *E. coli*, as a way to test whether EIN2 is also capable of transporting a divalent cation.

The N37K Substitution Does Not Disrupt the Ability of MntH to Transport a Metal, so Perhaps There is Hope for EIN2.

One highly conserved Nramp motif that is important for metal transport is the DPGN motif (Courville et al., 2004). EIN2 contains a DPGK in place of the DPGN motif (Figure 4.1), and the effect of this N37K substitution on metal transport in other organisms is unknown. It is possible that previous attempts to demonstrate metal transport ability with EIN2 have been unsuccessful because EIN2 contains a DPGK motif In the *E. coli* Nramp, MntH, substituting this particular asparagine residue with a serine, glutamine, or aspartate disrupted metal transport (Haemig and Brooker, 2004). It is possible that changing it to a lysine will have a different effect.

To test whether or not metal ion transport could possibly be disrupted due to this difference in motifs, I introduced a missense mutation encoding an N37K

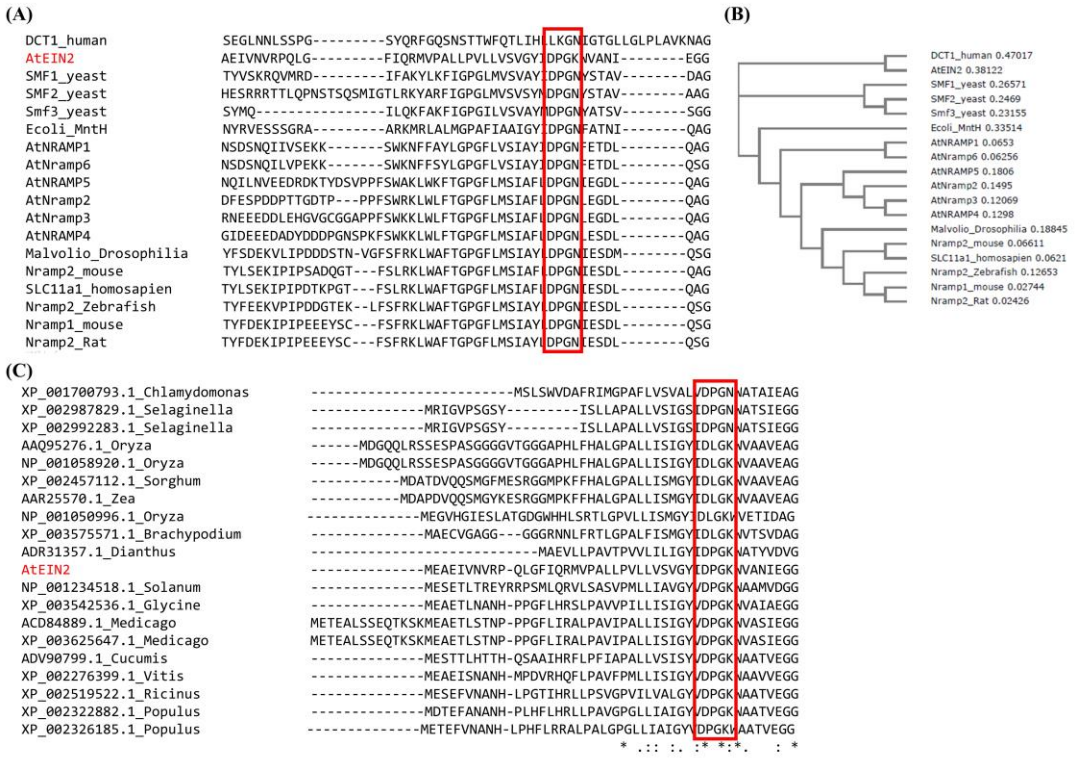

Figure 4.1. EIN2 shows homology to Nramp metal ion transporters. (A) Protein sequence alignment of EIN2 (AtEIN2 highlighted in red) and other Nramp proteins. The highly conserved DPGN motif is highlighted with a red box, but EIN2 contains a DPGK motif. (B) Phylogenetic tree of EIN2 and other Nramp proteins, demonstrating EIN2 is similar to *E. coli* MntH but diverged from the Arabidopsis Nramp proteins. (C) Protein sequence alignment of EIN2 sequences from vascular plants, demonstrating the conserved DPGK motif (also highlighted with a red box) in EIN2 proteins. Also shown in Chapter 3, Figure 3.1. Alignments were created using MUSCLE (Edgar, 2004) and the phylogenetic tree is a nearest neighbor joining tree without distance corrections. The calculated branch lengths are listed.

substitution into the *MntH* DNA sequence. To test for transport ability, I transformed this altered MntH N37K into an SL93 *E. coli* strain, also lacking MntH, and used a MICKEY (Metal Ion Compensation of Killing Efficiency and Yield) assay to test for growth inhibition in the presence of a high concentration of metal (Makui et al., 2000).

With the MICKEY assay (Makui et al., 2000), a lawn of bacteria is spread on a minimal media plate, in a very thin top coat layer. A small filter paper disk imbibed with a high concentration of metal solution is placed in the center of the plate. If the expressed protein is able to transport the metal then the growth of the *E. coli* around the disk would be inhibited, thus the "ring of death" would increase. The larger the difference the in "ring of death" between induced and non-induced samples, the better the protein is at transporting a metal.

This SL93 strain (*hflB1*Ts) mutant contains a point mutation in a metal-dependent protease/chaperone (HflB) that requires addition of divalent metals in order to grow at a permissive (42^{o}C) temperature (Herman et al., 1995). Makui et al., (2000) used this SL93 strain to additionally knock out the *MntH* gene and subsequently overexpressed MntH, which using a MICKEY assay enhanced the uptake of divalent metals, restoring the temperature sensitive phenotype of the SL93 strain. This, as well as other functional assays, suggests MntH functions as a divalent metal transporter.

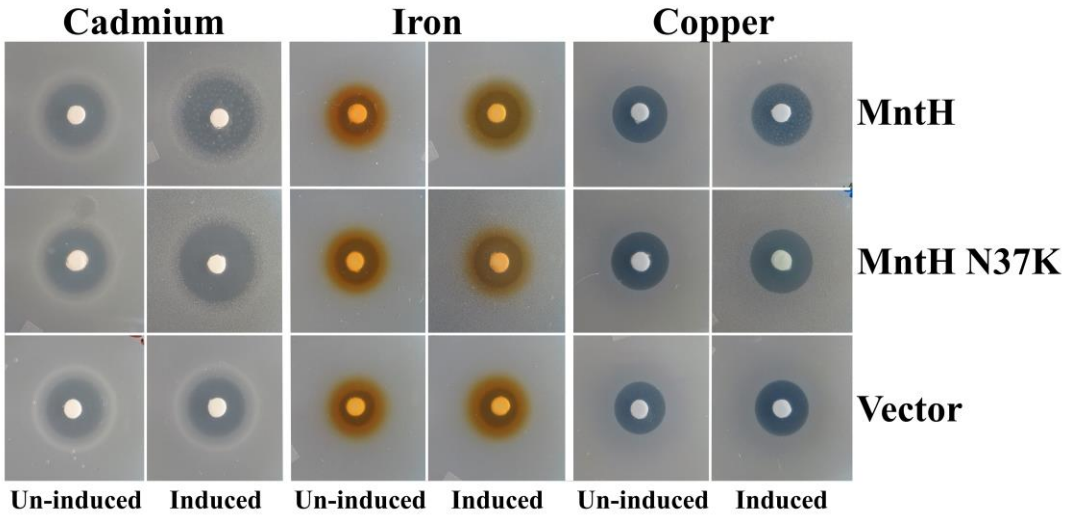

Figure 4.2. The N37K substitution does not prevent MntH from transporting a divalent metal. The MICKEY assay demonstrated that MntH can transport a divalent metal (Makui et al., 2000). EIN2 is different from other Nramp proteins in that it contains an N37K substitution (DPGK motif). When this N37K substitution was introduced into MntH, metal transport by MntH was not prevented. Constructs were transformed into the SL93 *E. coli* strain lacking the *mntH* gene. Empty vector (pBAD24) was used as a negative control, as were the un-induced cultures. These are representative sample plates, showing a close up of the filter paper disk imbibed with metal solution and the "ring of death". Bacteria was plated on 0.1% top agar GTA solution, with or without 0.06% arabinose (inducer). Filter paper disks were imbibed with metal solution (0.25 M $CdCl_2$, 1 M $FeSO_4$, or 1 M $CuSO_4$) then placed onto the top agar layer. Plates were incubated at 37 C for 16 hrs.

		MICKEY assay (mm)		
		- Arabinose	+ Arabinose	Δ
Iron	MntH	12.2±1.3	23.7±1.5	+11.7
	MntH N37K	15.7±1.2	17.3±0.6	+5.3
	Vector	11.7±0.6	12±1	-
Copper	MntH	18±1.4	20±1.4	+3
	MntH N37K	19.3±0.6	22.3±2.3	+5.3
	Vector	17±1.4	17±1.4	-
Cadmium	MntH	20.5±0.7	24±1.4	+5.5
	MntH N37K	22.7±0.6	26.8±1	+8.3
	Vector	20±0	18.5±2.2	-

Table 4.1. The N37K substitution in MntH does not disrupt metal transport of iron, copper or cadmium. Data for MICKEY assay shown in Figure 4.2. The effect of transport (Δ column) was calculated by subtracting the difference between induced empty vector (pBAD24) and induced samples (MntH or MntH N37K). Filter paper disks were imbibed with 1M $FeSO_4$, 1M $CuSO_4$, or 0.25M $CdCl_2$ and protein expression was induced with 0.06% arabinose. Values are calculated averages, where n = 3. The MntH N37K samples are a pool of three independent clones. The ring of death was measured in mm.

The addition of the N37K substitution did not disrupt divalent metal transport of iron, cadmium, or copper in MntH (Figure 4.2, Table 4.1). This suggests that the EIN2 N37K motif (Figure 4.1; Chapter 3, Figure 3.1) is compatible with transport of divalent metals. This would further support the possibility that EIN2 could be a metal transporter, or at least does not rule it out. I then proceeded to explore the possibility of EIN2 being a metal transporter using expression in *E. coli*.

Expression of the *Arabidopsis* EIN2 N-terminal Domain in *E. coli*

E. coli has an advantage in that it does not contain inner membranes, which can make eukaryotic protein localization more complicated. EIN2 shows homology to MntH A (Figure 4.1), so I decided to start by attempting to express both the full length and just the N-terminal domain of Arabidopsis EIN2 (residues 1-481) in an *E. coli* SL93 mutant, which contains a deletion of the MntH A gene (Herman et al., 1995; Makui et al., 2000). Unfortunately, however, when the expression of Arabidopsis EIN2 was probed using a Western Blot, the attached His epitope tags were undetectable for both full-length EIN2 and the truncated EIN2 N-terminal domain alone. This indicates that neither full-length EIN2 nor the truncated N-terminal domain alone were detectably expressed in *E. coli* (data not shown).

To aid in expression of Arabidopsis EIN2 in *E. coli*, an EIN2/MntH chimeric protein was created (termed "EIN2/MntH chimera"). Using gene synthesis (by Genewiz) we created a version of the N-terminal domain in which the first fifteen residues of the EIN2 N-terminus were replaced with those of MntH, with the goal of promoting protein stability and facilitating insertion of the protein into the bacterial membrane. In addition, the entire sequence was codon optimized for *E. coli* to

facilitate expression (Appendix B). However, when assayed for cell growth viability (Figure 4.3a) the EIN2/MntH chimera protein seemed to cause cell growth inhibition. Therefore, the EIN2/MntH chimera was unusable in further assays for metal transport, although it did express weakly (Figure 4.3b).

Beyond the N-terminal domain of EIN2, there is an additional protein domain, the coiled-coil domain (residues 485-515), followed by the C-terminal domain (residues 516-1294). Alonso et al. (1999) proposed that the coiled-coil domain could be the site of protein-protein interactions. However, it is possible that this coiled-coil domain is necessary for the function of the N-terminal domain. Therefore, I extended the codon-optimized chimeric protein to include this domain, ending at residue 524, to ensure this coiled-coil domain was not disrupted (Appendix B). Dr. Bret Cooper (USDA-ARS, Beltsville, MD) helped create the codon optimized extension piece via Gibson cloning. The new extended chimera protein (termed "EIN2 hybrid") did not confer such a drastic growth inhibition defect (Figures 4.3a and 4.4a) and the addition of the coiled-coil domain enhanced expression in *E. coli* (Figures 4.3b and 4.4b). Therefore, I used the EIN2 hybrid in my further bacterial transport assays.

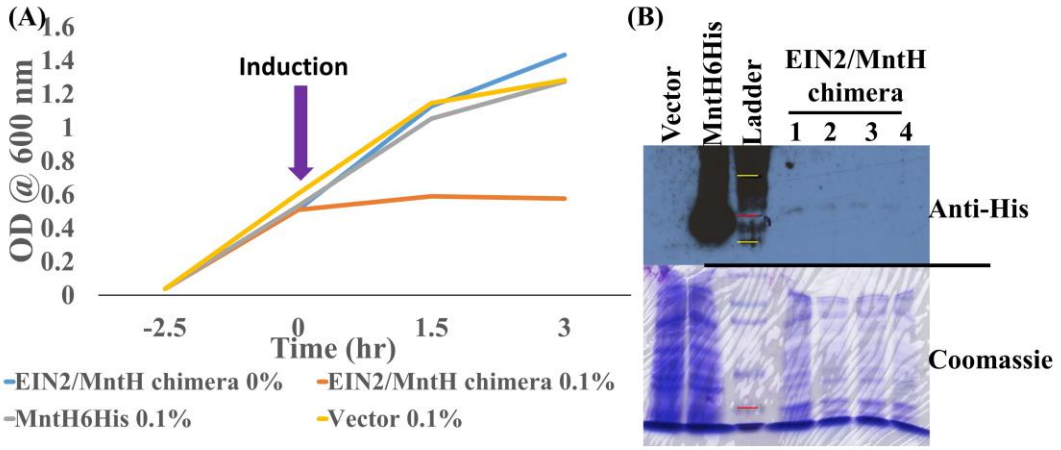

Figure 4.3. Expression of the EIN2/MntH chimeric protein causes growth inhibition in *E. coli*. Codon optimized EIN2/MntH chimeric protein was expressed in DH5α cells. Thirty milliliter cultures were synchronized to an OD of 0.0375 and grown at 37ºC for 2.5 hours (-2.5 hr) until they reached an OD of approximately 0.5. At time zero, protein expression was induced with 0.1% arabinose and growth, as monitored by absorbance readings at 600 nm, were recorded for 3 hrs post induction. Expression of EIN2/MntH chimera caused growth inhibition. MntH-6His (MntH with six His tags) and *E. coli* transformed with empty vector (pBAD24) were used as positive controls for growth. The EIN2/MntH chimera line is an average of three independent clones, and error bars represent the standard deviation. (B) Western Blot of the microsomal fraction of DH5α cells induced with 0.1% Arabinose, indicating EIN2/MntH chimera weakly expresses, as detected by an anti-His antibody. MntH6His was used as a positive control and empty vector (pBAD24) were used as a negative control. Ladder bands represent 50, 37 (red), and 25 kDa on Western Blot. Red bar (37 kDa) is also indicated on the Coomassie Gel, used as a loading control. Fifty µL of membrane fraction protein samples were first heated for 1 hr at 37 C

before loading into a 10% acrylamide gel. Protein expression was probed using attached 6-His epitope tags using anti-His antibody (Abcam). Signal detected using Femto HRP detection kit (ThermoFisher) using an overnight exposure.

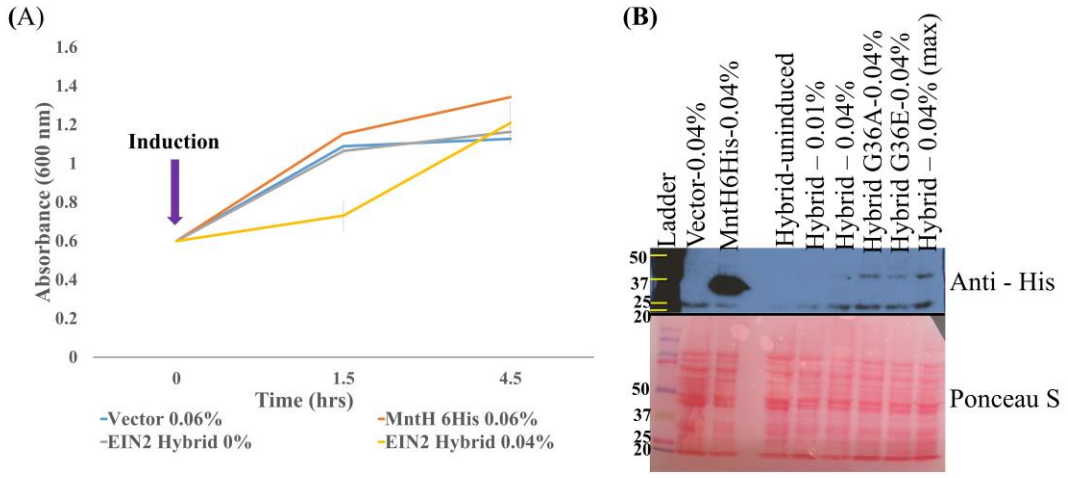

Figure 4.4. Expression of the EIN2 hybrid protein does not greatly inhibit growth of *E. coli* (A) The EIN2 hybrid (residues 1-524) was expressed in DH5α *E. coli* cells, where cultures were grown for approximately 3 hours (until they reached an OD of approx. 0.5). Protein expression was induced with 0.04% arabinose (time 0) and growth inhibition was monitored, via absorbance readings at 600 nm, for 4.5 hrs post induction. Expression of MntH (with 6 His tags) did not alter growth and grew similar to empty vector (pBAD24). Protein expression of EIN2 hybrid inhibited growth initially, but after 1.5 hrs growth was exponential. After 4.5 hrs post induction growth was similar to the un-induced cultures and empty vector. EIN2 hybrid lines represent an average of three independent clones and error bars represent standard deviation. (B) Western Blot from the microsomal fraction of EIN2 hybrid was probed with an anti-His antibody indicating that although the EIN2 hybrid does not express at strongly as MntH6His, it does express a protein. Addition of the G36E and G36A substitutions increased the EIN2 hybrid protein level compared to the wild-type EIN2 hybrid protein level. Fifty µL of protein extract was heated for 1 hr

at 37C before loading into a 10% SDS-PAGE gel. Hybrid 0.04% (max) contained 60 µL of protein sample and showed an increase in the EIN2 hybrid signal. Protein expression was detected using an anti-His antibody (Abcam) and visualized using a femto detection kit (Thermo Scientific) with an overnight exposure. Ladder bands are denoted

Evidence for Iron and Copper Transport by EIN2 Expressed in *E.coli*

To assay for metal transport by the EIN2 hybrid in *E. coli*, I used the MICKEY assay (Makui et al., 2000). The EIN2 hybrid protein showed an increase in the "ring of death" when the protein was induced under conditions of high Fe^{2+} and Cu^{2+} (Figure 4.5; Table 4.2). This would suggest that EIN2 might transport iron and copper. Interestingly, the EIN2 hybrid seemed to transport copper better than MntH (Makui et al., 2000). Copper does fit nicely into the ethylene pathway since the receptors require a copper cofactor to bind ethylene (Rodriquez et al., 1999). However, since the receptors act upstream of EIN2, it would not make sense that the copper would come directly from EIN2. If that was the case, however, and EIN2 was acting upstream of the receptors, then loss of the EIN2 Nramp domain should confer a receptor null phenotype (an enhanced ethylene response rather than insensitivity).

I also tested EIN2 with other metals, including Mn^{2+}, Cd^{2+} and Ni^{2+}. Since MntH is known to be a Mn^{2+} transporter, I was particularly interested in testing whether the EIN2 hybrid was capable of Mn^{2+} transport. Although manganese appeared to produce a definitive "ring of death" in the Makui et al., 2000 study, I had some trouble with that metal. For me, I was not able to see a definitive "ring of death" as I did with the other metals and therefore the data was not easily interpretable. Both Cd^{2+} and Ni^{2+} showed hints at transport (data not shown) but for each of these metals, two of the three independent EIN2 hybrid clones demonstrated hints of transport ability, one clone did not. In this case, there was no difference between the EIN2 hybrid induced and un-induced samples, they looked just like the empty vector.

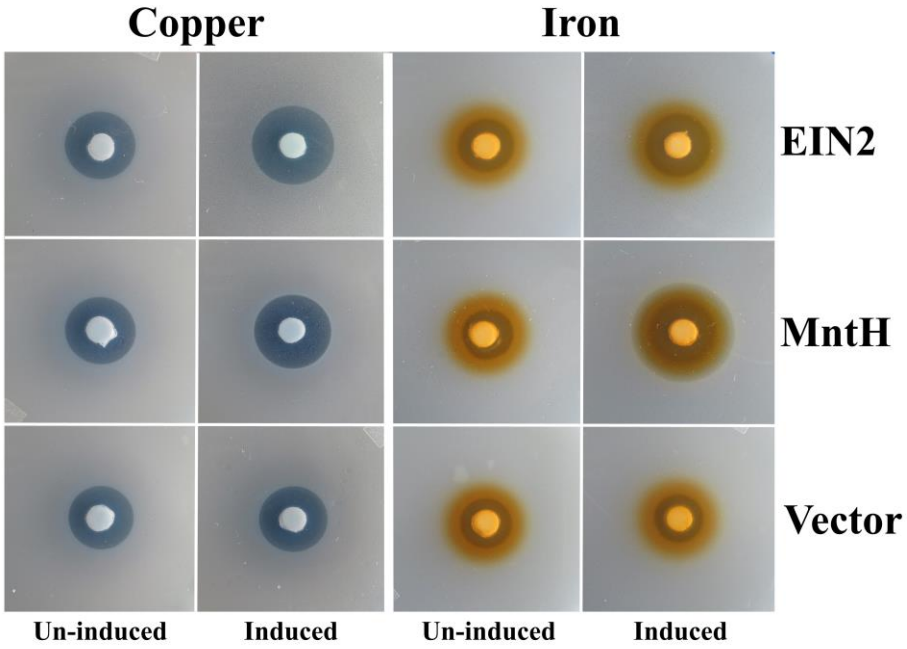

Figure 4.5. The EIN2 hybrid protein can transport iron and copper when expressed in *E. coli*. EIN2 hybrid was expressed in *E. coli* and tested for metal uptake using the MICKEY assay. The "ring of death" increased in the presence of both copper and iron suggesting EIN2 may be transporting both of these divalent metals. MntH, a broad range transporter, was used as a positive control and empty vector (pBAD24) was used as a negative. A representative sample of a close up of the filter paper disks and "ring of death" is shown. Disks imbibed with 10 µL of either 1 M $CuSO_4$ or 1 M $FeSO_4$, and the inducer (0.06% arabinose) was mixed into the GTA top layer (0.1% agar) with the bacteria. Filter paper disks with metal solution were placed on top of this thin top layer. Plates were then incubated at 37^oC for 16 hrs and the "ring of death" was measured in mm.

	Metal	Induced	Un-induced	Δ
Vector	$FeSO_4$	12.4 ± 1.3	12.8 ± 1.0	-
	$CuSO_4$	17.1 ± 0.9	17.3 ± 0.6	-
MntH	$FeSO_4$	12.5 ± 0.7	23 ± 0.8	10.3
	$CuSO_4$	17.1 ± 0.7	18.4 ± 0.8	1.1
EIN2 Hybrid	$FeSO_4$	12.1 ± 0.5	16.0 ±2.8	3.3
	$CuSO_4$	17.8 ± 0.7	21 ± 2.3	3.8
EIN2 Hybrid G36A	$FeSO_4$	12.8 ± 0.5	15.8 ± 1.1	3
	$CuSO_4$	17.3 ± 0.4	20.4 ± 0.7	3.2
EIN2 Hybrid G36E	$FeSO_4$	12.6 ± 0.3	15.9 ± 1.2	3.2
	$CuSO_4$	17.2 ± 0.6	21.3 ± 0.8	4.1

Table 4.2. The EIN2 hybrid can transport iron and copper when expressed in *E. coli*. Data for the MICKEY assay of Figure 4.5. When expressed in *E. coli* the EIN2 hybrid can uptake iron and copper. Addition of the G36E and G36A substitutions did not alter the ability of EIN2 hybrid to uptake these metals. Filter paper disks were imbibed with either 10μL of 1M $FeSO_4$ or 1M $CuSO_4$ and protein expression was induced with 0.04% arabinose. Effect of transport (Δ) was calculated by subtracting the induced vector amount from the induced sample (MntH or EIN2). Values are the average, where $n = 4$. The EIN2 hybrids (WT, G36E, and G36A) are a pool of three independent clones, where $n = 4$ technical replicates. Ring of death measured in mm.

Interestingly, it was a different EIN2 hybrid clone for each metal that did not show any transport ability suggesting it was not just a bad clone of EIN2 hybrid. Perhaps these metals are not the preferred substrates for EIN2 hybrid transport.

Since Nramp proteins are a broad-range divalent metal transporters, I was hoping to narrow down the possible substrates for EIN2. The MICKEY test provided at least two possibilities, copper and iron.

Substitution of Gly-36 Did Not Disrupt Transport by EIN2 in *E. coli*

Since the above findings provided evidence of metal transport by EIN2 and EIN2 is important for ethylene signaling, a key question was whether ethylene signaling depends on metal transport. The G36E substitution (Chapter 3) falls in a highly conserved Nramp motif, DPGN, which is important for metal transport (Haemig and Brooker, 2004; Chaloupka et al., 2005). In fact, Haemig and Brooker (2004) found that mutating the Glycine (in the DPGN) disrupted the metal transport ability of MntH because it was predicted to be an important residue for the conformation of the metal binding pocket, even a G36A substitution disrupted transport. However, to my knowledge, a G36E substitution has not been tested.

If the G36E substitution, which confers ethylene insensitivity (Chapter 3, Figure 3.2) disrupts metal transport by EIN2, then that would suggest EIN2 metal transport plays a role in ethylene signaling. To test this, I introduced mutations encoding both G36E and G36A (the substitution that is known to disrupt transport) (Haemig and Brooker, 2004) substitutions into the EIN2 hybrid and used the MICKEY assay to test if metal transport was disrupted. The G36E mutation was not able to disrupt transport of EIN2 hybrid and neither did G36A (Table 4.2). Thus it

remains unclear whether metal transport by EIN2 plays a role in ethylene signaling. Since neither the G36E nor the G36A mutations disrupted transport by MntH (data not shown), whereas G36A was previously shown to abolish transport (Haemig and Brooker, 2004), perhaps EIN2 expression in *E. coli* can only provide hints at divalent metal transport.

Interestingly, when expressed in bacteria, both the G36A and G36E mutations increased the protein expression level of the EIN2 hybrid (Figure 4.4b). This suggests that, although these mutations did not disrupt metal transport, they do have an effect on EIN2. This further suggests that these mutations should also be investigated, perhaps by other means.

Part 2 –Evidence for EIN2 Metal Ion Transport in the Yeast *Saccharomyces cerevisiae*

Saccharomyces cerevisiae (baker's yeast) can be a good system for assaying for metal transport, since yeast is eukaryotic and contains many transporters that are homologous with those in Arabidopsis. Previous attempts to test EIN2 for metal transport ability have mainly been carried out by using various sized fragments of EIN2 to complement yeast mutants (Alonso et al, 1999; Thomine et al., 2000; Thomine and Schroeder, unpublished data). In fact, much of the yeast work with EIN2 regarding metal transport, both published and unpublished, has been done attempting to complement the yeast *smf*1 Nramp mutant (Thomine et al., 2000, and unpublished). However, *S. cerevisiae* SMF1 is localized to the plasma membrane (Supek et al., 1996) while EIN2 is at the ER membrane in plants.

The EIN2 N-terminal Domain Localizes to Internal Membranes, in Yeast

Where does Arabidopsis EIN2 localize in yeast? To determine this, an undergraduate working with me, John Paul Ouyang, used a modified split-ubiquitin (Ub) assay where Arabidopsis EIN2 was fused to the split-Ub bait and each prey vector would express a protein located at a different cellular membrane, fused to the other half of Ub (Wittke et al., 1999). If EIN2-split Ub was located at that particular membrane, it would show an interaction with that particular prey. The Arabidopsis EIN2 N-terminal domain (residues 1-524) interacted with SEC62 and SED5 (Figure 4.6), which are ER and Golgi membrane markers, respectively, and did not interact with the plasma membrane marker (SSO1). This suggests that the Arabidopsis N-terminal domain of EIN2 localizes to the ER and Golgi membranes, or more generally to internal membranes, in yeast.

When John Paul also attempted to localize the full length EIN2 protein, it did not interact with any of the membrane proteins tested under stringent conditions (data not shown) suggesting that it perhaps did not localize properly in yeast. It is possible that the novel C-terminal domain interfered with yeast localization and therefore full length EIN2 did not localize to any specific membrane. Alternatively, the expression level of the protein might have been poor. Therefore, for all further yeast metal transport work, I used only the N-terminal domain of EIN2 (residues 1-524).

Since the question still remained, whether metal transport by EIN2 plays a role in ethylene signaling, I was curious as to whether the EIN2 G36E substitution could disrupt metal transport in a yeast system. Therefore, I was also curious as to whether the G36E substitution would interfere with the localization of the EIN2 N-

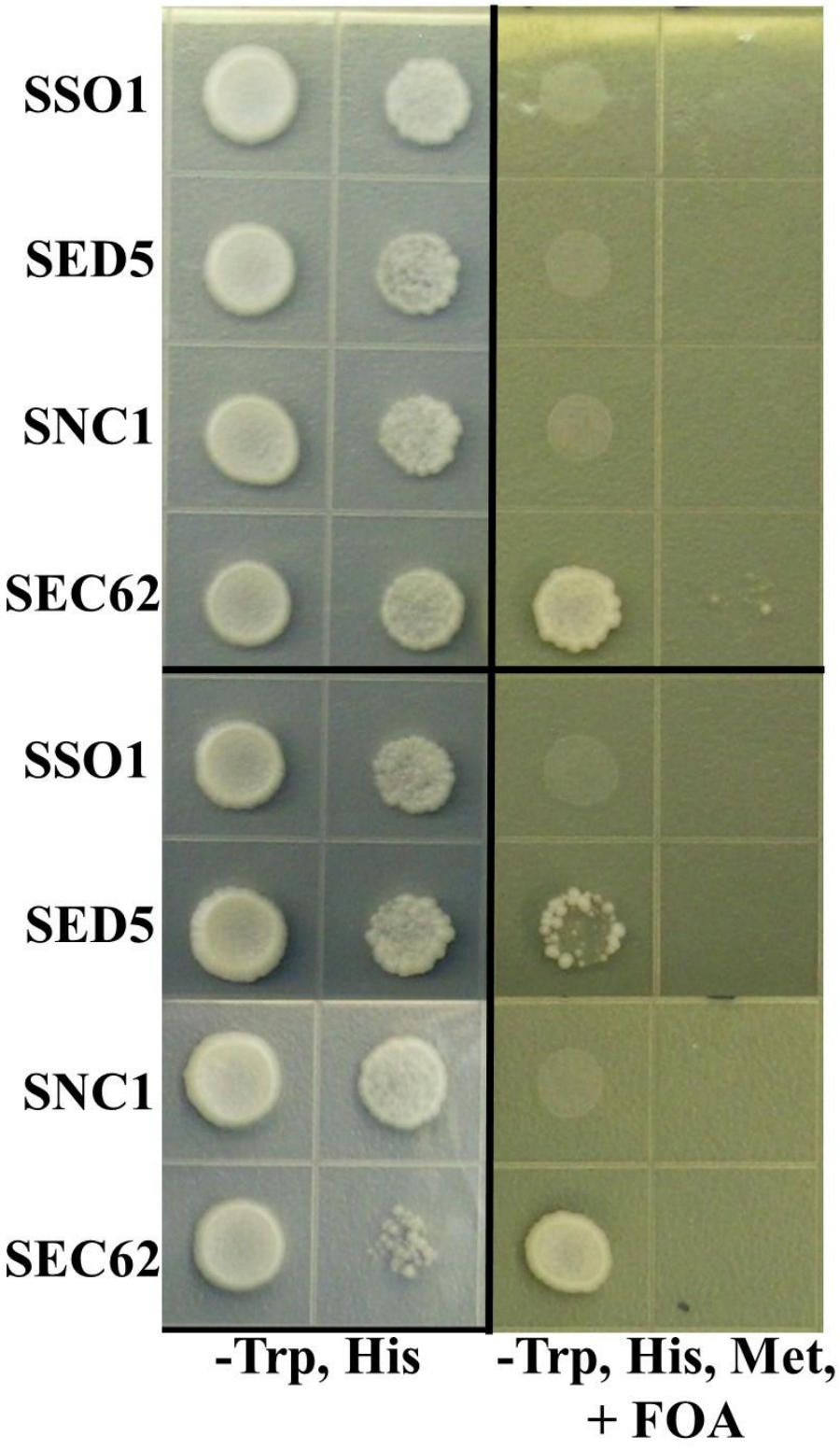
SSO1
SED5
SNC1
SEC62
SSO1
SED5
SNC1
SEC62
-Trp, His
-Trp, His, Met,
+ FOA

Figure 4.6. The Arabidopsis EIN2 N-terminal domain localizes to the ER and Golgi membranes, in yeast. The EIN2 N-terminal domain was fused to Cub (pMKZ) and the membrane markers were fused to Nub (pNUB-I). Two colonies of EIN2 are shown. EIN2 interacts with SEC62 (ER marker) and SED5 (early Golgi marker) but not SSO1 (plasma membrane) or SNC1 (Vesicles, late golgi). Yeasts were spotted on minimal media plates (-Trp, -His, growth control) and interactions were selected using minimal media plates (-Trp, His, Met) with the addition of 10 μM FOA (5-Fluoroorotic Acid) and were grown for 2 to 4 days at 30 C.

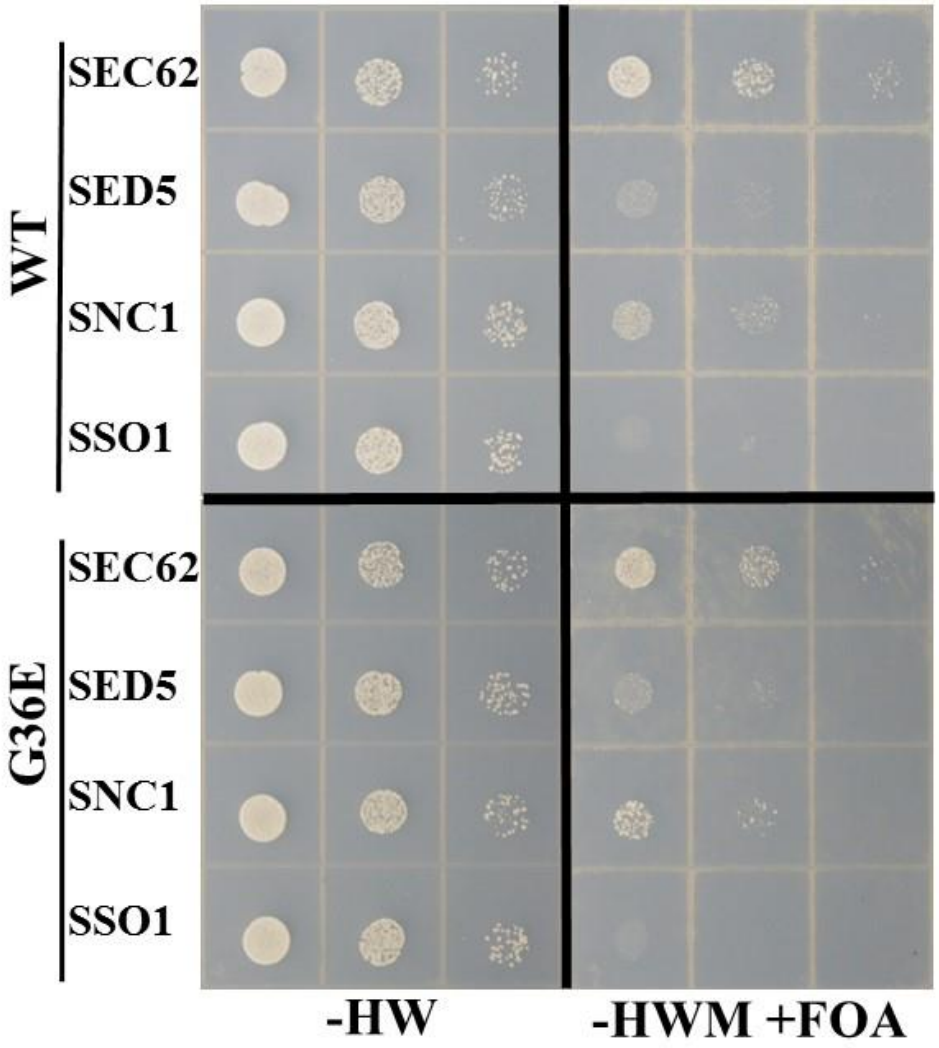

Figure 4.7. The EIN2 G36E substitution does not disrupt the localization of the EIN2 N-terminal domain, in yeast. Yeast was localized using a modified split-ubiquitin assay, where the EIN2 N-terminal domain (both wild-type and EIN2 G36E) were fused to Cub (pMKZ) while the membrane markers were fused to Nub (pNUB-I). Both wild-type and EIN2 G36E interacted with SEC62 (ER marker) and SNC1 (vesicle, late golgi marker) and not SED5 (early golgi) or SSO1 (plasma membrane marker). Yeasts were spotted on minimal media plates (-Trp, -His; growth control)

and interactions were selected using minimal media plates (-Trp, His, Met) with the addition of 10 uM FOA (5-Fluoroorotic Acid) and were grown for 2 to 4 days at 30C.

terminal domain in yeast. Another undergraduate working with me, Jordon Limsky, introduced the G36E substitution into the EIN2 N-terminal split-Ub construct and tested whether the G36E substitution had an effect on the localization the N-terminal domain of EIN2, in yeast. As in plants (Chapter 3) the G36E substitution did not interfere with localization (Figure 4.7) suggesting the G36E substitution does not affect the protein localization of EIN2 N-terminal domain in yeast.

Interestingly, both wild-type EIN2 and EIN2 G36E localized with the SNC1 (late golgi/vesicle) marker (Figure 4.7) and not the SED5 (early golgi) like it did in Figure 4.6. This could be a due to the EIN2 N-terminal domain localizing more generally to internal membranes, or broadly to the Golgi. It is also possible that the difference of localization was a result of the two independent transformations and the two colonies chosen.

Complementation of the *smf2* Yeast Mutant

The yeast Nramp homolog SMF1 localizes to the plasma membrane (Supek et al,, 1996) as stated above, but EIN2 N-terminal domain does not (Figure 4.6). However, yeast does contain another Nramp homolog, SMF2, which localizes to internal membranes (such as ER, Golgi, and vacuole; Luk and Culotta, 2001). Since, to my knowledge, no one had yet tried testing metal transport of EIN2 using the *smf2* mutant, and since the subcellular localization of EIN2 was more similar to the yeast SMF2 protein, I proposed that the *smf2* mutant would be a better choice to test for rescue. Therefore, to test transport ability of EIN2, yeast cells expressing the EIN2 N-terminal domain (residues 1-524) were transformed into an *smf2* mutant background.

SMF2 is a Mn^{2+} transporter (Portnoy et al., 2000) so I assayed for Mn^{2+} transport, using a spot assay (Thomine et al., 2000). Transformed yeast were spotted on plates with a high dose of EGTA (25 mM) to chelate divalent cations. Growth on the EGTA plate would suggest that the transgene encodes a transporter of divalent metals because the yeast cells can survive in low metal conditions, in particular Mn^{2+}. EGTA chelates divalent cations, but has a very high affinity for Mn^{2+} and Ca^{2+}.

The EIN2 N-terminal domain was able to complement the *smf*2 mutant (Figure 4.8) almost as well as AtNramp4, which is known to be involved in Mn^{2+} homeostasis (Lanquar et al., 2010), whereas the empty vector and GUS did not grow as efficiently. This suggests that EIN2 may function as a divalent metal ion transporter, possibly involved in transport of Mn^{2+}. I found that cell growth increased when the medium was spiked with 100 µM $MnSO_4$, but did not grow as well as with 0 µM or 1 µM $MnSO_4$, suggesting that EIN2 might not be a high affinity transporter of Mn^{2+} (Figure 4.8). Interestingly, growth of Nramp4 was slightly inhibited on the 100 µM $MnSO_4$ plate, which could suggest that uptake of this particular metal is causing some cytotoxicity. EIN2 did not show observable growth inhibition in the presence of 100 µM $MnSO_4$ compared to the lower doses.

Data suggests that AtNramp4 is a higher affinity Mn^{2+} transporter than EIN2, since growth was slightly increased on the 1 µM $MnSO_4$ plate compared to the 100 µM $MnSO_4$ plate. Since yeast cells require 2-10 µM manganese for optimal growth (Jones and Gadd, 1990) the 100 µM $MnSO_4$ supplemented in the plate be providing a toxic level of manganese to the cell, via uptake from AtNramp4, and thus inhibiting cell growth. A 100 µM concentration of $MnSO_4$ has been shown to cause DNA

damage in PC12 rat cells (Hirata, 2002). However, this growth inhibition at 100 µM $MnSO_4$ is an intriguing phenomenon since yeast growth inhibition from manganese was found to require at least 600 µM $MnCl_2$ (Gadd and Laurence, 1996). Again, this could indicate that AtNramp4 is a high affinity Mn^{2+} transporter.

The EIN2 N-terminal Domain Cannot Complement the *smf1* Mutant

Previous attempts to test EIN2 for metal transport ability were unsuccessful, and much of the previous work was done attempting to complement the *smf1* mutant (Thomine et al., 2000; unpublished data). Therefore, I was curious as to whether the N-terminal fragment that that partially rescued of *smf2* was able to rescue the *smf1* mutant as well, since each laboratory working on EIN2 tested slightly different portions of EIN2. I transformed the EIN2 N-terminal domain (residues 1-524) into the *smf1* mutant and tested EIN2 for transport ability using the spot assay as above. However, the EIN2 N-terminal domain was not able to complement this mutant (data not shown). This suggests that proper localization of the EIN2 N-terminal domain is important for transport ability and perhaps not just the particular portion of the EIN2 N-terminal domain used.

The EIN2 G36E Substitution Does Not Disrupt Transport Ability of EIN2

Since EIN2 plays such an essential role in ethylene signaling, the question still remains, does metal transport via EIN2 also play a role in ethylene signaling? The G36E substitution falls in a highly conserved motif (Figure 4.1) that is important for metal transport (Haemig and Brooker, 2004) and the *ein2 G36E* mutant confers ethylene insensitivity (Chapter 3-Figure 4.2). Therefore, disruption of metal transport by the EIN2 G36E substitution would suggest metal transport plays a role in ethylene

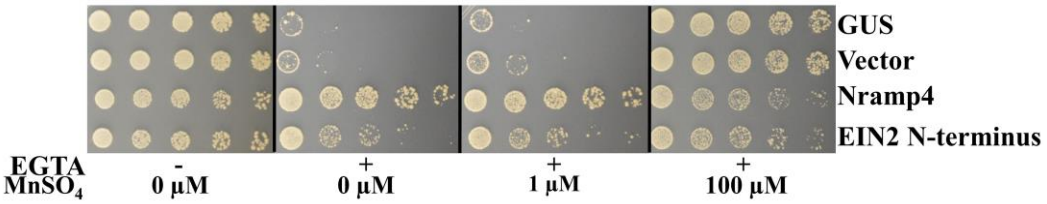

Figure 4.8. The EIN2 N-terminal domain can complement the *smf2* yeast mutant suggesting it is capable of divalent metal transport. The N-terminal domain of EIN2 (residues 1-524) was transformed into a *smf2* mutant background and plated on a high dose of EGTA (25 mM, all but left most panel). Growth on the EGTA plates suggest EIN2 is capable of divalent metal transport. EGTA plates spiked with $MnSO_4$, tested Mn^{2+} transport affinity however, growth on 1µM is similar to 0 µM suggesting EIN2 is not a high affinity transporter of Mn^{2+}. Yeast transformed with GUS and empty vector (pAG426 GPD –ccdB) were used as negative controls and yeast expressing AtNramp4 (from Arabidopsis) as a positive control. Left most panel is the growth control. All plates are minimal media, –Ura with G418, pH 6.0, buffered with 10 mM MES.

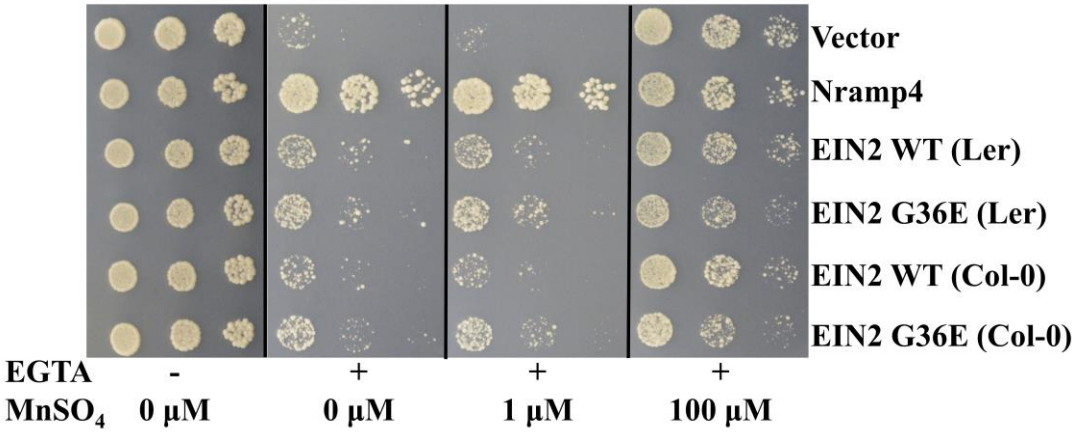

Figure 4.9. The EIN2 G36E substitution in the context of the L*er EIN2* sequence (Y160C) does not hinder the transport ability of the EIN2 N-terminal domain. Yeast expressing the EIN2 N-terminal domain (residues 1-524) were transformed into a *smf2* mutant background and plated on a high dose of EGTA (22 mM, all but left panel). Growth on EGTA plates suggests EIN2 is capable of divalent metal transport. Addition of the G36E substitution and the Y160C polymorphism (Col-0 to L*er* ecotype polymorphism) did not hinder the growth of yeast expressing EIN2 on the EGTA plates suggesting transport ability was not affected. Yeast transformed with empty vector (pDR195-GW) was used as a negative control and AtNramp4 was used as a positive control. Left most panel is the growth control. All plates contain minimal media, –Ura with G418, pH 6.0, buffered with 10 mM MES.

signaling. To test this possibility, I introduced the mutation encoding the G36E substitution into the EIN2 N-terminal domain construct and used the spot assay as above in the *smf2* yeast mutant background to test if transport was disrupted.

However, as with the expression of EIN2 hybrid in *E. coli*, the G36E substitution did not cause growth inhibition of the *smf2* yeast mutant in the presence of 25 mM EGTA (stringent divalent metal chelating conditions) and acted similar to the wild-type EIN2 N-terminal domain (Figure 4.9). This suggests that the G36E substitution does not disrupt Mn^{2+} transport of EIN2 N-terminal domain, at least in this yeast assay, and that the defect in G36E that results in ethylene insensitivity is unrelated to metal transport.

Landsberg EIN2 N-terminal Domain is Capable of Metal Transport

It is possible that the ecotype differences in the gene sequence could have an effect on the transport ability of the EIN2 N-terminal domain. There is one DNA polymorphism in EIN2 (L*er*) compared to EIN2 (Col-0), encoding an Y160C polymorphism that lies within the middle of the predicted transmembrane domain (number five) (ARAMEMNON). Since the *ein2 G36E* mutant was in the L*er* ecotype, but all of my constructs consisted of *EIN2* from Col-0, I was curious if the L*er* polymorphism had any effect on the transport ability of EIN2. To test this possibility, I introduced the nucleotide polymorphism encoding Y160C into both wild-type *EIN2* and the *EIN2 G36E* yeast constructs and expressed them in the yeast *smf2* mutant. However, when spotted on a high dose of EGTA (22 mM), this Y160C polymorphism did not affect the yeast growth in the assay, neither in wild-type EIN2

nor EIN2 G36E (Figure 4.9). This indicates that the Y160C polymorphism between L*er* and Col-0 does not alter the transport ability of the EIN2 N-terminal domain.

The EIN2 N-terminal Domain May be Involved in Cadmium Transport

Cadmium is a metal that can "piggy back" into the cell through iron transporters, such as IRT1 (IRON REGULATED TRANSPORTER 1; Eide et al., 1996; Rogers et al., 2000) and since it is a highly toxic metal, with no physiological function, cells are particularly sensitive. In addition, AtNramp1, AtNramp3, AtNramp4, and AtNramp6 have been shown play a role in Cd^{2+} transport (Thomine et al., 2000; Cailliatte et al., 2009). Therefore, I was curious whether EIN2 also could have a role in Cd^{2+} transport, and if EIN2 expression had any influence over the Cd^{2+} toxicity in yeast. Expression of EIN2 in a wild-type yeast background caused growth inhibition when plated on synthetic medium supplemented with 10 μM $CdCl_2$ (Figure 4.10) similar to the known Cd^{2+} transporter AtNramp4 (Thomine et al., 2000). As in the case with the *smf2* mutant, the addition of the G36E substitution and the Y160C polymorphism did not promote growth or slow inhibition. This suggests that EIN2 could be a possible Cd^{2+} transporter. It is also possible that EIN2 could be transporting another metal ion, such as Fe^{2+} or Mn^{2+}, and that Cd^{2+} is able to be transported at a lower affinity or is "piggy backing". This also further indicates that the Y160C polymorphism does not alter the transport ability of EIN2. Introducing the G36E substitution did not make the yeast less sensitive to the Cd^{2+}, further indicating that the Glycine residue is not essential for metal transport.

Complementation of Other Yeast Metal Transporter Mutants

Nramp proteins can transport a broad range of divalent metal cations. Therefore, the next question was, can the EIN2 N-terminal domain transport other divalent cations as well? To test this, I decided to use the EIN2 N-terminal domain, to attempt to complement other yeast transporter mutants, since the EGTA assay with the *smf2* mutant is mainly specific to Mn^{2+}.

The *E. coli* transport had assays provided hints that EIN2 could transport iron and copper. However, EIN2 N-terminal domain was not able to complement the yeast *fet3fet4* mutant, which is a high and low affinity yeast iron transporter mutant, under conditions of reduced iron (data not shown). Nor was EIN2 N-terminus able to complement copper, zinc, or cadmium yeast transporter mutants (see Appendix D). This could suggest that EIN2 does not transport iron, copper, zinc, or cadmium. However, it is also possible that EIN2 does not localize to the same membrane as these transporters and therefore was not able to complement them.

EIN2 May be a Calcium Transporter

Since the *smf2* mutant and Cd^{2+} toxicity results were promising, our collaborators, Dr. Sébastien Thomine and Pierre Longerstay (CNRS, Gif-sur-Yvette) tested the metal content of the transformed yeast cells directly, using atomic absorption spectroscopy. Liquid *smf2* mutant yeast cultures, overexpressing EIN2 N-terminal domain (as well as AtNramp4, GUS and empty vector), were grown and tested for their manganese, iron, copper, zinc, calcium, and magnesium accumulation levels. They found that calcium levels were statistically higher than GUS and empty vector in both Col-0 and L*er* wild-type EIN2, and L*er* EIN2 G36E (Appendix D);

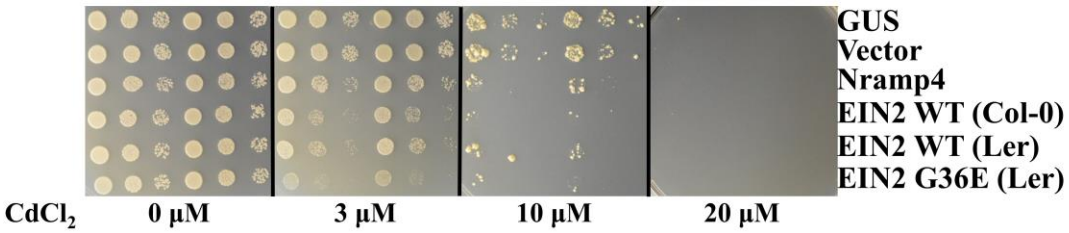

Figure 4.10. EIN2 expression increased Cd^{2+} sensitivity, in yeast. The EIN2 N-terminal domain (residues 1-524) was expressed in the BY4741 wild-type yeast strain. Plates were supplemented with 3, 10, or 20 µM $CdCl_2$, which caused growth inhibition of yeast transformed with the EIN2 or the Arabidopsis Nramp4 construct. Addition of the G36E substitution and Y160C polymorphism (creating the L*er* ecotype) to EIN2, did not decrease $CdCl_2$ sensitivity. GUS and empty vector (pDR195-GW) were used as negative controls and Nramp4 was used as a positive control. All plates were minimal medium, -Ura, with G418, pH 6.0, buffered with 10 mM MES.

Copper levels were higher in L*er* EIN2, and both Col-0 and L*er* EIN2 G36E; Manganese levels were higher in L*er* EIN2 and Col-0 EIN2 G36E. There was no statistical difference in metal concentration between EIN2 and empty vector for iron, magnesium or zinc. This suggests that EIN2 may play a role in the transport of calcium, copper, and manganese. (Longerstay and Thomine, unpub.). It also suggests that the G36E substitution does not disrupt transport by EIN2.

Calcium showed the highest yeast metal accumulation for EIN2 and was an exciting new avenue since, to my knowledge, no other Nramp have been shown to transport calcium (Appendix C). Therefore, I next asked whether EIN2 can transport Ca^{2+}. To test this, I first transformed the EIN2 N-terminal domain (residues 1-524) into different Golgi- and ER-localized calcium transporter yeast mutants (see Appendix D) and tested whether EIN2 is capable of complementing these mutants under Ca^{2+} deprived conditions. However, EIN2 was not able to complement these mutants (data not shown). I also tested the same mutants under conditions of elevated calcium (200 mM) to see if the overexpression of EIN2 could rescue the calcium hypersensitive phenotype of these mutants, however, the EIN2 N-terminal domain was not able to do so either (data not shown). This could suggest that EIN2 may not be transporting Ca^{2+}, but it also could suggest that EIN2 is too diverged from these transporters to be able to complement them.

Calcium Treatment Enhances the Triple Response Phenotype

Since the atomic absorption results indicate calcium is the strongest candidate for the preferred substrate of EIN2, I was curious as whether I could see an affect in the *ein2 G36E* mutant plant, again utilizing the insensitivity to ethylene as a read-out.

To test this, I grew the *ein2 G36E* mutant in the presence of additional calcium, in the presence and absence of ACC. Addition of calcium to the medium did make the hypocotyl of *ein2 G36E* mutant shorter on ACC, however the wild-type also became similarly shorter (Figure 4.11). Etiolated seedling growth in the presence of EGTA, which potentially blocks divalent metal transport, similarly had a pleiotropic response (data not shown). This suggests that calcium plays a role in inhibiting hypocotyl growth in the triple response. However, the exact role of EIN2 in growth inhibition, is not clear. These results are in agreement with a study done by Raz and Fluhr (1992) that suggested calcium is required for a variety of ethylene mediated responses, such as ethylene mediated-pathogenic response and the apical hook formation during the triple response phenotype.

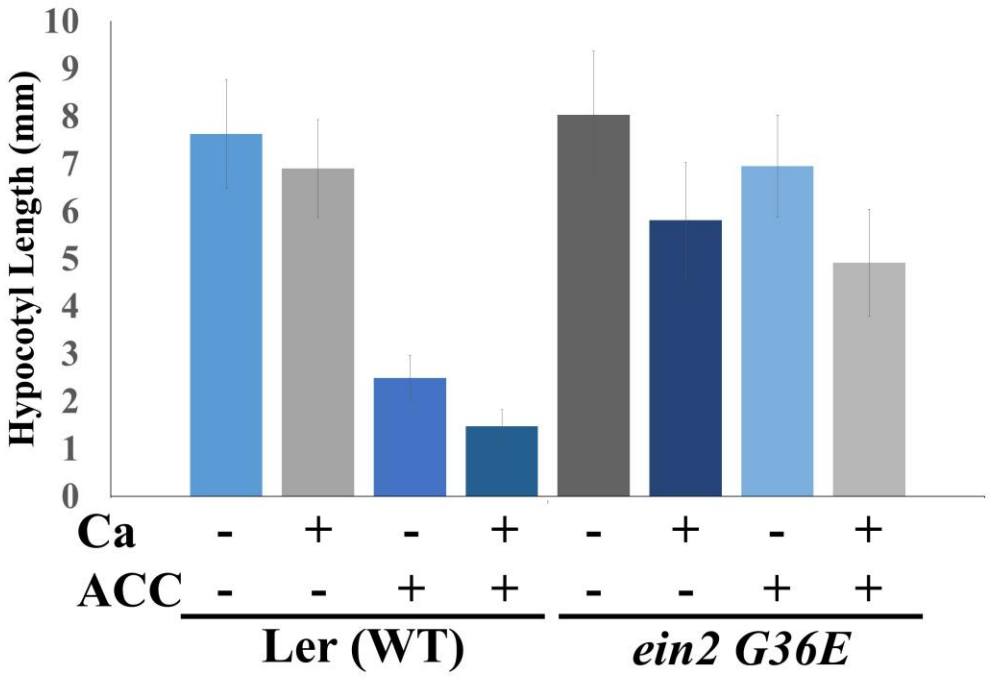

Figure 4.11. Addition of calcium enhanced the triple response phenotype. Four day-old etiolated seedlings were grown on agarose plates in the presence and absence of ACC (an ethylene precursor) and/or with 10 mM $CaCl_2$. Addition of calcium similarly enhanced the triple response phenotype for both L*er* (WT) and *ein2 G36E*. Bars represent $50<n<80$ seedlings and measurements were made using Image J.

Discussion

Expression of the EIN2 N-terminal Domain in *E.coli* Suggests that EIN2 Transports Copper and Iron

Whether EIN2 is capable of metal transport has been a question eluding the ethylene field for almost two decades. Since EIN2 is quite diverged from other Nramp proteins (Figure 4.1b), it is possible that EIN2 has diverged enough that it may look like an Nramp but not function like one. One of the motifs unique to EIN2, a DPGK motif (Figure 4.1a), fell in a highly conserved motif in Nramp proteins, the DPGN motif, important for metal transport (Haemig and Brooker, 2004). However, since the N37K substitution did not disrupt the transport ability of MntH (Figure 4.2, Table 4.1) it is possible that EIN2 could have retained this Nramp metal transport ability.

The MICKEY assays, where the EIN2 N-terminal domain was expressed in *E. coli* gave hints that EIN2 could be transporting copper and iron (Figure 4.5; Table 4.2). In fact, it was particularly interesting, since copper is not one of the preferred substrates of MntH (Makui et al., 2000). In addition, the N37K substitution allows MntH to transport copper slightly better (Figure 4.2; Table 4.1). Perhaps the N37K substitution in EIN2 helps change the metal specificity of the EIN2 binding pocket. This can be observed in the rice NRAT1 (NRAMP ALUMINUM TRANSPORTER1) protein (Xia et al., 2010), which is an Nramp-like protein that prefers binding M^{3+} (in particular Al^{3+}) metal ions instead of M^{2+}.

It is possible that the N37K substitution did not disrupt transport of MntH because only one residue was changed. If all the important residues in MntH were

substituted, so that they mimic EIN2, then the results might be different. However, since EIN2 looks to be functioning as a divalent metal ion transporter, I would hypothesize that additional mutations would most likely dampen the strong transport ability of MntH, compared to EIN2, and perhaps change the metal specificity. This possible change in specificity could explain why EIN2, expressed in yeast, transports calcium (Appendix C) and no other Nramp proteins have been shown to transport calcium.

EIN2 Expression and Transport of Iron and Copper in *E. coli*

The transport assays in *E. coli* gave hints as to the possible metal ion substrate of EIN2. They were indirect, however, since we were not measuring metal uptake directly. There were some issues due to trouble with expression, which was why EIN2 was also expressed in yeast. With the EIN2 N-terminal domain expression in yeast, metal transport was measured indirectly, via spot tests, and directly, via atomic absorption. EIN2 expression in bacteria was a major problem.

I originally tested metal transport of the EIN2 hybrid two different ways, with a MICKEY assay (Figure 4.5, Table 4.2) and a spot test (data not shown). Unfortunately, there were some complications with the spot test. For example, the EIN2 hybrid did not grow as well as the empty vector and MntH (the positive control), so therefore could not be assayed at the same time under the same conditions. The addition of the coiled-coil domain of EIN2 (in creating the EIN2 hybrid) to the hybrid helped with growth inhibition, but did not completely rectify the problem (Appendix B, Figure 4.3 and 4.4). Therefore, only the MICKEY assay yielded any real interpretable data.

The final EIN2 N-terminal piece (EIN2 hybrid - residues 1-524), was able to be expressed in *E.coli* (Figure 4.4), and growth of *E. coli* was better than with the previous smaller piece, EIN2/MntH chimera (residues 1-481). Growth was still affected somewhat (Figure 4.4), enough that I was unable to use the spot assay, but not enough to inhibit a lawn of growth, and therefore the MICKEY assay was still applicable. The EIN2/MntH chimera inhibited growth to the extent that the bacterial lawn growth was affected.

Interestingly, yeast expression of the smaller fragment of Arabidopsis EIN2 (residues 1-481), used in making the EIN2/MntH chimera, also caused growth inhibition (when used for split-ubiquitin assays). Whereas the larger Arabidopsis EIN2 fragment, used in making the EIN2 hybrid, did not alter the growth when expressed in yeast (Chapter 3, Figure 3.11). In fact, yeast transformed with the larger EIN2 N-terminus piece grew similar to the empty vector and yeast transformed with full length EIN2. This could suggest that the addition of the coiled-coil domain is necessary for proper growth.

Reliability of the independent clones was also an issue with bacterial expression. Three independent EIN2 hybrid clones were tested, and they would not always yield consistent results (between technical and biological replicates). One possible explanation is subtle expression level differences between each independent clone. Another possibility is that there were slight differences in the concentration of metal imbibed on the filter paper disk. A standard volume of a high concentration of metal solution was pipetted onto a filter paper disk for the MICKEY assay. If there were slight variations in the amount pipetted or how it absorbed into the filter paper

disk, it could possibly affect the size of the "ring of death" produced. This was one of the main reasons why we pursued expression in yeast as a second option. Also, most plant transport proteins in the literature were tested using yeast as an expression system (Thomine et al., 2000; Ishimaru et al., 2012; Pence et al., 2000; Vert et al., 2001).

Reliability of the clones was also an issue when using the MICKEY assay to test for transport of Cd^{2+} and Ni^{2+}. Some of the EIN2 hybrid clones showed transport ability and others did not demonstrate any transport ability (data not shown) and therefore the data was not interpretable. This could suggest that EIN2 is not able to transport Cd^{2+} and Ni^{2+} and what was interpreted as transport is simply due to a growth defect in the bacterial lawn. If the lawn does not completely develop properly, i.e. expression of the EIN2 hybrid caused some growth inhibition, it could artificially make the "ring of death" look larger than would have had the lawn fully developed. Another possibility is that EIN2 is transporting the divalent metal at a low affinity, and that transport affinity is effected by subtle variations in EIN2 expression, seen between the independent clones. It is also possible that EIN2 could transport Cd^{2+} and Ni^{2+} but this assay is not the best way to demonstrate that.

Chapter 2 of this thesis suggests that EIN2 functions in a haploinsufficient manner, so perhaps the hybrid is also sensitive to subtle variations in expression as well. Perhaps too much, once it reaches a certain threshold, is causing EIN2 to be degraded and therefore no transport was observed. That could explain why the same clone can transport metal sometimes, and not others. For example, there could be subtle variations in the metal concentration on the filter paper disk, as discussed

above, which may cause the same EIN2 hybrid clone to be expressed slightly differently. The weak protein level of the EIN2 hybrid seen on a Western Blot (Figure 4.4b) could suggest that it is being turned over. It is also possible that one clone expresses a higher level and therefore transports a divalent metal, while the slightly lower expressing clone does not transport as well.

The L*er* Version of EIN2 is Also Capable of Metal Transport

During sequencing of the *ein2 G36E* mutant, we discovered a polymorphism present in the *EIN2* N-terminal domain of the L*er* ecotype that was not present in the Columbia (Col-0) ecotype, a Tyrosine at residue 160 (Y160C) that is normally a Cysteine in Col-0. This amino acid substitution could potentially cause a drastic change in the EIN2 protein since tyrosine and cysteine residues are quite different from each other and residue 160 of EIN2 is predicted to fall within transmembrane domain five (ARAMEMNON). When used in the yeast spot assays (Figures 4.9 and 4.10) there was no noticeable difference in transport ability of EIN2, between ecotypes. However, when the same yeast from Figure 4.9 was measured for metal uptake with atomic absorption, there were subtle differences. The L*er* ecotype version seemed slightly better at metal uptake (Appendix C).

L*er* EIN2 could be slightly better at transporting a divalent metal because perhaps it is more beneficial to that ecotype. Interestingly enough, when both ecotypes were compared, Col-0 seemed to have a higher EIN2 protein level (Chapter 3-Figure 3.5). L*er* may require a slightly stronger ethylene signal, compared to the Col-0 ecotype, since L*er* has a shorter stature, thicker stem, and a shorter lifespan. This could suggest that the Y160C polymorphism could have some role in EIN2, such

as enhancing the function so as to compensate for the slightly decreased EIN2 protein level in the L*er* ecotype. This could be an interesting residue to investigate further.

Interestingly, the G36E substitution is predicted to fall in a loop region of EIN2 (ARAMEMNON), whereas in MntH the whole DPGN motif falls in the first transmembrane domain (Makui et al., 2000; Courville et al., 2004). This could account for the fact that the G36E substitution does not disrupt transport of EIN2, since it perhaps would not be part of the conserved metal binding pocket within the membrane, as in MntH, if it is in the loop region versus inside the transmembrane domain. This could suggest that the DPGK motif, in EIN2, is not as important for metal transport, as it is for the *E. coli* homolog. If this is the case, a different conserved amino acid within one of the transmembrane domains could disrupt transport. It would be interesting to see if a substitution that can disrupt transport also confers ethylene insensitivity, suggesting metal transport via EIN2 would play a role in ethylene signaling. However, it is also possible that metal transport by EIN2 does not play a role in ethylene signaling.

The expression level of the EIN2 hybrid carrying either the G36E or G36A substitution was increased compared to the wild-type EIN2 hybrid (Figure 4.4). This could suggest that these mutations do have an effect on transport, somehow. Yet another possibility is that the G36E substitution only dampens the transport ability of EIN2, so that EIN2 is still able to transport, just not as effectively. Perhaps they are functioning to increase EIN2 levels, in compensation for reduced activity, since the G36E substitution did not seem to increase EIN2 transport activity.

EIN2 Can Transport Copper, Manganese and Cadmium.

Yeast overexpressing EIN2 in the *smf2* mutant background were able to grow on plates with a high dose of EGTA (Figures 4.8 and 4.9). This suggests EIN2 is transporting Mn^{2+}. Since the complementation at 1 μM Mn^{2+} was similar to no additional added Mn^{2+}, this could suggest EIN2 is a low affinity transporter of Mn^{2+}. This is in agreement with the atomic absorption data (Appendix C) suggests that EIN2 may be transporting Mn^{2+} at a much lower affinity. It is possible that some of the growth seen on the yeast spot assay is a result of EIN2 induction due to a deficiency in Ca^{2+} as well as Mn^{2+}, since EGTA also chelates Ca^{2+}.

Since EIN2 expression caused growth inhibition in the presence of Cd^{2+}, in a wild-type yeast background (Figure 4.10), this suggests EIN2 could be transporting Cd^{2+}. However, this was not verified via atomic absorption and EIN2 could not complement the yeast cadmium transporter mutant (*ycf1,* Appendix D), but could be an interesting avenue for future study. As mentioned above, many of the other Arabidopsis Nramp proteins can transport Cd^{2+}, so it is possible that EIN2 also can transport Cd^{2+}. However, cadmium is known to "piggy back" into the cell from other transporters (Eide et al., 1996, Rogers et al., 2000). It is possible that the EIN2 expression is more sensitive to Cd^{2+} toxicity because more Cd^{2+} ions are "piggy backing" around the cell. It is also possible that the expression of EIN2 is inducing the expression of other transporters, allowing this to happen as well.

Copper is a very interesting choice of substrate for EIN2 (see Appendix C), since copper is a required cofactor for ethylene binding to the receptors (Rodriguez et al., 1999). It also was interesting since the *E. coli* transport data suggested copper as

a substrate for EIN2 as well (Figures 4.4 and 4.5; Tables 4.1 and 4.2). However, EIN2 was not able to complement the yeast copper transporter mutants tested (*ctr1, ctr1-3, ctr1-3 ctr2;* Appendix D). As with SMF1, this could be due to differences in protein localization, since CTR1 is localized to the plasma membrane and CTR2 to the vacuole (Dancis et al., 1994; Portnoy et al., 2001). However, it is also possible that EIN2 is functioning slightly differently than the yeast copper transporters (i.e. directionality of transport, conformation in membrane binding pocket, etc.) and therefore not similar enough to allow for complementation. This could also be why there was no complementation of any calcium transporter yeast mutants, or any of the other metal ion transporter mutants tested either (Appendix D). It was suggested that AtNramp1 was less efficient at complementing *fet3fet4* than AtNramp3 or AtNramp4 because it was evolutionarily more distant (Thomine et al., 2000). If this is the case, it would make sense that EIN2 is also less efficient, since it is not at the same membrane and evolutionarily much more diverged than all six Arabidopsis Nramp proteins (Figure 4.1b).

EIN2 - a Calcium Transporter

The most unexpected result was calcium uptake by EIN2 (Appendix C), suggesting EIN2 could be an ER-localized calcium transporter. No other Nramp proteins, to my knowledge, have been shown to transport calcium, so this is quite exciting and should definitely be an avenue for further exploration. It is possible that EIN2, being more evolutionarily diverged than other Nramp proteins (Figure 4.1b) has diverged enough in the critical binding pocket residues that the metal specificity has changed, and has therefore now become a calcium transporting Nramp protein.

This is somewhat similar to what is observed in Nrat1, an Nramp-like protein that can transport Al^{3+} instead.

Nevo and Nelson (2006) stated that it would be more beneficial for transcription factors to use non-redox active ions, such as Ca^{2+} and Zn^{2+}. It is possible that the EIN2 N-terminal domain is delivering a metal, such as Ca^{2+}, to the C-terminal domain. Unpublished data by Dr. Georg Groth suggests EIN2 C-terminal domain, purified from *E.coli*, binds three or four Ca^{2+} ions. This could suggest that the C-terminal domain may be one of the targets of metal transport by the N-terminal domain. The C-terminal domain may then act as a chaperone to deliver Ca^{2+} to some other downstream target in the nucleus, when it is cleaved and is translocated, in response to ethylene (Chapter 2- Figure 2.4). Since the next known downstream component in the ethylene pathway is EIN3, it is possible that the target of EIN2 C-terminal domain could be EIN3. Another possibility is calcium could be required for the EIN2 C-terminal domain interaction with the 3'UTR of EBF1/2 or with EIN5 and other P-body factors (Liu et al., 2015). However, it is also possible that the target is some other unknown protein in the ethylene pathway or some other related pathway.

Calcium is required for regulation of many cellular processes. Calcium could be required for other proteins in the ethylene-signaling pathway, besides EIN2, and therefore it is difficult to assay for within the signaling context. A study done by Kwak and Lee (1997) found an increased influx of Ca^{2+} at around 6 hrs of ethylene exposure, which was important for the ethylene signal transduction. They also hypothesized that there would be a local intracellular reservoir of Ca^{2+} for this purpose. Perhaps EIN2 has a role in distribution and maintenance of local levels of

Ca^{2+} at or near the ER membrane. Another possibility is that calcium is required for an unknown kinase (Hwang et al., 2000) or phosphorylation event (Raz and Fluhr, 1993) required in the ethylene signaling pathway, since there are many possible proteins phosphorylated within the ethylene signaling pathway.

EIN2 could be providing a metal ion for some unknown function as well. A few possibilities are that EIN2 provides a metal cofactor to a metalloprotease (e.g., the unknown protease that cleaves EIN2). A metallophosphatase is also a possibility, in the regulation of EIN2, or perhaps to help regulate some other protein downstream of EIN2. Another possibility is that metal transport is required for some additional function of EIN2 beyond ethylene signaling. For example, the *ein2 G36E* mutant was isolated from an ABA screen (Gong, unpublished), and *ein2* mutants have been isolated from other screens for ABA, auxin, and cytokinin (Su and Howell, 1992; Fujita and Syono, 1996; Ghassemian et al., 2000). It is possible that EIN2 is transporting a metal ion to a protein in another signaling pathway besides ethylene.

Materials and Methods

Protein Sequence Alignments – Nramp protein sequences were obtained from the NCBI database using AtEIN2 as a query. The accession numbers are as follows: AtNramp1 (AF165125.1), AtNramp2 (AF141204.1), AtNramp3 (AF202539.1), AtNramp4 (Q9FN18.1), AtNramp5 (Q9SN36.1), AtNramp6 (AEE29390.1), *E. coli* MntH (BAA16262.1), *S. cerevisiae* SMF1 (CAA64547.1), *S. cerevisiae* SMF2 (P38778.1), *S. cerevisiae* SMF3 (Q12078.1), *M. musculus* Nramp2 (AAA39838.1), *M. musculus* Nramp1 (AAC42051.1), *D. melanogaster* Malvolio (AAA82593.1), *R. norvegicus* Nramp2 (AAC53319.1), *H. sapien* SLC11a1/Nramp1 (NP_000569.3), *H.*

sapien DCT1 (ADB56966.1), *D. rerio* Nramp2 (NP_001035460.1). The phylogenetic tree is a Neighbor joining tree, which was also generated using the MUSCLE software (Edgar, 2004) without distance corrections. The calculated branch lengths are shown. (http://www.ebi.ac.uk/Tools/msa/muscle/). The EIN2 protein sequence alignment is also shown and described in the methods in Chapter 3. Accession numbers are displayed.

Creation and Growth of EIN2 Hybrid-The *E. coli* codon optimized EIN2/MntH chimera construct (encoding residues 1-481) was synthesized and cloned into the pBAD24 vector using *BspHI* and *XbaI* restriction sites by Genewiz. The EIN2/MntH chimera was extended to create the EIN2 hybrid (encoding residues 1-524, see Appendix B) was created by Dr. Bret Cooper via Gibson cloning and ligated to the EIN2/MntH chimera. Growth was induced with 0.1% arabinose Growth inhibition assays were done by synchronizing an overnight culture to an OD600 of 0.0375 and grown for approximately 2.5 hours (or until cultures reached an OD of approximately 0.5), at which time cultures were induced with arabinose and growth (as monitored by the OD600 readings) was recorded for 3-4.5 hours post induction.

Detection of Proteins Expressed in *E. coli* (Western Blotting)- Using osmotic shock, membrane fractions were extracted from synchronized bacterial cultures grown for approximately 3 hrs until reaching an OD600 of (0.55-0.65) before the protein expression was induced with 0.1% arabinose. After pelleting the culture, and washing with 1X PBS, the pellet was then resuspended in 150 µL of cold resuspension buffer (20% sucrose, 10 mM Tris HCl pH 7.5) and spiked with 5 µL of cold 0.5 M EDTA pH 8. To isolate just the membrane fraction, the proteins were

incubated on ice for 10 min prior to a 5 min centrifugation at 10K rpm. Resulting pellet was resuspended in ice-cold sterile water and incubate on ice for 10 min. After a second 10K rpm spin, the resulting pellet contains the cytoplasmic/membrane fraction and was resuspended in 100 μL of sterile ice cold water. Protein fractions were solubilized in 4X SDS buffer (composed of 40% glycerol, 0.5 M β-mercaptoethanol, 40 mM Tris HCl pH 7.2, 0.005% bromophenol blue) at 4 C for 1 hr before a 10 min incubation at 37 C and protein samples were separated by 10% SDS-PAGE. An identical gel was loaded and used for the Coomassie Blue stain. Proteins were transferred to a PVDF membrane via semi-dry transfer, stained with Ponceau S to verify sufficient protein transfer and then immunoblotted with a 1:1000 dilution of an anti-His antibody (Abcam) to detect the 6 His epitope tags (*Ara-MntH-6His, Ara-EIN2/MntH chimera-6His, Ara-EIN2 hybrid-6His, Ara-EIN2 G36A hybrid-6His, Ara-EIN2 G36E hybrid-6His*). Detection of EIN2 hybrid and EIN2/MntH chimera required a SuperSignal™ West Femto Maximum Sensitivity Substrate detection kit (Thermo Fisher) and overnight film exposure.

Metal Transport in *E. coli* - Both *Ara-MntH* and *Ara-MntH-6His* constructs were a gift from from Dr. Mathieu Cellier. The nucleotides encoding the N37K and G36A substitutions were introduced into *MntH* pBAD24 constructs via site directed mutagenesis (Agilent Technologies), using primers listed below. The G36E and G36A substitutions were also introduced into both EIN2/MntH chimera and the EIN2 hybrid via site directed mutagenesis (Agilent Technologies) using the primers listed below. All constructs were transformed into SL93 *E. coli* strain lacking the *mntH* gene (also a gift from Dr. Mathieu Cellier). Fresh transformations were used for each

assay. Mickey assay was performed as described in Makui et al., 2000. *Ara-MntH N37K* was induced with 0.06% arabinose, *Ara-EIN2/MntH chimera* with 0.1% arabinose, EIN2 Hybrid with 0.06% and 0.04% arabinose.

Primer name	Forward or Reverse	Primer Sequence (5'-3')
MntH N37K	F	CGATTGGTTATATCGATCCCGGTAAGTTTGCGACCAATAT
	R	ATATTGGTCGCAAACTTACCGGGATCGATATAACCAATCG
MntH G36A	F	GATTGGTTATATCGATCCCGCTAACTTTGCGACCAATATTC
	R	GAATATTGGTCGCAAAGTTAGCGGGATCGATATAACCAATC
Hybrid G36A	F	TTGGCAACCCATTTGGCCGGGTCGATATAGC
	R	GCTATATCGACCCGGCCAAATGGGTTGCCAA
Hybrid G36E	F	GTGGGCTATATCGACCCGGAAAAATGGGTTGCCAATATCG
	R	CGATATTGGCAACCCATTTTTCCGGGTCGATATAGCCCAC

EIN2 N-terminal Domain Localization in Yeast- Both wildtype *EIN2 (1-524) (no stop*) pDONR221 and *EIN2 G36E (1-524) (no stop)* pDONR221 were transferred to the pMKZ vector, created by John Paul Ouyang and Jordon Limsky, respectively. The destination plasmids were transformed with each of the membrane markers; *SS01-Nub*, *SEC62-Nub*, *SED5-Nub*, and *SNC1-Nub* (Wittke et al., 1999) in the THY.AP4 yeast strain. For full-length EIN2 self-interaction, split Ub interactions were selected on plates lacking methionine with the addition of 10 μM FOA (5-Fluoroorotic Acid, GoldBio.com) Yeasts were spotted in serial dilutions (10^{-1} each) on both growth control (only lacking histidine and tryptophan) and selection plates, then grown at 30C for two to four days. Wildtype EIN2 was localized thanks to help from John Paul Ouyang and EIN2 G36E was localized thanks to help from Jordon Limsky.

Primer name	Forward or Reverse	Primer Sequence (5'-3')
EIN2 G36A	F	GTCGGATATATTGATCCCGCGAAATGGGTTGCAAATATC
	R	GATATTTGCAACCCATTTCGCGGGATCAATATATCCGAC
EIN2 G36E	F	GTCGGATATATTGATCCCGAGAAATGGGTTGCAAATATC
	R	GATATTTGCAACCCATTTCTCGGGATCAATATATCCGAC

Yeast Mutant Complementation – To recreate the Landsberg polymorphism, the nucleotides encoding the Y160C substitution were introduced into the *EIN2 (1-524, with stop)* pDONR221 and the *EIN2 G36E (1-524, with stop)* pDONR221 constructs via site directed mutagenesis (Agilent Technologies) using the primers listed below. *EIN2 (1-524, with stop)* pDONR221, *EIN2 G36E (1-524, with stop)* pDONR221, *EIN2 Y160C (1-524, with stop)* pDONR221, *EIN2 G36E Y160C (1-524, with stop)* pDONR221, *NRAMP4* pDON207 (a gift from Dr. Sébastien Thomine) and *GUS* pENTR (Invitrogen) were transferred to the pAG426-GPD-ccdB vector (obtained from Addgene) and the pDR195-GW vector (a gift from Dr. Sébastien Thomine). All plasmids were transformed into both the BY4741 wildtype and *smf2* mutant yeast strains. Yeasts were grown on minimal medium lacking uracil with the addition of 200 mg/L G418, pH 6.0, buffered with 10 mM MES. Yeast complementation of the *smf2* mutant (plates contained either 22 or 25 mM EGTA) and growth inhibition with cadmium (using 3, 10, and 20 μM $CdCl_2$) were done as described in Thomine et al.,

2000) Plates were grown at 30C for two to four days.

Primer name	Forward or Reverse	Primer Sequence (5'-3')
EIN2 Y160C	F	CAGGCCTGCAGAGCAAATGGATACTGTATTTGCCATAC
	R	GTATGGCAAATACAGTATCCATTTGCTCTGCAGGCCTG

Calcium Triple Response Assay- Seeds for both *Arabidopsis thaliana* ecotype Landsberg (L*er*, used as the wild-type) and the *ein2 G36E* mutant were plated onto 0.8% agar with or without the addition of 10 mM $CaCl_2$. For ethylene response, 20 μM ACC (Sigma Aldrich) was added to the plates. Plates were cold stratified at 4 C, in the dark, for 4 days prior to the 20 C dark treatment for 4 days. Seedlings were photographed and hypocotyls were measured using the ImageJ software (https://imagej.nih.gov/ij/).

Chapter 5: RTE3: a Member of a Large Nuclear Protein Complex, Related to Ethylene Signaling

Introduction

Discovery of the *rte3* Alleles

In an attempt to find novel components of the ethylene signaling pathway, a previous lab member, Dr. Chunhai Dong, performed an EMS suppressor screen of *etr1-2*, a weak insensitive allele of *ETR1*. By isolating mutants with the ability to suppress the insensitivity of just one of the redundant ethylene receptors, we were hoping to uncover new mutants not found in previous screens. This screen yielded *rte3* (REVERSION TO ETHYLENE SENSITIVITY 3) a recessive extragenic suppressor mutant *of etr1-2* (data not shown). Two alleles were isolated from this suppressor screen, *rte3-1* (W1187*) and *rte3-2* (W1321*) (Figure 5.1, McClellan, PhD thesis), both alleles show the same phenotype and are predicted to encode truncated proteins, therefore the majority of the work was done using the *rte3-1* allele. (McClellan, PhD thesis).

Dr. Christopher McClellan started the project and did the initial characterization of the *rte3* mutants, mapping, and RTE3 localization. *RTE3* (also called *SAC3b*) contains 19 exons and 18 introns (Figure 5.2, McClellan, PhD thesis) and is located on chromosome 3. Interestingly, when cloning *RTE3*, two alternative splice forms were found. The first splice form differs from the predicted annotation in TAIR (The *Arabidopsis* Information Resource, www.arabidopsis.org) by 54 nucleotides (385-438 of the 8.1 kb genomic sequence). These nucleotides are located at the 5' end of the second exon,

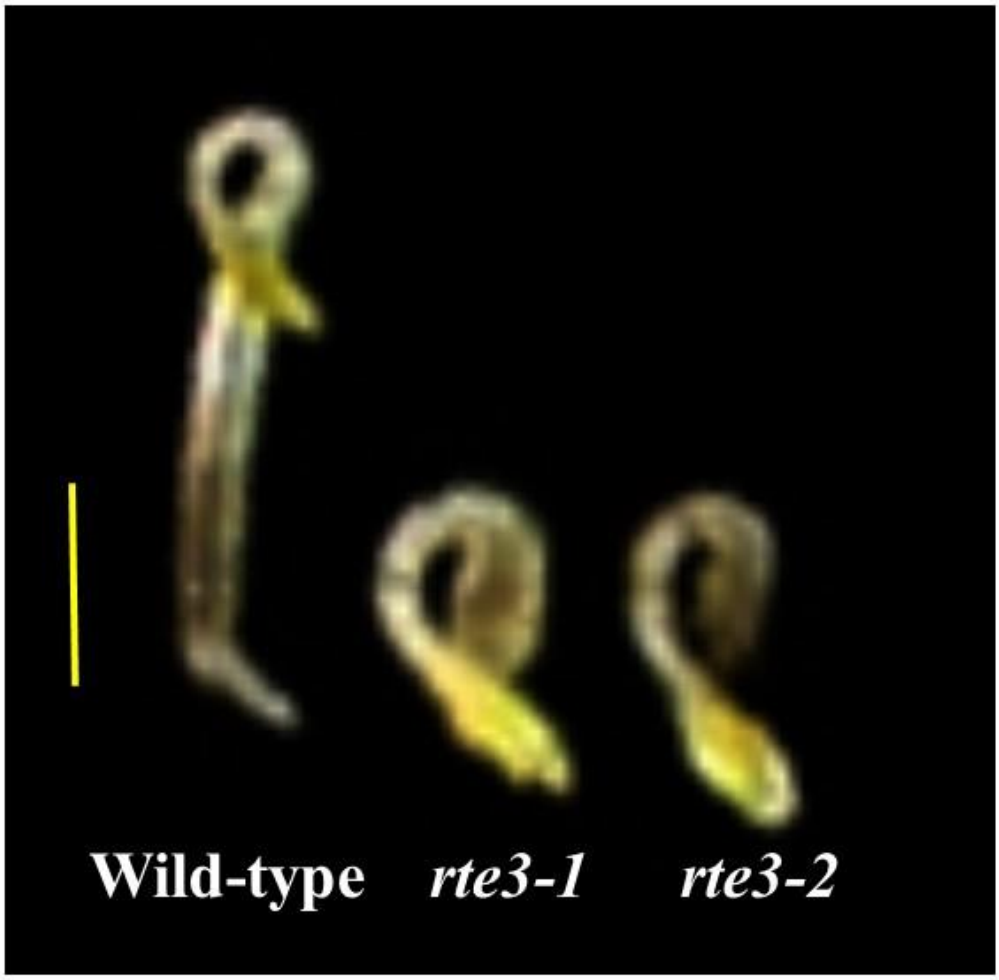

Figure 5.1. The *rte3-1* and *rte3-1* mutants have a similar phenotype. Although the *rte3-1* (W1187*) and *rte3-2* (W1321*) both potentially encode most of the RTE3 protein, both alleles show the same hypersensitive ethylene phenotype, much more dramatic than wild-type (Col-0). Representative sample of four day-old etiolated seedlings were grown on plates containing 20 µM ACC. Scale bar represents 1 mm. Similar figure also shown in McClellan, PhD thesis.

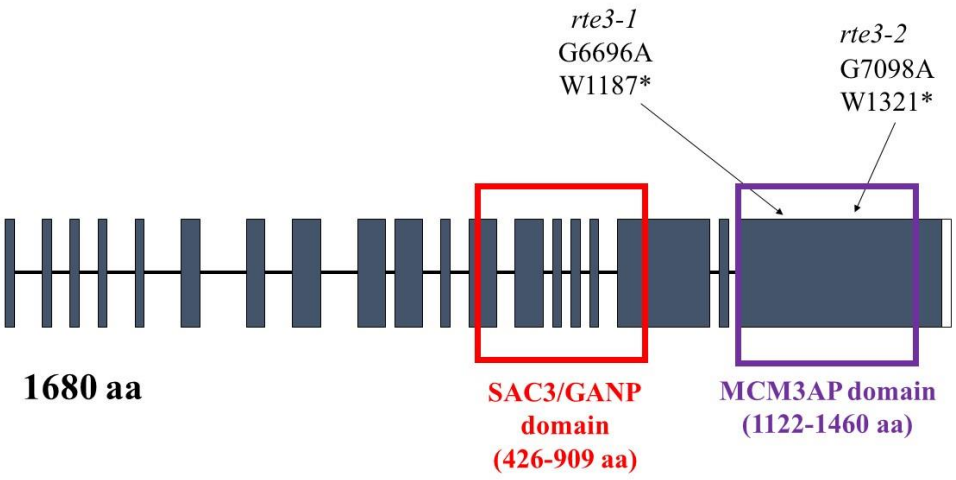

Figure 5.2. Gene structure of *RTE3* showing the two different protein domains. *RTE3* gene is approximate 8.2 kb long (genomic sequence), contains 19 exons (blue boxes) and 18 introns (black lines) and encodes a 1680 residue protein. The RTE3 protein encodes two different protein domains, a SAC3/GANP domain (red box, residues 426-909) and a MCM3AP domain (purple box, residues 1122-1460). Two different alleles of *RTE3* were isolated, *rte3-1* and *rte3-2*, both denoted above and encode premature stop codons at residues 1187 and 1321, respectively. Both alleles would potentially encode truncated proteins. Figure taken from McClellan, PhD thesis and slightly modified.

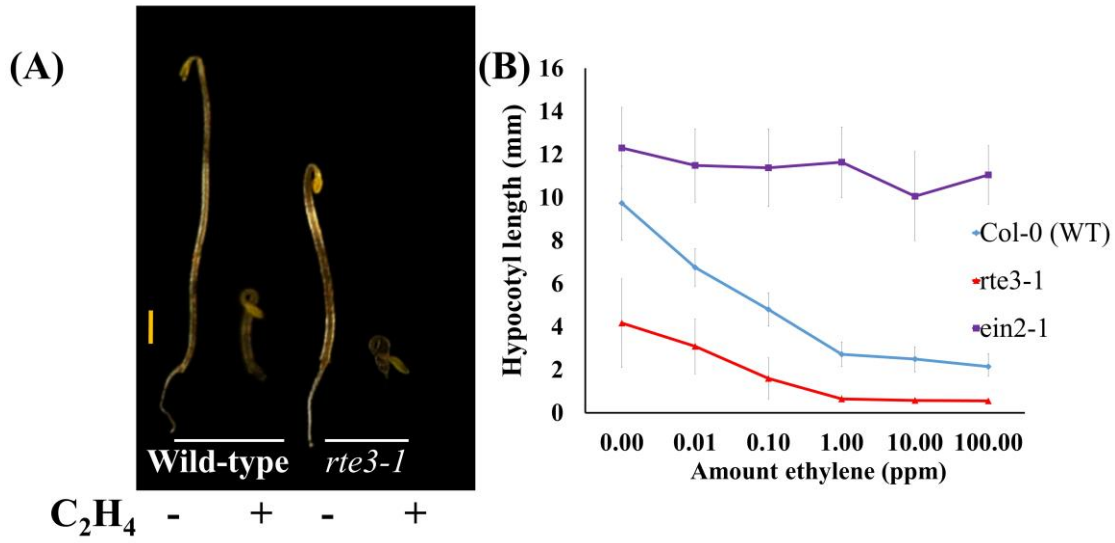

Figure 5.3. The *rte3-1* mutant is hypersensitive to ethylene, but inhibition of hypocotyl elongation is more of a pleiotropic response. Four day-old etiolated seedlings were grown at various concentrations of ethylene (from 0 to 100 ppm). The *rte3-1* mutant shows a hypersensitive response, compared to wild-type (Col-0). However, without ethylene, the *rte3-1* mutant is also shorter than wildtype, suggesting *RTE3* has a more pleiotropic response on hypocotyl growth. (A) A representative sample of seedlings grown at 0 and 100 ppm ethylene. Scale bar represents 1 mm. (B) Ethylene dosage response curves for Col-0 and *rte3-1*. The *ein2-1* mutant was used a negative control. Hypocotyls were measured using Image J. Error bars represent standard deviation, where $40<n<75$ seedlings.

and are spliced out with the first intron. This was the splice form used for all subsequent applications since the predicted coding sequence on TAIR was not found with RT-PCR (no supporting cDNA) (McClellan, PhD thesis). The second splice form has a 215 nucleotide deletion (1428-1642 of the genomic sequence) at the 5' end of the sixth exon. This deletion leads to a frameshift in the *RTE3* cDNA, and a stop codon is soon encountered, potentially producing a severely truncated protein (McClellan, PhD thesis).

The *rte3* mutants were isolated from the *etr1-2* suppressor screen due to their extreme hypersensitive phenotype in the presence of ethylene. However, they were also proportionally shorter than wild-type without ethylene (Figure 5.3; McClellan, PhD Thesis). The addition of silver nitrate (an ethylene signaling inhibitor) and AVG (an ethylene biosynthesis inhibitor) were not able to rescue the *rte3* mutant phenotype back to wild-type length, suggesting that the shortening of the hypocotyl is not purely due to ethylene (McClellan, PhD thesis). This indicates that *RTE3* is involved in some parallel pathway that similar to ethylene, affects hypocotyl growth.

RTE3 Protein Analysis

Further analysis of *RTE3* indicated that it encodes a 1680 residue protein, which localized to the nuclear periphery (McClellan, PhD thesis) and contains both a SAC3/GANP domain (residues 426-909) and an MCM3AP domain (residues 1122-1460) (Figure 2). GANP (GERMINAL CENTER ASSOCIATED NUCLEAR PROTEIN) is the mammalian homolog of yeast SAC3 (SUPPRESSOR OF ACTIN). SAC3 protein domains are usually found in large protein complexes with diverse functions, throughout eukaryotes, such as TREX-2 mRNA export complex, eIF3

initiation factor, and the 26S proteasome lid (Lei et al., 2003; Burks et al., 2001; Gordon et al., 1996).

MCM3AP (MINI CHROMOSOMAL MAINTAINENCE 3 ASSOCIATED PROTEIN, also called Map80: 80 kDa MCM3 ASSOCIATED PROTEIN) is a mammalian splice variant of the GANP protein, where only the MCM3AP protein is expressed. Even though MCM3AP is part of the GANP protein, the MCM3AP protein functions independently of GANP (Abe, et al., 2000; Wickramasinghe, et al., 2010b). Yeast SAC3 does not contain this additional MCM3AP domain.

One of the differences between GANP and MCM3AP, is that MCM3AP is found in both the nucleus and cytoplasm (Takei, et al., 2002) whereas GANP (as well as SAC3 in yeast) is nuclear localized (Wickramasinghe, et al., 2010b; Jones, et al., 2000). Binding of MCM3AP to, and the subsequent acetylation of MCM3 by MCM3AP facilitates this nuclear localization and formation of the pre-replication complex (Takei and Tsujimoto, 1998; Takei, et al., 2002). MCM3 (MINI CHROMOSOMAL MAINTENANCE 3) is one of six MCM proteins that form the pre-replication complex, essential for the initiation of DNA replication in eukaryotes (Forsburg, 2004). Although RTE3, like GANP, contains both a SAC3 domain and an MCM3AP domain, no MCM3AP splice variant have been identified in *Arabidopsis.*

EER5 May Have a Similar Function to RTE3 or Found in a Similar Pathway

In studying the *rte3* phenotype, we noticed that it has a similar phenotype to an *eer5* mutant (Figure 5.4; McClellan, PhD thesis; Christians et al., 2008). Like RTE3, EER5 (ENHANCED ETHYLENE RESPONSE 5) also was found to localize to the nuclear periphery (McClellan, PhD thesis). In addition, the double mutant with

eer5-1 ein3-1 has a similar partial suppression as the *rte3-1 ein3-1* double mutant when grown on plates containing ACC (Christians et al., 2008; data not shown). This could suggest that RTE3 and EER5 may have similar functions or are in a similar pathway.

EER5 contains a PAM domain (PCI/PINT ASSOCIATED MODULE), which are known to interact with proteins containing PCI/PINT (PROTEASOME, COP9, INITIAITION FACTOR) domains as well as SAC3 domains. PCI/PINT and PAM domains, similar to SAC3 domains, are found in proteins involved in large complexes such as the 26S proteasome lid and the TREX-2 mRNA export complex (Ciccarelli, et al., 2003). However PCI/PINT and PAM domains are also found in other complexes, such as the subunits of the COP9 signalosome (CSN) (Ciccarelli, et al., 2003). CSN homology to the 26S proteasome lid extends beyond the PCI/PINT and PAM domains (Wei and Deng, 2003).

EER5, EIN2 C-terminal Domain and the COP9 Signalosome are in a Large Nuclear Protein Complex

Christians et al. (2008) discovered that EER5 interacts with EIN2 C-terminal domain (residues 516 to 1294) and CSN8 (COP9 signalosome, subunit 8) using the yeast 2-hybrid assay. They also found that EIN2 C-terminal domain interacts with CSN3, CSN6A, and CSN6B (additional subunits of the COP9 signalosome). This could suggest that EIN2 C-terminal domain, EER5, and the COP9 signalosome may function in a complex together. It could also suggest that RTE3 may be a member of the same hypothesized complex, since SAC3 domains are also found in similar complexes as PAM and PCI/PINT domains (Ciccarelli et al., 2003).

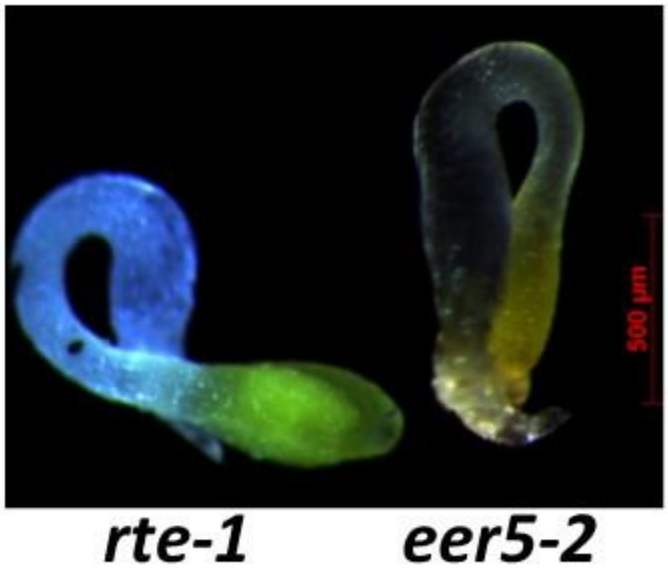

Figure 5.4. The *rte3-1* and *eer5-2* mutants have a similar ethylene hypersensitive phenotype. Four day-old etiolated seedlings were grown on plates containing 20 µM ACC. Representative sample of seedlings. Images taken using a Zeiss Axioscope. Scale bar represents 500 µm.

COP9 signalosome (CSN) mutants were originally identified as constitutively photomorphogenic mutants, because they look like light-grown seedlings when grown in the dark (Wei and Deng, 1992). The CSN is a large, highly conserved protein complex, composed of nine subunits (CSN1-8 and CSNAP), shows homology to the 26S proteasome lid, and found in eukaryotes **(**Wei and Deng, 2008; Mundt et al., 1999; Glickman et al., 1998; Rozen et al, 2015). CSN has been shown to play a role in many cellular processes, such as; cell cycle progression, nuclear export, and the DNA damage repair pathway (Tomoda et al., 2001; Doronkin et al., 2002; Doronkin et al., 2003; Liu et al., 2013; Füzesi-Levi et al., 2014). The *csn* subunit mutants show the same seedling lethal phenotype, suggesting that this complex functions as a holoenzyme. Interestingly, both CSN3 and CSN5 have been shown to have additional independent functions, beyond the COP9 signalosome (Kwok et al., 1998; Wang et al., 2002; Huang et al., 2013).

The Arabidopsis TREX-2 mRNA Export Complex

RTE3 and EER5 were shown to be members of the Arabidopsis TREX-2 mRNA export complex (Liu et al., 2010). The TREX-2 complex is evolutionarily conserved amongst eukaryotes and plays a role in many cellular processes, such as; transcription and mRNA export (Gallardo et al., 2003), DNA replication (Bermejo et al., 2011), gene gating (Cabal et al., 2006), and genome stability (González-Aguilera et al., 2008).

The *Arabidopsis* TREX-2 mRNA export complex is an example of a nuclear pore complex not as highly conserved in plants, since not all the yeast homolog interactions were observed in *Arabidopsis* (Lu, et al., 2010). For example, in yeast the

SAC3 (SUPRESSOR OF ACTIN) protein component of this complex interacted with two SUS1 proteins, but in Arabidopsis, RTE3 (REVERSION TO ETHYLENE SENSITIVITY 3, also called SAC3B) did not interact with the AtSUS1 protein (Jani et al., 2009; Liu et al., 2010). In addition, yeast SAC3 interacted with NUP1, which allows the TREX-2 complex to dock directly at the nuclear pore (Jani et al, 2009). However, in the Arabidopsis TREX-2 complex, EER5 (ENHANCED ETHYLENE RESPONSE 5, also known as THP1) acted as a mediator protein and forms a bridge between RTE3 and AtNUP1 since a direct interaction between RTE3 and AtNUP1 was not detected (Liu et al., 2010). This could suggest that the *Arabidopsis* TREX-2 complex may be composed of slightly different proteins (or protein interactions) and behaving differently than its yeast counterpart.

Results

RTE3 is in a Large Nuclear Protein Complex with EER5, CSN3 and EIN2

RTE3 protein contains a SAC3/GANP domain, which are known to interact with PAM domain containing proteins and found in large protein complexes (Ciccarelli, et al., 2003). Christians et al. (2008) found that EER5 and EIN2 C-terminal domain can interact with members the Arabidopsis COP9 complex, when expressed in yeast. Additionally, RTE3 and EER5 also both localize to the nuclear periphery (McClellan, PhD thesis) and both the *eer5-2* and *rte3-1* mutants have a similar enhanced ethylene phenotype (Figure 5.4), suggesting they might somehow be functioning together or in a similar pathways. This suggests that perhaps EER5, EIN2 C-terminal domain and the COP9 complex could be in a large protein complex with RTE3.

To test this possibility, Dr. Chris McClellan and I used a yeast 2-hybrid assay to test whether RTE3 also interacted with CSN3 (and other subunits of the COP9 complex), EER5, and EIN2 C-terminal domain. We found RTE3 interacted with EER5, EIN2 C-terminal domain, and CSN3 (Figure 5.5; McClellan, PhD thesis), but did not interact with CSN5, 6 or 8 (data not shown). I further verified these interactions *in planta*, using BiFC expressed in tobacco leaf epidermal cells (Figure 5.6) placing RTE3 in a large protein complex in the nucleus. However, the function of this complex is not known.

Lu et al., (2010) published the RTE3-EER5 (SAC3B-THP1) interaction and suggested that RTE3 is involved with EER5 in the TREX-2 mRNA export complex. However, it is not understood how the COP9 complex and EIN2 play a role in this. One possibility is that they are involved in nuclear protein export of EIN2 C-terminal domain to the P-bodies (Li et al., 2015; Merchante et al., 2015). The subunits of the COP9 complex are also known to have independent functions, beyond their role in the signalosome (Stuttmann et al., 2009). Perhaps this is a novel role for CSN3.

Genetic Evidence for the RTE3 - EER5 Interaction

For genetic evidence to further support these physical protein interactions, a previous graduate student, Dr. Christopher McClellan, created the double mutants, *rte3-1 eer5-2* and *rte3-1 ein2-1*. The *rte3-1 eer5-2* seeds were given to me at the segregating F_2 stage, whereas the *rte3-1 ein2-1* seeds luckily were already homozygous. The *rte3-1 csn3* double mutant was not investigated. Unfortunately, *csn* mutants are notoriously difficult to work with, due to their seedling lethality, and therefore I did not create a double mutant with *rte3* and *csn3*. I figured assumed a

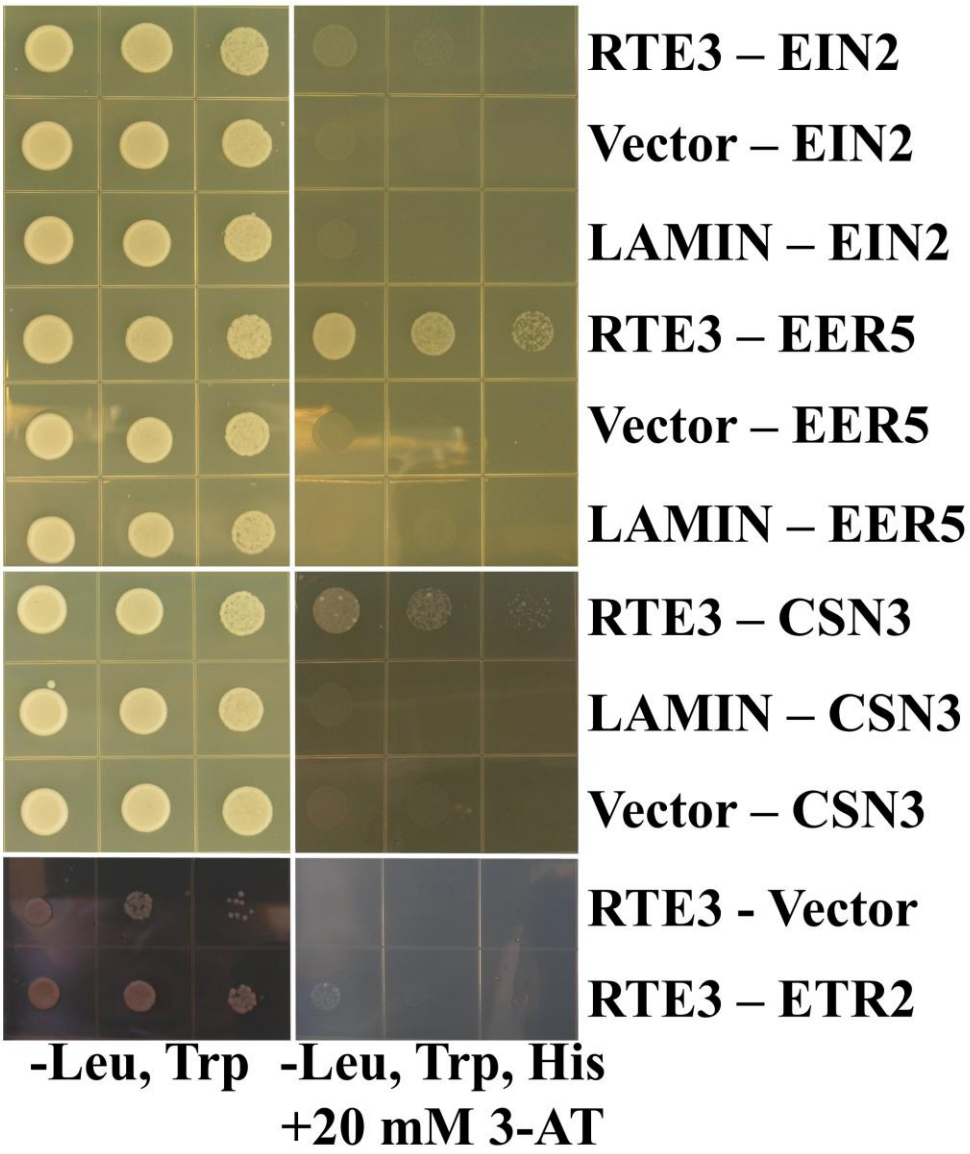

Figure 5.5. RTE3 interacts with the EIN2 C-terminal domain, EER5 and CSN3, in yeast. Using a yeast 2-hybrid assay RTE3 was found to interact with the EIN2 C-terminal domain (residues 516-1294), EER5, and CSN3. Yeasts were spotted on minimal medium plates lacking leucine and tryptophan (left panel, growth control) and interactions selected using minimal media (lacking leucine, tryptophan, and histidine, with the addition of 20 mM 3-AT (3-Amino-1,2,4-triazole), right panel). Interaction with either LAMIN, ETR2, and/or empty vector (pACTII or pLEXA) was

used as a negative control. Plates were grown for 2-5 days at 30 C. Similar results also shown in McClellan PhD thesis.

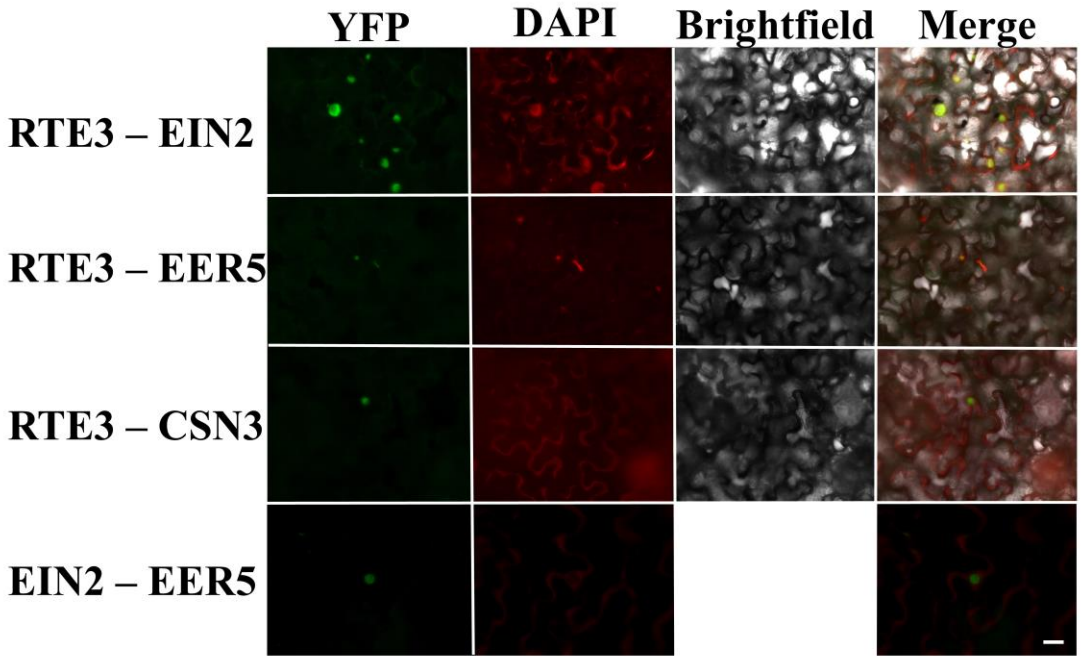

Figure 5.6. RTE3 interacts with EER5, CSN3 and EIN2 C-terminal domain in the nucleus, *in planta*. BiFC interaction of RTE3 with EIN2 C-terminal domain (residues 516-1294), EER5, and CSN3 in tobacco leaf epidermal cells. Also shown is the BiFC interaction of EIN2 C-terminal domain with EER5. The YFP (BiFC signal) overlaying with the DAPI signal suggests these interactions occur in the nucleus. Tobacco leaves were infiltrated with Agro bacteria containing the BiFC constructs (both EIN2 and RTE3 expressed the N-terminal half of YFP while EER5, EIN2 and CSN3 expressed the C-terminal half of YFP), and allowed to incubate for 3 days before being imaged using a Zeiss AxioObserver. Merged image shows YFP (BiFC signal), DAPI (20 mg/mL, falsely colored red for clarity in merged image), and Brightfield. Scale bar represents 50 µm.

weaker allele of *csn3*, which may not be lethal, perhaps would not be as informative.

The *rte3-1 eer5-2* double mutant is extremely dwarfed, produces many leaves, and sterile (Figure 5.7) suggesting a synergistic role for the two genes. Reducing the expression of *EER5* results in a prolonged lifespan and reduced fertility, since the wildtype were already dead. Plants heterozygous for the *eer5* mutation were shown starting to senesce and plants homozygous for *eer5* mutation were still green and much less fertile (Figure 5.7a). Loss of *RTE3* seems to slightly extend lifespan, since the homozygous *rte3* plants were much more fertile and pictured senescing (Figure 5.7a and 5.7b). However, even at earlier stages of development, the *rte3-1 eer5-2* double mutant had an extremely dwarfed phenotype (Figure 5.7c). Perhaps this could suggest a more general role for these two proteins in plant growth and development. Although sterile, the *rte3-1 eer5-2* double mutant did eventually produce a few flowers. When I looked at these flowers, it is clear why they are sterile, since the flowers are not properly developed (Figure 5.7d). The petals did not form properly and neither did the sepals. Most importantly, the stamen are under developed and too short to reach the top of the stigma, which also looks under developed. The anthers did produce a little pollen, but nothing that would stick to the stigma. So basically, the few flowers that did form were unable to be pollinated and therefore resulted in a sterile plant.

This is different than what was observed in the Lu et al., 2010 study. In this study, they produced an *rte3 eer5* double mutant using two different alleles. Although their phenotype was also dramatic, still suggesting a genetic interaction between these two proteins, the phenotype produced had a small stature and reduced

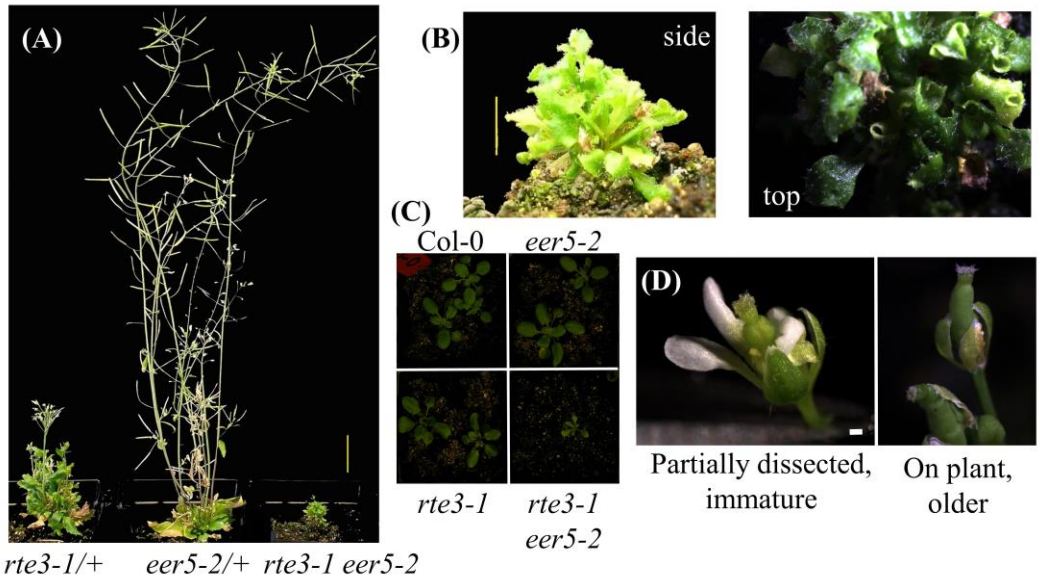

Figure 5.7. The *rte3-1 eer5-2* double mutant has extremely stunted growth and is sterile. (A) Representative sample of 10 week old plants. From left to right: *rte3-1/+ eer5-2/eer5-2; rte3-1/rte3-1 eer5-2/+; rte3-1/rte3-1 eer5-2/eer5-2.* The *rte3-1 eer5-2* double mutant is extremely dwarfed and delayed in growth. Col-0 wild-type was already dead and seeding, so not depicted. Scale bar represents 10 mm. (B) Close-up image of just the *rte3-1 eer5-2* double mutant from the side and top. Scale bar represents 5 mm. (C) Representative sample of 4 week old plants, showing just the double mutant and wild-type (Col-0), again showing that the double mutant is extremely dwarfed in development. (D) Representative image of flowers on the *rte3-1 eer5-2* double mutant, show flower development defect. Images taken with Zeiss AxioScope. Scale bar represents 200 µM.

fertility. However, their double mutant was not sterile and not just basically a little bush of leaves, like the *rte3-1 eer5-2* double mutant (Figure 5.7a and 5.7b). Perhaps because stronger alleles have a stronger phenotypes? This was quite intriguing since the *rte3-1* mutant is not a null (McClellan, PhD thesis) and Lu et al., (2010) suggested the *sac3b-2* mutant is a null allele.

Naturally, I was curious as to how the phenotype of the *sac3b-2* mutant compared to the *rte3-1* mutant, so I obtained the *sac3b-2* mutant used in the Lu et al. (2010) study. When compared, the phenotypes were very similar to each other (Figure 5.8). This suggests that the *rte3-1* mutant could be behaving like a null mutant. However, data suggests that there is a transcript expressed in this mutant, suggesting that *rte3-1* is probably producing a protein (data not shown, McClellan, PhD Thesis). It is possible that this truncated protein is untranslated or non-functional and therefore rte3-1 functions like a null allele.

Genetic Evidence for the Interaction Between RTE3 and the EIN2 C-terminal Domain

To provide genetic evidence of the RTE3-EIN2 interaction, *rte3-1 ein2-1* double mutant was created by Dr. Christopher McClellan. Originally this mutant was created as another way to determine if RTE3 was in the ethylene pathway, via epistasis analysis. However, when the triple response assay was attempted, it became obvious that this assay was not possible due to a germination defect. So, instead, we assayed the *rte3-1 ein2-1* double mutant for germination, and found that although *ein2-1* had a slight germination delay, the *rte3-1 ein2-1* double mutant had an enhanced delayed in germination (Figure 5.9; McClellan, PhD Thesis). In fact, even

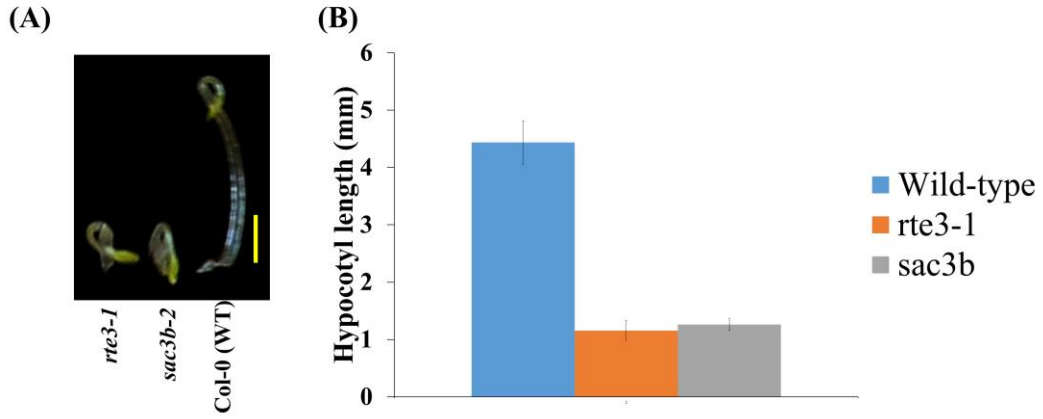

Figure 5.8. The *rte3-1* mutant has the same phenotype as the *sac3b-2* null mutant. Four day-old seedlings were grown on plates containing 20 µM ACC. (A) Representative sample of seedlings showing the *rte3-1* mutant has the same phenotype as the *sac3b-2* mutant used in the Lu et al. 2010 study. Scale bar represents 1 mm. (B) Hypocotyl measurements of seedlings grown on 20 µM ACC, measured using Image J. Error bars show standard deviation.

after two weeks there was still only 84% germination.

To help aid germination and to test whether osmotic stress played a role, I also grew the seeds with 2% sucrose or 1% mannitol, respectively, and neither caused a dramatic difference in germination (data not shown). The enhanced germination defect of the *rte3-1 ein2-1* double mutant suggests a synergistic role for the RTE3 and EIN2. This suggests RTE3 and EIN2 could be functioning in parallel pathways to affect germination.

Dr. Christopher McClellan found that the S-phase cyclin gene marker CYCA3;2 was increase in both *rte3-1* and *rte3-1 ein2-1*, suggesting that a role for RTE3 in cell cycle regulation (McClellan, PhD thesis). However, it is unclear how and if the cell cycle plays a role, or if it is just an artifact of the *rte3-1* mutant. Interestingly, yeast SAC3 was found to play a role in normal cell cycle progression (Bauer and Kölling, 1996).

The RTE3-1 Substitution Disrupts the Interaction of RTE3 with CSN3 and the EIN2 C-terminal Domain

The *rte3-1* mutant, which would potentially produce a truncated protein (Figure 5.2), has the same phenotype as the null *sac3b-2* mutant (Figure 5.6) yet is not a null allele (data not shown, McClellan, PhD thesis). It is possible that this *rte3-1* phenotype is a result of a loss of an essential protein interaction. In the *rte3-1* allele, the premature stop codon is located 65 residues into the 338 residue MCM3AP domain, potentially resulting in a truncated protein without a complete MCM3AP domain. However, it is unknown, the extent to which this potential truncated MCM3AP domain is functional.

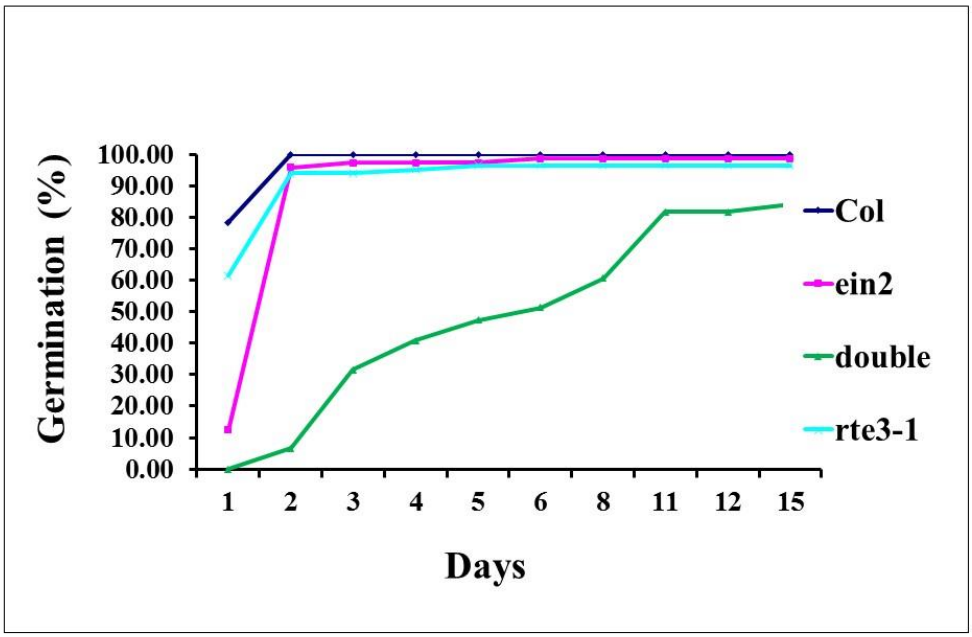

Figure 5.9. The *rte3-1 ein2-1* double mutant shows a severely enhanced germination delay. When grown in the light on MS media, both the *rte3-1* and *ein2-1* single mutants showed a slight germination delay. However, this germination delay (as measured by rupture of the seed coat) was greatly enhanced in the *rte3-1 ein2-1* double mutant. Even after two weeks, only 84.2% germination was achieved, whereas 100, 98.6, and 96.4% germination was achieved for the wild-type (Col-0), *ein2-1*, and *rte3-1* single mutants, respectively. Seed germination scored (as a crack in the seed coat) using a Zeiss Axio Scope, where $70<n<80$ seeds.

To test whether the *rte3-1* mutation causes a loss of an essential protein interaction, I used a yeast 2-hybrid assay, introducing the W1187* mutation into the previously created RTE3 construct, creating yeast expressing RTE3-1. I used this new RTE3-1 protein to test with the known interacting proteins: EER5, CSN3, and EIN2 C-terminal domain (residues 516-1294). RTE3-1 still was still able to interact with EER5, but lost the ability to interact with EIN2 C-terminal domain and CSN3 (Figure 5.10), suggesting that EIN2 and CSN3 may be interacting with the MCM3AP domain. This also suggests that EER5 may be interacting with the SAC3 domain, which was expected since the SAC3 domain is the component of the yeast TREX-2 complex, which interacts with the EER5 homolog (Jani et al., 2009). It is possible that the enhanced phenotype seen in the *rte3-1* mutant allele is due to a loss of either/both of the protein interactions with CSN3 and EIN2 C-terminal domain.

The *rte3-1* substitution also seemed to reduce the strong self-activation seen with RTE3 and empty vector since the X – gal assay did not show an interaction for RTE3-1 with empty vector, but did show a positive interaction for wild-type RTE3 and empty vector (data not shown). This suggests that there might be some sort of a transcriptional activation domain within the last 500 residues of RTE3. Another possibility is that the *rte3-1* substitution is disrupting the confirmation of RTE3.

EER5, CSN3 and EIN2 C-terminal Domain Interact With the MCM3AP Domain of RTE3

If EER5 interacted with the SAC3 domain of RTE3, do CSN3 and the EIN2 C-terminal domain interact with the remaining MCM3AP domain? To test this, an undergraduate working with me, Andrew Scaggs, used the yeast 2-hybrid assay to test

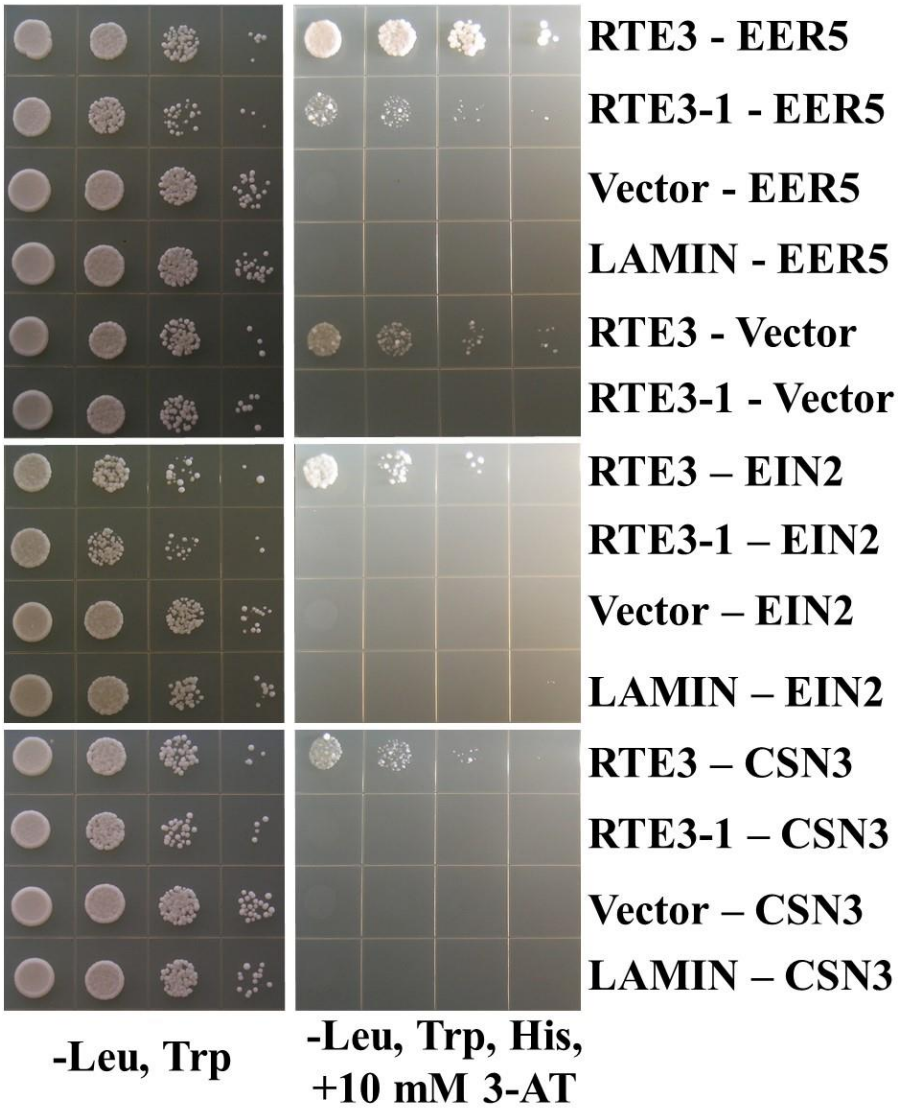

Figure 5.10. The *rte3-1* substitution disrupts the interaction with EIN2 C-terminal domain and CSN3, in yeast. A W1187* substitution was inserted into the previously created RTE3 pLEXA construct (from Figure 5.5), to mimic the *rte3-1* mutant allele (termed RTE3-1). The RTE3-1 protein was no longer able to interact with EIN2 C-terminal domain (residues 516-1294) and CSN3, but the RTE3-EER5 interaction remained intact. Growth plates (left panel) consisted of minimal media lacking leucine and tryptophan. Selection plates (middle panel) consisted of minimal media

(lacking leucine, tryptophan, and histidine) with the addition of 10 mM 3-AT (3-Amino-1,2,4-triazole). Empty vectors (pACTII or pLEXA) and LAMIN were used as a negative controls. Yeast plates grown for 2 or 5 days at 30 C.

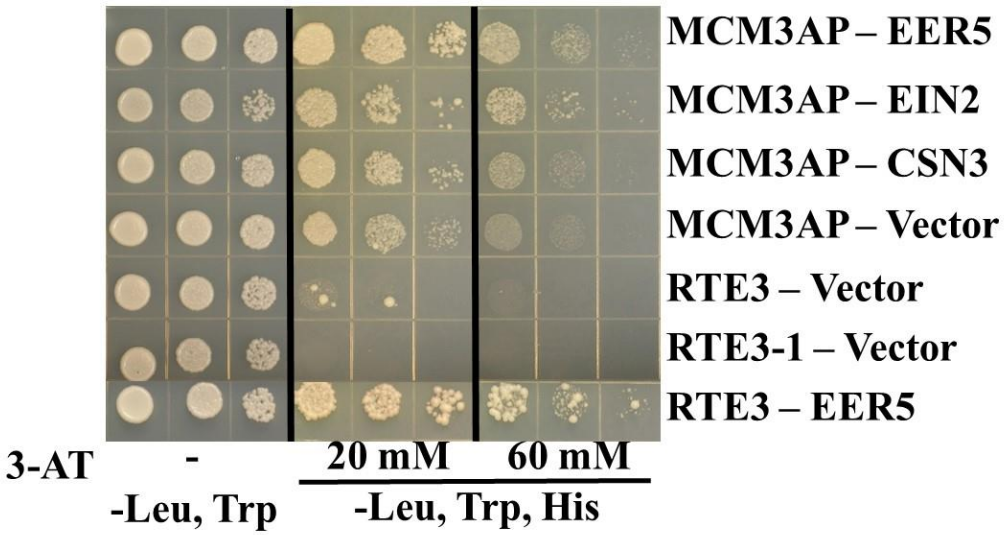

Figure 5.11. EER5, EIN2 C-terminal domain and CSN3 interact with the MCM3AP domain of RTE3, in yeast. The MCM3AP domain of RTE3 (from residues 1122-1460) was cloned into the pLEXA vector and tested against the interacting proteins of RTE3. All three proteins; EER5, EIN2 C-terminal domain (residues 516-1294), and CSN3 were found to interact with the MCM3AP domain, since there was more growth observed in these interactions than with yeast transformed with both the MCM3AP domain and empty vector. However, even at 60 mM 3-AT, growth was observed with the yeast transformed with both the MCM3AP domain and empty vector, whereas growth was inhibited at this concentration when transformed with the full length RTE3 protein. Growth plates (left panel) consisted of minimal media lacking leucine and tryptophan. Selection plates (right panel) consisted of minimal media (lacking leucine, tryptophan, and histidine) with the addition of 20 or 60 mM 3-AT (3-Amino-1,2,4-triazole). Empty vectors (pACTII or pLEXA) were used as a

negative controls. The RTE3-EER5 interaction was used as a positive control. Yeast plates were grown for 2 or 4 days at 30 C.

whether CSN3, EIN2 C-terminal domain and EER5 interact with the MCM3AP domain of RTE3. All three proteins interacted with the MCM3AP domain (Figure 5.l1) suggesting the CSN3 and the EIN2 C-terminal domain interactions are specific to the MCM3AP domain of RTE3, while the EER5 interaction spans both SAC3 and MCM3AP domains. This further suggests that it is possible that the *rte3-1* phenotype could be a result of the loss of the protein interaction with CSN3 and/or the EIN2 C-terminal domain.

The *rte3-1* Allele Does Not Have an mRNA Export Defect

In yeast, SAC3 is an important part of the TREX-2 mRNA export complex and the *Δsac3* yeast mutants have an mRNA export defect (Fischer et al., 2002; Lei et al., 2003). However, the Arabidopsis s*ab3b-2* allele did not have an mRNA export defect (Lu et al., 2010), suggesting that the Arabidopsis TREX-2 complex may be functioning differently than the yeast complex. Our *rte3-1* allele had a more severe phenotype than the published null *sac3b-2* mutant (Lu et al., 2010). However, when I compared the two alleles, they were very similar (Figure 5.6). Nonetheless, I was curious as to whether the *rte3-1* mutant allele would show an mRNA export defect. However, when the location of cellular mRNAs were visualized using an *in situ hybridization* mRNA export assay, the *rte3-1* mutant did not have an mRNA export defect (Figure 5.12). This suggests the Arabidopsis TREX-2 complex is functioning differently than the yeast homolog since the yeast homolog does have an mRNA export defect and is an essential component of the mRNA export function (Fischer et al., 2002; Lei et al., 2003; Jani et al., 2009). Additionally, it further indicates that the *rte3-1* mutant is behaving similar to the null *sac3b* mutant (Figure 5.11) and suggests

that RTE3 may not play as important a role in mRNA export as the yeast SAC3 homolog.

RTE3 Interacts With an EF-HAND Protein

In order to isolate other interacting proteins with RTE3, other possible components of this large nuclear protein complex, a previous graduate student, Dr. Christopher McClellan, used a yeast 2-hybrid cDNA library screen, where RTE3 was used as the bait protein. The cDNA library consisted of RNA from three-day old etiolated seedlings (McClellan, PhD Thesis). One positive clone was isolated, containing the protein from At4g27280, which was called "EF-HAND" since it contained a calcium binding EF-Hand domain.

I was curious whether this EF HAND protein was also in this complex, with EER5, CSN3 and EIN2 C-terminal domain. In the yeast TREX-2 complex, SAC3 interacts with CDC31, an EF Hand containing protein (Jani et al., 2009), so it is possible that an EF Hand containing protein was also in this complex. Therefore, I wanted to test if our EF-HAND protein could also interact with the other proteins that were known to interact with RTE3, placing it in the same complex. Using a yeast 2-hybrid assay, I found that EF-HAND could not interact with EER5, EIN2 C-terminal domain, or CSN3, suggesting that the EF-HAND protein is not in the same complex with the other proteins. Another possibility is that this EF-HAND was isolated due to the EF-Hand protein domain's affinity for SAC3 domains in yeast (the EF-HAND just happened to stick to RTE3).

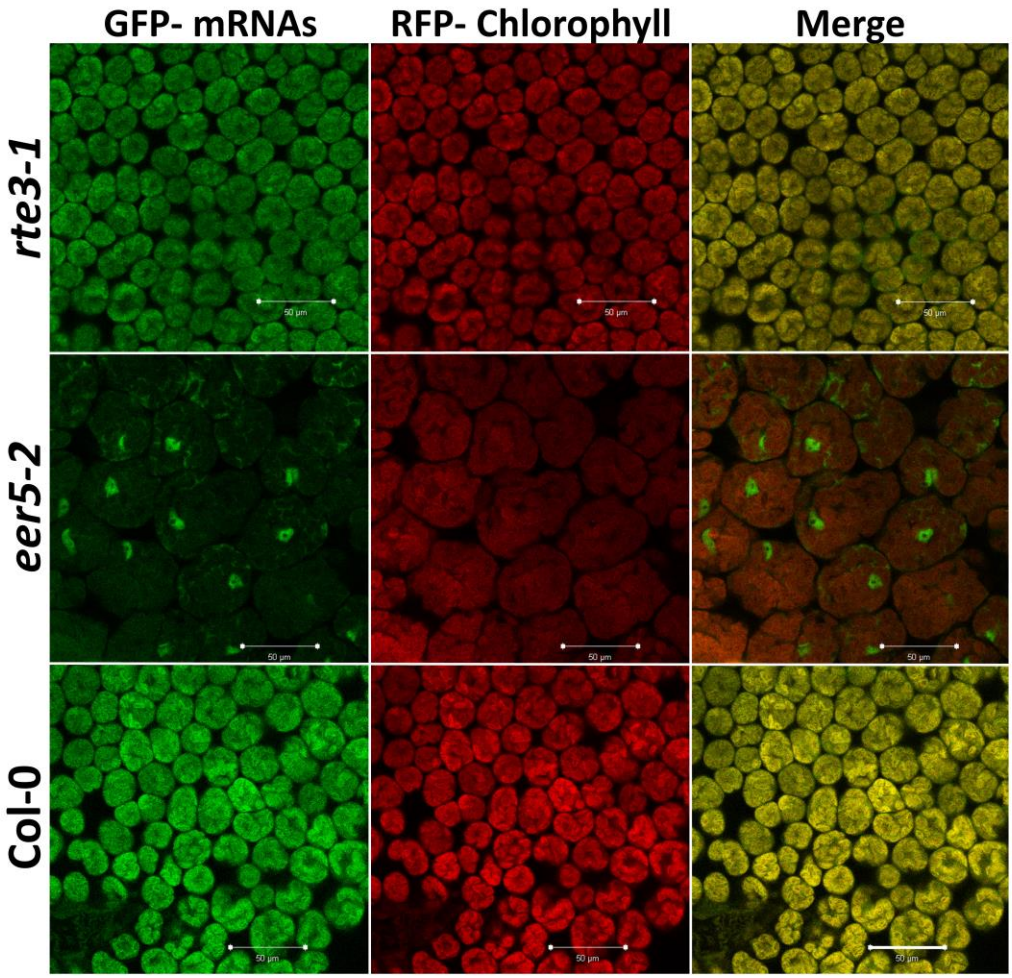

Figure 5.12. The *rte3-1* mutant does not show an mRNA export defect. Plants were grown on MS plates for two weeks, then used for *in situ hybridization* with a fluorescein-labeled oligo (dT) probe. While the *eer5-2* mutant shows an mRNA export defect, the *rte3-1* mutant, like Col-0 wild-type, does not. Arabidopsis leaves were observed using a Zeiss LSM 710 confocal microscope. Merged image is an overlay of GFP (mRNA location) and chlorophyll. Scale bar represents 50 µM.

Creation of TAP-Tag Lines

To attempt to identify other proteins that interact with RTE3, and identify other components of this large nuclear protein complex, I implicated a different approach. I created RTE3 TAP-Tagged Lines (Tandem Affinity Purification), to pull down proteins that interact with RTE3 *in plantae*. The goal was to use the 3 tandem Flag and 6 tandem His epitope tags attached to RTE3, under control of a double 35S promoter and isolate RTE3 as well as other interacting proteins, in a pull down assay. The interacting proteins would then be identified using mass spectrometry. Two different constructs were created and (an N-terminally tagged- and a C-terminally tagged-RTE3) transformed into an *rte3-1* mutant background. Homozygous lines showed phenotypic rescue to wild-type phenotypic ethylene responses (Figure 5.13). However, no RTE3 was detected in total protein extracts, from etiolated seedlings (data not shown). Therefore, I did not further pursue this project, since I cannot purify something I cannot see. One possibility is that the protein was too big, and did not transfer efficiently on to the membrane, during the Western Blot procedure. However, not even a faint trace of RTE3 was ever detected.

EIN2 Protein Levels are Increased in the *rte3-1* Mutant

The *rte3-1* mutant has an enhanced ethylene response phenotype, reminiscent of the U-shaped phenotype seen with overexpression of EIN2 (Appendix A; An et al., 2010). The SAC3 yeast protein plays a role in nuclear protein export (Jones et al., 2000), perhaps RTE3 has a similar role. Since the RTE3-1 substitution caused loss of the CSN3 and EIN2 C-terminal domain protein interactions (Figure 5.10), it is possible that the *rte3-1* phenotype is a result of an accumulation of nuclear EIN2.

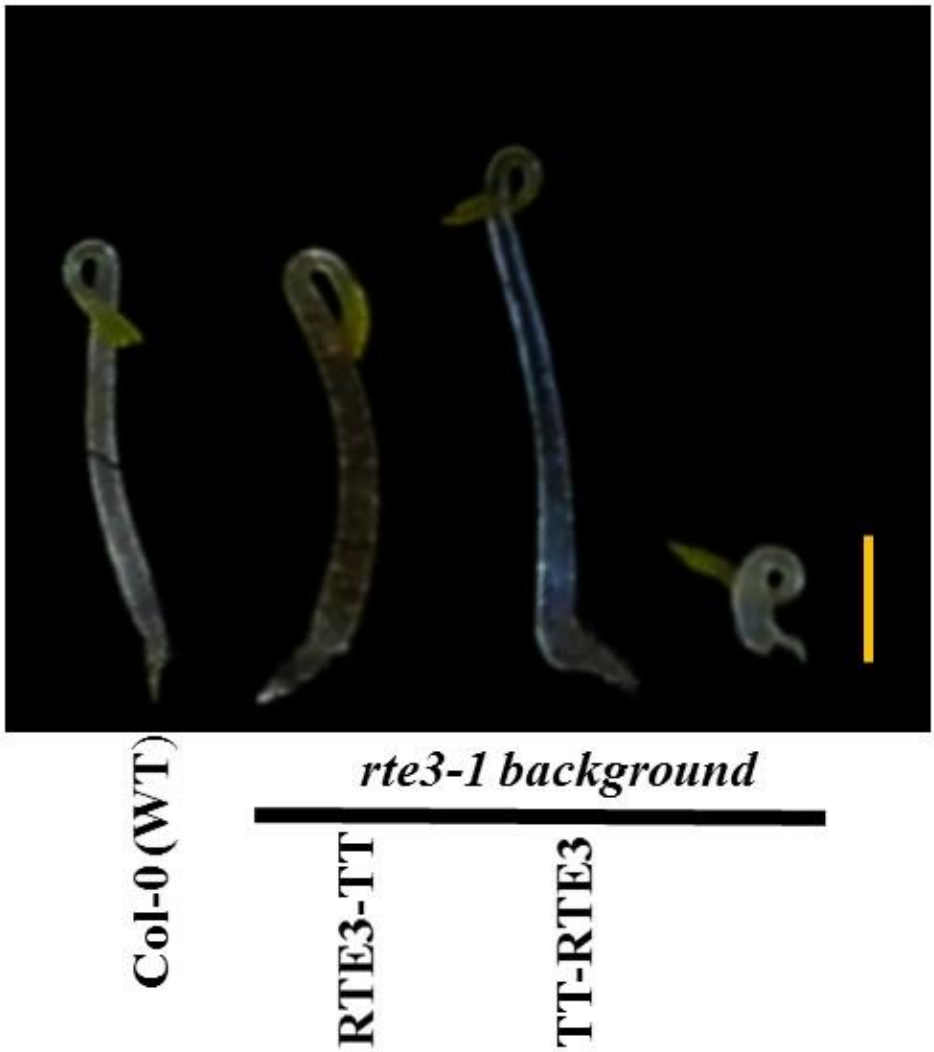

Figure 5.13. Both N-terminally and C-terminally TAP-tagged RTE3 constructs phenotypically rescued the *rte3-1* mutant. Representative sample of one transgenic line each. Constructs were created expressing 3-Flag and 6-His epitope tags attached to either the N-terminus or the C-terminus of RTE3. These were then transformed into an *rte3-1* mutant background, resulting in phenotypic rescue. However, no protein was detected on a Western Blot (data not shown). Scale bar represents 1 mm.

To test this possibility, I compared EIN2 levels between the *rte3-1* mutant and Col-0 (wild-type). I extracted total protein from 4 day-old etiolated seedlings and probed for the EIN2 levels using an anti-EIN2 antibody (YenZym Antibodies, LLC). Unfortunately, I was not able to detect full length EIN2, however I did detect a band that could be the controversial nuclear C-terminal fragment. The band looks to be around 65 kDa, which is similar to what is seen in the other studies (Qiao et al., 2012; Wen et al., 2012). This band was increased in the *rte3-1* mutant, compared to wild-type, and EIN2 levels were increased in response to ethylene, and most importantly the EIN2 level was not detected in the *ein2-1* mutant (Figure 5.13). This further supports the RTE3-EIN2 C-terminal domain interaction by suggesting that *rte3-1* mutant could be hypersensitive to ethylene due to a loss of the EIN2 C-terminal domain interaction, resulting in an accumulation of EIN2 in the nucleus.

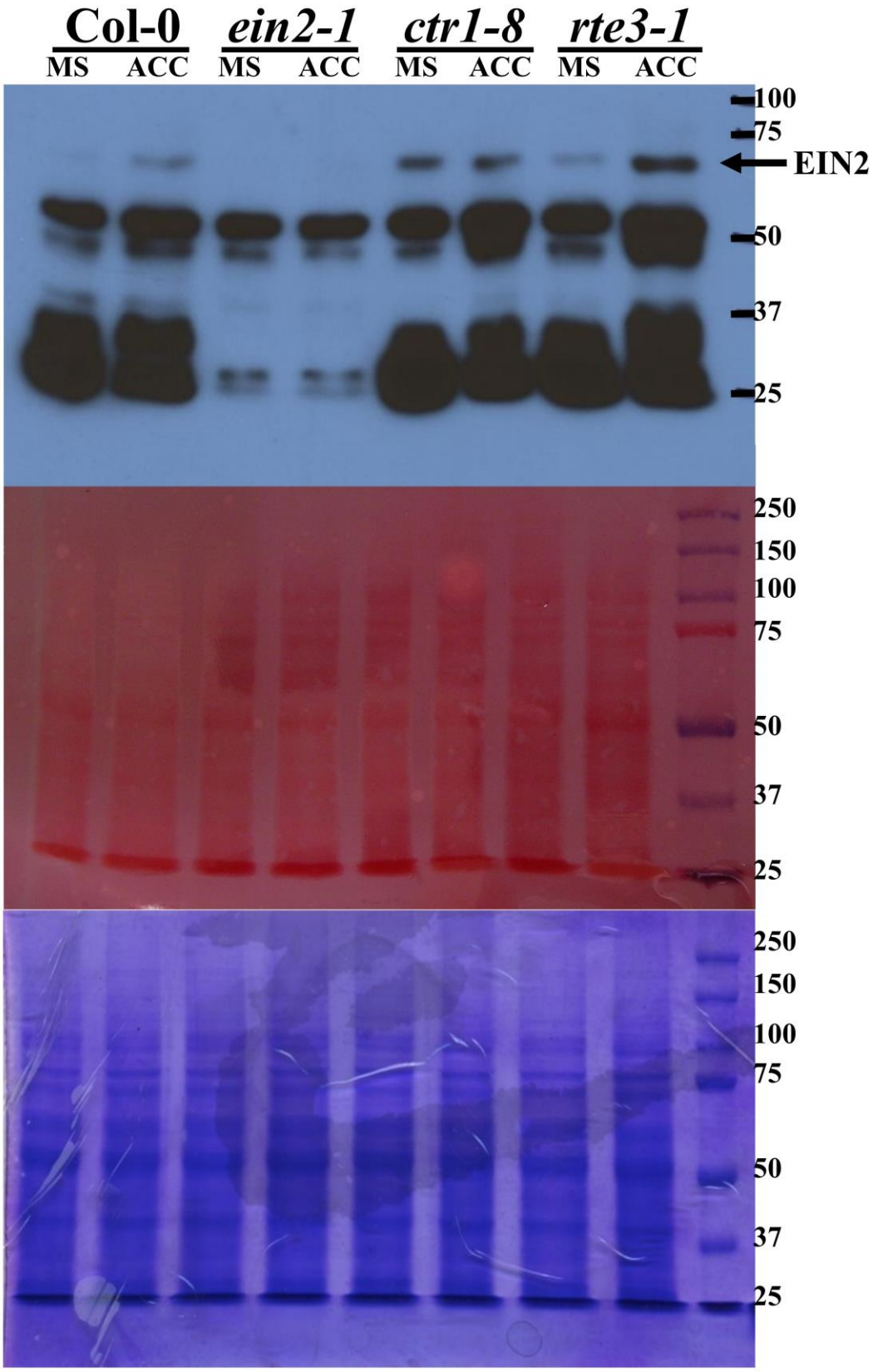
Col-0
ein2-1
ctr1-8
rte3-1
MS
ACC
MS
ACC
MS
ACC
MS
ACC
100
75
EIN2
50
37
25
250
150
100
75
50
37
25
250
150
100
75
50
37
25

Figure 5.14. The protein level of the EIN2 C-terminal domain is increased in the *rte3-1* mutant. Total protein was extracted from four day-old etiolated seedlings, and was probed for EIN2 levels using an anti-EIN2 C-terminal domain antibody (YenZym Antibodies, LLC). Western Blot reveals the *rte3-1* mutant shows increased EIN2 levels, compared to wildtype (Col-0), which are also enhanced when seedlings were grown on plates with 20 µM ACC (an ethylene precursor). The EIN2 C-terminal domain protein is denoted with an arrow (as EIN2) and is approximately 65 kDa. The *ein2-1* mutant was used as a negative control and *ctr1-8* was used as a positive control. Ponceau S and Coomassie stains were used as a loading controls.

Discussion

My progress on this RTE3 project dwindled after the Lu et al., (2010) paper was published. That is when I switched my focus to the N-terminal domain of EIN2 (Chapters 2-4). Since working with RTE3, it has now been published that the EIN2 C-terminal can move into the nucleus in the presence of ethylene (Chapter 2; Ju et al., 2012, Qiao et al., 2012), where it would be available to interact with RTE3, EER5, and the COP9 complex. At the time of working on RTE3, EIN2 was only speculated to have a nuclear function. The EIN2 C-terminal domain was also recently shown to be localized to P-bodies, where it interacts with the 3' UTR of EBF1/2 mRNA and can inhibit their translation (Li et al., 2015).

RTE3 is Part of the TREX-2 mRNA Export Complex.

Lu et al., (2010) published the RTE3-EER5 interaction (also called SAC3B-THP1 interaction), suggesting that RTE3 is involved with EER5 in the TREX-2 mRNA export complex. However, in this same study Lu et al. (2010) also discovered the Arabidopsis TREX-2 complex has lacks some of the essential protein interactions compared to the yeast TREX-2 mRNA export complex suggesting that the Arabidopsis TREX-2 complex may be functioning differently. Figures 5.5 and 5.6 suggest that EIN2 C-terminal domain and CSN3 are also part of a complex with RTE3 and EER5. Since there are no homologs of either of these proteins in the yeast TREX-2 complex, it is not known how the CSN3 and EIN2 C-terminal domain play a role, or if they are also part of this novel Arabidopsis TREX-2 complex. One possibility is that they are involved in nuclear protein export of EIN2 C-terminal

domain to the P-bodies, since the yeast TREX-2 complex has been shown to be involved in nuclear protein export (Jones et al., 2000).

In addition, over-expression of EIN2 C-terminal domain results in a U-shaped constitutive response (Appendix A) phenotype and reduced fertility (Alonso et al., 1999). The *rte3-1 eer5-2* double mutant has short hypocotyl, is sterile (Figure 5.7), and has a constitutive response (data not shown). This could suggest that EIN2 C-terminal domain is accumulating in this mutant, since both of these proteins (RTE3 and EER5) are known to be involved in a homologous nuclear protein export complex (Jones et al., 2000, Lu et al., 2010).

The *rte3-1* mutant has a higher level of EIN2 protein (Figure 5.14). I would speculate that the level of EIN2 would synergistically increase in the *rte3-1 eer5-2* double mutant. However, due to the sterility of that mutant, very slow development, and difficulty identifying the double mutant in the triple response assay (data not shown) it was difficult to obtain enough tissue to test this hypothesis. Due to this protein export defect, is possible that the EIN2 C-terminal domain could be trapped in the nucleus and not exported to the P-bodies (Li et al., 2015).

This suggest that perhaps RTE3 plays an important role in either turnover of EIN2 (perhaps with CSN3 and the rest of the COP9 signalosome), or perhaps with nuclear export of the EIN2 C-terminal domain (an additional role of CSN3 beyond the COP9 signalosome). This could possibly provide a mechanism for how the EIN2 C-terminal domain is being exported from the nucleus to the P-bodies, where it interacts with EIN5 and is involved in the mRNA decay pathway (Li et al., 2015).

EIN2 C-terminal Domain and CSN3 Interactions are Specific to the MCM3AP Domain of RTE3

To gain better insight into the function of the *rte3-1* phenotype, it is possible that the hypersensitivity to ethylene could be due to a loss of an essential protein interaction. Using a yeast 2-hybrid assay, and mutating RTE3 to mimic the *rte3-1* mutant, I was able to disrupt the RTE3 interactions with EIN2 C-terminal domain and CSN3. This suggests that both of these protein interact with the MCM3AP domain, since this substitution would potentially leave a non-functional MCM3AP domain. When tested against just the MCM3AP domain, both proteins interacted (Figure 5.11) indicating that they interact with the MCM3AP domain of RTE3.

The EER5 interaction spanned both the MCM3AP and the SAC3 domains, since the *rte3-1* mutation (Figure 5.10) was not able to interrupt this interaction, yet EER5 was still able to interact with the MCM3AP domain. One possibility is that EER5 is in such a confirmation with RTE3 in that it spans both SAC3 and MCM3AP domains. Another possibility is that it has a function with both SAC3 and MCM3AP domains of RTE3.

RTE3 contains an MCM3AP domain, which is a novel component of the TREX-2 complex. Both EIN2 C-terminal domain and CSN3, interact solely with the MCM3AP domain, therefore, it is possible that these interactions are part of the different functioning of the Arabidopsis TREX-2 complex. EER5 could represent a part of the homologous TREX-2 functioning, i.e. mRNA export or protein export, since EER5 interacts with the SAC3 domain, and also part of the novel functioning as well since it also interacts with the MCM3AP domain (Figure 5.11).

Similar to MCM3, CSN3 is also in a large protein complex, the COP9 signalosome. Although the COP9 signalosome mainly functions as a holoenzyme complex, the CSN5 and CSN3 subunits are also known to have independent functions outside the holoenzyme (Kwok et al., 1998; Wang et al., 2002; Huang et al., 2013). The CSN3 interaction with RTE3 (Figure 5.5 and 5.6) could suggest another independent function of CSN3 beyond the COP9 signalosome. Perhaps the double mutant analysis using a weak *csn3* mutant allele (Huang et al., 2013) since null *csn* alleles are seedling lethal, would give more insight into the functioning of this protein interaction with RTE3, and within the large nuclear protein complex.

RTE3 is Probably Not Involved in mRNA Export But in Some Large Nuclear Protein Complex.

Yeast SAC3 is an essential part of the TREX-2 complex and therefore mutants show an mRNA export defect (Fisher et al., 2002). However, both *rte3-1* (Figure 5.12) and the *sac3b-2* mutant used in the Lu et al., (2010) study do not show an mRNA export defect. This suggests that perhaps RTE3 is not involved in mRNA export. Again, this further suggests the Arabidopsis TREX-2 complex is functioning differently from the homologous yeast complex.

Another possibility is that RTE3 is involved in the export of specific mRNAs. In this case, it may not look like there was an mRNA export defect, since the probe used was for mRNAs in general. If RTE3 is specific for a subset of mRNAs, then the level of mRNAs that were defective in the *rte3-1* mutant would be lower than the overall pool of mRNAs in the cell. This could explain a phenotype but not an mRNA defect. Unfortunately, the only way to test this would be to narrow down the possible

targets. The EIN2 C-terminal domain is involved in the regulation of EBF1 and EBF2 mRNA (Li et al., 2015). Perhaps RTE3 also has a role in this process.

The RTE3-TAP-Tagged Lines

To attempt to isolate other components of this novel nuclear protein complex, I created TAP-Tagged transgenic lines, overexpressing RTE3 in an *rte3-1* mutant background. I was hoping to use the isotope tags attached to RTE3 to pull down other protein components, which would then be identified using mass spectrometry. Unfortunately, this did not work. I did obtain phenotypic rescue (Figure 5.13), yet no RTE3 protein was detected on a Western Blot. It is possible that this phenomenon is due to the fact that dark grown seedlings were used in the protein extraction. RTE3 was shown to have reduced expression in the dark, compared to the light (McClellan, PhD Thesis). Dark grown seedlings were chosen for this assay since there was phenotypic rescue and because of the easily distinguishable triple response phenotype. It is possible that RTE3 was still expressed, but below the detection limit.

Another possibility is that RTE3 was at the nuclear periphery, and only found in a membrane fraction, and therefore perhaps not efficiently extracted and not highly represented in a total protein extract. SAC3 in yeast (as well as mammalian GANP) is nuclear localize and functions by binding to the target protein and moving said target protein to the proximity of the nuclear pore (Wickramasinghe et al., 2010; Jones et al., 2000). MCM3AP on the other hand, is found in both the nucleus and cytoplasm and the binding and subsequent acetylation of MCM3 by MCM3AP facilitates nuclear localization (Takei and Tsujimoto, 1998; Takei et al., 2002). I was hoping RTE3 was functioning more like MCM3AP than SAC3 in the dark. However,

undetectable protein levels of RTE3 in the TAP-Tagged lines suggest that RTE3 was not expressed in the dark or at extremely low levels. Further studies are needed to better understand what is happening to RTE3 in dark.

RTE3 is a very large protein, 1680 residues, approximately 190 kDa without any epitope tags. It is possible that RTE3 was not able to be detected because the protein was too large to transfer efficiently. Larger proteins do not always transfer as easily or as efficiently as smaller proteins, during the Western Blotting transfer process. However, I think that this was not likely the case since as mentioned above not even a trace of the protein was detected on a Western Blot and therefore it was likely not an inefficient transfer problem. In addition, the ladder efficiently transferred to the membrane. The largest molecular weight band on the ladder is 250 kDa suggesting that larger bands should also transfer to the membrane under those conditions.

If RTE3 protein expression was extremely low, future studies could be done on a much larger scale, perhaps using older plants and much more tissue. Nuclear fractions could also be used in attempts to increase the representation of RTE3 protein in the protein sample. The rescue of the RTE3 TAP-Tagged lines (Figure 5.13) was promising. Future studies using these lines could help to identify other components of this nuclear RTE3, EER5, CSN3, and the EIN2 C-terminal domain complex. It could also give insight into the function of this complex and help to better understand why these proteins interact with each other and how this complex fits into the ethylene signaling cascade.

Materials and Methods

Plant Growth and Conditions- *Arabidopsis thaliana* ecotype Col-0 (Col-0) was used as the wild-type. For the triple response assay, seeds were plated onto Murashige and Skoog (MS) medium (Caisson Labs) containing 0.8% agar. For ethylene response, 20 μM ACC (Sigma Aldrich) was added to the plates. Plates were cold stratified at 4 C, in the dark, for 4 days prior to the 20 C dark treatment for 4 days. For dosage response, plates were place in jars and injected with ethylene gas and stored in the dark for 4 days at 20C. Seedlings were photographed and hypocotyls were measured using the ImageJ software (https://imagej.nih.gov/ij/). Soil grown plants were first screened on ACC plates for triple response phenotype and then transferred to soil. Close up images of the *rte3-1 eer5-2* double mutant leaves and flower buds, the *rte3-1* and the *eer5-2* mutant were taken with the Zeiss AxioScope.

Yeast 2-Hybrid Assays-Genes were PCR amplified from cDNA (using primers below) created from RNA extracted from 4-day old light grown seedlings using an RNeasy Isolation kit (Qiagen), with help from Dr. Christopher McClellan. cDNA was created using an iScript Select cDNA synthesis kit (Bio-Rad). The *RTE3* pLEXA-NLS, *LAMIN* pLEXA-NLS, and *EIN2 C-terminus (residues 516-1294)* pACTII constructs were created by Dr. Christopher McClellan (McClellan PhD, thesis). The *EER5* pACTII and *CSN3* pACTII constructs were created with help from Chris, as described in McClellan, PhD thesis. The RTE3-1 substitution (W1187*) was inserted into the *RTE3 pLEXA* construct using site directed mutagenesis (Agilent Technologies) using the primers listed below. The MCM3AP domain was PCR amplified using the existing *RTE3 pLEXA* clone by Andrew Scaggs using the primers

listed below. MCM3AP fragment (nucleotides encoding residues 1122-1690) was first cloned into the pGEMT vector (Invitrogen) and then digested using the added *XmaI* and *SalI* restriction sites, before ligation into the pLEXA-NLS vector. All plasmids were transformed into the L40 yeast strain. Yeast 2-hybrid interactions were selected on plates lacking histidine with the addition of 20 mM 3-AT. RTE3-1 interactions were selected with the addition of 10 mM 3-AT. The MCM3AP domain interactions were tested (thanks to help from Andrew Scaggs) using the addition of either 20 mM 3-AT or 60 mM 3-AT to plates. Plates were grown for 2 to 5 days at 30C.

Primer name	Forward or Reverse Primer Sequence (5'-3')	
rte3-1 mutagenesis	F	CTCCCGGCGTGTCTGTATGATAGAAATGGGTTGCAAATGGGT
	R	ACCCATTTGCAACCCATTTCTATCATACAGACACGCCGGGAG
MCM3AP pLEXA	F	CCCGGGATGTCATGGT CAAGGCTG
	R	GTCGACGAAGTAAATACAGAGCTTC

Bimolecular Fluorescence Complementation Assay- The coding sequences for *RTE3 (no stop)* pDONR221, *EIN2 C-terminal domain (encoding residues 516-1294, no stop)* pDONR221, *EER5 (no stop)* pDONR221, and *CSN3 (no stop)* pDONR221 were created by Dr. Christopher McClellan (McClellan, PhD thesis) and transferred into the pSPYCE-35S and pSPYNE-35S vectors (Schütze et al., 2009). *RTE3 (no stop)* pDONR221, *EIN2 C-terminal domain (encoding residues 516-1294, no stop)* pDONR221 were transferred to the pSPYNE-35S vector and *EIN2 C-terminal domain (encoding residues 516-1294, no stop)* pDONR221, *EER5 (no stop)* pDONR221, and *CSN3 (no stop)* pDONR221 were transferred to the pSPYCE-35S

vector (Schütze et al., 2009). All plasmids were transformed into the *Agrobacterium* strain C58C1 and then co-expressed via infiltration into tobacco leaf epidermal cells (Schütze et al., 2009). After a 3 day incubation, leaf epidermal pieces leaf pieces were incubated in 20 μg/mL DAPI for 15 min before BiFC interactions were visualized using a Zeiss AxioObserver. Z1 fluorescent microscope. The artificial color for the DAPI was changed using the Zeiss imaging software.

Germination Assay – A homozygous line of the *rte3-1 ein2-1* double mutant was created by Dr. Christopher McClellan. Seeds were sterilized with a 50% bleach solution before being plated on MS and grown in the light for 2 weeks at 20C. Seeds were scored for germination by rupture of seed coat, as observed using the Zeiss Axioscope.

mRNA Export Assay – Arabidopsis seedlings were grown on MS plates for 2 weeks prior to *in situ hybridization* with an oligo (dT) probe as described in Gong et al., 2005. Fixed leaves were imaged using a Zeiss LSM 710 confocal microscope.

Creation of Stably Transformed TAP-Tagged Arabidopsis Lines – The RTE3 lull length genomic sequence (both stop and no stop versions) were cloned into the pDONR221 vectors by Dr. Christopher McClellan (McClellan, PhD thesis). The *RTE3 no stop* pDONR221 construct was transferred to the pC-TAPa-GW vector and the *RTE3 with a stop codon* pDONR221 construct was transferred to the pN-TAPa-GW vector. The pN-TAPa and pC-TAPa vectors were created by Rubio et al., 2005 and modified to contain a gateway cassette by Dr. Ruiqiang Chen. The *35S-35S-RTE3 TAP-Tagged* constructs were transformed into the *Agrobacterium tumefaciens* strain GV3101, and Arabidopsis plants were then transformed using the floral dip method

(Clough and Bent, 1998) into the *rte3-1* mutant background, where positive transformants were selected using 90 mg/L gentamycin. Homozygous lines obtained in the T3 generation and phenotypes verified using the triple response assay (on MS plates with addition of 20 μM ACC). Seedlings were photographed and hypocotyls were measured using the ImageJ software (https://imagej.nih.gov/ij/).

Western Blot- Total protein was extracted from 4-day old etiolated seedlings using RIPA buffer (BioWorld). The Col-0 (wild-type) served as the control for the *rte3-1* mutant and the *ein2-1* mutant served as a negative control and the *ctr1-8* served as a constitutive positive control. Tissue was quickly collected in green light, so as not to evoke a light response, and frozen in liquid nitrogen. Powder tissue was incubated in RIPA buffer with 1x protease inhibitor cocktail (Sigma) at 4C for 2 hrs before collecting the supernatant. Protein samples were incubated for 10 min at 95 C before separation by 10% SDS-PAGE. An identical gel was loaded and used for Coomassie Blue stain. Proteins were transferred to a PVDF membrane via semi-dry transfer, stained with Ponceau S prior to verify protein transfer and then immunoblotted with a 1:1000 dilution of an anti-EIN2 antibody (YenZym Antibodies, LLC).

Chapter 6: Conclusion and Future Directions

Introduction

The goal of this thesis was to discover the roles and functions of EIN2, a master regulator protein of the ethylene signaling pathway. The major findings of this body of work have been subdivided into three main categories; 1. The function of EIN2 as a metal transporter 2. How EIN2 functions in the context of ethylene signaling 3. A novel functioning of EIN2 C-terminal domain in the nucleus.

1. EIN2 is an ER Membrane Metal Transporter of Ca^{2+}, Cu^{2+} and Mn^{2+}

Whether EIN2 is capable of metal transport has been an elusive question for almost two decades (Alonso et al., 1999). The first major finding of this body of work is evidence of divalent transport by EIN2. Proper subcellular localization, of EIN2 in the *smf2* mutant in *S. cerevisiae* proved to play a vital role in this discovery. This finding suggests that EIN2 has an important role in controlling local reservoirs of metal concentrations specifically at the ER membrane.

The DGPK substitution in MntH and the G36E substitution in EIN2 did not disrupt transport suggesting the DPGK motif might not be as important for transport as in other Nramp proteins. In addition, some monocots contain a DLGK motif in EIN2 (Chapter 3-Figure 3.1), further evidence of less conservation of the Nramp DPGN motif in EIN2. Interestingly, more primitive plants (like the green algae *Chlamydomonas* and the vascular moss *Selaginella*) have a DPGN motif, suggesting that the lysine substitution had evolved sometime after the evolution of vascular plants. In the future, these lysine and proline substitutions (or generally the evolution

of the DPGN motif) could give evolutionary insight into the function of the DPGK motif in EIN2.

The location of DPGK motif also differs between EIN2 and other Nramp proteins (MntH for example). In MntH, the DPGN motif is found within the first transmembrane domain (Courville et al., 2004) however, in EIN2 the DPGK motif is predicted to reside in the loop region, in the lumen, outside the membrane (ARAMEMNON). The DPGN is important for metal transport in Nramp proteins because it is predicted to be involved in formation of the metal binding site within the membrane (Haemig and Brooker, 2004). The DPGK motif is predicted to be outside of the membrane in EIN2, which might explain why the DPGK motif does not seem as important for metal transport.

The evolutionary differences in the DPGN motif could also help to explain the preference for calcium as a substrate for EIN2. Nramp proteins are known to transport a wide range of divalent cations, however, to my knowledge, transport of calcium has not been shown. Evidence of residues changing metal ion transport specificity was observed in the Nrat1 protein, an Nramp-like protein with specificity for M^{3+}, in particular Al^{3+} (Xia et al., 2010).

The recipient of the divalent cation from EIN2 is unknown. Unpublished data from both G. Groth and H. Guo suggest the C-terminal domain of EIN2 can bind a metal ion. In fact data from G. Groth suggests the C-terminal domain can bind three to four Ca^{2+} ions. It is very appealing to propose that the N-terminal domain provides a metal to the EIN2 C-terminal domain, which either needs the metal as a cofactor for its activity, or alternatively transports it to the nucleus for some other essential

process (perhaps a metalloprotease or a metallophosphatase in the nucleus) or to the P body.

Another possibility is that EIN2 could provide a metal for various proteins in proximity to EIN2 at the ER membrane. It could be providing a metal ion to ETR1, for example, which has been shown to require manganese for autophosphorylation activity (Gamble et al., 1998). Perhaps EIN2 provides the required manganese ion since ETR1 is one of the proteins that EIN2 interacts with at the ER (Chapter 2-Figure 2.1). The protease that cleaves EIN2 has yet to be discovered. It is possible that this unknown protease is a metalloprotease and that EIN2 provides the metal cofactor for its own cleavage.

Future Directions

EIN2 is capable of divalent metal transport, however, the preferred substrate and residues critical for transport are yet to be determined. Site-directed mutagenic studies, testing whether other highly conserved residues in EIN2 are capable of disrupting divalent transport of EIN2 would give insight into the function of EIN2 as a metal transporter and specifically which residues are important for transport ability. For example, there is a highly conserved Nramp protein motif, the MPH motif, in transmembrane domain six. EIN2 contains a VPH motif. However, this motif could also highlight an evolutionary functional difference between EIN2 and other Nramp proteins, like the DPGK motif (as discussed above).

Other possible candidates for mutagenesis are His211 and His216 (located within transmembrane domain six) were shown to be involved in pH regulation in MntH (Haemig et al., 2010), both of which are conserved in the EIN2 sequence. The

transport assays with *smf2* were pH dependent in that subtle variations in the pH of the yeast media drastically altered the results. EIN2 was able to complement the smf2 mutant at pH 6.0 but not when the pH deviated from 6.0. This could suggest that EIN2, like other Nramp proteins is a pH dependent transporter. Perhaps substitution of these conserved Histidine residues (His 211 and His 216) potentially altering the pH regulation of EIN2 may disrupt transport. To test if transport is disrupted, the yeast spot assay using *smf2* mutant background (like Chapter 4 – Figures 4.8 and 4.9) could be used as well as atomic absorption to test metal uptake directly, like in Appendix C.

Another way to address the location of the conserved residues in EIN2 is by determining the topology of the transmembrane domain of EIN2. The location of the conserved residues within the transmembrane domains could give insight into the function, such as give insight into the confirmation of the metal binding pocket and the residue involved, as well as help identify critical residues in EIN2 for potential mutagenic studies. One method to determine the topology of the EIN2 N-terminal domain would be with a protease cleavage assay, which was how the topology of MntH was determined (Makui et al., 2000).

Determining the crystal structure of the N-terminal domain of EIN2 is perhaps a more informative and exciting avenue. However, crystal structures of membrane proteins are notoriously difficult (especially large proteins like EIN2) and can take years. Advances in technology, allowing for better crystal structures and structures determined directly from purified protein, such as EPR (electron paramagnetic resonance) or NMR (nuclear magnetic resonance) (Rice et al., 2013; Zook et al.,

2013) could help facilitate a structure of the EIN2 N-terminal domain. Both EPR and NMR have the advantage over traditional crystal structures because the protein structure is determined in the native environment. Using traditional methods, during the crystallization process, an artificial environment may need to be created in order for the protein to form a crystal, which may alter the metal ion present in the binding pocket. Improperly identifying the metal substrate is a major problem with metal binding proteins (Zheng et al., 2013). However, with the right technology and experimental conditions, a wealth of information can be obtained.

Future studies also need to address transport of EIN2 *in planta*. One possibility is to measure the uptake of calcium or other divalent cations directly in an *ein2* Arabidopsis mutant compared to wild-type using ICP-MS. This technique could not only give insight into the particular metal substrates for EIN2 *in planta*, but also confirm that EIN2 is a novel calcium transporting Nramp protein. Yet another possibility is to directly visualize the cellular and subcellular distribution of different divalent metal cations in an *ein2* mutant (presumably one containing a substitution disrupting metal transport compared to wild-type and an *ein2* mutant) using a synchrotron-X-ray fluorescence (S-XRF) and high-resolution secondary ion mass spectrometry (NanoSIMS). Using a combination of these techniques, Moore et al. (2014) were able to detect the subcellular distribution of divalent cations in rice tissues.

It is possible that due to the subcellular location (at the ER membrane) and the presence of six other Nramp proteins in Arabidopsis (and many other metal transporters) an *ein2* mutant may not demonstrate a difference in metal uptake

compared to wild-type. This was observed with the *nramp3-1* mutant, where although NRAMP3 was shown to transport manganese, iron, and cadmium, it did not show a difference in metal uptake compared to controls when analyzed using ICP-MS (Thomine et al., 2000). However, when NRAMP3 was overexpressed, the plants became hypersensitive to cadmium and over accumulated iron (Thomine et al., 2000). Therefore, the transgenic lines overexpressing the N-terminal domain of EIN2 (Chapter 3 –Figure 3.16b) in a wild-type background could prove useful. By enhancing the metal transport function of EIN2, the metal related phenotype could also be enhanced as well as any measurable metal uptake by the plant.

Does divalent metal transport, via EIN2, play a role in ethylene signaling? That is the ultimate next question, and unfortunately the G36E substitution was not able to address this question. However, in the future, a substitution will eventually be discovered that is capable of disrupting transport. It will be interesting to find out if this same substitution also confers ethylene insensitivity, which would suggest that metal transport via EIN2 does play a role in ethylene signaling. One possibly faster way to test the potential substitutions that disrupt transport is using particle bombardment in onion epidermal cells. Do those same substitutions in EIN2 that disrupt transport also prevent the C-terminal domain from translocating to the nucleus? These potential substitutions could be inserted into the full-length wild-type EIN2 and the subcellular localization could be visually compared to wild-type to see if these substitutions prevent nuclear localization of the EIN2 C-terminal domain, suggesting ethylene insensitivity. A second approach using the same overexpression constructs would be to look at reporter gene expression (such as ERF1, PDF1.2, etc.)

as a result of overexpression of EIN2 with the substitution compared to overexpression of wildtype EIN2 (in either onion cells or protoplasts). Over-expression of EIN2 should cause the reporter gene expression to increase, but if the substitutions that prevents transport also causes insensitivity, then the reporter genes would not increase in expression.

If metal transport is linked to ethylene signaling, can an Nramp stimulate the translocation of the EIN2 C-terminal domain? To test this, one could create a chimeric protein where an Nramp protein (which would be modified to localize to the ER membrane) could be fused to the C-terminal domain of EIN2. Perhaps one such as NRAMP4, which was also able to complement the *smf2* mutant (Chapter 4 – Figures 4.8 and 4.9). A non-functional Nramp fused to EIN2 C-terminal domain could be used as a control. I would probably first test this in onion cells, because it is much faster than creating transgenic lines. In the presence of ethylene, if the C-terminal domain of EIN2 of this Nramp chimeric protein is cleaved, it would suggest that metal transport is essential for the cleaving of EIN2 C-terminal domain. If the chimeric protein does not cleave in the presence of ethylene, then that would suggest the N-terminal domain has other essential regulatory roles on the C-terminal domain, besides metal transport.

2. Insight Into the Regulation and Function of EIN2

Although much is known regarding the function of EIN2 function, there are still many questions remaining regarding this enigmatic protein. Only in the presence of ethylene was the EIN2 C-terminal domain found to interact with ETR1 (Bisson and Groth, 2010), however as discussed previously, this seemed a bit counterintuitive.

Data suggests that full-length EIN2 interacts with ETR1 (Chapter 2-Figure 2.1) in the presence and absence of ethylene. It is possible that the N-terminal domain could be involved in the interaction of EIN2 with ETR1 in the absence of ethylene. Future studies will determine the role of the interaction of EIN2 and ETR1 in ethylene signaling. However, this interaction suggests EIN2 functions in a signaling complex with CTR1 and ETR1. Previously, it was unknown whether these components function at the same time, at the same membrane.

A novel finding is that EIN2 can self-interact (Chapter 3-Figures 3.10-3.16). The receptors and EIN3 are also known to function as dimers (Gao et al., 2008; Solano, et al., 1998) and provides a possible novel mechanism for EIN2 functioning. To test this possibility, one would want to disrupt the interaction, which I attempted by testing the G36E and H1143P (*ein2-9* mutation) substitutions. Since both confer ethylene insensitivity, if one of the mutations disrupted the EIN2 self-interaction, then it would have suggested the self-interaction of EIN2 plays a role in ethylene signaling. However, since neither substitutions disrupted the self-interaction, it can only be concluded that those particular substitutions do not play a role in self-interaction. When the smaller fragments encompassing the highly conserved C-terminal region of EIN2 and (where the NLS is located) were tested for self-interaction, the interaction seemed to get stronger (Chapter 3-Figure 3.13, data not shown). This could further suggest a role of the EIN2 self-interaction in ethylene signaling.

Other novel findings are that EIN2 functions *in cis* (Chapter 3-Figure 3.19) in a haploinsufficient manner (Chapter 3- Figure 3.17). Additionally, data suggests the

N-terminal domain is required for proper functioning of the C-terminal domain (Chapter 3- Figure 3.20), as suggested by Alonso et al. (1999). These findings address a mechanism for how EIN2 functions, helping to advance our understanding of this master regulator of ethylene signaling. Not enough EIN2 protein (such as seen with a null allele, *ein2-5*) results in ethylene insensitivity, and too much results in extreme ethylene hypersensitivity (Appendix A). EIN2 functioning in a haploinsufficient manner describes a mechanism for how the protein level of EIN2 can possibly be regulated in the cell. EIN2 protein is rapidly induced in the presence of ethylene (Qiao et al., 2009) and therefore any mutant versions would quickly be amplified and could potentially have deleterious effects on any one of EIN2's many functions. By EIN2 N-terminal domain functioning *in cis* to regulate the C-terminal domain, versus *in trans,* it results in a slightly slower ethylene response with tighter regulation over EIN2 C-terminal domain. Overexpression of EIN2 C-terminal domain confers constitutive ethylene responses in adult plants (Alonso et al., 1999). It also provides a means for selective pressures to act upon EIN2 via different mutations.

Since in Arabidopsis there are six Nramp proteins plus EIN2, another possibility is that EIN2 evolved a different function than the other Nramp proteins. EIN2 contains a C-terminal domain and functions in ethylene signaling, yet it also appears to retain its function as a metal transporter (Chapter 4). It was observed that many proteins families that are retained, like EIN2, are resistant to removal from the genome because they either function in a dosage dependent manner, function in signal transduction pathways, encode components of protein modification complexes, and/or form an interconnected interaction networks (Thomas et al., 2006), again like

EIN2. It is possible that the most primitive function of EIN2 is metal transport and the signaling function was somehow an evolutionary advantage for transport function and/or ethylene signaling and therefore the C-terminal domain became attached to an Nramp protein. The attachment of the N-terminal domain to the C-terminal domain guaranteed the retention of EIN2 in the genome, since it has a unique function from other Nramp proteins.

Future Directions

Since the function of the EIN2 self-interaction is novel, further study could provide insight into the function of EIN2. Perhaps EIN2 function requires self-interaction? To test this possibility, one would want to find a residue to disrupt this self-interaction. Since the very C-terminus is highly conserved and the self-interaction interaction appeared stronger with fragments encompassing a smaller section of just the C-terminus (residues 1041-1294 was the smallest tested, data not shown), it is possible that the residue critical for disruption of self-interaction is in this region. The NLS sequence is contained in this region (Bisson and Groth, 2011) and since the NLS is critical for EIN2 function in ethylene signaling (Qiao et al., 2012), I would probably start by site directed mutagenesis of residues in the NLS sequence (or in one of the residues in the highly conserved region surrounding it). The EIN2 self-interaction could be retested using the new EIN2 with the amino acid substitution using a yeast 2-hybrid assay and later verified *in planta* using BiFC. An Arabidopsis mutant defective in the NLS sequence of EIN2 would be most likely be ethylene insensitive, but if one of the residues of the NLS sequence (or in the highly conserved region around it) did disrupt the self-interaction, I would want to verify the

phenotype *in planta* with creation of transgenic lines. If these lines also show the predicted ethylene insensitivity, it would suggest that the nuclear localization and the EIN2 self-interaction are important for ethylene signaling.

Interestingly, when treated with ethylene, the EIN2 self-interaction remained at the ER membrane (Chapter 3-Figure 3.14). This is contrary to how EIN2 is known to function (Chapter 2- Figure 2.4; Ju et al., 2012; Qiao et al., 2012). It is possible that EIN2 functions as a monomer in the nucleus. However, it is also possible that the tag at the C-terminus is interferes with the proper function of the C-terminal domain. As a way to test this, one could make additional BiFC full-length EIN2 constructs tagging the N-terminus of EIN2 instead of the C-terminus. Using particle cell bombardment using onion epidermal cells (because it is much faster than creating transgenic lines) one could test both the N-terminally tagged EIN2 as well as the C-terminally tagged EIN2 for self-interaction, in the presence and absence of ethylene. Although data suggests that they would all localize to the ER, one could extract the protein from these onion cells, and use a Western Blot to detect the EIN2 levels by detecting the YFP BiFC signal. If EIN2 is a monomer in the nucleus, then the N-terminally tagged EIN2 sample would be cleaved when treated with ethylene and result in a smaller sized protein band. If the tag at the C-terminus of EIN2 interferes with its function, there could be no cleavage or cleavage at an incorrect site.

Interestingly, the localization of ETP1/2 have only been predicted to be cytoplasmic, due to regulation of the EIN2 C-terminal domain protein level (which is soluble) (Qiao et al., 2009). These ETP proteins were never actually localized in the cell. It is possible that there are two ETPs in Arabidopsis due to a difference of

localization. For example, it is possible that one is regulating EIN2 C-terminal domain in the cytoplasm and one in the nucleus. It is also possible that the G36E substitution is interfering with the proper functioning of the EIN2-ETP1/2 interactions, since this substitution seems to cause the C-terminal domain to be misregulated. For example, if the G36E substitution is somehow changing the confirmation of EIN2 in such a way that the site of the ETP1/2 interaction is somehow more available, EIN2 could be turned over more readily causing reduced EIN2 protein levels and an ethylene insensitive phenotype. This possibility could be further explored by testing the interaction between EIN2 C-terminal domain and ETP1/2, using first the yeast 2-hybrid assay and followed by in planta studies using BiFC (if needed). If the G36E substitution is causing a conformational change, making the ETP site more available, the interaction between EIN2 and the ETPs would potentially become stronger. In addition, the strength of the protein interaction could be quantified using a FRET or split luciferase assay.

3. EIN2 C-terminal Domain is in a Large Nuclear Protein Complex with RTE3, EER5 and CSN3

One of the major remaining questions in the ethylene signaling field is, what happens to the EIN2 C-terminal domain in the nucleus? The next known downstream component is EIN3 however, EIN3 and EIN2 C-terminal domain do not interact directly (data not shown). This thesis provides data suggesting the EIN2 C-terminal domain is in a large nuclear protein complex with RTE3, EER5, and CSN3 (Chapter 5- Figures 5.5, 5.6, 5.9 and 5.11). RTE3 and EER5 have been shown to be a part of the Arabidopsis TREX-2 mRNA export complex (Lu et al., 2010). EIN2 could also

be a part of this TREX-2 complex and could be a novel function of the EIN2 C-terminal domain in the nucleus.

The yeast TREX-2 complex was shown to play a role in protein export (Jones et al., 2000) and the *rte3-1* mutant showed an increase in EIN2 protein level (Chapter 5 – Figure 5.14). It is possible that RTE3 is important for the protein export function of the TREX-2 complex, and the substrate in this case is the EIN2 C-terminal domain.

Overexpression of EIN2 results in extreme hypersensitivity to ethylene (Appendix A) and the *rte3-1* phenotype is quite hypersensitive (Chapter 5-Figure 5.3). In addition, the RTE3-1 substitution resulted in loss of the protein interaction with the EIN2 C-terminal domain. This loss of interaction might result in a build-up of EIN2 in the nucleus resulting the hypersensitive phenotype seen in the *rte3-1* mutant, reminiscent of the phenotype seen with overexpression of *EIN3* caused by overstimulation of the ethylene response pathway (An et al., 2010).

How the EIN2 C-terminal domain is exported from the nucleus is unknown. Recent studies indicate that the EIN2 C-terminal domain is also present in the P-bodies (Liu et al., 2015). It is unknown, however, if a subset of the C-terminal domain goes directly to the P-bodies instead of the nucleus. If the EIN2 C-terminal domain interaction with RTE3 is involved with nuclear export of the EIN2 C-terminal domain, this nuclear export could help to provide insight into how the EIN2 C-terminal domain can be simultaneously present in the nucleus and the P-bodies.

Future Directions

What happens to the EIN2 C-terminal domain in the nucleus, and why does it interact with RTE3 and EER5? How does the EIN2 C-terminal domain fit into the

TREX-2 complex? The TAP-Tagged lines did show phenotypic rescue (Chapter 5-Figure 5.13), which were promising, however no RTE3 protein was detected by Western Blotting. It is possible that RTE3 protein could have been detected by scaling up the protein isolation and/or by, isolating just the nuclear fraction. Isolation of the RTE3 complex could give insight into the function of RTE3, EER5, COP9, as well as EIN2 C-terminal domain in the nucleus, as well as identify other components in this hypothesized large complex. In addition, isolation of the RTE3 complex could yield information on the Arabidopsis TREX-2 complex, since it seems to be functioning differently than the yeast TREX-2 complex (Jani et al., 2009; Lu et al., 2010). I created TAP-Tagged lines expressing TBP2 (TATA-BOX BINDING PROTEIN2) to use as a nuclear protein control for such studies in the future.

Additionally, the same technique could be used to isolate a nuclear EIN2 C-terminal domain complex. Transgenic lines could be created expressing a TAP-Tagged EIN2 C-terminal domain (residues 516-1294) and subsequently used in a pull down to isolate the EIN2 C-terminal domain. Interacting proteins could then be identified using mass spectrometry. This technique could yield insight into the functions of EIN2 in the nucleus as well as identify some other potentially unknown component(s) of the ethylene signaling pathway. As a nuclear protein control, the same TBP2 TAP-Tagged lines (mentioned above) could be used.

Since EIN2 the C-terminal domain interacts with components of the TREX-2 complex, is EIN2 also part of this complex and also involved in mRNA export? To test these possibilities, I would first test the EIN2 C-terminal domain, using a yeast 2-hybrid assay, against known proteins in the TREX-2 complex (such as NUP1 and

SUS1) to see if they also interact, placing EIN2 in the TREX-2 complex. Additionally, these TREX-2 components could also have functions with the EIN2 C-terminal domain, providing additional components in the ethylene signaling pathway. These protein interactions could be further verified in plants, with BiFC and co-immunoprecipitation.

If EIN2 is involved in the mRNA export function of the TREX-2 complex (assuming it part of the TREX-2 complex) then *ein2* mutants should show an mRNA export defect, like *eer5* mutants do (Chapter 5 – Figure 5.12). To test this, one could use an *in situ* hybridization mRNA export assay, with an *ein2* mutant, to see if they have an mRNA export defect, which would suggest that, like EER5, the EIN2 C-terminal domain would play an important role in the mRNA export function of the TREX-2 complex. If the *ein2* mutants do not show an mRNA export defect, like *rte3* mutants, then it could suggest that EIN2 might not be as essential for the mRNA functioning of the TREX-2 complex.

The *rte3-1* mutant showed an increased level of EIN2 protein (Chapter 5-Figure 5.14), suggesting that the hypersensitive phenotype of the *rte3-1* mutant is due to an over accumulation of EIN2 C-terminal domain. It is possible that the *rte3-1* mutants are accumulating EIN2 C-terminal domain in the nucleus due to a protein export defect. To test this possibility, I created transgenic lines, overexpressing EIN2 C-terminal domain in an *rte3-1* background. These lines could be further studied to determine the subcellular localization of the EIN2 C-terminal domain in the *rte3-1* background compared to the Col-0 (wild-type) background.

Proposed Model

In summary, EIN2 is probably involved in redistribution of metal ion reserves across the ER membrane, namely Ca^{2+}, Mn^{2+}, Fe^{2+}, Cu^{2+}, and possibly Cd^{2+}. The ER is predicted to have Ca^{2+} concentrations in the mM magnitude levels compared to the nucleus and cytosol, which have predicted concentrations in the nM magnitude levels (Vaz Martins et al., 2013). Since the yeast assays were very pH dependent, EIN2 is also most likely functioning as a proton pump, like other Nramp proteins. Therefore, EIN2 is most likely actively pumping ions with the concentration gradient, from the ER membrane towards the nucleus. It is possible that the EIN2 self-interaction helps EIN2 to form larger pores/larger reserves in the membrane to help promote metal ion transport, to help stimulate a more rapid response.

The substrate of EIN2 metal transport could be anything, but my preferred model involves the C-terminal domain. Since the N-terminal domain was found to be important for regulation of the C-terminal domain, it is possible that this also extends to metal transport, or that this regulation of the C-terminal domain is via metal transport. In this model, the N-terminal domain provides the metal ion for the C-terminal domain, which is then cleaved in the presence of ethylene and translocated to the nucleus. While in the nucleus, the C-terminal domain acts as a metal chaperone to deliver the metal ion to other downstream targets. An additional possibility is that the C-terminal domain also translocates to the P-body and also acts as a metal chaperone to provide downstream targets in the P-body with their essential metal cofactor.

As for the G36E substitution, it is possible that it does have a modest dampening effect on the transport ability of EIN2. However, this substitution seems

to increase the expression of EIN2, which may compensate for the reduction in transport ability. This substitution seems to affect the regulation of the C-terminal domain of EIN2, perhaps through miscleavage or mislocalization. For example, it is possible that this substitution is causing the EIN2 C-terminal domain to be cleaved at the wrong location creating the wrong sized fragment. This wrong sized fragment may not localize properly or not properly active the downstream ethylene response, resulting in the observed ethylene insensitivity in the *ein2 G36E* mutant. Perhaps this wrong sized fragment is not able to carry a metal ion to the nucleus or sends it to the vacuole instead. Another possibility is that this G36E substitution is causing EIN2 turnover and then the C-terminal domain would never reach its target, perhaps due to some difference in confirmation of protein modification

In the future, it will be interesting to see how the story of "EIN2 the Nramp metal transporter" unravels. The *ein2 G36E* mutant has uncovered many functions of EIN2 and allowed for great advances in our understanding of how EIN2 functions. This work will be one of many stepping stones along the way. With better advances in technology, perhaps the remainder of the EIN2 story will not take another two decades…

Appendices

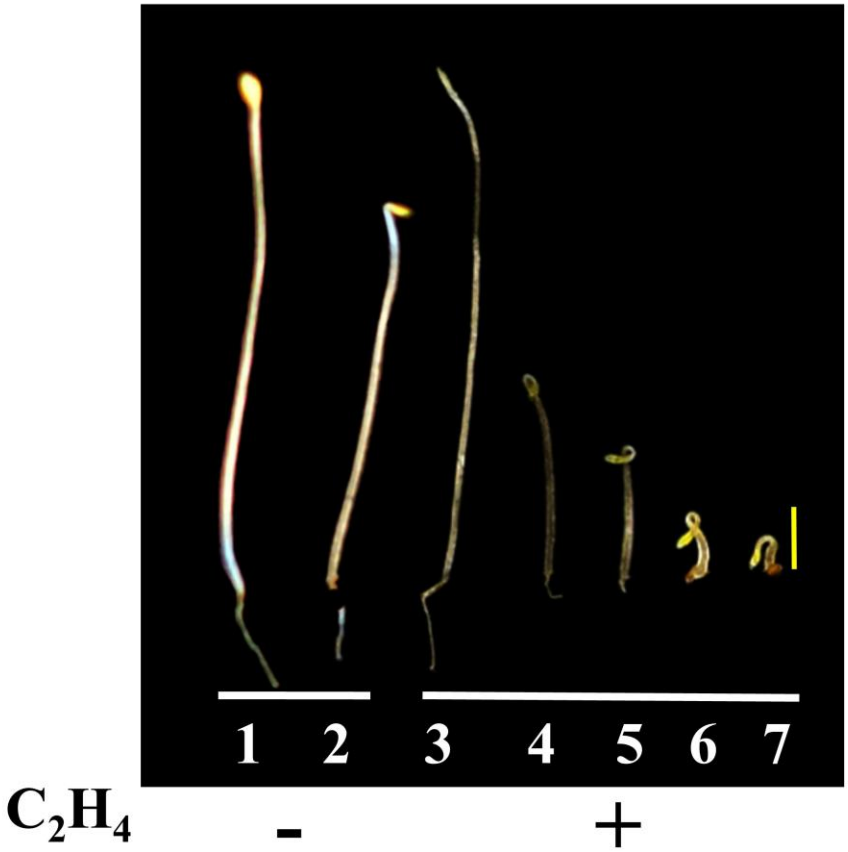

Appendix A. Ethylene phenotypes. Four day-old etiolated seedlings were grown on media containing just MS (1 and 2) or with 20 μM ACC (an ethylene precursor, 3-7). Seedlings 1 and 3 are the ethylene insensitive *ein2-5* mutant, whereas lanes 2 and 5 are Col-0 wild-type, showing the wildtype etiolated response and a wildtype triple response, respectively. A partial ethylene insensitivity (lane 4) was observed in the cross between *ein2-5* and Col-0. Seedlings overexpressing full length EIN2 (using a 35S promoter in a Col-0 background) confer both ethylene hypersensitivity (lane 6) and an extreme overexpression phenotype known as the "U-shape" (lane 7). This "U-

shape phenotype is similar to the phenotype seen with overexpression of EIN3 (An et al., 2010). Scale bar represents 2 mm.

Materials and Methods

Plant Growth and Conditions– *Arabidopsis thaliana* ecotype Col-0 (Col-0) was used as the wild-type. For the triple response assay, seeds were plated onto Murashige and Skoog (MS) media (Caisson Labs) containing 0.8% agar. For ethylene response, 20 μM ACC (Sigma Aldrich) was added to the plates. Plates were cold stratified at 4 C, in the dark, for 4 days prior to the 20 C dark treatment for 4 days. Seedlings were photographed and hypocotyls were measured using the ImageJ software (https://imagej.nih.gov/ij/). The transgeneic lines shown in lanes 6 and 7 are described in the methods (in "Creation of stably transformed Arabidopsis lines"**)** in Chapter 3.

TCATGAMTNYRVESSSGRAARQRMVPALLPVLLVSVGYIDPGKWVANIEGG
ARFGYDLVAITLLFNFAAILCQYVAARISVVTGKHLAQICNEEYDKWTCMFL
GIQAEFSAILLDLTMVVGVAHALNLLFGVELSTGVFLAAMDAFLFPVFASFLE
NGMANTVSIYSAGLVLLLYVSGVLLSQSEIPLSMNGVLTRLNGESAFALMGL
LGASIVPHNFYIHSYFAGESTSSSDVDKSSLCQDHLFAIFGVFSGLSLVNYVLM
NAAANVFHSTGLVVLTFHDALSLMEQVFMSPLIPVVFLMLLFFSSQITALAW
AFGGEVVLHDFLKIEIPAWLHRATIRILAVAPALYCVWTSGADGIYQLLIFTQ
VLVAMMLPCSVIPLFRIASSRQIMGVHKIPQVGEFLALTTFLGFLGLNVVFVV
EMVFGSSDWAGGLRWNTVMGTSIQYTTLLVSSCASLCLILWLAATPLKSASN
RAEAQIWNMDAQNALSYPSVQEEEIERTETRRNEDESIVRLESRVKDQLDTTS
VTSSVHHHHHHTGATCTAGA

Appendix B. - Protein sequence of EIN2/MntH hybrid. Pink highlighted region denotes MntH protein sequence that replaced the EIN2 sequence. The EIN2/MntH hybrid (residues 1-524) differed from the EIN2/MntH chimera (residues 1-481) by the extension of the green highlighted region, gene extension kindly added via Gibson cloning by Dr. Bret Cooper (USDA-ARS, Beltsville, MD). The yellow highlighted region denotes the added 6-His epitope tags. This EIN2/MntH hybrid gene was codon optimized for *E. coli* and the gene construct was synthesized into the pBAD24 vector by Genewiz.

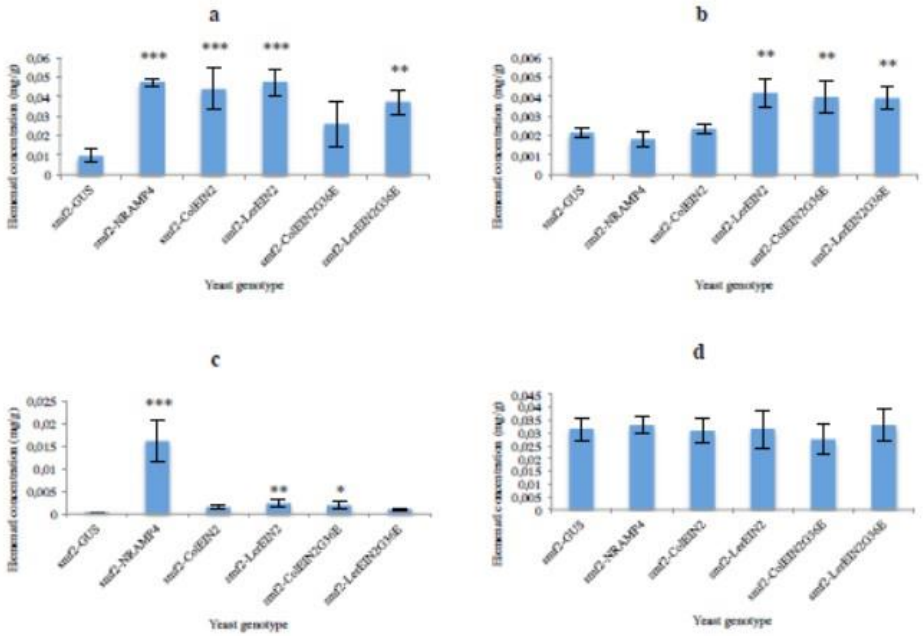

Appendix C. Elemental concentration analysis of yeast cells. *smf2* mutant yeast cells expressing EIN2 N-terminal domain (residues 1-524) were analyzed for metal uptake of (a) Ca (b) Cu (c) Mn and (d) Zn using atomic absorption. The gene sequence of EIN2 from both Col-0 and Ler were analyzed, as well as yeast expressing the G36E substitution. Asterisks denote different levels of significant difference compared to the negative control (smf2-GUS) (*: $p<0.05$, **: $p<0.01$, ***: $p<0.001$). *smf2*-NRAMP4 (expressing Arabidopsis NRAMP4) was used as a positive control. Error bars represent standard deviation. Data from Longerstay and Thomine, CNRS, Gif-sur-Yvette, France, unpublished.

Materials and Methods

Metal uptake measurements were performed by collaborators Pierre Longerstay and Dr. Sébastien Thomine using an AA240FS flame spectrometer. The yeast

transformants in the smf2 background (expressing GUS, NRAMP4, EIN2 (1-524, denoted ColEIN2), EIN2 G36E (1-524, denoted ColG36E), EIN2 Y160C (1-524, denoted LerEIN2), and EIN2 G36E Y160C (1-524, denoted LerG36E)) were grown for 4 days at 30 C in minimal medium lacking uracil, before diluting to an OD of 0.2 in minimal media lacking uracil supplemented with 50 μM $MnSO_4$ and buffered with 20 mM MES to pH 6.0. Cultures were grown for 48 hrs at 30 before centrifuged and pellets washed and dried. Samples were digested in 70% HNO_3, and diluted in ultrapure water, total Ca, Cu, Fe, Mg, Mn, and Zn were measured using the flame spectrometer. Four replicates were done for each genotype.

Gene	Strain	EIN2 complement	Background	Function
COT1	Y01613	no	BY4741	zinc transporter of the vacuole
CTR1	Y05539	no	BY4741	High affinity Copper transporter of PM
	ctr1-3 (83)	no	CM3262	
CTR2				low affinity copper transporter of vacuole
	ctr1-3ctr2Δ	no	CM3262	
CCC1		no	DY150	iron and manganese transporter of the vacuole
FET3 FET4	DEY1453	no	-	high and low affinity iron transporters
YCF1	Y04069	no	BY4741	cadmium transporter of the vacuole
ZRC1	Y10829	no	BY4742	zinc transporter of the vacuole
K667	Δvcx1 cnb1 pmc1	no	W303	Vacuolar Ca and K antiporter (VXC1), calcium dependent protein phosphatase (regulatory subunit of Calcineurin, CNB1)), Vacuolar Ca^{2+} ATPase that depletes cytosol of Ca^{2+} ions (PMC1)
K665	pmc1 vcx1	no	W303	
K616	pmr1 pmc1 cnb1	no	W303	High affinity Ca^{2+}/Mn^{2+} P-type ATPase of the golgi (PMR1)
SPF1		no	BY4741	P-type ATPase of ER involved in Ca^{2+} homeostasis
PMR1		no	BY4741	High affinity Ca^{2+}/Mn^{2+} P-type ATPase of the golgi (PMR1)
	pmr1spf1	no	BY4741	
	pmr1smf2	no	BY4741	Divalent ion transporter (Nramp) involved in Mn^{2+} homeostasis (SMF2)

Appendix D. Other yeast strains used to test whether EIN2 is capable of metal ion transport. The functions of these yeast genes are listed. EIN2 N-terminal domain (residues 1-524) was transformed into these mutants and spotted on various yeast media plates in attempt to complement these mutants, under conditions of low metals (chelated with EGTA, similar to 4.8 and 4.9) and in death assays with high doses of the various metals (similar to the cadmium assay, Figure 4.10). EIN2 was not able to complement any of these other yeast mutants under the conditions tested. The *cot1*, *ctr* mutants, *ccc1*, *fet3fe4*, *ycf1* and *zrc1* mutants were obtained from S. Thomine, as well as the *smf2* and *smf1* mutants. The K616 and K667 mutants were obtained from H. Sze. The K665 and K667 mutants were obtained from K. Hirschi. The *spf1*, *pmr1*, *pmr1smf2*, and *pmr1spf1* mutants were obtained from R.E. Willinger.

Materials and Methods

Yeast constructs in either the pDR195-GW vector (modified to include the gateway cassette by S. Thomine) or the pAG426-GPD-ccdB vector (Addgene) were transformed into all yeast strains listed in Appendix D. (expressing GUS, NRAMP4,

EIN2 (1-524), EIN2 G36E (1-524), EIN2 G36A (1-524), EIN2 Y160C (1-524), and EIN2 G36E Y160C (1-524)). Yeasts were grown on minimal media lacking uracil, with the addition of G418 for *cot1, ctr1, ycf1 and zrc1* mutant strains. The *ccc1* and *ctr1-3 ctr2Δ* double mutant were grown on plates lacking histidine and uracil, while the *fet3fet4* mutant was grown on medium lacking leucine, histidine, and uracil. All plates buffered with 10 mM MES to pH 6.0 unless otherwise stated. The *fet3fet4* mutant required spiking with 0.1 mM $FeCl_3$ to grow, and complementation was tested by the addition of 100 μM BPDS (bathophenanthrolinedisulfonic acid, and iron chelator), supplemented with 0-30 μM $FeCl_3$. The yeast assays with the *ccc1, cot1*, and *zrc1* mutants were repeated as described in Menguer et al., 2013, both the *cot1* and *zrc1* mutants were grown on plates adjusted to pH 5.5. The *ctr* yeast mutants were tested by Dr. Sébastien Thomine. All of the above listed mutants were a gift from Dr. Sébastien Thomine.

To test for calcium transport, the K667, K665, K601, *spf1, pmr1, smf2 pmr1, spf1 pmr1* mutants were used. The K667, K665, and K601 mutants were a gift from Dr. Heven Sze, the K667 and K665 mutants were also obtained from Dr. Kendal Hirschi. The *spf1, pmr1, smf2 pmr1, spf1 pmr1* mutants were obtained from Dr. Ralf Erik Wellinger. Yeasts transformed with all of the above plasmids were spotted on minimal media lacking uracil and containing 22 mM EGTA buffered with 50 mM MES to a pH 6.0 (like with the *smf2* mutant yeast assay in Chapter 4), but spiked with 10 mM $CaCl_2$, and with just 10 mM $CaCl_2$ (no EGTA), similar to described in García-Rodríguez et al., 2015). Calcium sensitivity was tested as described in Cheng et al., 2003.

Bibliography

Abel, L., Sánchez, F.O., Oberti, J., Thuc, N.V., Hoa, L.V., Lap, V.D., Skamene, E., Lagrange, P.H., and Schurr, E. (1998). Susceptibility to leprosy is linked to the human NRAMP1 gene. *J. Infect. Dis.*, 177(1): 133-145.

Abeles, F., Morgan, P., and Saltveit, M.J. (1992). *Ethylene in plant biology, Second Edition*. San Diego: Academic Press, Inc.

Adie, B.T.A, Pérez- Pérez, J., Pérez- Pérez, M.M., Godoy, M., Sánchez-Serrano, J.J., Schmelz, E.A, and Solano, R., (2007). ABA is an essential signal for plant resistance to pathogens affecting JA biosynthesis and the activation of defenses in Arabidopsis. *Plant Cell*, 19: 1665-1681.

Alonso, J.M., Hirayama, T., Roman, G. Nourizadeh, S. and Ecker, J.R. (1999). EIN2, a bifunctional transducer of ethylene and stress responses in Arabidopsis. *Science*, 284(5423): 2148-2152

Alscher, R.G. Erturk, N., and Heath, L.S. (2002). Role of superoxide dismutase (SODs) in controlling oxidative stress in plants. *J. Exp. Bot*., 53: 1331-1341.

An, F., Zhao, Q., Ji, Y., Li, W., Jiang, Z., Yu, X., Zhang, C., Han, Y., He, W., Liu, Y., Zhang, S., Ecker, J.R., and Guo, H. (2010). Ethylene-induced stabilization of ETHYLENE INSENSITIVE3 and EIN3-LIKE1 is mediated by proteasomal degradation of EIN3 binding F-box 1 and 2 that requires EIN2 in Arabidopsis. *Plant Cell*., 22: 2384-2401.

An, F., Zhang, X., Zhu, Z., Ji, Y., He, W., Jiang, Z., Li, M., and Guo, H. (2012). Coordinated regulation of apical hook developed by gibberellins and ethylene in etiolated *Arabidopsis* seedlings. *Cell Research*, 22: 915-927.

Arredondo, M., Muñoz, P. Mura, C.V., and Núñez, M.T. (2003). DMT1, a physiologically relevant apical Cu^{1+} transporter of intestinal cells. *Am J. Cell Physiol.*, 284: 1525-1530.

Bakshi, A., Shemansky, J.M., Chang, C., and Binder, B.M. (2015). History of research on the plant hormone ethylene. *J. Plant Growth Regul.,*. 34: 809-827.

Bauer, A., and Kölling, R. (1996). The *SAC3* gene encodes a nuclear protein required for normal progression of mitosis. *J. Cell Sci*. 109: 1575-1583.

Berg, J. (1976.) A potent inhibitor of ethylene action in plants. *Plant Physiol*., 58: 286-371.

Bermejo, R., Capra, T., Jossen, R., Colosio, A., Frattini, C., Carotenuto, W., Cocito, A., Doksani, Y., Klein, H., Gómez-González, B., Aguilera, A., Katou, Y., Shirahige, K., and Foiani, M. (2011). The replication checkpoint protects fork stability by releasing transcribed genes from nuclear pores. *Cell,*. 146: 233-246.

Bleecker AB, Estelle MA, Somerville C, and Kende H (1988) Insensitivity to ethylene conferred by a dominant mutation in Arabidopsis thaliana. *Science*, 241:1086–1089.

Binder, B.M., Walker, J.M., Gagne, J.M., Emborg, T.J., Hemmann, G., Bleecker, A.B., and Vierstra, R.D. (2007). Arabidopsis EIN3 binding F-Box proteins EBF1 and EBF2 have distinct but overlapping roles in ethylene signaling. *Plant Cell,* 19(2): 509-523.

Birchler, J.A, and Vietia, R.A. (2007). The gene balance hypothesis: from classical

genetics to modern genomics. *Plant Cell*, 19: 395-402.

Bisson, M.M., Bleckmann, A., Allekotte, S., and Groth, G. (2009). EIN2, the central regulator of ethylene signaling is localized at the ER membrane where it interacts with the ethylene receptor ETR1. *Biochem J,*. 424(1): 1-6.

Bisson, M.M.A. and Groth. G. (2010). New insight in ethylene signaling: autokinase activity of ETR1 modulates the interaction of receptors and EIN2. *Molec Plant*., 3(5): 882-889.

Bisson, M.M.A., and Groth, G. (2011). New paradigm in ethylene signaling, EIN2, the central regulator of the signaling pathway, interacts directly with the upstream receptors. *Plant Signal & Behav*., 6(1): 164-166.

Blobel, G. (1985) Gene gating: a hypothesis. *Proc. Natl. Acad. Sci. USA*, 82: 8527-8529.

Burg S.P. and Burg E.A. (1967). Molecular requirements for the biological activity of ethylene. Plant Physiol., 42:144–152

Burks, E.A., Bezerra, P.P., Le, H., Gallie, D.R., and Browning, K.S. (2001). Plant initiation factor 3 subunit composition resembles mammalian initiation factor 3 and has a novel subunit. *J. Biol. Chem.*, 276: 2122-2131.

Cabal, G.G., Genovesio, A., Rodiquez-Navarro, S., Zimmer, C., Gadal., O., Lesne, A., Buc, H., Feuerbach-Fournier, F., Olivo-Marin, J.C., Hurt, E.C., and Nehrbass, U. (2006). SAGA interacting factors confine sub-diffusion of transcribed genes to the nuclear envelope. *Nature*, 441: 770-773.

Cailliatte, R., Lapeyre, B., Briat, J.F., Mari, S., and Curie, C. (2009). The

NRAMP6 metal transporter contributes to cadmium toxicity. *Biochem. J.*, 422(2): 217-228.

Cancel, J.D. and Larsen, P.B. (2002). Loss-of-Function mutations in the ethylene receptor ETR1 cause enhanced sensitivity and exaggerated response to ethylene in Arabidopsis. *Plant Physiol*., 129: 1557–1567.

Cao, S., Chen, Z., Liu, G., Jiang, L., Yuan, H., Ren, G., Bian, X., Jian, H., and Ma, X. (2009). The Arabidopsis Ethylene-Insensitive 2 gene is required for lead resistance. *Plant Phys. Biochem.*, 47: 308-312.

Cellier, M. and Gros, P. (2004). *The Nramp family*. New York: Kulwer Academic.

Chang, K. N., Zhong, S., Weirauch, M. T., Hon, G., Pelizzola, M., Li, H., Huang, S.C., Schmitz, R.J., Urich, M.A., Kuo, D., Nery, J.R., Qiao, H., Yang, A., Jamai, A., Chen, H., Ideker, T., Ren, B., Bar-Joseph, Z., Hughes, T.R., and Ecker, J. R. (2013). Temporal transcriptional response to ethylene gas drives growth hormone cross-regulation in *Arabidopsis*. *eLife*, *2*, e00675. http://doi.org/10.7554/eLife.00675

Chaloupka, R., Courville, P, Veyrier, F, Knudsen, B., Tompkins, T.A, and Cellier, M.F. (2005). Identification of functional amino acids in the Nramp family by a combination of evolutionary analysis and biophysical studies of metal proton cotransport *in vivo*. *Biochem*., 44(2): 726-33.

Chao, Q., Rothenberg, M., Solano, R., Roman, G., Terzaghi, W., and Ecker, J.R. (1997). Activation of the ethylene gas response pathway in Arabidopsis by the nuclear protein ETHYLENE-INSENSITIVE3 and related proteins. *Cell*, 89: 1133-1144.

Chen, R.Q., Binder, B.M., Garrett, W.M., Tucker, M.L., Chang, C., and Cooper, B. (2011). Proteomic responses in Arabidopsis thaliana seedlings treated with ethylene. *Mol Biosyst*., 7(9): 2637-2650.

Chen, T., Liu, J., Lei, G., Liu, Y.F., Li, Z.G., Tao, J.J., Hao, Y.J., Cao, Y.R., Lin, Q., Zhang, W.K., Ma, B., Chen, S.Y., and Zhang, J.S. (2009). Effects of tobacco ethylene receptor mutations on receptor kinase activity, plant growth and stress responses. *Plant Cell Physiol*., 50:1636-1650.

Chen, X.Z., Peng, J.B., and Cohen, A. (1999). Yeast SMF mediates H(+)-coupled iron uptake with concomitant uncoupled cation currents. *J. Biol. Chem*., 274: 35089-35094

Chen, Y.F., Gao, Z., Kerris, R.J. III, Wang,W., Binder, B.M., and Schaller, G.E. (2010). Ethylene receptors function as components of high-molecular-mass protein complexes in Arabidopsis. *PLoS ONE,* 5(1):e8640. DOI:10.1371/journal.pone.0008640.

Cheng, N.H., Pittman, J.K., Zhu, J.K., and Hirschi, K.D. (2003). The protein kinase SOS2 activates the *Arabidopsis* H^+/Ca^{2+} antiporter CAX1 to integrate calcium transport and salt tolerance. *J. Biol. Chem*., 279: 2922-2926.

Christians, M.J. and Larsen, P.B. (2007). Mutational loss of the prohibition AtPHB3 results in an extreme constitutive ethylene response phenotype coupled with partial loss of ethylene-inducible gene expression in Arabidopsis seedlings. *J. Exp. Bot*., 58(8): 2237-2248.

Christians, M.J., Robles, L.M., Zeller, S.M., Larsen, P.B. (2008). The *eer5*

mutation, which affects a novel proteasome-related subunit, indicates a prominent role for the COP9 signalosome in resetting the ethylene-signaling pathway in Arabidopsis. *Plant J*., 55: 467-477.

Ciccarelli, F.D., Izaurralde, E., and Bork, P. (2003). The PAM domain, a multi-protein complex-associated module with an all-alpha-helix fold. *BMC Bioinform.,* 4: 64-68.

Clark, K.L., Larsen, P.B., Wang, X., and Chang, C. (1998). Association of the Arabidopsis CTR1 Raf-like kinase with the ETR1 and ERS ethylene receptors. *Proc. Natl. Acad. Sci. USA*, 95: 5401-5406.

Clemens, S., Antosiewicz, D. M., Ward, J. M., Schachtman, D. P., and Schroeder, J. I. (1998). The plant cDNA LCT1 mediates the uptake of calcium and cadmium in yeast. *Proc. Natl. Acad. Sci. USA*, 95**:** 12043–12048.

Clough, S.J. and Bent, A.F. (1998). Floral dip: A simplified method for Agrobacterium-mediatedtransformation of Arabidopsis thaliana. *Plant J*., 16(6):735–743.

Cohen, C. K., Nelson, H., and Nelson, N. (2000). The family of SMF metal ion transporters in yeast cells. *J. Biol. Chem*., 275: 33388-33394.

Cooper B. (2013). Separation anxiety: An analysis of ethylene-induced cleavage of EIN2. *Plant Signal. Behav.*, 8: e24721, DOI: 10.4161/psb.24721.

Cope, G.A., Suh, G.S., Aravind, L., Schwarz, S.E., Zipursky, S.L., Koonin, E.V., and Deshaies, R.J. (2002). Role of predicted metalloprotease motif of Jab1/Csn5 in cleavage of Nedd8 from Cul1. *Science*, 298: 608-611.

Courville, P., Chaloupka, R., Veyrier, F., and Cellier, M.F.M. (2004).

Determination of transmembrane topology of the *Escherichia coli* natural resistance-associated macrophage protein (Nramp) ortholog. *J. Biol. Chem.*, 279(5): 3318-3326.

Courville, P., Chaloupka, R., and Cellier, M.F.M. (2006). Recent progress in structure-function analyses of Nramp proton-dependent metal-ion transporters. *Biochem. Cell Biol.,* 84: 960-978.

Curie, C., Alonso, J.M., Le Jean, M., Ecker, J.R. and Briat, J.F. (2000). Involvement of NRAMP1 from Arabidopsis thaliana in iron transport. *Biochem J.,* 347: 749-755.

Dancis, A., Yuan, D.S., Haile, D., Askwith, C., Eide, D., Moehle, C., Kaplan, J., and Klausner, R.D. (1994). Molecular characterization of a copper transport protein in *S. cerevisiae*: an unexpected role for copper in iron transport. *Cell*, 76(2): 393-402.

De Paepe, A., De Grauwe, L., Bertrand, S., Smalle, J., and Van der Straeten, D. (2005). The Arabidopsis mutant *eer2* has enhanced ethylene responses in the light. *J. Exp. Bot.,* 56(419): 2409-2420.

Dong, C.H., Rivarola, M., Resnick, J.S., Maggin, B.D., and Chang, C. (2008). Subcellular co-localization of Arabidopsis RTE1 and ETR1 supports a regulatory role for RTE1 in ETR1 ethylene signaling. *Plant J.*, 53:275-286.

Doronkin, S., Djagaeva, I., and Beckendorf, S.K. (2002). CSN5/Jab1 mutations affect axis formation in the *Drosophila* oocyte by activating a meiotic checkpoint. *Development*, 129:5053–64.

Doronkin, S., Djagaeva, I., and Beckendorf, S.K. (2003). The COP9 signalosome

promotes degradation of Cyclin E during early Drosophila oogenesis. *Dev. Cell,* 4(5): 699-710.

Earley, K.W., Haag, J.R., Pontes, O., Opper, K., Juehne, T., Song, K., and Pikaard, C.S. (2006). Gateway-compatible vectors for plant functional genomics and proteomics. *Plant J.,* 45(4):616–629.

Edgar, R.C. (2004). MUSCLE: multiple sequence alignment with high accuracy throughput. *Nucleic Acids Res.* 32(5): 1792-1797.

Eide, D., Broderius, M., Fett, J., and Guerinot, M.L. (1996). A novel iron-regulated metal transporter from plants identified by functional expression in yeast. *Proc. Natl. Acad. Sci. USA,* 93: 5624-5628.

Ferrari, S., Plotnikova, J.M., De Lorenzo, G., and Ausubel, F.M. (2003). *Arabidopsis* local resistance to *Botrytis cinerea* involves salicylic acid and camalexin and requires *EDS4* and *PAD2,* but not *SID2, EDS5,* or *PAD4. Plant J*., 35(2): 193-205.

Fischer, T., Strässer, K., Rácz, A., Rodrigues-Navarro, S., Oppizzi, M. Ihrig, P., Lechner, J., and Hurt, E. (2002). The mRNA export machinery requires the novel Sac3p-Thp1p complex to dock at the nucleoplasmic entrance of the nuclear pores. *The EMBO J*., 21: 5843-5852.

Fleming, M.D., Trenor III, C.C., Su, M.A., Foernzler, D., Beier, D.R., Dietrich, W.F., and Andrews, N.C. (1997). Microcytic anaemia *Nramp2*, a candidate iron transporter gene. *Nature Genetics*, 16: 383-386.

Fujita, H. and Syono, K. (1996). Genetic analysis of the effects of polar auxin transport inhibitors on root growth in Arabidopsis thaliana. *Plant Cell Physiol*., 37(8): 1094-1101.

Füzesi-Levi, M.G., Ben-Nissan, G., Bianchi, E., Zhou, H., Deery, M.J., Lilley,

K.S., Levin, Y., and Sharon, M. (2014). Dynamic regulation of the COP9 signalosome in response to DNA damage. *Mol. Cell Biol*., 34(6): 1066-1076.

Gadd, G.M. and Laurence, O.S. (1996). Demonstration of high-affinity Mn^{2+} uptake in *Saccharomyces cerevisiae*: specificity and kinetics. *Microbio.*, 142: 1159-1167.

Gagne, J.M., Smalle, J., Gingerich, D.J., Walker, J.M., Yoo, S.D., Yanagisawa, S., and Vierstra, R.D. (2004). Arabidopsis EIN2-binding F-box 1 and 2 form ubiquitin-protein ligases that repress ethylene action and promote growth by directing EIN3 degradation. *Proc. Natl. Acad. Sci. U.S.A,* 101(17): 6803-6088.

Gallardo, M., Luna, R., Erdjument-Bromage, H., Tempst, P., and Aguilera, A. (2003). Nab2p and the Thp1p-Sac3p complex functionally interact at the interface between transcription and mRNA metabolism. *J. Biol. Chem*., 278: 24225-24232.

Gamble, R.L., Coonfield, M.L., and Schaller, G.E. (1998). Histidine kinase activity of the ETR1 ethylene receptor from Arabidopsis. *Proc. Natl. Acad. Sci. U.S.A,* 95: 7825–7829.

Gao, Z., Chen, Y., Randlett, M.D., Zhao, X., Findell, J.L., Kieber, J.J., and Schaller, G.E. (2003). Localization of the Raf-like kinase CTR1 to the endoplasmic reticulum of Arabidopsis through participation in ethylene receptor signaling complexes. *J. Biol. Chem.,* 278: 34725-34732.

Gao, Z., Wen, C.K., Binder, B.M., Chen, Y.F., Chang, J., Chiang, Y.H. Kerris

3rd, R.J., Chang, C. and Schaller, G.E. (2008) Heteromeric interactions among ethylene receptors mediate signaling in Arabidopsis. *J. Biol. Chem*., 283: 23801–23810.

García-Rodríguez, N., Manzano-López, J., Muñoz-Bravo, M., Fernández-García, E., Muñiz, M., and Wellinger, R.E. (2015). Manganese redistribution by calcium stimulated vesicle trafficking bypass the need for P-type ATPase function. *J. Biol. Chem*., 290: 9335-9347.

Gazouli, M., Atsaves, V., Mantzaris, G., Economou, M., Nasioulas, G., Evangelou, K., Archimandritis, A.J., and Anagnou, N.P. (2008). Role of functional polymorphisms of NRAMP1 gene for the development of Crohn's disease. *Inflamm. Bowel. Dis.*, 14(10): 1323-1330.

Ghassemian, M., Nambara, E., Cutler, S., Kawaide, H., Kamiya, Y., and McCourt, P. (2000). Regulation of abscisic acid signaling by the ethylene response pathway in Arabidopsis. *Plant Cell*, 12(7): 1117-1126.

Glickman, M.H., Rubin, D.M., Coux, O., Wefes, I., Pfeifer, G., Cjeka, Z., Baumeister, W., Fried, V.A., and Finley, D. (1998). A subcomplex of the proteasome regulatory particle required for ubiquitin-conjugated degradation and related to the COP9-signalosome and eIF3. *Cell*, 94: 615-623.

Gong, Z., Dong, C.H., Lee, H., Zhu, J., Xiong, L., Gong, D., Stevenson, B., and Zhu, J.K. (2005). A DEAD Box RNA helicase is essential for mRNA export and is important for development and stress responses in Arabidopsis. *Plant Cell*, 17: 256-267.

González-Aguilera, C., Tous, C., Gómez-González, B., Huertas, P., Luna, R., and

Aguilera, A. (2008). The THP1-SAC3-SUS1-CDC31 complex works in transcription elongation-mRNA export preventing RNA-mediated genome instability. *Mol. Biol. Cell*, 19: 4310-4318.

Gordon, C., McGurk, G., Wallace, M., and Hastie, N.D. (1996). A conditional lethal mutant in the fission yeast 26S protease subunit mts3+ is defective in metaphase to anaphase transition. *J. Biol. Chem.*, 271: 5704-5711.

Grefen, C., Städele, K., Růžička, K., Obrdlik, P., Harter, K., and Horák, J. (2008). Subcellular localization and *in vivo* interactions of the *Arabidopsis thaliana* ethylene receptor family members. *Mol. Plant*, 1: 308-320.

Guo, H. and Ecker, J.R. (2003). Plant responses to ethylene gas are mediated by SCF EBF1/EBF2-dependent proteolysis of EIN3 transcription factor. *Cell*, 115: 667–677.

Guzmán, P. and Ecker, J.R (1990). Exploiting the triple response of Arabidopsis to identify ethylene-related mutants. *Plant Cell*, 2: 513–523.

Haemig, H.A.H. and Brooker, R.J. (2004). Importance of conserved acidic residues in MntH, the Nramp homolog of *Escherichia coli*. *J. Membr. Biol*., 201(2): 97-107.

Haemig, H.A.H., Moen, P.J., and Brooker, R.J. (2010). Evidence that highly conserved residues of transmembrane segment 6 of *Escherichia coli* MntH are important for transport activity. *Biochem*., 49(2): 4662-4671.

Hall, A.E., Chen, G.C., Findell, G.C., Schaller, G.E., and Bleecker, A.B. (1999)

The relationship between ethylene binding and dominant insensitivity conferred by mutant forms of the ETR1 ethylene receptor. *Plant Physiol*., 121: 291-299.

Hall, A.E. and Bleecker, A.B. (2003) Analysis of combinatorial loss-of-function mutants in the Arabidopsis ethylene receptors reveals that the *ers1 etr1* double mutant has severe developmental defects that are EIN2 dependent. *Plant Cell*, 15: 2032-2041.

Hall, B.P., Shakeel, S.N., Amir, M., Ul Haq, N., Qu, X., and Schaller, G.E. (2012).Histidine kinase activity of the ethylene receptor ETR1 facilitates the ethylene response in Arabidopsis. *Plant Physiol*., 159: 682–95.

He, W., Brumos, J., Li, H., Ji, Y., Ke, M., Gong, X., Zeng, Q., Li, W., Zhang, X., An, F., Wen, X., Li, P., Chu, J., Sun, X., Yan, C., Yan, N., Xie, D.Y., Raikhel, N., Yang, Z., Stepanova, A.N., Alonso, J.M., and Guo, H. (2011). A small-molecule screen identifies L-kynurenine as a competitive inhibitor of TAA1/TAR activity in ethylene-directed auxin biosynthesis and root growth in *Arabidopsis. Plant Cell*, 23: 3944-3960.

Herman, C., Lecat, S., D'Ari, R., and Bouloc, P. (1995). Regulation of the heat-shock response depends on divalent metal ions in an hflB mutant of *Escherichia coli*. *Molec. Microbio.*, 18(2): 247-255.

Hirata, Y. (2002). Manganese-induced apoptosis in PC12 cells. *Neurotxicol. Teratol.*, 24: 639-53.

Hirayama, T., Kieber, J.J., Hirayama, N., Kogan, M., Guzmán, P., Nourizadeh,

S., Alonso, J.M., Dailey, W.P., Dancis, A., and Ecker, J.R. (1999). RESPONSIVE-TO-ANTAGONIST1, a Menkes/Wilson disease-related copper transporter, is required for ethylene signaling in Arabidopsis. *Cell*, 97: 383-393.

Hoffmann, K. and Bucher, P. (1998). The PCI domain: a common theme in three multiprotein complexes. *Trends Biochem. Sci.*, 23:204-205.

Hollender, C.A. and Liu, Z. (2010) Bimolecular fluorescence complementation (BiFC) assay for protein-protein interaction in onion cells using the helios gene gun. *J. Vis. Exp.*, 40(40): 1963.

Hsu, Y.H., Chen, C.W., Sun, H.S., Jou, R., Lee, J.J., and Su, I.J. (2006). Association of *NRAMP1* gene polymorphism with susceptibility to tuberculosis in Taiwanese Aboriginals. *J. Formos. Med. Assoc*., 105(5): 363-369.

Hua, J. and Meyerowitz, E.M. (1998). Ethylene responses are negatively regulated by a receptor gene family in *Arabidopsis thaliana*. *Cell*, 94: 261–271.

Huang, H., Quint, M., and Gray, W.M. (2013). The *eta7/csn3-3* auxin response mutant of Arabidopsis defines a novel function for the CSN3 subunit of the COP9 signalosome. *PLoS ONE*, 8: e66578. DOI:10.1371/journal.pone.0066578

Huang, Y., Li, H., Hutchison, C.E., Laskey, J., and Kieber, J.J. (2003) Biochemical and functional analysis of CTR1, a protein kinase that negatively regulates ethylene signaling in Arabidopsis. *Plant J*., 33: 221–33.

Hwang, I., Sze, H., and Harper, J.F. (2000). A calcium-dependent protein kinase

can inhibit a calmodulin-stimulated Ca^{2+} pump (ACA2) located in the endoplasmic reticulum of Arabidopsis. *Proc. Natl. Acad. Sci. U.S.A*, 97(11): 6224-6229.

Ishimaru, Y. Takahashi, R., Bashir, K., Shimo, H., Senoura, T., Sugimoto, K., Ono, K., Yano, M., Ishikawa, S., Arao, T., Nakanishi, H., and Nishizawa, N.K. (2012). Characterizing the role of rice NRAMP5 in manganese, iron, and cadmium transport. *Sci. Rep*., 2: 286. DOI:10.1038/srep00286

Jani, D., Lutz, S., Marshall, N.J., Fischer, T., Kohler, A., Ellisdon, A.M., Hurt, E., and Stewart, M. (2009). Sus1, Cdc31, and the Sac3 CID region form a conserved interaction platform that promotes nuclear pore association and mRNA export. *Mol. Cell*, 33: 727-737.

Jones, A.L., Quimby, B.B., Hood, J.K., Ferrigno, P., Keshava, P., Silver, P.A., and Corbett, A.H. (2000). *SAC3* may link nuclear protein export to cell cycle progression. *Proc. Natl. Acad. Sci. U.S.A*, 97: 3224-3229.

Jones, R.P. and Gadd, G.M. (1990). Ionic nutrition of yeast – the physiological mechanisms involved and applications for biotechnology. *Enzym. Microbiol. Tech.,* 12: 402-418.

Ju, C., Yoon, G.Y., Shemansky, J.M., Lin, D.Y., Ying, I.Y., Chang, J., Garrett, W.M., Kessenbrock, M., Groth, G., Tucker, M.L., Cooper, B., Kieber, J.J., and Chang, C. (2012). CTRI phosphorylates the central regulator EIN2 to control ethylene hormone signaling from the ER membrane to the nucleus in Arabidopsis. *Proc. Natl. Acad. Sci. U.S.A.*, 109(47): 19486-19491.

Kieber, J..J., Rothenberg, M., Roman, G., Feldmann, K.A., and Ecker, J.R.

(1993). CTR1, a negative regulator of the ethylene response pathway in Arabidopsis, encodes a member of the Raf family of protein kinases. *Cell*, 72: 427-441.

Kim, J., Patterson, S.E., and Binder, B.M. (2013). Reducing jasmonic acid levels causes *ein2* mutants to become ethylene responsive. *FEBS Letters*. 587: 226-230.

Kim, J., Chang, C. and Tucker, M.L. (2015). To grow old: regulatory role of ethylene and jasmonic acid in senescence. *Frontiers in Plant Science*. 6:20. doi:10.3389/fpls.2015.00020.

Kim, T., Hofmann, K., von Arnim, A.G., and Chamovitz, D.A. (2001). PCI complexes: pretty complex interactions in diverse signaling pathways. *Trends Plant Sci*,. 6:379–386.

Knight, L.I. and Crocker, W. (1913) Toxicity of smoke. *Bot. Gaz.*, 55: 337–371.

Kubo, M., Furuta, K., Demura, T., Fukuda, H., Liu, Y.G., Shibata, D., and Kakimoto, T. (2011). The *CKH1/EER4* gene encoding a TAF12-Like protein negatively regulates cytokinin sensitivity in Arabidopsis thaliana. *Plant Cell Physiol*., 52(2): 629-637.

Kushwah, S., Jones, A.M. and Laxmi, A. (2011). Cytokinin interplay with ethylene, auxin, and glucose signaling controls *Arabidopsis* seedling root directional growth. *Plant Physiol.*, 156: 1851-1866.

Kwak, S.H. and Lee, S.H. (1997). The requirements for Ca^{2+}, protein phosphorylation, and dephosphorylation for ethylene signal transduction in *Pisum sativum* L. *Plant Cell Physiol*., 38(10): 1142-1149.

Kwok, S.F., Solano, R., Tsuge, T., Chamovitz, D.A., Ecker, J.R., Matsui, M., and Deng, X.W. (1998). Arabidopsis homologs of a c-Jun coactivator are present both in monomeric form and in the COP9 complex, and their abundance is differentially affected by pleiotropic *cop/det/fus* mutations. *Plant Cell*, 10(11): 1779-1790.

Lam-Yuk-Tseung, S., Govoni, G., Forbes, J., and Gros, P., (2003). Iron transport by Nramp2/DMT1: pH regulation of transport by 2 histidines in transmembrane domain 6. *Blood*, 101(9): 3699-3707.

Lanquar, V., Lelièvre, F., Barbier-Brygoo, H., and Thomine, S. (2004). Regulation and function of AtNRAMP4 metal transporter protein. *Soil Sci. Plant Nutrit*., 50: 1141-1150.

Lanquar, V., Lelièvre, F., Bolte, S., Hamès, C., Alcon, C., Neumann, D., Vansuyt, G., Curie, C., Schröder, A., Krämer, U., Brabier-Brygoo, H., and Thomine, S. (2005). Mobilization of vacuolar iron by AtNRAMP3 and AtNRAMP4 is essential for seed germination on low iron. *EMBO J*., 24: 4041-4051.

Lanquar, V., Ramos, M.S., Lelièvre, F., Barbier-Brygoo, H., Krierger-Liszkay, A., Krämer, U., and Thomine, S. (2010). Export of vacuolar manganese by AtNRAMP3 and AtNRAMP4 is required for optimal photosynthesis and growth under manganese deficiency. *Plant Physiol.*, 152: 1986-1999.

Larsen, P.B. and Chang, C. (2001). The Arabidopsis *eer1* mutant has enhanced ethylene responses in the hypocotyl and stem. *Plant Physiol.*, 125(2): 1061-1073.

Lei, E.P., Stern, C.A., Fahrenkrog, B., Krebber, H., Moy, T.I., Aebi, U., and Silver, P.A.

(2003). Sac3 is an mRNA export factor that localizes to cytoplasmic fibrils of nuclear pore complex. *Mol. Biol. Cell*., 14: 836-847.

Li, W., Ma, M., Feng, Y., Hongjiang, L., Wang, Y., Ma, Y., Li, M., An, F., and Guo, H. (2015). EIN2-directed translational regulation of ethylene signaling in Arabidopsis. *Cell*, 163(3): 670-683.

Liu, C., Guo, L.Q., Menon, S., Jin, D., Pick, E., Wang, X., Deng, X.W., and Wei, N. (2013). COP9 signalosome subunit Csn8 is involved in maintaining proper duration of the G1 phase. *J. Biol. Chem*., 288(28): 20443-20452.

Lu, Q., Tang, X., Tian, G., Wang, F., Liu, K., Nguyen, V., Kohalmi, S.E., Keller, W.A., Tsang, E.W.T., Harada, J.J., Rothstein, S.J., and Cui, Y. (2010). Arabidopsis homolog of the yeast TREX-2 mRNA export complex: components and anchoring nucleoporin. *Plant J*., 61: 259-270.

Liu, X.F., Supek, F., Nelson, N., and Culotta, V.C. (1997). Negative control of heavy metal uptake by the *Saccharomyces cerevisiae BSD2* gene. *J. Biol. Chem*., 272: 11763-11769.

Luk, E.E.C. and Culotta, V.C. (2001). Manganese superoxide dismutase in *Saccharomyces cerevisiae* acquires its metal co-factor through a pathway involving the Nramp metal transporter, Smf2p. *J. Biol. Chem*., 276(50): 47556-47562.

Makui, H., Roig, E., Cole, S.T., Helmann, J.D., Gros, P., and Cellier, M.F. (2000). Identification of the *Escherichia coli* K-12 Nramp orthologue (MntH) as a selective divalent metal ion transporter. *Molec. Microbiol*., 35(5): 1065-1078.

Mayerhofer, H., Panneerselvam, S., and Muller-Dieckmann, J. (2012). Protein

kinase domain of CTR1 from *Arabidopsis thaliana* promotes ethylene receptor cross talk. *J. Mol. Biol*., 415: 768-779.

McClellan, C. (2009). Suppressors of *etr1-2*: I *etr1-11* is a loss-of-function mutation of the *ETR1* ethylene receptor. II. *REVERSION TO ETHYLENE SENSITIVITY3* is a regulator of seedling growth. *PhD thesis*, University of Maryland, College Park.

Meier, I. and Brkljacic, J. (2010). The Arabidopsis nuclear pore and nuclear envelope. *The Arabidopsis Book*. 8: e0139. DOI: 10.1199/tab.0139

Menguer, P.K., Farthing, E., Peaston, K.A., Ricachenevsky, F.K., Fett, J.P., and Williams, L.E. (2013). Functional analysis of the rice vacuolar zinc transporter OsMTP1. *J. Exp. Bot*., 64: 2871-2883.

Merchante, C., Brumos, J., Yun, J., Hu, Q., Spencer, K.R., Enríquez, P., Binder, B.M., Heber, S., Stepanova, A.N., and Alonso, J.M. (2015). Gene-specific translation regulation mediated by the hormone-signaling molecule EIN2. *Cell*, 163(3): 684-697.

Merkle, T. (2011). Nucleo-cytoplasmic transport of proteins and RNA in plants. *Plant Cell Rep*. 30: 153-156.

Moore, K.L., Chen, Y., van de Meene, A.M.L., Hughes, L., Liu, W., Gerake, T., Mosselmans, F., McGrath, S.P., Grovenor, C., and Zhao, F.J. (2014). Combined NanoSIMS and synchrotron X-ray fluorescence reveal distinct cellular and subcellular distribution patters of trance elements in rice tissues. *New Phytol*., 201: 104-115.

Moussatche, P. and Klee, H.J. (2004) Autophosphorylation activity of the Arabidopsis ethylene receptor multigene family. *J. Biol. Chem*. 279:48734-48741.

Mundt, K.E., Porte, J., Murray, J.M., Brikos, C., Christensen, P.U., Caspari, T., Hagan, I.M., Millar, J.B., Simanis, V., Hofmann, K., Carr, A.M. (1999). The COP9/signalosome complex is conserved in fission yeast and has a role in S phase. *Curr. Biol.,* 9: 1427–1430

Neljubow, D. (1901) Uber die horizontale nutation der stengel von *Pisum sativum* und einiger anderen pflanzen. *Beih. Bot. Zentralb.,* 10: 128–139.

Nelson, B.K., Cai, X., and Nebenführ, A. (2007). A multicolored set of in vivo organelle markers for co-localization studies in Arabidopsis and other plants. *Plant J*., 51(6):1126–1136.

Nevo, Y. and Nelson, N. (2006). The NRAMP family of metal-ion transporters. *Biochem. Biophys. Acta*. 1763: 609-620.

Nevo, Y. (2008). Site-directed mutagenesis investigation of coupling properties of metal ion transport by DCT1. *Biochim.Biophys. Acta*., 1778: 334-341.

Novikova, G.V., Moshkov, I.E., Smith, A.R., and Hall, M.A. (2000), The effect of ethylene on MAPKinase-like activity in Arabidopsis thaliana. *FEBS Lett.,* 474: 29–32.

Obrdlik, P., El-Bakkoury, M., Hamacher, T., Cappellaro, C., Vilarino, C., Fleischer, C., Elllerbrok, H., Kamuzinzi, R., Ledent, V., Blaudez, D., Sanders, D., Revuelta, J.L., Boles, E., André, B., and Frommer, W.B. (2004). K^+ channel interactions detected by a genetic system optimized for systematic studies of membrane protein interactions. *Proc. Natl. Acad. Sci. U.S.A.,* 101: 12242-12247.

Olmedo, G., Guo, H., Gregory, B.D., Nourizadeh, S.D., Aguilar-Henonin, L., Li,

H. An, F., Gúzman, P., and Ecker, J.R. (2006). ETHYLENE-INSENSITIVE5 encodes for a 5'->3' exoribonuclease required for regulation of the EIN3-targeting F-box proteins EBF1/2. *Proc. Natl. Acad. Sci. U.S.A.,*. 103: 13286–13293.

O'Malley, R.C., Rodriguez, F.I., Esch, J.J., Binder, B.M., O'Donnell, P., Klee, H.J. and Bleecker, A.B. (2005). Ethylene-binding activity, gene expression levels, and receptor system output for ethylene receptor family members from Arabidopsis and tomato. *Plant J*., 41: 651–659.

Palmiter, R.D., and Findley, S.D. (1995). Cloning and functional characterization of a mammalian zinc transporter that confers resistance to zinc. *EMBO J*., 14 (4): 639-649.

Pence, N.S., Larsen, P.B., Ebbs, S.D., Letham, D.L.D., Lasat, M.M., Garvin, D.F., Eide, D., and Kochian, L.V. (2000). The molecular physiology of heavy metal transport in the Zn/Cd hyperaccumulator *Thlaspi caerulescens. Proc. Natl. Acad. Sci. U.S.A.*, 97: 4956-4960.

Pinner, E., Gruenheid, S, Raymond, M., and Gros, P. (1997). Functional complementation of the yeast divalent cation transporter family *SMF* by *NRAMP2*, a member of the mammalian natural resistance-associated macrophage protein family. *J. Biol. Chem*., 272: 28933-28938.

Portnoy, M.E., Liu, X.F., and Culotta, V.C. (2000). *Saccharomyces cerevisiae* expresses three functionally distinct homologues of the Nramp family of metal transporters. *Mol. Cell Biol*., 20(21): 7893-7901.

Portnoy, M.E., Schmidt, P.J., Rogers, R.S., and Culotta, V.C. (2001). Metal transporters that contribute copper to metallochaperones in *Saccharomyces cerevisiae*. Mol. Genet Genomics, 265(5): 873-882.

Portnoy, M.E., Jensen, L.T., and Culotta, V.C. (2002). The distinct methods by which manganese and iron regulate the Nramp transporters in yeast. *Biochem J*., 362(1): 119-124.

Potuschak, T., Lechner, E., Parmentier, Y., Yanagisawa, S., Grava, S., Koncz, C., and Genschik, P. (2003). EIN3-dependent regulation of plant ethylene hormone signaling by two Arabidopsis F Box proteins : EBF1 and EBF2. *Cell*, 115: 679–689.

Potuschak, T., Vansiri, A., Binder, B.M., Lechner, E., Vierstra, R.D., and Genschik, P. (2006). The exoribonuclease XRN4 is a component of the ethylene response pathway in Arabidopsis. *Plant Cell*, 18: 3047–3057.

Qiao, H., Chang, K.N., Yazaki, J., and Ecker, J.R. (2009). Interplay between ethylene, ETP1/2 F-box proteins, and degradation of EIN2 triggers ethylene responses in Arabidopsis. *Genes & Dev*., 23: 512-521.

Qiao, H., Shen, Z., Huang, S.C., Schmitz, R.J., Urich, M.A., Briggs, S.P., Ecker, J.R. (2012). Processing and subcellular trafficking of ER-tethered EIN2 control response to ethylene gas. *Science*, 338(6105): 390-393.

Qiao, H., Shen, Z., Huang, S.S.C., Schmitz, R.J., Urich, M.A., Briggs, S.P., and Ecker, J.R. (2013)**.** Response to perspective: "Separation anxiety: An analysis of ethylene-induced cleavage of EIN2". *Plant Signal. Behav*., 8:8, e25037. DOI: 10.4161/psb.25037

Qu, X. and Schaller, G.E. (2004). Requirement of the histidine kinase domain for signal transduction by the ethylene receptor ETR1. *Plant Physiol.,* 136: 2961–2970.

Qu, X., Hall, B.P., Gao, Z., and Schaller, G.E. (2007). A strong constitutive ethylene-response phenotype conferred on Arabidopsis plants containing null mutations in the ethylene receptors *ETR1* and *ERS1*. *BMC Plant Biol.,* 7: 3. DOI:10.1186/1471-2229-7-3.

Quaked, F., Rozhon, W., Lecourieux, D., and Hirt, H. (2003). A MAPK pathway mediates ethylene signaling in plants. *EMBO J*., 22: 1282-1288.

Raz, V. and Fluhr, R. (1992). Calcium requirement for ethylene-dependent responses. *Plant Cell*, 4: 1123-1130.

Rice, A.J., Alvarez, F.J.D., Schultz, K.M., Klug, C.S., Davidson, A.L., and Pinkett, H.W. (2013). EPR spectroscopy of $MolB_2C_2$-a reveals mechanism of transport for a bacterial type II molybdate importer. *J. Biol. Chem.,* 288: 21228-21235.

Richer, E., Courville, P., and Cellier, M. (2004). Molecular evolutionary analysis of the Nramp family. In Cellier, M. and Gros, P. (Eds.) *The Nramp family*. (pp. 178-194). New York: Kulwer Academic.

Rodriguez, F.I, Esch, J.J., Hall, A.E., Binder, B.M., Schaller, G.E., and Bleecker, A.B. (1999). A copper cofactor for the ethylene receptor ETR1 from Arabidopsis. *Science*, 283: 996-998.

Rogers, E.E, Eide, D.J., and Guerinot, M.L. (2000). Altered selectivity in an

Arabidopsis metal transporter. *Proc. Natl. Acad. Sci. USA*, 97(22): 12356-12360.

Roman, G., Lubarsky, B., Kieber, J.J., Rothenberg, M., and Ecker, J.R. (1995). Genetic analysis of ethylene signal transduction in *Arabidopsis thaliana*: five novel mutant loci integrated into a stress response pathway. *Genet.*, 139: 1393–1409.

Rozen, S., Fuzesi-Levi, M. G., Ben-Nissan, G., Mizrachi, L., Gabashvili, A., Levin, Y., Ben-Dor, S., Eisenstein, M., and Sharon, M. (2015). CSNAP Is a Stoichiometric Subunit of the COP9 Signalosome. *Cell Rep.*, 13(3): 585–598.

Rubio, V., Shen, Y., Saijo, Y., Liu, Y., Gusmaroli, G., Dinesh-Kumar, S.P., and Deng, X.W. (2005). An alternative tandem affinity purification strategy applied to Arabidopsis protein complex isolation. *Plant J*., 41: 767-778.

Rudolph, H.K., Antebi, A., Fink, G.R., Buckley, C.M., Dorman, T.E., LeVitre, J., Davidow, L.S., Mao, J., and Moir, D.T. (1989). The yeast secretory pathway is perturbed by mutations in *PMR1*, a member of the Ca^{2+} ATPase family. *Cell*, 58: 133-145.

Schaller, G.E., and Bleecker, A.B. (1995). Ethylene-binding sites generated in yeast expressing the Arabidopsis *ETR1* gene. *Science*, 270: 1809–1811.

Schaller, G.E., Ladd, A.N., Lanahan, M.B., Spanbauer, J.M., and Bleecker, A.B. (1995). The ethylene response mediator ETR1 from Arabidopsis forms a disulfide-linked dimer. *J. Biol. Chem.*, 270(21): 12526–12530.

Schütze, K., Harter, K., and Chaban, C. (2009). Bimolecular fluorescence

complementation (BiFC) to study protein-protein interactions in living plant cells. *Methods Mol. Biol.,* 479: 189–202.

Schwechheimer, C. and Deng, X.W. (2001). COP9 signalosome revisited: a novel mediator of protein degradation. *Trends Cell Biol*., 11: 420-426.

Seeger, M., Kraft, R., Ferrell, K., Bech-Otschir, D., Dumdey, R., Schade, R., Gordon, C., Naumann, M., and Dubiel, W. (1998). A novel protein complex involved in signal transduction possessing similarities to 26S proteasome subunits. *FASEB J.,* 12: 469-478.

Serino, G. and Deng, X.W. (2003). The COP9 signalosome: regulating plant development through the control of proteolysis. *Annu. Rev. Plant Biol.,* 54:165–182.

Sharon, M., Mao, H., Boeri Erba, E., Stephens, E., Zheng, N., and Robinson, C.V. (2009). Symmetrical modularity of the COP9 signalosome complex suggests it multifunctionality. *Structure*, 17: 31-40.

Solano, R., Stepanova, A., Chao, Q., and Ecker, J.R. (1998). Nuclear events in ethylene signaling: a transcriptional cascade mediated by ETHYLENE-INSENSITIVE3 and ETHYLENE-RESPONSE-FACTOR1. *Genes Dev*., 12: 3703–3714.

Stohs, S.J. and Bagchi, D. (1995). Oxidative mechanisms in the toxicity of metal ions. *Free Radical Biol. Med*., 18(2): 321-336.

Stuttmann, J., Parker, J.E., and Noel, L.D. (2009). Novel aspects of COP9 signalosome functions revealed through analysis of hypomorphic *csn* mutants. *Plant Signal. Behav.,* 4: 896-898.

Su, W. and Howell, S.H. (1992). A single genetic locus, Ckr1, defines Arabidopsis mutants in which root growth is resistant to low concentrations of cytokinin. *Plant Physiol.*, 99(4): 1569-1574.

Supek, F., Supekova, L., Nelson, H., and Nelson, N. (1996). A yeast manganese transporter related to the macrophage protein involved in conferring resistance to mycobacteria. *Proc. Natl. Acad. Sci. USA*, 93: 5105-5110.

Takei, Y. and Tsujimoto, G. (1998). Identification of a novel MCM3-associated protein that facilitates MCM3 nuclear localization. *J. Biol. Chem.,* 273: 22177-22180.

Takei, Y., Assenberg, M., Tsujimoto, G., and Laskey, R. (2002). The MCM3 acetylase MCM3AP inhibits initiation, but not elongation, of DNA replication via interaction with MCM3. *J. Biol. Chem*., 277: 43121-43125.

Thomas, B.C., Pedersen, B., and Freeling, M. (2006). Following tetraploidy in an Arabidopsis ancestor, genes were removed preferentially from one homolog leaving clusters enriched in dose-sensitive genes. *Genome Res*., 16: 934-946.

Thomine, S., Wang, R., Ward, J.M., Crawford, N.M., and Schroeder, J.I. (2000). Cadmium and iron transport by members of a plant metal transporter family in Arabidopsis with homology to Nramp genes. *Proc. Natl. Acad. Sci. USA*, 97(9): 4991-4996.

Thomma, B.P.H.J., Eggermont, K., Tierens, K.F.M.-J., and Broekaert, W.F. (1999). Requirement of functional ethylene resistance of *Arabidopsis* to infection by *Botrytis cinerea*. *Plant Physiol*., 121(4): 1093-1101.

Tomoda, K., Kubota, Y., Arata, Y., Mori, S., Maeda, M., Tanaka, T., Yoshida,

M., Yoneda-Kato, N., and Kato, J. (2002). The cytoplasmic shuttling and subsequent degradation of $p27^{Kip1}$ mediated by Jab1/CSN5 and the COP9 signalosome complex. *J. Biol. Chem*., 277(3): 2302-2310.

Tsukihara, T., Aoyama, H., Yamashita, E., Tomizaki, T., Yamaguchi, H., Shinzawa-Itoh, K., Nakashima, R., Yaono, R., and Yoshikawa, S. (1995). Structures of metal sites of oxidized bovine heart cytochrome c oxidase at 2.8A. *Science*, 269: 1069-1074.

Vaz Martins, T., Evans, M.J., Woolfenden, H.C. and Morris, R.J. (2013). Towards the physics of calcium signaling in plants. *Plants*, 2(4): 541-588.

Veitia, R.A. (2007). Exploring the molecular etiology of dominant-negative mutations. *Plant Cell*, 19: 3843-3851.

Vert, G., Briat, J.F., and Curie, C. (2001). *Arabidopsis IRT2* gene encodes a root-periphery iron transporter. *Plant J*., 26: 181-189.

Wang, W., Hall, A.E., O'Malley, R., and Bleecker, A.B. (2003). Canonical histidine kinase activity of the transmitter domain of the ETR1 ethylene receptor from Arabidopsis is not required for signal transmission. *Proc. Natl. Acad. Sci. USA*, 100: 352–357.

Wang, X., Kang, D., Feng, S., Serino, G., Schwechheimer, C., and Wei, N. (2002). CSN1 N-terminal dependent activity is required for *Arabidopsis* development but not for Rub1/Nedd8 deconjugation of cullins: a structure-function study of CSN1 subunit of COP9 signalosome. *Mol. Biol. Cell*, 13: 646–655.

Wang, Y., Liu, C., Li, K., Sun, F., Hu, H., Li, Y., Zhao, Y., Han, C., Zhang, W.,

Duan, Y., Liu, M., and Li, X. (2007). *Arabidopsis* EIN2 modulates stress response through abscisic acid response pathway. *Plant Mol. Biol.* 64: 633-644.

Wei, N. and Deng, X.W. (1992). COP9: A new genetic locus involved in light-related development and gene expression in Arabidopsis. *Plant Cell*, 4: 1507-1518.

Wei, N. and Deng, X.W. (1998). Characterization and Purification of the mammalian COP9 complex, conserved nuclear regulator initially identified as a repressor of photomorphogenesis in higher plants. *Photochem. Photobio*., 68(2): 237-241.

Wei, N., Serino, G., and Deng, X.W. (2008). The COP9 signalosome: more than a protease. *Trends Biochem. Sci*., 33(12): 592-600.

Wen, X., Zhang, C., Ji, Y., Zhao, Q., He, W., An, F., Jiang, L., and Guo, H. (2012). Activation of ethylene signaling is mediated by nuclear translocation of the cleaved EIN2 carboxyl terminus. *Cell Res*., 22: 1613-1616.

Wickramasinghe, V.O., McMurtrie, P.I.A., Mills, A.D., Takei, Y., Penrhyn-Lowe, S., Amagase, Y., Main, S., Marr, J., Stewart, M., and Laskey, R.A. (2010). mRNA export from mammalian cell nuclei is dependent on GANP. *Curr. Biol.*, 20: 25-31.

Wilkie, A.O.M. (1994). The molecular basis of genetic dominance. *J.Med. Genet.*, 31:

89-98.

Wittke, S., Lewke, N., Müller, S., and Johnsson, N. (1999). Probing the molecular

environment of membrane proteins in vivo. *Molec. Biol. Cell*, 10: 21519-2530.

Xia, J., Yamaji, N., Kasai, T., and Ma, F. (2010). Plasma membrane-localized transporter for aluminum in rice. *Proc. Natl. Acad. Sci. USA*, 107 (43): 18381-18385.

Xie, F., Liu, Q., and Wen, C.K. (2006). Receptor signal output mediated by the ETR1 N-terminus is primarily subfamily I receptor dependent. *Plant Physiol.*, 142:492-508.

Yoo, S.D., Cho, Y.H., Tena, G., Xiong, Y., and Sheen, J. (2008). Dual control of nuclear EIN3 by bifurcate MAPK cascades in C_2H_4 signaling. *Nature*, 451:789–796.

Zheng, H., Chordia, M.D., Cooper, D.R., Chruszcz, M., Müller, P., Sheldrick, G.M., and Minor, W. (2014). Validation of metal-binding sites in macromolecular structures with the CheckMyMetal web server. *Nat. Protoc.*, 9: 156-170.

Zhu, Z., An, F., Feng, Y., Li, P., Xue, L., A, M., Jiang, Z., Kim, J.M., To, T.K., Li, W., Zhang, X., Yu, Q., Dong, Z., Chen, W.Q., Seki, M., Zhou, J.M. and Guo, H. (2011). Derepression of ethylene-stabilized transcription factors (EIN3/EIL1) mediates jasmonate and ethylene signaling synergy in Arabidopsis. *Proc. Natl. Acad. Sci. U.S.A.*, 108: 12539-12544.

Zook, J.D., Molugu, T.R., Jacobsen, N.E., Lin, G., Soll, J., Cherry, B.R., Brown,

M.F., and Fromme, P. (2013). High-resolution NMR reveals secondary structure and folding of amino acid transporter from outer chloroplast membrane. *PLoS One*. 8: e78116. DOI:10.1371/journal.pone.0078116.